Using RNA aptamers to manipulate the functions of Human papillomaviruses (HPV)

By

Ozlem Cesur

Submitted in accordance with the requirements for the degree of Doctor of Philosophy

The University of Leeds

School of Molecular and Cellular Biology

February 2015

The candidate confirms that the work submitted is her own, except where work which has formed part of jointly authored publications has been included. The contribution of the candidate and the other authors to this work has been explicitly indicated below. The candidate confirms that appropriate credit has been given within the thesis where reference has been made to the work of others

Chapters 3 (Sections 3.2.2 and 3.4.1.1):

NICOL, C., CESUR, O., FORREST, S., BELYAEVA, T. A., BUNKA, D. H., BLAIR, G. E. & STONEHOUSE, N. J. 2013. An RNA aptamer provides a novel approach for the induction of apoptosis by targeting the HPV16 E7 oncoprotein. *PLoS One,* 8**,** e64781.

Chapter 3 (Section 3.4.2.2):

BELYAEVA, T. A., NICOL, C., CESUR, O., TRAVE, G., BLAIR, G. E. & STONEHOUSE, N. J. 2014. An RNA Aptamer Targets the PDZ-Binding Motif of the HPV16 E6 Oncoprotein. *Cancers (Basel),* 6**,** 1553-69.

Chapter 5 (Section 5.2.1):

DOBLE, R., MCDERMOTT, M. F., CESUR, O., STONEHOUSE, N. J. & WITTMANN, M. 2014. IL-17A RNA aptamer: possible therapeutic potential in some cells, more than we bargained for in others? *J Invest Dermatol,* 134**,** 852-5.

Chapter 5 (Section 5.3) and Chapter 4 (Sections 4.2.2 and 4.2.3):

CESUR, O., NICOL, C., GROVES, H., MANKOURI, J., BLAIR, G. E & STONEHOUSE, N. J. The subcellular localisation of the Human papillomavirus (HPV) 16 E7 protein in cervical cancer cells and its perturbation by RNA aptamers. *Viruses (Besel)* (in press).

Acknowledgements

I am extremely grateful to my supervisor, Professor Nicola Stonehouse for an enormous amount of support and guidance over the past four years. It was a real privilege for me to be a member of her research group. I would also like to thank my co-supervisor Professor Eric G. Blair for his support and advice throughout my PhD, and for reviewing parts of this manuscript.

I would like to thank all members of the Stonehouse lab, past and present for creating such an amazing and inspiring environment to work and do experiments. My particular thanks go to Dr Clare Nicol, a great scientist whom I owe great appreciation. I also would like to thank my friends, Dr Marietta Müller, Dr Emma Prescott, Dr Chris Wasson, Oluwapelumi Adeyemi and Refik Bozbuga for all chats, scientific discussions and lunchtime get-togethers.

I would also like to express my sincere gratitude to Dr Jamel Mankouri for giving me advice and reagents for aptamer internalisation experiments in Chapter 5.

I would like to thank all my close friends, in particular Zahide Tekin, Yonca Yüzügüllü, Burçak Kocuklu, Anastasia Kazaltzi, Pavlos Xenitidis, Irene Yah-Ling Hung and Paraskevi Mallini who have made my time in Leeds very special.

I would like to express my sincere gratitude to the Turkish Ministry of National Education for sponsoring my studies in the UK.

I would like to thank my family, mum and dad for their endless love, unconditional support and constant encouragement, without them I would not have come this far. My special thanks go to my sister, Dr Sinem Cesur for being my other half and my best friend. Last but not least, I am so thankful to my brother Ilker Serkan Cesur and my sister-in-law Damla Cesur for all fantastic times we have shared together and most importantly bringing my beautiful nephew, Ali Koru into this world.

Hiçbir zaman sevgi ve desteklerini benden esirgemeyen canim ailem; iyi ki varsınız…

Abstract

HPV is the most common viral infection of reproductive tract, affecting both females and males. High-risk oncogenic types are the cause of cervical cancer by the expression of E6 and E7 viral oncoproteins. High-risk oncogenic types are also responsible for up to 90% of anal and 12 % of oropharyngeal cancers. The well-characterised interaction of HPV16 E7 is with the cell cycle control protein pRb, promoting pRb degradation and resulting in cell cycle misregulation. E7 can interact with many other cellular proteins. In this study, RNA aptamers identified against HPV16 E7 were used to study E7 interactions further. The aptamers were generated previously by an *in vitro* technique known as the systematic evolution of ligands by exponential enrichment (SELEX), in which molecules from a random pool are isolated for binding to the target with a high affinity and specificity. Aptamers are single-stranded oligonucleotides that can form complex structures and bind target molecules in a conformation-dependent manner. The E7 aptamers have been stabilised by the inclusion of modified pyrimidines. Aptamers have therapeutic potential; examples include the aptamer Macugen (also called Pegaptanib). Several HPV16 E7 aptamers were able to induce apoptosis in an HPV16-transformed cervical carcinoma cell line (SiHa) that actively express both E6 and E7. Of particular interest is the E7 aptamer A2. In order to ensure apoptosis is not due to the innate immune response, immune stimulatory effects of E7 aptamers were studied by quantitative PCR. Effects of aptamers on the steady state levels of E7 and cellular proteins were analysed by western blotting. Treatment of cells with A2 resulted in loss of the E7 oncoprotein and a rise in cellular pRb levels. We have evidence that some of the HPV16 E7 aptamers can also target HPV18 E7. Several inhibitor molecules of protein degradation were used to determine the pathway of E7 loss following aptamer transfection in HPV16-transformed cervical carcinoma cell line, CaSki. Results suggested that aptamer transfection did not appear to alter normal degradation pathway of E7, which was mainly 26S proteasome-mediated. Co-localisation of aptamers (model aptamers) with cellular markers was studied by immunofluorescence. Co-localisation of E7 with cellular markers in the presence or absence of HPV16 E7 aptamers suggested the accumulation of E7 in the endoplasmic reticulum (ER) in A2 transfected cells, suggesting an alternative pathway, leading to a model for E7 degradation. Aptamers can be advantageous in terms of developing novel potential therapeutics. In Chapter 5, model aptamers were shown to internalise into keratinocytes and cervical cancer cells without the need for lipofection. This novel ability of aptamers might enable topical use of aptamers. The mechanism of aptamer entry was also studied using

endocytosis inhibitors for receptor-mediated uptake as well as macropinocytosis. The result suggested that reagent-free internalisation can be both energy-dependent (receptor-mediated) and passive (macropinocytosis) and that uptake can be sequence-dependent.

Contents

List of Figures

List of tables

Abbreviations

3D pol	3D polymerase
A	Adenine
Aβ	Amyloid beta
AAV	Adeno-Associated Virus
ADA3	Alternation/deficiency in activation-3
Ad E1A	Adenovirus
AIDS	Acquired immunodeficiency syndrome
AIV	Avian influenza virus
AML	Acute myeloid leukaemia
Ang-2	Angiopoietin
AP-1	Activator protein-1
APC	Allophycocyanin
APS	Ammonium persulphate
ATCC	American tissue culture collection
ATL	T-cell leukaemia
ATP	Adenosine 5′-triphosphate
ATR	ATM and Rad3-related
AUC	Analytical ultracentrifugation
Bak	Bcl-2-antagonist
Bax	Bcl-2-associated protein X
BCE	Before the Current Christian Era
Bcl-2	B-cell lymphoma 2
bp	Base pair
BRCA1	Breast cancer gene 1
BrdU	5-bromo-2-deoxyuridine
BSA	Bovine serum albumin
°C	Degree Celsius
C	Cysteine, Cytosine
CAT	Chloramphenicol acetyltransferase
CBP	CREB-binding protein
CCR5	Chemokine (C-C motif) receptor 5
CD	Circular dichroism
CDC	Centre for Disease Control
Cdk	Cyclin-dependent kinase

cDNA	Complementary DNA
c-IAP	Cellular inhibitor of apoptosis
CIN1/2/3	Cervical intraepithelial neoplasia 1/2/3
CIP-1	CDK-interacting protein 1
CK2	Casein kinase 2
CMCT	1-cyclohexyl-(2-morpholinoethyl) carbodiimide metho-p-toluenesulfonate
c-Myc	Cellular myelocytomatosis viral oncogene homologue
Co-IP	Co-immunoprecipitation
CRPV	Cottontail rabbit papillomavirus
CR1/2/3	Conserved region 1/2/3
CREB	cAMP response element-binding
C-terminus	Carboxyl terminus
CTP	Cytosine 5′-triphosphate
Da	Dalton
DAPI	4′,6-diamidino-2-phenylindole
dATP	Deoxyadenosine 5′-triphosphate
dCTP	Deoxycytidine 5′-triphosphate
ΔG	Gibbs free energy
ΔΔCt	Difference in threshold cycles
dGTP	Deoxyguanosine 5′-triphosphate
DMEM	Dulbecco's modified Eagles' medium
DMSO	Dimethyl sulphoxide
DNA	Deoxyribonucleic acid
DNase	Deoxyribonuclease
dsDNA	Double-stranded DNA
dsRNA	Double-stranded RNA
DTT	Dithiothreitol
dTTP	Deoxythymidine 5′-triphosphate
E1	Early gene 1
E1A	Early gene 1A
E2	Early gene 2
E4	Early gene 4
E5	Early gene 5
E6	Early gene 6
E6-AP	E6-associated protein

E6-BP	E6-binding protein
E6TP-1	E6 targeted protein-1
E7	Early gene 7
EBV	Epstein-Barr virus
EDC	1-Ethyl-3-[3-dimethyl-aminopropyl] carbodiimide
EDTA	Ethylenediamine tetra-acetic acid
EEA1	Early endosome antigen 1
EGF	Epidermal growth factor
EGFR	Epidermal growth factor receptor
EGTA	Ethylene glycol tetra-acetic acid
ELISA	Enzyme-linked immunosorbent assay
EMBL-EBI	European Molecular Biology Laboratory - European Bioinformatics Institute
EMCV	Encephalomyocarditis virus
EMSA	Electrophoretic mobility shift assay
ERAD	Endoplasmic reticulum associated degradation
FACS	Fluorescence-activated cell sorting
FBS	Foetal bovine serum
FDA	Food and drug administration
FITC	Fluorescein isothiocyanate
Fl	Fluoro
FMDV	Foot-and-mouth disease virus
G0	Growth phase 0
G1	Growth phase 1
G2	Growth phase 2
GAPDH	Glyceraldehyde 3-phosphate dehydrogenase
GFP	Green fluorescent protein
GM-beads	Glutathione magnetic-beads
gp120	Glycoprotein 120
GRO	G-rich oligonucleotide
GST	Glutathione S-transferase
GTP	Guanosine 5′-triphosphate
HA	Haemagglutinin
HBV	Hepatitis B virus
HCC	Hepatocellular carcinoma
HCl	Hydrochloric acid
HCV	Hepatitis C Virus

HDAC	Histone deacetylase
hDLG	Human homologue of the *Drosophila* discs large tumour suppressor
HSP70	Heat shock protein-70
HSPG	Heparan sulphate proteoglycan
HEK	Human embryonic kidney
HEPES	(4-(2-hydroxyethyl)-1-piperazineethanesulfonic acid
HHSC	Hydrophobic hyaluronic acid–spermine conjugates
HIV	Human immunodeficiency virus
HPV	Human papillomavirus
HRP	Horseradish peroxidase
hScrib	Human Scribble homologue
hTERT	Human telomerase reverse transcriptase
HTLV-1	Human T-cell leukaemia virus type 1
IC_{50}	Half maximal inhibitory concentration
IDP	Intrinsically disordered protein
IFIT	Interferon induced protein with tetratricopeptide repeat
IFN-α/β	Interferon-α/β
IGFBP-3	Insulin-like growth factor binding protein 3
Ig	Immunoglobulin
IP	Immunoprecipitation
IPTG	Isopropyl β-D-1-thiogalactopyranoside
IRES	Internal ribosome entry site
IRF	Interferon regulatory factor
ISG	Interferon stimulating genes
K	Lysine
kb	Kilobase
kcal	Kilocalorie
kDa	Kilodalton
K_{Dapp}	Apparent dissociation constant
K_i	Inhibition constant
KSHV	Kaposi`s sarcoma herpesvirus
L	Leucine, Litre
L1	Late gene 1
L2	Late gene 2
LAMP1	Lysosomal-associated membrane protein 1
LANA	Latency-associated nuclear antigen

LB	Luria-Bertani
LC3	Microtubule-associated protein 1A/1B-light chain 3
LCR	Long control region
LNA	Locked nucleic acid
M	Marker, Methionine, Mitosis, Molar
MAGI-1-2-3	Membrane-associated guanylate kinase-1-2-3
MAN	Mannosidase
MAP	Mitogen-activated protein kinase
MCM	Mini chromosome maintenance complex
MCV	Merkel cell carcinoma virus
MDA5	Melanoma differentiation-associated gene 5
mg	Milligram
µg	Microgram
MHC	Major Histocompatibility Complex
min	Minutes
ml	Millilitre
µm	Micrometre
µM	Micromolar
µmol	Micromole
mM	Milimolar
mmol	Millimole
MPP2	M phase phosphoprotein
mRNA	Messenger RNA
MUPP1	Multi-PDZ-domain protein
MW	Molecular weight
MWCO	Molecular weight cut-off
MX1	Myxovirus resistance-1
n	Sample number
NC	Nucleocapsid
NF-κB	Nuclear factor-κB
NFX1-91	Nuclear transcription factor, X-box binding 1-91
ng	Nanogram
NLS	Nuclear localisation signal
nm	Nanometre
nM	Nanomolar
nmol	Nanomole

NMR	Nuclear magnetic resonance
NP	Nanoparticle
NP-40	Nonidet P-40
NS3/5B	Non-structural protein 3/5B
O(6)-MGDMT	O-6-methylguanine-DNA methyltransferase
Oct-1	Octamer-binding protein 1
OD	Optical density
OmpT	outer membrane protease
ORF	Open reading frame
PAGE	Polyacrylamide gel electrophoresis
pA_E	Early polyadenylation sites
pA_L	Late polyadenylation site
PAMP	Pathogen-associated molecular pattern
Pap	Papanicolaou
PaVE	Papillomavirus Episteme
PBS	Phosphate buffered saline
pCAF	p300/CBP-associated factor
PCNA	Proliferating cell nuclear antigen
PCR	Polymerase chain reaction
PDGF-β	Platelet-derived growth factor-β
PDZ	Post synaptic density protein-*Drosophil*a disc large tumour suppressor-zonula occludens-1 protein
PEG	Polyethylene glycol
PEI	Polyethylenimide
PI	Propidium iodide
PI3K	Phosphatidylinositol-3-kinase
pM	Picomolar
PML	promyelocytic leukaemia
pmol	Picomole
PPI	Protein phosphatase 1
pRb	Retinoblastoma protein
PS	Phosphatidylserine
PSD	Postsynaptic density protein
PSMA	Prostate-specifc membrane antigen
PtdIns3P	Phosphatidylinositol-3-phosphate
p-value	Probability-value

Qdots	Quantum dots
Rev	Regulator of virion
RIG-I	Retinoic acid-inducible gene 1
RIPA	Radio-immuno precipitation assay
RLR	RIG-I like receptor
RNA	Ribonucleic acid
RNA-IP	RNA-immunoprecipitation
RNase	Ribonuclease
rNTP	Ribonucleoside tri-phosphate
RSV	Rous sarcoma virus
rpm	Revolutions per minute
RT	Reverse transcriptase
RT-PCR	Real-time PCR
S	DNA synthesis
SAP	Signalling lymphocytic activation molecule associated protein
SCC	Squamous cell carconima
SDS	Sodium dodecyl sulphate
SDS-PAGE	SDS-polyacrylamide gel electrophoresis
SELEX	Systematic evolution of ligands by exponential enrichment
shRNA	Short hairpin RNA
SID	Systemic siRNA deficient
SIL	Squamous intraepithelial lesions
siRNA	Short interfering RNA
SIV	Simian immunodeficiency virus
snRNA	small nuclear RNA
SNX17	Sorting nexin 17
SP-1	Specificity protein-1
SPR	Surface plasmon resonance
SRC-1	Steroid receptor co-activator-1
ssDNA	Single-stranded DNA
ssRNA	Single-stranded RNA
Stat3	Signal transducer and activator of transcription 3
Stauro	Staurosporine
STI	Sexually transmitted infections
SV40	Simian virus 40
T	Thymidine

TAF	TATA-binding protein-associated factor
TAg	Large T antigen
Tat	Transactivator of transcription
TBE	Tris-borate-EDTA
TBP	TATA-binding protein
TBST	Tris buffered saline-Tween 20
TE	Tris-EDTA
TGase	Transglutaminase
TGF-β	Transforming growth factor-β
TGN	Trans-Golgi network
thio-NTP	Thio-ribonucleoside
TLR	Toll-like receptor
TNF	Tumour necrosis factor
TPR	Tetratricopeptide repeat domain
TUNEL	Terminal deoxynucleotidyl transferase-mediated dUTP nick-end labelling
U	Uridine
Ubch7 (UBE2L3)	Ubiquitin-conjugating enzyme H7 (Ubiquitin-conjugating enzyme E2L 3
UTP	Uridine 5′-triphosphate
UK	United Kingdom
USA	United States of America
UV	Ultraviolet
V	Voltage
v/v	Volume/volume
VEGF	Vascular endothelial growth factor
VLP	Virus-like particle
VPg	Viral protein genome-linked
W	Watts
w/v	Weight/volume
WB	Western blot
WHO	World Health Organisation
YIP	Yeast inorganic pyrophosphatase
ZO-1	Zona occuldens protein-1

1 INTRODUCTION

1.1 Tumour Virology

Cancer is characterised by uncontrolled cell proliferation and the ability to invade other tissues through the blood and lymph systems. Cancer can be referred to as carcinoma, sarcoma, leukaemia, lymphoma and myeloma and central nervous system cancer. These are the cancer types that originate from skin, bone, blood-producing tissues, immune system and brain-spinal cord tissues, respectively. The earliest cancers documented are bone cancers seen in 4-million year old fossils and nasopharyngeal carcinomas and osteogenic sarcomas seen in ancient Egyptian mummies from 3000 BCE, reviewed in (Javier and Butel, 2008). The development of microbiology in 19th century led to the proposition of links between cancer and several infectious agents such as bacteria, yeasts, fungi and protozoa. Most importantly, research which showed a nematode worm as the causative agent of stomach cancer in rats was awarded a Nobel Prize in 1926, reviewed in (Javier and Butel, 2008). When a new class of infectious agents, viruses, were discovered, studies focussed on molecular mechanisms in virus-induced tumours. The first known tumour virus to be identified was from a Plymouth Rock chicken with spindle cell carcinoma and named Rous sarcoma virus (RSV); an RNA virus (Rous, 1993). This was followed with the discovery of the first DNA tumour virus, cottontail rabbit papillomavirus (CRPV) from warts obtained from wild cottontail rabbits (Shope and Hurst, 1933). CRPV was then showed to induce the formation of skin carcinomas in domestic rabbits (Rous and Beard, 1935). DNA tumour viruses infecting humans were also discovered. Human adenovirus was discovered from explants of adenoid and tonsil tissues and shown to cause human acute respiratory disease (Hilleman and Werner, 1954, Rowe et al., 1953). Adenoviruses were also reported to induce tumour formation in experimentally infected animals (Trentin et al., 1962). The first human tumour virus, Epstein-Barr virus (EBV), was identified and visualised by electron microscopy from cell lines derived from Burkitt`s lymphoma (Epstein et al., 1965), which is a cancer of antibody producing B-cells. It should however be noted that most tumour viruses do not replicate to produce virions in tumour cells, thus making electron-microscopy imaging challenging. Studies later suggested that EBV was necessary but not sufficient to induce lymphomas; some other cofactors were also required such as *myc* translocation (*myc-IgH* and *myc-IgL*) resulting in the abnormal expression of *myc* oncogene (Javier and Butel, 2008). In common with EBV, hepatitis B virus (HBV) was shown to be a human tumour virus (Blumberg et al., 1975). It was

shown that individuals with chronic HBV infection developed hepatocellular carcinoma (HCC) with a 100-fold increase when compared to uninfected individuals (Beasley et al., 1981). The first cancer vaccine (offering protection against liver cancer) was developed by large-scale purification of HBV surface antigens from the serum of HBV-positive individuals. However, this vaccine was later replaced by a second generation recombinant HBV surface antigen vaccine which was safer due to the production of the vaccine in human-plasma free environment with a cost effective way. Later, a non-A, non-B hepatitis virus, hepatitis C (HCV) was identified and linked to chronic hepatitis and HCC (Tan et al., 2008). There were also retroviruses found to be associated with human cancer as in the case of human T-lymphotropic virus-I (HTLV-I) causing adult T-cell leukaemia (ATL). Their association was supported with the facts that first ATL was mainly distributed in specific geographic locations where HTLV-I infection was disperse, second almost all ATL patients were infected with HTLV-I, third in the molecular basis, all leukaemia cells from infected individuals contained HTVL-I proviral DNA, and fourth when HTLV-I introduced into healthy T-cells it induced transformation (Javier and Butel, 2008). Most animal retroviruses such as avian and murine leukaemia viruses lack viral oncogenes, therefore they can cause cancer through a mechanism called insertional mutagenesis in which the provirus integrates near a cellular proto-oncogene and modify its expression (Butel, 2000). Despite being a retrovirus, HTLV-I do not use this mechanism for carcinogenesis. This virus behaves more like a DNA virus, and encodes its own oncogene, *Tax* that is required for replication (Matsuoka and Jeang, 2011). This gene can also play roles in cellular transformation by e.g. acceleration of transition between G1 and S phase of cell cycle, interference with cellular DNA repair mechanisms, and activation of certain transcription factors (Matsuoka and Jeang, 2011).

In 1994, Kaposi`s sarcoma herpesvirus (KSHV) (or human herpesvirus type 8) was discovered in 90% of Kaposi`s sarcoma tissues from patients with acquired immunodeficiency syndrome (AIDS) by Chang and Moore by representational difference analysis (Chang et al., 1994). In this method, fragmented cDNA sequences obtained by restriction digestion with an enzyme (e.g. *Dpn*II) from healthy and diseased tissues from the same individual can be cross-hybridised and following PCR amplification can specifically enrich the DNA obtained from diseased tissue due to the presence of additional viral genes (Lisitsyn et al., 1993). The newest member of the tumour viruses is Merkel cell carcinoma virus (MCV) discovered in 2008 by computational subtraction of cDNA sequence data by digital transcriptome subtraction

(Feng et al., 2008). A recent review summarised the key facts including genome organisation, virus life-cycle and pathogenesis of MCV (Stakaityte et al., 2014).

There is a strong selection amongst viruses (tumour and non-tumour viruses) to maintain viral genes that have a potential to induce cellular transformation, and the products of these viral genes can target similar tumour suppressor pathways. For instance, oncoproteins from most of the human tumour viruses destabilise retinoblastoma 1 (Rb1) and p53 tumour suppressors using unique mechanisms. Other cellular targets of tumour virus oncoproteins include telomerase reverse transcriptase (TERT), cytoplasmic PI3K-AKT-mTOR, nuclear factor-κB (NF-κB), β-catenin and interferon signalling pathways (Moore and Chang, 2010). The KSHV LANA1 oncoprotein targets pRb, p53 and interferon signalling and at the same time it prevents the virus to progress from latency to lytic replication (Cloutier and Flamand, 2010, Friborg et al., 1999, Radkov et al., 2000). Human papillomaviruses are small DNA tumour viruses and most small DNA tumour viruses encode oncogenes in order to function as deregulators of the cell cycle entry and prepare cellular conditions for the viral replication (Moore and Chang, 2010). Since, host replication machinery is inactive and nucleotide pools are not enough for their replication in the G0 phase of the cell cycle of the differentiated host cells. Therefore, these viruses force cells for the S-phase transition in order to enrich cellular resources for their genome replication. In normal conditions, when cell cycle regulation is disrupted, cell death signalling pathways (e.g. p53) become activated. However, in tumour virus infected cells, viral oncoproteins inhibit the function of these pathways by targeting these tumour suppressor proteins to ensure the export of the progeny viruses (e.g. p53). For example, HPV oncoproteins E6 and E7 can maintain infected cells in a proliferative state, preventing apoptosis.

These above described viruses are all linked to tumourigenesis. However, virus infection alone is not always sufficient for the development of cancer apart from few cases such as KSHV and HPV for Kaposi`s sarcoma and cervical cancer due to the fact that these viruses can ubiquitously be found present in the respective tumours (Moore and Chang, 2010). Immunity is an important factor in determining if the exposure to a tumour virus will result in cancer. Some individuals can have propensities for the development of cancer due to defects in immunity. An example of this is the signalling lymphocytic activation molecule associated protein (SAP) mutations in males that can result in immunodeficiency and X-linked lymphoproliferative syndrome following EBV infection (Purtilo et al., 1975). Another factor causing immunodeficiency is AIDS caused by HIV infection. A study in USA

showed that the incidence of the KSHV-related Kaposi`s sarcoma cases rocketed with the increase in HIV infection amongst the population (Engels et al., 2006).

The evasion of innate immunity can be one of the major elements in viral tumourigenesis. Tumour viruses can achieve this with the expression of oncogenes. Oncogenes do not only target tumour suppressor proteins but also key effector proteins in innate immune signalling. In fact, this key effector proteins such as p53 and p21 cyclin-dependent kinase inhibitor are shared in both tumour suppressor and immune signalling mechanisms. Therefore, while targeting tumour suppressor pathways, these viruses also inactivate anti-viral pathways to evade innate immunity. This can be one of the crucial steps in the cancerous transformation of infected cells. KSHV encodes four interferon regulatory factor (IRF) homologues which play roles in the inhibition of interferon signalling and cellular transformation. IRFs are family of transcription factors that regulates the induction of interferons, therefore providing a host defence mechanism against pathogens.

Association of papillomavirus infection with cancer was first reported in 1935 by Rous and Beard. In this study, CRPV was shown to cause carcinomas in domestic rabbits. Since then, research on papillomaviruses had been limited for a certain period of time due to the benign nature of skin warts in addition to the lack of tissue culture systems. When bovine papillomavirus was shown to induce malignant tumours in animals, studies on papillomaviruses and their association with cancer gained importance. Harald zur Hausen linked human papillomavirus infection (in particular HPV type 16 and 18) with cervical cancer by demonstrating the presence of HPV DNA in cervical tumours, reviewed by (zur Hausen, 2002). Similar to HBV, there are vaccines generated to protect against HPV infection. These vaccines are produced by overexpression of HPV structural proteins (VLPs) in recombinant systems and contain no oncogenic HPV genome (see section 1.2.6).

1.2 Human papillomavirus (HPV) and cervical cancer

1.2.1 Classification of papillomaviruses

Papillomaviruses have been discovered and studied in many vertebrates including human, cattle, dogs, birds, reptiles etc. More than 300 distinct types were classified in 37 genera, which makes them one of the largest family of vertebrate viruses. Within papillomavirus family, around 170 human and 130 animal different types have been sequenced and identified to date (see Papillomavirus Episteme (PaVE) on http://pave.niaid.nih.gov/#home).

Human papillomaviruses (HPVs) are classified into five genera (Alpha, Beta, Gamma, Mu and Nu) based on their L1 capsid DNA sequences. These HPV genera contain numerous HPV types with different life-cycle properties and propensities to disease conditions. Many HPV types within the cutaneous Beta and Gamma genera do not cause symptoms in infected individuals (Doorbar et al., 2012). However, when immunosuppressed individuals are infected with these types, cancer e.g. skin cancer may result. Cutaneous HPV types in Gamma, Beta and especially Alpha genera are more diverse than that in Mu and Nu genera (Doorbar et al., 2012). The Alpha PVs contain species that cause cervical cancer as well as benign lesions. The Alpha group consists of cutaneous and mucosal HPVs. The mucosal HPVs are further classified as high-risk or low-risk types (Bernard et al., 2010). The Alpha types can also include low-risk cutaneous species such as HPV2 and 57, causing common warts, and HPV3 and 10, causing flat warts (Bernard et al., 2010, Hsueh, 2009). Twelve HPVs (alpha 5, 6, 7 and 9); 16, 18, 31, 33, 35, 39, 45, 51, 52, 56, 58, and 59 are defined by the World Health Organisation (WHO) as being high-risk types with additional types, 68 and 73 under investigation. Mucosal high-risk Alpha species that are responsible for cervical cancer have been relatively well-studied e.g. in the case of HPV16 infecting the ectocervix and cervical transformation zone (zur Hausen, 2009). However, HPV16 and also other Alpha types at other sites e.g. the anus, endocervix and the penis have not been so well studied, reviewed by (Doorbar et al., 2012). Some of the low-risk types can also cause cutaneous genital lesions, however infection, mostly, does not lead to neoplasia (Middleton et al., 2003). The low-risk Alpha types (alpha 10) i.e. HPV6 and 11 can cause genital warts and might also be responsible for a very rare condition, juvenile respiratory papillomatosis (RRP) (Major et al., 2005). Approximately 5% of children with the persistent infection can later develop lung cancer (Derkay, 1995).

1.2.2 Burden of HPV-associated cancers

HPV is the most common viral infection of reproductive tract, affecting both females and males. High-risk oncogenic types are the main cause of cervical cancer. However, all women infected with high-risk HPV do not develop cervical cancer. Since, the majority (70% – 90%) of HPV infections with both high and low risk genotypes do not cause symptoms and are cleared spontaneously within 1–2 years. Squamous cell carcinoma (SCC) and adenocarcinoma are two main histological types of cervical cancer. SCC accounts for 90–95% of invasive cancer cases. Only small percentage of persistent infections (around ~5–10%) with specific oncogenic types (especially type 16 and 18) can result in precancerous lesions and eventually SCC if

untreated (Bosch et al., 2002). Persistent infection has been shown by the presence of DNA from specific HPV types in biological specimens over a period of time e.g. 6 months. Progression to invasive carcinoma can take around 10 years or longer upon infection with high-risk HPV. This period is dependent on several predisposing conditions and risk factors. These include oncogenic potential of the HPV type, the immune status of the individual (e.g. HIV infected, treated with immunosuppressant), presence of co-infection with other sexually transmitted infections (STI) e.g. herpes simplex and/or chlamydia, smoking and childbirth at young age and number of childbirths (WHO, 2014).

HPV types 18 and especially 16 were shown to be the most common types in cervical biopsies (Smith et al., 2007). However, the most common high-risk HPV types were found to be HPV-16 and HPV-52 amongst men (WHO, 2014). The risk of developing cervical cancer is found to be 400 and 250 times higher in HPV16 and HPV18, respectively, infected women when compared to that in uninfected women (de Sanjose et al., 2010). HPV infection with low-risk types (HPV6 and 11) may lead to anogenital warts (condyloma acuminata) both in females and males, which are difficult to treat. These warts, rarely, can progress to become malignant as in the case of Buschke-Lowenstein tumours. These low-risk HPV can also result in a rare condition termed recurrent respiratory papillomatosis (RRP) mainly in younger children (≤5 years old) or people in their 30s (Sinal and Woods, 2005, Humans, 2007). This condition can be serious due to the blockage of respiratory tract and larynx where warts are formed. HPV infection can also cause (20 – 90%) squamous carcinomas of the anus, the oropharynx, the vulva and vagina, and of the penis (Bosch et al., 2002).

According to the Cancer Research UK statistics, cervical cancer is the twelfth most common female cancer in the UK and the third most common gynaecological cancer following uterus (womb) and ovary cancers. However, it is the most common female cancer of under 35 in the UK. Around 3,100 new cases of cervical cancer were diagnosed in 2011 in the UK most of which (more than 75%) were in woman aged 25 – 64. Around 900 women died from cervical cancer in 2012 in the UK. Main risk factor for cervical cancer is the infection with high-risk human papillomavirus (HPV) which is linked to the almost 100% of cervical cancer cases in the UK. Other factors leading to cervical cancer in the UK include smoking, human immunodeficiency virus (HIV), and oral contraceptives.

The World Health Organisation (WHO) indicated that cervical cancer is the second most common cancer in women worldwide, with an estimated 530 000 new cases in

2012 (WHO, 2014) with around 270 000 deaths in the same year. Approximately 85% of these deaths occurred in developing countries, in Africa, Latin America and especially Asia (WHO, 2014). Protection from cervical cancer can be achieved by the use of barrier methods and vaccination (see chapter 1.2.6 for more info on HPV vaccination). WHO announced that HPV vaccination has been successful in 45 developed countries (WHO, 2014). However, in order to cure global burden of cervical cancer, HPV vaccination needs to be widely introduced in the developing countries as part of their national public health service.

1.2.3 Diagnosis and treatment of HPV

There is no HPV-specific treatment of cervical lesions or cancer. However, there are clinical trials ongoing for T-cell based immunotherapy for cervical cancer e.g. with the use of T-cell immune checkpoint inhibitors including anti-cytotoxic T-lymphocyte associated protein 4 (anti-CTLA-4) (trial number NCT01693783 in Phase II) and anti-programmed cell death ligand (anti-PD-L1) (trial number NCT01693562 in Phase I/II) targeting antibodies. Current treatment includes surgical removal of affected tissue or cryotherapy of precancerous lesions. Diagnosis of HPV infection is based on the detection of HPV-DNA on cervical or vaginal swabs by PCR, and of the HPV-induced changes (exfoliated cells) in the cervical epithelium by cytology under a microscope, known as the Papanicolaou (pap) smear test. Another method used in low-resource facilities is the visual inspection using acetic acid. There is an ongoing clinical trial testing the efficacy and sensitivity of E6/E7 mRNAs versus HPV DNA for cervical cancer screening based on RT-PCR (trial number NCT02116920). An alternative detection method for cervical cancer can be developed using aptamer molecules recognising E6 and E7 oncoproteins due to the fact that these proteins are overexpressed in malignant tissues.

1.2.4 Genome organisation, life-cycle and pathogenesis of HPV

Papillomaviruses are double-stranded (ds) DNA viruses from the family of *Papillomaviridae* that also includes polyomavirus, simian vacuolating virus and human papillomaviruses (HPVs).

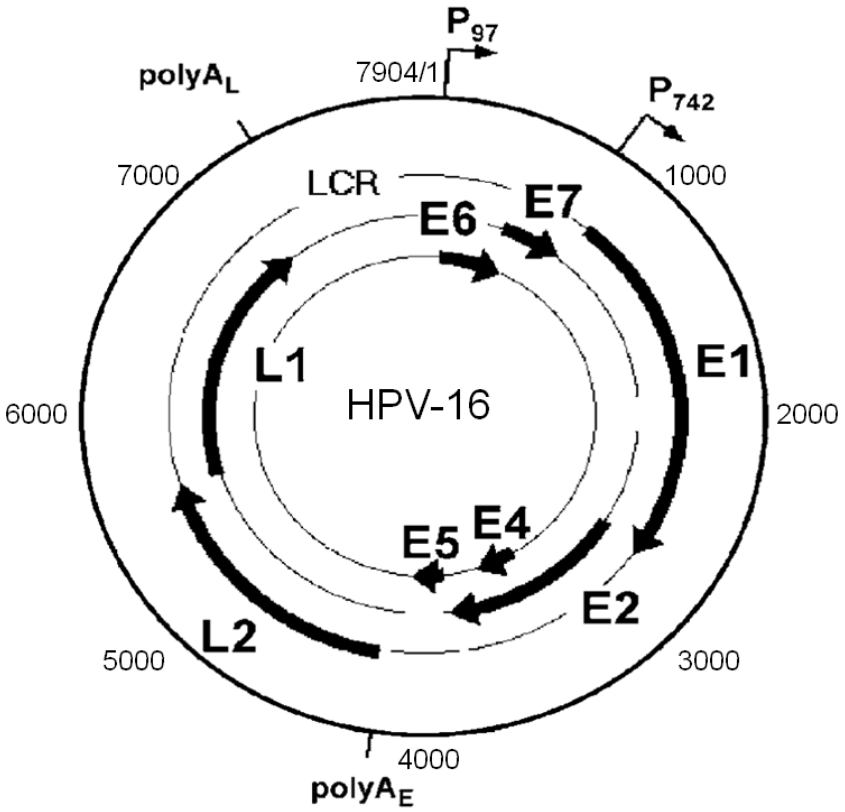

Figure 1.1 High-risk HPV 16 genome. Papillomaviruses contain a double-stranded and circular DNA genome around ~8 kb. Genome consists of three major regions; early, late and a long control region (LCR) (or non-coding region [NCR]). The LCR region consists of 850 bp and covers around ~10% of the papillomavirus genome. It contains regulatory sequences that are important for viral replication and transcription. The three regions in papillomaviruses are separated by two polyadenylation sites (pA). These are early pA (pA_E) and late pA (pA_L) polyadenylation sites. Early region cover around ~50% of whole HPV genome and encodes non-structural early genes, E1, E2, E4, E5, E6 and E7. The expression of these early genes are controlled by p97 promoter in HPV16 and 31 (p105 in HPV18) prior to productive replication. Late region covers almost 40% of papillomavirus genome on the downstream of early region. This region encodes L1 (major) and L2 (minor) ORFs. The late capsid proteins are expressed from p742 in HPV31 (or p670 in HPV16) late promoter during virus production. Modified from (Fehrmann and Laimins, 2003).

These are non-enveloped viruses with icosahedral capsids. They replicate their genomes within the nuclei of infected host cells. The HPV genome (~8 kb) contains three major regions with an average of 8 open reading frames (ORFs). Gene expression occurs from polycistronic mRNAs transcribed from a single DNA strand. A non-coding long control region (LCR) with around ~1 kb, ORFs with early genes (3 kb) E6, E7, E1, E2, E4, E5, regulating viral DNA replication and gene expression. The late region encodes two genes responsible for capsid formation; L1, major capsid protein and L2, minor capsid protein (Section 1.2.6)

Two other ORFs, E3 and E8, were previously thought to be present, however only the E8 ORF was shown to encode a protein, a spliced E8^E2C fusion protein functioning as a negative regulator of virus replication and transcription, in bovine papillomavirus 1 (BPV1) and HPV31 (Zheng and Baker, 2006). The rabbit papillomavirus genome also contains an E8 ORF, but it functions as an oncogene similar to the functions of E5 oncoprotein (Han et al., 1998).

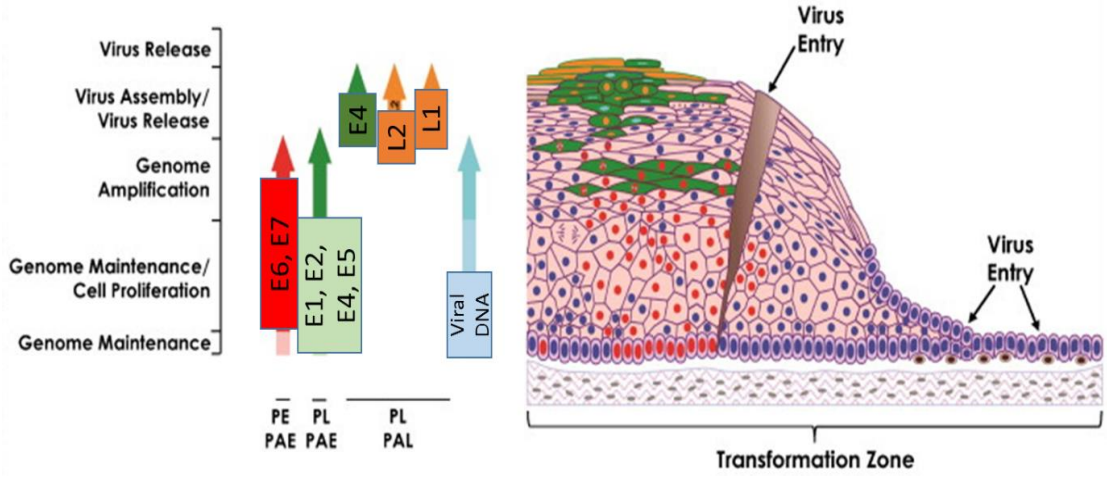

Figure 1.2 The life cycle of high-risk HPVs in infected epithelium. Virus enters the basal layer via micro wounds and is maintained as a low copy number episome. The E6 and E7 proteins (red nuclei) are expressed from the early promoter, p97 in HPV16, in the lower layers of epithelium (red arrow). Uninfected cells were represented with dark blue circles. The expression of E4 and other early proteins (green) occurs from late promoter (p670 in HPV16) (green arrow). Their expression will reduce the expressions of E6 and E7. The green cells containing red nuclei express both E4 and E7. These cells were suggested to possess all the necessary proteins to facilitate genome amplification. Once genome amplification is completed, virus capsid proteins L1 and L2 are expressed (orange arrow) in cells expressing E4 (green). This allows the packaging of the amplified HPV genomes. PAE: Position of the early polyadenylation site; PAL: Position of the late polyadenylation site; PE: Early promoter (p97); PL: late promoter (p670 or p742 in HPV31). Modified from (Doorbar et al., 2012).

The life cycle of the virus in an infected epithelium is shown schematically above (Figure 1.2). Upon infection, virus can complete its reproductive life cycle depending on the site and nature of the infection, and presence of other factors including hormones and cytokines. The life cycle of HPV is strongly related to the differentiation status of keratinocytes. Virus entry is believed to occur in the basal layers of the epithelium via micro wounds. Papillomavirus particles can bind many epithelial cell

via a conserved receptor region which is called heparan sulphate proteoglycans (HSPGs) present on the cell surface (Giroglou et al., 2001). Laminin can possibly help virus attachment (Culp et al., 2006). L1 can be one of the major determinants for the attachment of virus to the cell surface (Giroglou et al., 2001). Virus entry is believed to occur through clathrin-dependent endocytosis (Bousarghin et al., 2003). Upon attachment, virus undergoes structural changes including the cleavage of L2 capsid protein (Doorbar et al., 2012). This facilitates the interaction with a second receptor (e.g. alpha 6 integrin) involved in the internalisation of the virus in cells and subsequent transport of the virus genome to the nucleus (Evander et al., 1997). L2 can function to destabilise the endosomal membrane by e.g. possibly interacting with an adaptor protein, sorting nexin 17 (SNX17) (Bergant Marusic et al., 2012). This function of L2 is important for the endosomal release of the genome (Kamper et al., 2006). In addition, L2 can mediate the transport of the viral genome to nucleus. It is suggested to contain nuclear localisation signals at the both termini (Fay et al., 2004). Whereas, L1 stays in the endosomes and is degraded by lysosomes (Doorbar et al., 2012).

The infection is followed by genome amplification. Virus genome is maintained as episomes in each cell of undifferentiated basal layer with around 200 extrachromosomal copies (Doorbar et al., 2012). The functions of E1 and E2 are required for genome amplification and replication of the virus. The E1 protein is around 68 kDa in size and expressed in HPV infected cells at low levels. It plays an important role in HPV replication by recognizing the AT-rich sequences at the origins in the LCR as well as exhibiting ATPase and 3' - 5' helicase activities (Hughes and Romanos, 1993, Seo et al., 1993). The E2 protein is a DNA-binding protein with approximately 50 kDa. It is active as a dimer and functions as transcriptional regulator recruiting the cellular factors, specificity protein-1 (Sp-1), octamer-binding protein-1 (Oct-1), TATA-binding protein and activator protein-1 (AP-1) to regions in the long control region (LCR) in addition to its role in viral DNA replication (Longworth and Laimins, 2004). E2 binds the viral origin of replication in the LCR and recruits E1. E1 protein produces hexamers with a strong affinity for DNA similar to other helicases (Sedman and Stenlund, 1998) which then unwinds the viral DNA and recruits cellular proteins (such as DNA polymerase) involved in DNA replication. Apart from the functions above, E2 was shown to induce apoptosis by p53-independent mechanisms. Overexpression of E2 was demonstrated by western blotting to cause an accumulation of p53 tumour suppressor protein (Dowhanick et al., 1995, Goodwin et al., 2000), leading to apoptosis even with the co-expression of E6 (an HPV

oncoprotein targeting p53) (Desaintes et al., 1999). Another study showed by the examination of chromatin condensation by epifluorescence microscopy that the expression of E2 in several HPV-transformed and non-transformed cells induced apoptosis (Webster et al., 2000). Resulting apoptosis was shown to be through p53-dependent mechanisms due to the fact that co-expression of E2 and a mutant form of p53 or expression of E2 in cell lines containing non-functional or mutated p53 such as C33A did not appear to induce apoptosis (Webster et al., 2000). Therapeutic potential of E2 was also evaluated using a fusion protein expressed in *E. coli* containing VP22 (a protein from herpes simplex virus-1 [HSV-1] that can be transferred by mammalian cells) and a mutant E2 (E2p53m) which cannot bind p53 as efficiently as wild-type (Green et al., 2007). This fusion protein was shown by terminal deoxynucleotidyl transferase dUTP nick end labelling (TUNEL) assays to induce apoptosis in HPV transformed but not non-HPV transformed cells, providing cell type specificity for possible therapeutic applications (Green et al., 2007). The effects of E2 in transcription levels were also investigated. It was shown by northern blotting against E6 and E7 mRNAs that upon introduction of an E2 expression vector into HeLa cells, the transcription of E6 and E7 was suppressed, leading to apoptosis (Goodwin and DiMaio, 2000). These studies have supported the hypothesis that continuous expression of E6 and E7 is required for cancer cells to maintain their transformed phenotype (Goodwin and DiMaio, 2000, Wells et al., 2000).

The expression of E6 and E7 in the upper epithelial layers allows the infected cell to re-enter S phase, and subsequently virus copy-number increases. Differentiation signals allow the epithelial cell where genome amplification occurs to express several differentiation markers such as keratins 1 and 10 (cutaneous epithelia) or 4 and 13 (mucosa) in addition to the expression of markers involved in cell cycle entry, such as mini chromosome maintenance complex (MCM), Ki-67 (a cellular marker for proliferation), proliferating cell nuclear antigen (PCNA), Cyclin E and Cyclin A.

In addition to E1 and E2, E4 and E5 expressions also contributes genome amplification and virus release. The E4 from HPV is expressed as a fusion (E1^E4) with the first 5 amino acids of E1 (Longworth and Laimins, 2004). This is because E4 does not have an AUG start codon and uses E1 sequence for the initiation of translation (Longworth and Laimins, 2004). The high-risk E1^E4 proteins alters the cytoskeleton network associating with keratin intermediate filaments in the host cells (Doorbar et al., 1991). In the case of overexpression of this fusion protein in transient-transfection assays, cells start to collapse, facilitating the virus release. However, during the natural course of infection, the amount of collapse is limited. High-risk HPV

E4 can also associate with an RNA helicase, E4-DBD, involved in mRNA splicing, transport and translation initiation and acts as a regulator of gene expression (Yoshioka et al., 2000). Another study showed that overexpression of HPV11 and 16 E1^E4 in various cell types induced cell cycle arrest in the G2 phase (Davy et al., 2002). This can counteract the effects of E7 oncoprotein, a known facilitator of the S-phase entry. E5 is a hydrophobic transmembrane protein shown to have pore-forming capability (Krawczyk et al., 2010, Wetherill et al., 2012). E5 oncoprotein can interfere with the intracellular trafficking of endocytotic vesicles (Thomsen et al., 2000). E5 can contribute to genome amplification indirectly via its ability to stabilise epidermal growth factor (EGF) receptor (EGFR) and enhance EGF signalling and mitogen-activated protein (MAP) kinase activity (Doorbar et al., 2012). E5 was also observed by flow cytometry staining of E5 expressing cells to downregulate the major histocompatibility complex (MHC) class I molecules, playing another role in immune evasion (Campo et al., 2010).

The completion of virus cycle involves the expressions of major and minor capsid proteins L1 and L2, respectively from the late promoter p670 in HPV16. Cryoelectron microscopy and image reconstruction analysis showed that HPV16 particles contain 360 molecules of L1 arranged into 72 pentameric capsomeres, and each capsomer was observed to be associated with a single L2 protein (Buck et al., 2008). The ability of L1 to self-assemble to produce virus-like particles helped to the development of vaccines for HPV (see section 1.2.6). Virus maturation occurs on the most upper layers of epithelium where cells are dying. The changes in the cellular environment (converting from a reducing to an oxidising environment) enables to production of extremely stable and infectious viruses through disulphide linkage of L1 proteins. Although L1 and L2 capsid proteins are highly immunogenic, their detection by immune system is difficult due to the fact that their expression is only activated on the upper layer of cells where the immune surveillance is very limited (Badaracco et al., 2002).

Replication cycle of the virus, from the infection to the virus release, takes around ~3 weeks (Stanley et al., 2007). From infection to the appearance of lesions can take even longer from weeks to months. Histological detection of cervical and other ano-genital cancers shows intra-epithelial abnormalities, CIN (cervical intraepithelial neoplasia). These abnormalities ranges from low-grade (CIN 1), moderate (CIN 2) and high-grade (CIN 3). High- grade lesions (CIN 3) is followed by cervical cancer. Around 90% of these lesions were found to contain high-risk HPV (HPV16 mostly and 18) DNAs (Clifford et al., 2006).

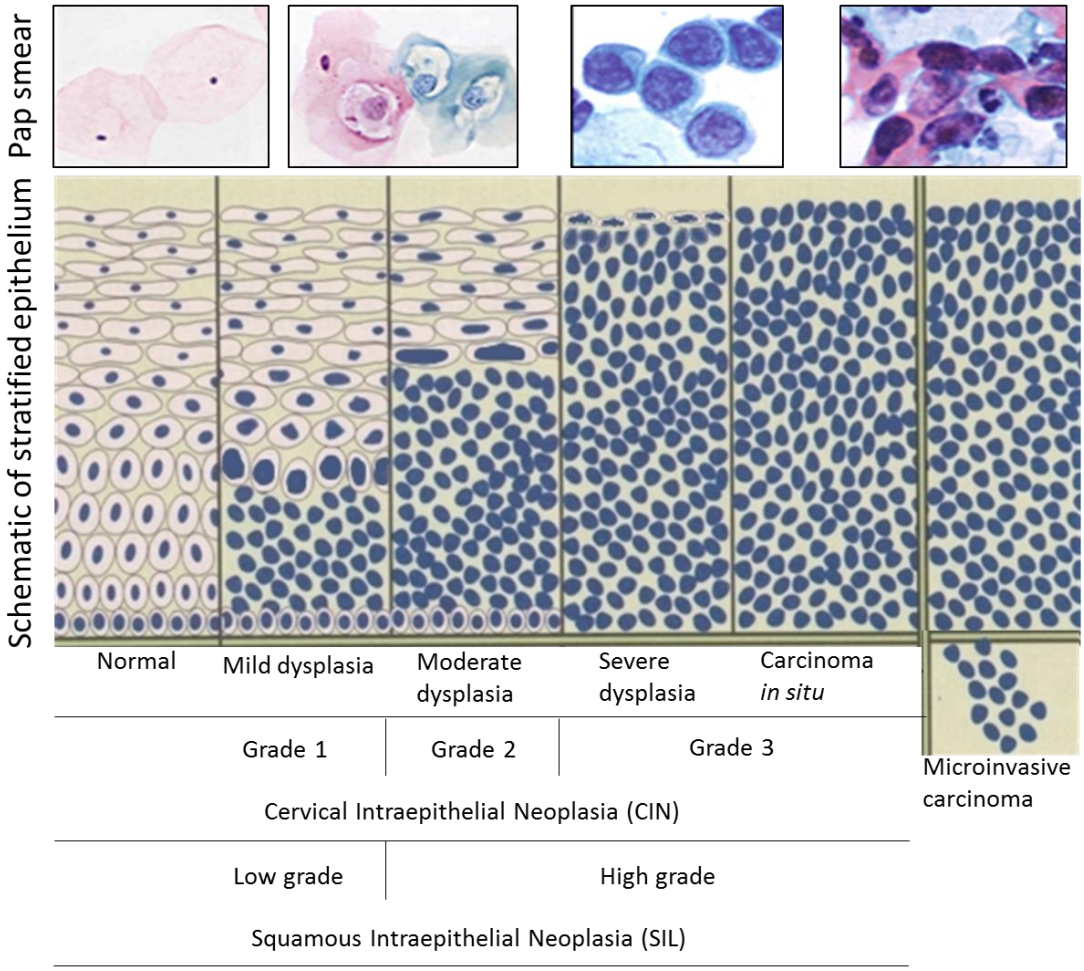

Figure 1.3 Classification of cervical cancer with a representative schematic and Pap smear images. WHO terminology classifies cervical cancer as mild, moderate and severe dysplasia, carcinoma *in situ*, microinvasive squamous carcinoma, invasive squamous carcinoma. Whereas the classification of the Bethesda system is either low grade (LG) or high grade (HG) squamous intraepithelial lesions (SIL) based on the cytological abnormalities reported in a Pap smear. LG-SIL and HG-SIL indicate mild and moderate/severe dysplasia, respectively. If an abnormal cytology is observed, it will be followed by a colposcopy and/or biopsy, if necessary. Histopathological observations lead to classify biopsied lesions based on their location and severity as cervical intraepithelial lesions (CIN1, CIN2 and CIN3), carcinoma *in situ* and invasive carcinoma (Hellner and Munger, 2011). Schematic of infected epithelium and Pap smear images are modified from www.eurocytology.eu and (Martha Lucía et al., 2012).

Figure 1.3 shows the different methods used for classification of cervical cancer. HPV can still complete its life cycle in CIN 1 category lesions and can cause the appearance of flat warts. The increase in E6 and E7 expression during high-risk HPV infection can result in the development of CIN 2+ where cell starts to accumulate

mutations, contributing to cancer progression. CIN 2 and CIN 3+ lesion can also facilitate the integration of viral episome in to the host genome. It was suggested that here are common fragile sites in the host genome where the integration event occurs (Thorland et al., 2003). Integration can often cause the disruption of some of the early genes, E1 and E2 with regulatory functions from the LCR region (Yu et al., 2005). E2 is the key transcription factor that regulates E6 and E7 expression. With the loss of E1 and E2 expression upon integration, cells start to aberrantly express E6 and E7 oncogenes and to accumulate genetic mutations leading to cancer. Malignant progression is often correlated with insertion of the viral genome into the host genome. Around 70% of HPV16 positive cervical cancers contains integrated HPV genome, whereas the genome of HPV18 is almost always found to be integrated to the host genome (Doorbar et al., 2012).

1.2.4.1 E6 oncogene

E6 is a relatively small protein with around ~150 amino acids and expressed in two forms; a full-length form of around ~16 kDa and a smaller form (~8 kDa) containing the N-terminal region only (Garnett and Duerksen-Hughes, 2006). E6 contains two CXXC-X_{29}-CXXC zinc binding domains (C, cysteine; X, any amino acid). The first structural data of the entire HPV16 E6 protein including the structures of these zinc-binding domains as well as a model structure of the N-terminal domain homodimer was obtained by high-resolution NMR spectroscopy (Zanier et al., 2012). Mutagenesis of N-terminal homodimer increased the solubility of E6 (Zanier et al., 2012). The oncoprotein plays an important role in immortalisation of human keratinocytes together with the E7 oncoprotein. One of the major targets of E6 is the tumour suppressor p53. In healthy cells, aberrant cell proliferation results in e.g. DNA damage, p53 level increases which induces the expression of cell cycle control proteins such as cyclin kinase inhibitor, p21. This process leads to cell cycle arrest or apoptosis. The E6 protein interacts with E6-associated protein (E6AP), a ubiquitin ligase, (Huibregtse et al., 1991) causing the degradation of p53 by the 26S proteasome, reducing the half-life of p53 from a few hours to around 20 minutes in keratinocytes (Hubbert et al., 1992, Huibregtse et al., 1993). E6 is also involved in down-regulation of p53 through its association with a p53 co-activator, p300/CBP4 (Zimmermann et al., 1999). Interaction of E6 with other proteins such as PDZ proteins is also important for its immortalising activity. PDZ protein can localise at cell-cell adhesion in epithelial cells. High-risk HPV E6 proteins associates with certain cellular proteins with a PSD95/Dlg/ZO-1 (PDZ) domain. These cellular proteins include human homologues of *Drosophila melanogaster* disc large (hDlg) and scribble tumour

suppressors (hScrib), post-synaptic density protein 95 (PSD95), multiple PDZ domain-containing protein 1 (MUPP1) via formation of complexes with E6AP and E6 targets them for proteasomal degradation (Longworth and Laimins, 2004). High risk E6 protein can bind members of this family proteins through the C-terminus and mediate their degradation. This interaction seems to be important. Since, the use transgenic mice expressing E6 with no PDZ binding domain resulted in a decrease in the proliferation of cells although p53 was still being inactivated (Nguyen et al., 2003).

E6 oncoprotein can interact with myc and Sp-1 and subsequently induce the expression of the catalytic subunit of telomerase, hTERT (human telomerase reverse transcriptase) (Oh et al., 2001). Telomerase is an enzyme containing four subunits, which incorporates hexamer repeats to the telomeric regions of chromosomes. Telomeric ends are shortened following repeated cell divisions due to the absence of telomerase activity, resulting in cell death. Other interacting partners of E6 include interferon regulatory factor-3 (IRF-3), E6 targeted protein-1 (E6TP1) and alternation/deficiency in activation-3 (ADA3) involved in DNA replication, Bak, c-Myc, tumour necrosis factor (TNF) receptor 1 involved in apoptosis and immune evasion, membrane-associated guanylate kinase (MAGI 1-3) involved in cell-cell adhesion (Longworth and Laimins, 2004).

1.2.4.2 E7 oncogene

HPV E7 is a highly phosphorylated and acidic polypeptide with approximately 100 amino acid residues. E7 shares sequence similarities with the adenovirus (Ad) E1A protein and the simian vacuolating virus 40 (SV40) large tumour (Large T) antigen (McLaughlin-Drubin and Munger, 2009), in particular, in a conserved protein motif, LXCXE (L, leucine; C, cysteine; E, glutamate; X, any amino acid) which is required for the physical interaction with pRb. A variety of cellular proteins contain the LXCXE (or closely related) motifs, including cyclinD1 (Brehm et al., 1998, Ewen et al., 1993), histone deacetylase (HDAC) 1-2 (Brehm et al., 1998, Chan et al., 2001) and BRG1 (Dunaief et al., 1994). The E7 phosphoprotein has two conserved regions: CR1 (amino acids 2-15), CR2 (amino acids 16-38) and the carboxyl terminal region containing a zinc finger domain (amino acids 39-98) (Figure 1.4).

CR1 and CR2 domains are conserved between HPV E7 proteins from different types and connected to each other through non-conserved sequences. The carboxyl terminal contains a conserved zinc binding site with two C-X-X-C motifs separated by around ~29 amino acid residues. The E6 oncoprotein also consists of these zinc binding sequences in common with E7 (Section 1.2.4.1), suggesting that E6 and E7

might have evolved from the same ancestors. The 3-dimensional (3D) structures of entire HPV45 E7 and C-terminal domain of HPV45 has been demonstrated by nuclear magnetic resonance spectroscopy (NMR) and X-ray crystallography, respectively (Liu et al., 2006, Ohlenschlager et al., 2006). This study indicated that the N-terminus is intrinsically disordered while the C-terminus is highly structured with zinc binding pocket involved in dimerisation. E7 was shown to be in dimeric forms when expressed in a recombinant system e.g. in *Escherichia coli* by gel filtration column (size-exclusion chromatography [SEC]) and non-denaturing acrylamide gel electrophoresis of purified E7 (McIntyre et al., 1993). Although E7 was reported to form tetramers (Clements et al., 2000) and higher order oligomers (Alonso et al., 2004) by sedimentation equilibrium experiments, an analytical ultracentrifugation (AUC) method, E7 dimers were suggested as being the dominant forms (Clements et al., 2000).

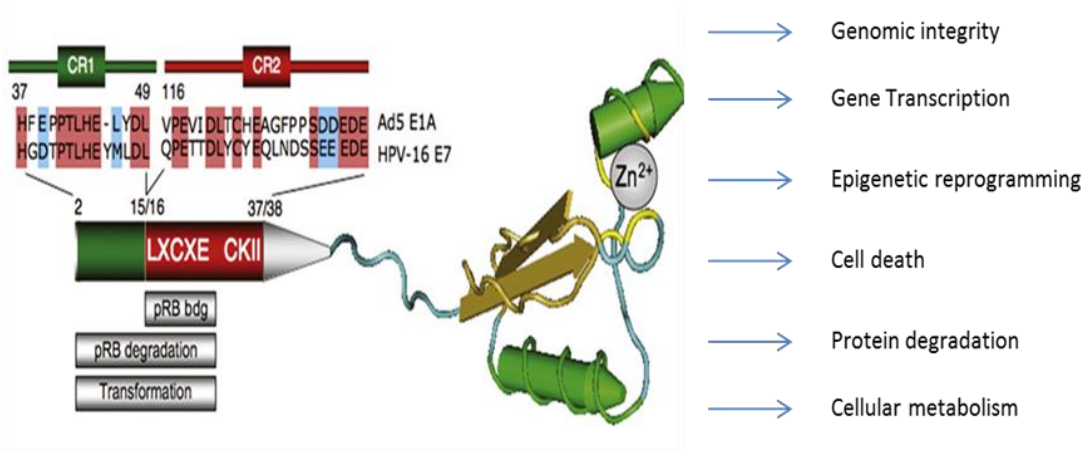

Figure 1.4 A representative schematic of HPV16 E7 oncoprotein with the cellular processes interfered. The amino terminus of HPV16 E7 is unstructured with 37 amino acids and contains two major domains, CR1 (green) and CR2 (red). These domains share a sequence similarity with Ad5 E1A protein (blue-identical and light red-chemically similar residues). CR2 domain contains pRb binding site, LXCXE motif, which is required for pRb degradation and subsequent cellular transformation. CR1 is also required for pRB binding. CR2 contains also a casein kinase 2 phosphorylation site (CKII) downstream of LXCXE, which is conserved in SV40 T, Ad E1A and other alpha virus HPV E7 (Barbosa et al., 1990). The X-ray crystallography structure of the carboxyl terminus HPV45 E7 was solved and included here (Ohlenschlager et al., 2006). This region contains two zinc binding cysteine motifs (Cys-X-X-Cys) (yellow). The list of cellular processes disrupted by E7 was placed on the right hand side of the figure. Figure was adapted from (McLaughlin-Drubin and Munger, 2009).

The predicted molecular weight of HPV16 E7 is ~11 kDa (Smotkin and Wettstein, 1987). However, it migrates on SDS polyacrylamide gels with a molecular size of ~17 kDa (Armstrong and Roman, 1993), possibly due to the high content of acidic, negatively charged amino acid residues. When the negative charges were neutralised through incorporation of 1-Ethyl-3-[3-dimethyl-aminopropyl] carbodiimide (EDC) to free carboxyl groups, HPV16 E7 was observed to migrate with its predicted molecular size (11 kDa) (Armstrong and Roman, 1993). The amino terminal CR1 domain is suggested to mediate the aberrant migration of E7 on SDS polyacrylamide gels (Munger et al., 1991). There are antibodies for the detection of HPV16 E7 some of which was used here (see Section 2.3). Another method commonly used for E7 detection is epitope tagging. Fusing epitopes to the amino terminus of HPV16 E7 might affect the stability and interaction of E7 with cellular proteins (Huh et al., 2005, Reinstein et al., 2000). This can also affect the transforming ability of E7 oncoprotein. However, tagging the C-terminus did not seem to alter the functions of E7 (Huh et al., 2005). HPV16 E7 is known to accumulate in the cytoplasm in addition to nuclear and nucleolar localisation. The half-life of E7 was shown to be around ~2 hrs (Smotkin and Wettstein, 1987) and the degradation of E7 occurs through a ubiquitin-mediated proteasomal mechanism following the conjugation of ubiquitin to the amino terminus of E7 (Reinstein et al., 2000). Ubch7 (UBE2L3) and a Cullin 1/Skp2-containing E3 ubiquitin ligase were also reported as involved in the ubiquitination of HPV16 E7 (Oh et al., 2004). Low risk- HPV6 and 11 was shown to be ubiquitinated similar to the high risk HPV16 and 18 using oestrogen-receptor (ER) tagged HPV E7 proteins (Roman and Munger, 2013). This study, however, showed that E7 from these low risk types had a longer half-life than HPV16 and 18**.**

HPV16 E7 possess a consensus phosphorylation site for casein kinase 2 (CK2) in the CR2 domain (Firzlaff et al., 1989). Phosphorylation occurs on serine residues (Smotkin and Wettstein, 1987). CK2, a serine/threonine-selective protein kinase involved mainly in cell cycle control and DNA repair pathways, was shown to phosphorylate HPV18 E7 two and four times faster when compared to HPV16 E7 and HPV6 E7, respectively (Barbosa et al., 1990). There is a cellular complex expressed in normal keratinocytes with inhibitory function on CK2, macrophage-inhibitory related factor protein (MRP) 8 and 14 (Tugizov et al., 2005). The expression of this complex was abolished in HPV-immortalised human keratinocytes with an accompanying rise in CK2 activity (Tugizov et al., 2005). The detection of three different isoforms of HPV16 E7, E7a1 (17.5 kDa), E7a (17 kDa) and E7b (16 kDa), showing different cellular localisation properties is possibly suggesting the presence of other post-

translational modifications (Valdovinos-Torres et al., 2008). In fact, HPV18, but not HPV16 E7, contains glutamine residues (position 87 or 88) that can be polyaminated by transglutaminase 2 (TGase 2), a family of enzymes involved in the catalysis of protein modification via the incorporation of polyamines in to substrate molecules, in the zinc binding region (Jeon et al., 2003). This post-translational modification of HPV18 E7 was reported to reduce its pRb binding. The inability of TGase 2 to associate and destabilise HPV16 E7 may be one of the explanation of the high prevalence of HPV16 over HPV18 in cervical cancer.

The major functions of E7 ensure that DNA synthesis phase of differentiated cells are retained and the viral genome is maintained in undifferentiated cells. E7 interferes with various cellular processes e.g. cell cycle entry and apoptosis in order to allow the virus to complete its life cycle. In order to study virus life cycle, monolayer human primary keratinocytes can be induced to differentiate with calcium and methylcellulose. Another method can be the use of *in vitro* engineered organotypic skin rafts. To produce these skin-like structures, keratinocytes are grown at the air-liquid interface on an artificial dermis. The resulting system has the key features of differentiating epithelia, allowing amplification of the viral genome, expression of late genes and generation of new virus in the upper differentiated layer. Such system adopted previously to study the effects of a mutation in the E6 protein kinase A (PKA) recognition motif of HPV18 genome on the virus life cycle (Delury et al., 2013). The phosphorylation of the E6 PDZ-binding motif (PBM) by PKA negatively regulates the interaction between high-risk E6 protein and their targets containing PDZ domains.

pRb is a tumour suppressor protein involved in cell cycle control. Defects in pRb can be seen in most cancer types. pRb regulates the transition from the G1 to the S phase of cell cycle by inhibiting the E2F family proteins: These are transcription factors and include E2F1, 2, 3a, 3b, 4, 5, 6, 7a, 7b and 8, upregulating the expression of genes involved in the S-phase entry. E2F1-6 can form heterodimer with proteins from a related family, DP factors. Hyphophosphorylated pRb binds and inhibits the activity of E2F1-3/DP complexes to control the entry to the S-phase (Dyson, 1998). Following the phosphorylation of pRb by cdk4 and/or cdk6/cyclin D complexes in the G1, E2F1-3/DP-pRb complex is disrupted and dissociated E2Fs can subsequently activate the transcription of genes required for S-phase entry including cyclin dependent kinase 2 (cdk2), cyclin A and E and DNA polymerase α. Overexpression of E7 has been reported to cause an increase in pRb-E2F1 complexes resulting in the rise of free E2F levels (Chellappan et al., 1992, Wu et al., 1993).

HDACs are transcriptional co-repressors and responsible for inducing chromatin remodelling with acetyl modifications of lysine residues on histones. Histone acetylation is responsible for weakening the interaction between histone N-terminal region and genomic DNA, opening up the chromatin structure which helps activating transcription factors to access to DNA. In normal cells, pRb forms a complex with HDAC and associates with the E2F transcription factor in the G1-phase (Garnett and Duerksen-Hughes, 2006). This causes the repression of E2F-inducible promoters, preventing the activation of genes necessary for proliferation. E7 protein can also bind HDAC (independently of its binding to retinoblastoma protein) (Brehm et al., 1999). This binding results in the release of the repression on the E2F regulated promoters and subsequent activation of E2F-inducible genes, which facilitates the S-phase entry and thus cell proliferation.

The interaction of HPV E7 with the pRb through the conserved LXCXE sequence motif within the CR2 domain was reported using co-immunoprecipitation (co-IP) assays (Dyson et al., 1989, Munger et al., 1989). The SV40 Tag and the Ad E1A proteins were shown by mutational studies to target pRB family proteins through LXCXE motifs and retain cells in the S-phase (DeCaprio et al., 1988, Whyte et al., 1988). High-risk HPV E7 protein binds pRB with an approximately 10-fold greater efficiency than low-risk HPV E7 protein. This difference was suggested to result from a single amino acid residue present in high-risk but not low-risk HPVs upstream the LXCXE motif (e.g. aspartate 21 in HPV16 E7 and glycine 22 in HPV 22 E7) (Barbosa et al., 1990, Heck et al., 1992). The HPV16 E7 protein binds hypophosphorylated form of pRb (Dyson et al., 1992) and targets this for degradation through interaction with a cullin 2 containing ubiquitin ligase complex (Huh et al., 2007). Degradation of pRb (caused by HPV E7) was studied using 26S proteasome inhibitor, MG132 (see section 4.1.2) and reported to be via proteasomal pathways (on a phosphorylation-dependent manner) (Boyer et al., 1996, Gonzalez et al., 2001). Since, treatment with MG132 resulted in the recovery of pRb levels in E7 expressing cells.

Crystal structure analysis showed that E7 interacts with pRb through a highly conserved groove on the β-box, also known as pocket domain where E2F/DP interaction takes place through a nine amino acid residue region containing LXCXE (Xiao et al., 2003). The role of high risk HPV E7 in pRb degradation is very important for transformation of infected cells. HPV E7 can activate cdk2 through interaction with cyclin E, cyclin A and cdk inhibitors (CKIs) including $p21^{CIP1}$ and $p27^{KIP1}$. These interactions can alter cell cycle regulation and result in the blockage of the responses

against anti-proliferative signals such as growth factor receptor withdrawal, activation of p53 and loss of cellular adhesion (McLaughlin-Drubin and Munger, 2009).

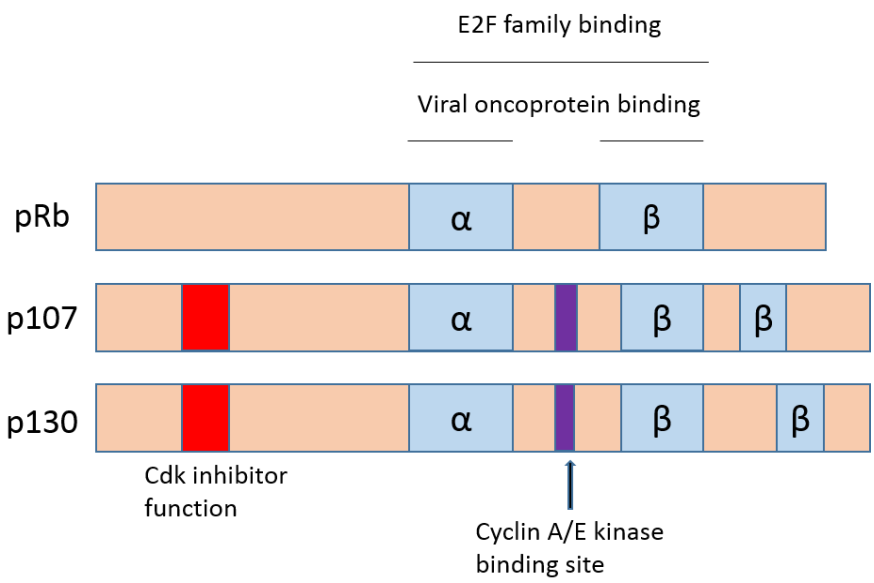

Figure 1.5 A schematic of pRb family proteins, pRb, p107 and p130 with homology domains. pRb family of pocket proteins shows a sequence homology in the C-terminal region. This region consists of α and β domains separated by a spacer region. p107 and p130 contains an additional β domains in addition to a cyclin A/Cdk2 and cyclin E/Cdk4 binding sites in between α and β domains. P107 and p130 also possess a region with Cdk inhibitor function in the amino terminus.

Other targets of HPV E7 includes pRb family proteins, p107 and p130. pRb family proteins show a sequence homology in the C-terminal or pocket region. The pocket region of all pRb family members consists of α and β sub-domains which are separated by a spacer region. p107 and p130 proteins include an additional region where the association with cyclin A/Cdk2 and Cyclin E/Cdk4 occurs (Figure 1.5).

Pocket proteins, pRb, p107 and p130 are involved in cell cycle control through their association with E2F1-3, E2F4 or E2F4-5, respectively (Classon and Dyson, 2001). E2F1-3 are transcriptional activators involved in DNA synthesis and S-phase entry, whereas E2F4-5 are transcriptional repressors which promotes cell cycle exit/growth arrest. p130 is expressed to function as a transcriptional regulator during G0/G1-phase transition (p130 localises in the nucleus during G0/G1 and is transported to the cytoplasm during S-phase for degradation by the 26S proteosome after being targeted through a ubiquitin ligase complex (E3) called SCF complexes (Barrow-Laing et al., 2010, Deshaies, 1999, Tedesco et al., 2002)), whereas p107 is expressed during G1/S-phase transition and in the G2-phase. The interaction of HPV16 E7 with

p107 and p130 results in the inhibition of the transcriptional repression of E2F4-5 promoters, leading to the disruption of pRB/E2F1-3 complexes. This will cause consequent expression of transcription factors as mentioned above.

HPV E7 binds many other proteins besides pRb family proteins and cell cycle control proteins mentioned above. This includes proteins involved in transcription regulation e.g. TATA box-binding protein (TBP) and the activator protein-1 (AP1) transcription factors, and other proteins with different functions e.g. TATA-binding protein-associated factor-110 (TAF-110), S4 ATPase of 26 proteaseome, interferon (IFN) regulatory factor-1 (IRF-1), Insulin-like growth factor binding protein-3 (IGFBP-3), protein phosphatase 2A (PP2A) and pyruvate kinase isoenzyme type M2 (M2-PK). Interaction partners of E7 along with a list of cellular processes affected were reviewed previously (Roman and Munger, 2013). The presence of various E7 interaction partners can be due to the highly unstructured amino terminus domain proving a flexibility to the E7 protein to associate with a variety of cellular proteins and even other viral proteins such as HPV E2 and Adeno-associated virus (AAV) Rep78 protein (Gammoh et al., 2006, Hermonat et al., 2000, Wang et al., 2012). Alternative explanation of possessing a large list of interaction partners can be the ability of E7 to alter its conformation for optimal target binding. For example, the E7 dimer can undergo a conformational change when subjected to small changes in the pH (from pH 7 to pH 5), increasing the solvent accessibility to hydrophobic surfaces (Alonso et al., 2002).

Apart from the functions of E7 explained above in cell proliferation and virus replication, E7 is also involved in apoptosis. By looking at some studies, anti-apoptotic actions of E7 can be suggested to be both direct and indirect. E7 was shown to upregulate the transcription of cellular inhibitor of apoptosis (c-IAP2), a protein involved in apoptosis inhibition, by c-IAP2 promoter-controlled luciferase reporter assays and to inhibit tumour necrosis factor (TNF)-mediated apoptosis by caspase activity assays and *in situ* terminal deoxynucleotidyl transferase-mediated dUTP nick-end labeling (TUNEL) analysis (which measures DNA fragmentation as a result of apoptosis) in keratinocytes (Yuan et al., 2005). Another study demonstrated a delay in Fas-mediated apoptosis and the inhibition of TNF-mediated apoptosis, based on the identification of apoptotic nuclei by bisbenzimide (Hoechst) staining by fluorescence microscopy, through a mechanism which involves the suppression of caspase-8 activation (analysed by caspase activity assays) (Thompson et al., 2001). E7 can also have a pro-apoptotic function. For example, E7 makes mouse lymphoma cells (JD3) more sensitive to IFN-alpha induced apoptosis (Thyrell et al., 2005) while

overexpression of E7 in genital keratinocytes can make cells sensitive to TNF-mediated apoptosis (Stoppler et al., 1998).

1.2.5 Inhibitory molecules targeting E6 and E7

The current strategies for the treatment of HPV related diseases are primarily anti-cancer, not anti-viral. In addition to surgical removal of affected lesions, cytotoxic agents such as podophyllin and trichloroacetic acid, 5-fluorouracil and arsenic trioxide (As_2O_3), photodynamic therapy (PDT) and immunotherapy (interferons) are available as anti-cancer treatment. However, there are propspective HPV-specific treatments including therapeutic vaccines, immunotherapies, RNA interference-based therapies and anti-virals. Some antivirals such as acyclic nucleoside phosphonate (ANP) and Cidofovir [(S)-1-[3-hydroxy-2-phosphonyl methoxy propyl] cytosine 'HPMPC'] reported to inhibit the proliferation of HPV-positive cells (Andrei et al., 1998, Johnson and Gangemi, 2000). The latter was shown to downregulate E6 and E7 mRNA levels with an accompanying increase in p53 and pRb, which radiosensitise HPV-positive cells as well as tumours in mice xenografts (Abdulkarim et al., 2002). The abundant expression of E6 and E7 in cervical cancer led to the development of inhibitory molecules against these proteins. Some of them are aptamers that will be mentioned in section 1.3.5.1. Apart from aptamers, siRNAs, single chain antibody fragments (scFV) and E6/E7 therapeutic vaccines have been studied. RNA interference technology has been used to target HPV E6 and E7 mRNA expression, preferably without disturbing the cellular RNA pool. siRNAs specific to E6/E7 mRNA was shown to inhibit cellular growth in HPV16 and HPV18 positive cervical cancer cell and induced apoptosis via p53-dependent mechanisms (Zhou et al., 2012, Hall and Alexander, 2003, Jiang and Milner, 2002). An *in vivo* xenograft study showed that intratumoural injection of siRNAs resulted in the regression of the tumour in mice (Chang et al., 2010). The functions of these oncoproteins can also be targeted by specific single-chain antibodies (scFV) expressed as intracellular antibodies (intrabodies). The successful expression (in endoplasmic reticulum) and anti-proliferative effects of an MS2D intrabody specific for HPV16 E7 was shown previously (Accardi et al., 2011). MS2D inhibited the tumour growth when introduced by a retroviral vector into mice models (Accardi et al., 2014). Therapeutic HPV vaccines have been developed against HPV16 viral oncogenes E6 and E7 as peptide/protein-based or DNA-based vaccines. Aim of these vaccines is to enhance T-cell immune response using e.g. a viral vector, a recombinant DNA or peptides/proteins derived from HPV oncoproteins. There is an ongoing phase II clinical trial testing the safety of a therapeutic HPV vaccine (e.g. the ProCervix, trial

number NCT01957878). ProCervix contains recombinant adenylate cyclase (CyaA) proteins, CyaA-HPV16 E7 and CyaA-HPV18 E7 in a 1:1 ratio and is being administered to the injection sites by Aldara™, a topical cream containing 5% of imiquimod (an immune modulator), as a vaccine adjuvant. An example of a therapeutic DNA vaccine for HPV is pNGVL4a-Sig/E7(detox)-HSP70, which aims to target HPV16 E7. This vaccine contained a mutated non-functional E7 (detox) recombinant that was unable to interact with pRb. E7 (detox) was linked to a heat shock protein, HSP70 (in order to enhance uptake by antigen presenting cells [APC] and MHC class I processing] and a signal sequence (for vaccine to target active APC) (Trimble et al., 2009). This vaccine is currently in a Phase I clinical trial in combination with imiquimod (trial number NCT00788164). There are also studies on E6 vaccines e.g. an HPV16 E6 related peptide can be promising for vaccine development (Dochez et al., 2014).

1.2.6 HPV vaccination

Current prophylactic vaccines were generated using recombinant technology based on the production of HPV L1 (major capsid protein). Since, HPV is very difficult to culture in addition to the presence of three potent oncogenes (E5, E6 and E7). Therefore, the production of an inactivated HPV vaccine would have been difficult and its human use would be unsafe. In order to express large amounts of L1 protein for vaccine production, L1 gene was inserted into a host i.e. baculovirus and yeast. These L1 proteins produced virus-like particles, resembling HPV virion in size and shape. However, they did not contain viral DNA, therefore did not cause infection or cancer, although they are highly immunogenic and protective due to the presence of neutralising serum antibodies (Dochez et al., 2014). These antibodies can coat virions, preventing their binding to cell surfaces (Dochez et al., 2014). Currently, there are two prophylactic vaccines available: Cervarix™ and Gardasil™. The bivalent vaccine, Cervarix™ was expressed in a baculovirus expression system and contained HPV16 (20 µg) and 18 (20 µg) VLP antigens in combined with an adjuvant, ASO4 (in order to enhance the immune response) and 3-*O*-desacyl-4 monophosphoryl lipid A and aluminium salt. The quadrivalent vaccine, Gardasil™ was produced using yeast substrate and contained HPV16 (40 µg) and 18 (20 µg), as well as low-risk HPV6 (20 µg) and 11 (40 µg) in combined with amorphous aluminium hydroxyl-phosphate sulphate as an adjuvant. Both vaccines can be administered by intramuscular injections in three doses; 0, 1 and 6 months for bivalent vaccine and 0, 2, and 6 months for quadrivalent vaccine. Upon 3-dose vaccination, highest immune response was observed in girls aged 9-15 years, and high antibody titres maintained for at least

8.4 years for the bivalent vaccine with 100% seropositivity and at least 5 years for the quadrivalent vaccine with around ~98% seropositivity (Romanowski, 2011). Both vaccines showed some cross-protection against non-vaccine HPV types. The quadrivalent vaccine was shown to cross-protect against HPV31, while the bivalent vaccine was cross-protecting against HPV31, 33 and 45. This was possible owing to phylogenetic similarities between L1 genes among HPV types. For example, HPV16 is phylogenetically related to HPV31, 33, 52 and 58, whereas HPV18 is related to HPV45 (Kemp et al., 2011, Malagon et al., 2012). One concern with the HPV vaccination is the type replacement. Although, HPV DNA is very stable, preventing escape mutations and generation of new HPV types (Dillner et al., 2011, Tota et al., 2013). There might be a strong natural competition between HPV types which cannot be compensated by vaccine cross-protection as mentioned above. It was shown by a study performed in the USA that while the prevalence of HPV vaccine types decreased in both vaccinated (by 31.8%) and non-vaccinated (by 30.2%) individuals, that of non-vaccine types increased by 14% for all individuals (Kahn et al., 2012). However, the risk of developing cancer caused by HPV16 or 18 is much greater than that by other HPV types (Tota et al., 2013).

There is another HPV vaccine, nine-valent, which is undergoing clinical trials (trial number NCT00943722). Current quadrivalent HPV vaccine (containing HPV6, 11, 16 and 18 antigens) is suggested to protect against around 70% of all SCC cases, whereas this nine-valent vaccine is estimated by mathematical modelling to protect against 90% of all SCC worldwide. Since, the nine-valent vaccine (V503) contains some other high-risk types, HPV31, 33, 45, 52 and 58 VLPs, in addition to the quadrivalent vaccine types (Serrano et al., 2012). Since, women face cervical cancer, but not men, HPV studies and HPV vaccination are focussed on women. However, HPV-related cancers can also be developed at other sites in men due to the fact that high-risk HPVs can cause around ~90%, ~40%, ~12% and ~3% of anal, penile, oropharyngeal and oral cancers, respectively (WHO, 2014). Therefore, vaccination of males might help to the prevention of these HPV-related cancers. In addition, vaccination of men was suggested to aid the protection of women through herd immunity (Angelo et al., 2014). However, the reduction of the cervical cancer rates through vaccination of men resulting in herd immunity could not be comparable to that through broad vaccination of women (Einstein et al., 2009).

Human papillomaviruses contains mainly L1 in addition to smaller quantities of L2 as capsid proteins. L1 protein is highly abundant and strongly stimulates B cells. Contrarily, L2 protein is almost invisible for the immune system. Once virus binds to

the basement membrane, conformational changes occurs and L2 protein becomes more exposed. However, this is still not enough for the induction of an anti-L2 neutralising antibody response. A small proportion of the L2 capsid protein, especially between amino acid 20 and 38, is highly conserved amongst various high-risk HPV types and several antibodies against this region can neutralise the activities of various papillomaviruses (Karanam et al., 2009). Although poor immunogenicity of L2 antigens makes them unsuitable candidates for vaccine development, recent studies conducted in mice using bacteriophage (*Lactobacillus casei*) VLPs expressing L2 on their surface were promising (Yoon et al., 2012). Oral administration of this vaccine candidate triggered the production of IgA, providing a moderate vaginal mucosal immunity for at least early phases of the viral infection.

1.3 Nucleic acid molecules as molecular tools

Aptamers, antisense oligonucleotides (ASOs), siRNAs and ribozymes each have therapeutic potentials. The sequence of an antisense oligonucleotide is complementary to a specific mRNA target, and binding the target results in the degradation of mRNA or inhibition of translation. siRNAs are short synthetic double-stranded RNA molecules, leading to the degradation of mRNA target upon binding. Ribozymes (catalytic RNAs) are used for site-specific cleavage of target RNA or site-specific RNA *trans*-splicing i.e. repair of mutant mRNA molecules causing a genetic disease. Antisense oligonucleotides, ribozymes and siRNAs act to inhibit the protein expression at the mRNA level through traditional hydrogen bond interactions. Aptamers accomplish tight and specific binding to the target ligand taking advantage of their three-dimensional (3D) structures. Upon binding, aptamer can become encapsulated by the ligand which subsequently becomes a part of the aptamer`s intrinsic structure (Huang et al., 2003). Aptamers were used as therapeutic agents for the first time in 1990 for a study in which overexpression of TAR (a regulatory RNA element in the HIV-1 required for *trans*-activation of viral promoter and for viral replication)-containing sequences (TAR decoys) inhibited human immunodeficiency virus type 1 (HIV-1) replication in CEM-SS cells (a human CD4 positive T-cell line) (Sullenger et al., 1990). Since then, aptamer studies have raised a considerable interest. As far as our knowledge, there are three nucleic acid molecules approved by Food and Drug Administration (FDA) to date. Two of those are antisense oligonucleotides (ASO), Fomivirsen (Vitravene®) and Mipomersen (Kynamro®) approved by FDA in 1998 and 2013, respectively. Fomivirsen is a 21-nucleotide phosphorothioate oligonucleotide which is complementary to the mRNA for the major immediate-early region proteins of human cytomegalovirus (CMV). The injection of

fomivirsen into a human eye can result in the inhibition of CMV retinitis. This is an inflammation of the retina of the eye that can lead to blindness. Mipomersen is a 20-nucleotide second-generation synthetic phosphorothioate oligonucleotide (see section 1.3.3.1) with 2'-O-methoxyethyl modifications (2'-MOE) at the 2' moiety of the ribose. It mediates the RNase H-mediated degradation of the mRNA for apolipoprotein B (apoB), a metabolic precursor of low-density lipoprotein (LDL). This antisense oligonucleotide has been used for the treatment of homozygous familial hypercholesterolemia which is a genetic disease characterized by high levels of LDL in the bloodstream and by early cardiovascular disease. Only one aptamer, termed Macugen (Pegaptanib) is approved by the FDA and in clinical use, which will be explained in detail in section 1.3.4.

1.3.1 Aptamers

Aptamers are short (15-100 nucleotides), chemically synthesised, single stranded (ss) RNA or DNA oligonucleotides. They fold into specific three-dimensional (3D) structures often with dissociation constants for their targets ranging between pico- and nano-molars (Nimjee et al., 2005). In contrast to most oligonucleotide therapies which mostly target the translational mechanism on the mRNAs level, aptamers directly bind target proteins through structural recognition (similar to antigen-antibody interaction) and interfere with functions of target protein by blocking the active site, disrupting the interactions with other target protein/DNA/receptor or inhibiting a specific protein domain with multiple subunits (Kaur and Roy, 2008). Therefore, aptamers are also termed “chemical antibodies”.

Aptamers have several advantages over antibodies. First, their molecular weight is considerably lower (8 – 25 kDa) when compared to antibodies (~ 150 kDa), which provides a faster and better target accessibility and more efficient penetration into tissues. Second, aptamers are considered non-immunogenic *in vivo* in contrast to antibodies, which are highly immunogenic especially after repeat administration. An example is the studies with anti-VEGF aptamer in *in vivo* models. These clinical studies in animal models as well as in humans illustrated no severe adverse effects resulting from immune stimulation against the aptamer (Eyetech Study, 2002, Eyetech Study, 2003). Third, aptamers are thermally stable, even with treatment at 95°C. When returned in to the room temperature, they can refold in to their correct secondary structures. However, antibodies, with protein properties, are not resistant to heat treatment; thus lose their activity. In addition, aptamers can be easily and rapidly synthesised in large scales with low costs using a well-established protocol

and in addition they can be modified by a variety of functional groups (Sun et al., 2014) and reporter molecules such as fluorescent dyes. Most importantly aptamer selections can be performed against a wide range of targets, such as metal ions (Hofmann et al., 1997, Rajendran and Ellington, 2008), amino acids (Mannironi et al., 2000), antibiotics (Wallace and Schroeder, 1998), toxins (Huang et al., 2015, Ye et al., 2014), peptides (Williams et al., 1997), proteins (Belyaeva et al., 2014, Nicol et al., 2013), virus glycoprotein (Liang et al., 2014), bacteria (Park et al., 2014), whole cells (Kim et al., 2014, Kunii et al., 2011) and organisms (Lorger et al., 2003) and even tissue samples (Noma et al., 2005). There are also some disadvantages including their susceptibility to nuclease degradation. However, this can be reduced by chemical modifications of nucleotides as further discussed in section 1.3.3.1. Another disadvantage is that an aptamer sequence can form several different secondary structures with similar ΔG (free energy) (see section 3.2.2). This can cause a reduction in the concentration of the desired and effective aptamer structure.

Aptamers against all these targets are identified through a process called SELEX (systematic evolution of ligands by exponential enrichment) which will be explained in detail in section below. This selection process *in vitro* allows the manipulation of specificity, binding affinity and selection conditions. Therefore, aptamers with desired properties that can bind to the target of interest at desired conditions i.e. particular temperature, pH, salt concentration or other buffer compositions can be generated.

1.3.2 Generation of aptamers by SELEX (Systematic Evolution of Ligands by Exponential Enrichment)

SELEX, an *in vitro* selection process, includes two steps; selection and amplification. Iterative rounds of SELEX serve to reduce the complexity of nucleic acid library (around ~10^{14} - 10^{15} molecules) (Tuerk and Gold, 1990).

As shown in Figure 1.6, technique is based on the incubation of a target of interest with a random pool of oligonucleotide library (single-stranded DNA or RNA) at a temperature which promotes the formation of most stable structures. The nucleic acid library contains a random sequence (30-40 nucleotides) flanked by constant regions located at the 5' and 3' ends. Constant regions consists of primer binding sites and also a T7 RNA polymerase recognition site (for RNA aptamers only). Oligonucleotide–target complex is washed and remaining bound sequences are eluted using appropriate buffer compositions. These sequences are then incubated with the control target if negative selection is necessary in order to eliminate the sequences that could also recognise the control. Recovered sequences are then

amplified by PCR or reverse transcription PCR for the synthesis of DNA and RNA aptamers, respectively. In the case of DNA SELEX, double stranded DNA aptamers need to be subjected to strand separation (in order obtain the sense strand of PCR products for the next round of selection) by i.e. using biotinylated primers (Bock et al., 1992) or fluorophore–labelled forward primers which allows the monitoring of the process by affinity separation or flow cytometry, respectively (Pei et al., 2014). However, for RNA SELEX, the pool of DNA is used as the template for *in vitro* transcription to produce a new pool of RNAs that goes in to the next round of selection. RNAs with a higher affinity for the target out-compete those with a lower affinity which are then removed and the whole cycle is repeated. The selection process is repeated (~10–20 rounds) to increase the binding affinity of aptamers resulting in K_d (the equilibrium dissociation constant) values ranging from nanomolar to picomolar. A stringent negative selection is generally included in the selection process in order to ensure target specificity. All nucleic acid sequences binding to affinity tags or closely related target proteins are discarded and remaining sequences (following amplification by PCR or reverse transcriptase PCR) are subjected to the next round of positive and negative selection.

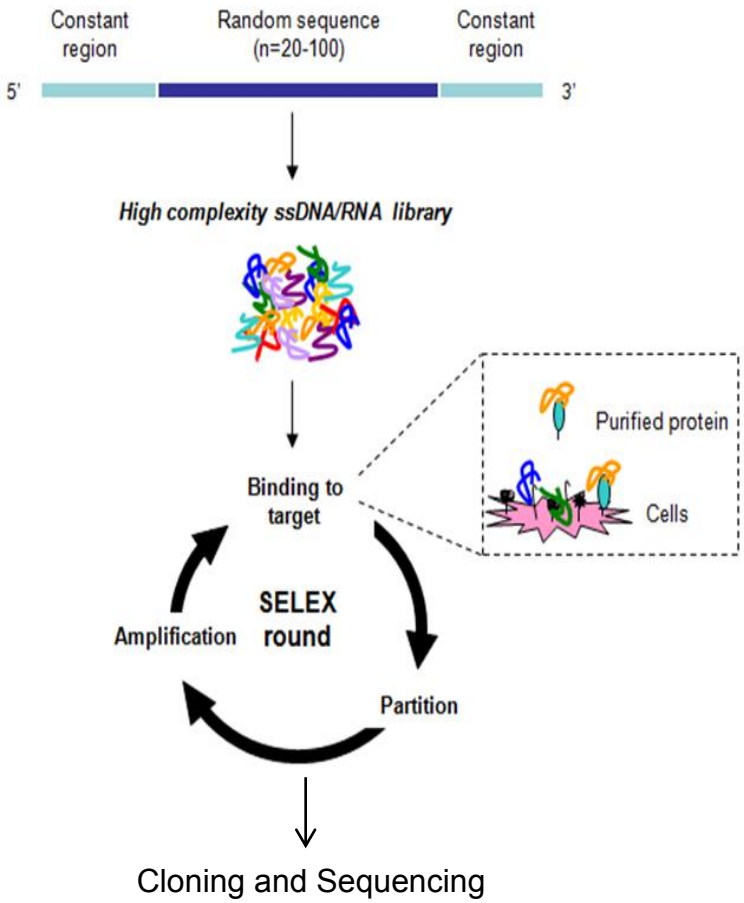

Figure 1.6 A schematic representation of SELEX process.The RNA or DNA aptamer library includes a variable region flanked by two constant regions. These constant regions contain primer binding sites for PCR amplification and a consensus promoter sequence for the T7-RNA polymerase. SELEX is based on incubation of target proteins/cells in a random pool of RNA/DNA, followed by washes to remove the unbound sequences. Then, bound RNA/DNA are eluted from target protein/cell, and amplified by PCR before moving on to next cycle generation. Resulting template pool is cloned into an appropriate plasmid and clones are picked and sequenced.

Aptamers can be identified from DNA or RNA pools. SELEX process for the selection of DNA aptamers requires fewer steps that of RNA aptamers which includes an *in vitro* transcription step as mentioned above. Chemical synthesis of RNA aptamers is more expensive than that of DNA aptamers, although synthesis of DNA aptamers requires an asymmetric PCR using labelled forward primers i.e. with biotin as mentioned above. DNAs are more stable and have longer shelf-life when compared to their RNA counterparts due to the fact that RNAs are more susceptible to hydrolysis than DNAs. This is why manipulation with RNA aptamers requires RNase-free conditions, although stability of RNA aptamer can be improved by incorporation of several modifications that will be discussed in section 1.3.3.1. In order to maintain the

aptamer at an effective concentration, high doses need to be administered in to animals or humans with several repeats, due to the issues with nuclease susceptibility. However, possibility of genetic encoding of RNA aptamers offers a great advantage over DNA aptamers due to the expression of aptamers directly by the target cells through vectors bearing sequences of aptamers of interest. In addition, base-pairing properties and presence of modified nucleotides (for RNA aptamers) within their 3D structures can provide structural diversity and versatility to RNA molecules as in the case of riboswitches. These are naturally occurring, non-coding and structured RNA sequences found in the 5'-untranslated region of mRNA molecules (Santosh and Yadava, 2014). Riboswitches are widespread in prokaryotic organisms i.e. bacteria and can recognise specific cellular metabolites (effector ligands) through their aptamer binding domain and can subsequently modulate metabolic gene expression through their expression platform domain (Santosh and Yadava, 2014). Main roles of riboswitches are premature termination of transcription, inhibition of translation and cleavage of mRNA itself (acting as ribozymes) when metabolite concentrations are sufficient. Similar to 3D RNA molecules found as riboswitches, DNA molecules with tertiary structures can also be found in organisms especially in telomere and promoter regions (Cogoi and Xodo, 2006, Oganesian and Bryan, 2007). They are observed to form G-quadruplex structures which can be considered major structural elements of DNA aptamers as in the case of thrombin aptamer, NU172 and nucleolin aptamer, AS1411 (section 1.3.4 and 5.2.4). These inter- and intramolecular G-quadruplex structures (G-quartets) formed by G-rich nucleic acid sequences have unique biophysical and biological properties (Dapic et al., 2003). Formation of these structures enhances the binding properties and also internalisation of aptamers into cells (Dapic et al., 2003, Reyes-Reyes et al., 2010). Based on considerations summarised above, DNA and RNA aptamers have specific advantages and disadvantages all of which needs to be taken into account before preferring one over the other.

A variation of traditional *in vitro* SELEX process is cell-SELEX (cell-based selection of aptamers). While traditional SELEX process is achieved by incubating the nucleic acid library with purified protein targets, cell-SELEX is performed using whole living cells. This protocol can be used even though cell marker proteins are unknown. Cells express certain marker proteins on the cellular membrane. Some of these are up-regulated or modified in a disease condition i.e. cancer or new markers might appear on the cell surface. This approach allows the isolation of RNA aptamers against cell surface markers with anti-cancerous, anti-inflammatory and anti-infectious effects for

the development of new therapies or biomarker discovery (Cibiel et al., 2012, Mi et al., 2010). One of the limitations of this approach is that presence of multiple markers on the cell membrane might result in non-specific binding. However, this can be overcome by inclusion of a stringent negative selection against negative control cells. A modified SELEX protocol, termed cross-over SELEX (if disease markers are known) can be used in order to eliminate these non-specific binding events. In this method, cell-SELEX are followed by traditional *in vitro* SELEX using purified cell marker proteins as targets. For example, this protocol was utilised to generate aptamers to human tenascin C (TN-C), an extracellular matrix protein involved in tumour growth, expressing U251 glioblastoma cells (Hicke et al., 2001). Following initial nine rounds of cell-SELEX, enriched pools were subjected to incubation with purified TN-C protein for two more rounds to identify sequences with higher affinity for the target.

Tissue-SELEX is another alternative selection process and used to identify aptamers against a tissue section i.e. from tumour including a negative selection against healthy tissues of the same origin. In this process, aptamers identified are supposed to bind several components of the tumour tissue i.e. cellular membranes, extracellular and intracellular molecules. In addition, another approach (*in vivo* SELEX) was described for the selection of RNA oligonucleotides that are localising to tumour cells *in vivo* using tumour bearing mice (Mi et al., 2010).

1.3.3 Challenges of aptamers in therapy

In vivo administration of aptamers are performed by intravenous (IV), subcutaneous (SC), or intravitreal (IVT) injections (Bouchard et al., 2010). However, other routes i.e. dermal, mucosal or inhalation can possibly be utilised to administer aptamers. Characterisation of aptamers that can internalise into keratinocytes without any chemical based introduction might allow topical application of aptamers i.e. to treat skin conditions involving inflammation (Doble et al., 2014). Alternative delivery mechanisms need to be established as well as subcellular localisation of aptamers upon administration. Therapeutic aptamers mostly target cell surface protein, abundant in the blood and body fluids. Therefore, aptamers need to remain functional and stable in these compartments for longer period of time. However, unmodified aptamers are highly unstable and prone to degradation with nucleases (and released nucleosides are subjected to purine and pyrimidine metabolism pathways) and rapidly eliminated by renal clearance (Sundaram et al., 2013). Aptamers might also result in nonspecific immune response in transfected cells which will be discussed below.

1.3.3.1 Requirement for modifications for the stabilisation of aptamers

Nucleic acids consist of base, ribose, and phosphate moieties. Each moiety can potentially be modified with various chemical groups in order to increase the half-life of unmodified aptamers, which observed to be less than 2 min (Griffin et al., 1993). For example, base moiety of pyrimidines and purines are modified at the 5', and 7' and 8' positions, respectively; sugar moiety is modified at the 2' or 4' position; and phosphate group is modified by substitution of oxygen with other chemical species (Kuwahara and Sugimoto, 2010). Modification of the phosphate group leads to the formation of inter-nucleotide phosphodiester linkages. An example of this is oligonucleotides synthesised using 5'-α-P-boranonucleotide triphosphates (Lato et al., 2002) and α-thio nucleotide triphosphates (phosphorothioate) (Kang et al., 2008) in which one of the oxygen atoms of the α-phosphate moiety is replaced by a boron atom or sulphur, respectively. Amongst several others, use of nucleotides with fluoro (-F), O-Methyl (OCH_2) and amino (NH_2) substitutions at the 2' OH position of the ribose are the most common modifications (Keefe and Cload, 2008). The presence of the –OH at the 2' ribose makes RNA more susceptible to nucleophilic attack when OH ions are present on the 5' phosphate group (2'–OH group can generate 2'–O ion, which attacks the phosphorous atom). This results in the breakage of phosphodiester bonds, and 2'-3' cyclic phosphate intermediates are formed. Hydrolysis of cyclic nucleotides generates a mixture of 2' and 3' nucleoside monophosphates. Amongst other 2' ribose modifications, fluorine is used more often due to its small size and also its neither hydrophobic nor hydrophilic nature (Pallan et al., 2011). Therefore, fluorine seem to be good mimics of the 2' hydroxyl group. Substitution with fluorine locks the ribose in the C3'-endo conformation, which can increase the binding affinity to the target (Pallan et al., 2011). The 2'-fluoro modification also reduces non-specific immune stimulation by nucleic acid molecules (Deleavey et al., 2010, Yu et al., 2009). An alternative position to modify the ribose is the replacement of 4' oxygen atom with sulphur compound. SELEX process using these modified 4'-thio UTP and CTPs was previously reported (Kato et al., 2005). Uridine or thymidine can also be modified at the 5' position (substitution of this position is likely to be ignored by polymerases) i.e. 5-pentynyl-2'-deoxy uridine (Latham et al., 1994). Mutant T7 RNA polymerase can be used in order to incorporate these modifications into aptamers before or after SELEX process (Chelliserrykattil and Ellington, 2004, Huang et al., 1997, Sousa and Padilla, 1995). However, if aptamers are modified after selection, it might be taken into consideration that their binding properties might have altered, although this was found to be negligible for aptamers selected to the RNA-dependent RNA polymerase

(RdRp) of foot-and-mouth disease virus, FMDV (Ellingham et al., 2006, Forrest et al., 2014).

Nucleotide capping by incorporation of an inverted nucleotide at the 3'- terminus (through 3'-3' phosphodiester bond) is also used to increase the stability of aptamers by protecting them from serum nucleases (Beigelman et al., 1995). In this case, oligonucleotide contains no 3'-termini, which increase the stability due to the fact that 3'- exonuclease activity in serum is considerably greater compared to 5'- exonuclease activity.

Locked nucleic acid aptamers and Spiegelmers (containing mirror imaged oligonucleotides) are resistant to nucleases with enhanced metabolic stability. Locked nucleotides contain a methylene bridge between 2'-O and 4'-C of the ribose group, which presents more stable base-pairing structures due to the fact that bridge locks the ribose in the 3'-endo (N-type) conformation (Schmidt et al., 2004). Spiegelmers are generated by the replacement of D-ribose with L-ribose, resulting in the production of unnatural L-nucleotides. These L-nucleotides (mirror images of natural oligonucleotides) are subsequently used in the chemical synthesis of L-RNAs (Spiegelmers) that are highly resistant to nuclease degradation (Eulberg and Klussmann, 2003). Several Spiegelmer aptamers (L-RNA aptamers) are currently undergoing clinical trials as presented in Table 1.1. A modified SELEX protocol is applied to generate these Spiegelmers owing to the fact that L-ribonucleotide triphosphates cannot be recognised by wild-type RNA polymerases that are used during selection process i.e. PCR. Therefore, SELEX is performed using the enantiomer (mirror image) of the desired protein target (that can be made synthetically using L-amino acids) and wild-type RNA sequences. Isolated aptamers are then synthesised with L-ribonucleotides and expected to bind to the desired protein target (synthesised with D-amino acids) in a similar way.

1.3.3.2 Conjugation of polymers to enhance the bioavailability of aptamers

Other concern using aptamers as therapeutics is their rapid renal clearance. Although low molecular mass (8 – 25 kDa) provides aptamers certain advantages (Section 1.3.1), this can also be a drawback due to the poor bioavailability of aptamers in plasma. As the molecular weight cut-off for the renal glomerulus is 30 – 50 kDa, conjugation of aptamers to polymers (30 – 50 kDa) prevents exclusion by renal clearance. Cholesterol and mostly polyethylene glycol (PEG) *N*-hydroxysuccinimide polymers are used for this purpose. When 20 kDa or 40 kDa PEG polymer was

conjugated to the aptamer, the half-life of the aptamer in circulation was found to be increased with reduced distribution to the kidneys (Healy et al., 2004). Use of 2'-ribose modified nucleotides i.e. 2'-O-methyl as well as 40kDa PEG conjugation can increase the circulation half-life of an aptamer by up to 23 h in mouse models (Burmeister et al., 2005) and up to 10 (±4) days in human (Macugen; Pfizer/Eyetech) (see clinical pharmacology section on the prescribing information of pegaptanib). PEG is conjugated to the protein generally in a random manner through lysine side chains. This could lead to heterogeneity (mixed PEGylated and unPEGylated species) and also loss of protein`s function. However, taking advantage of being chemically synthesised molecules, aptamers can be engineered to contain an additional functional moiety (i.e. alkyl amine) that can be used as a conjugation site for further modifications i.e. PEG polymer. Conjugation of PEG through an additional moiety helps to protect the 3D structure and function of the aptamer.

1.3.3.3 Potential toxicity due to the activation of innate immunity

Another challenge using aptamers as therapeutics results from their potential toxicity. In fact, there is very limited information available on the activation of innate immunity by aptamers unlike viral, bacterial nucleic acids and other DNA or RNA oligonucleotides. Host cells present pathogen-recognition receptors (PRRs) in order to recognise a pathogen invasion by detecting particular molecules associated with the pathogens (Bowie and Unterholzner, 2008). Recognition of viral RNA occurs in the endolysosomal compartments by membrane-bound Toll-like receptors (TLRs) 3 (responds to double-stranded DNA or RNA), mouse TLR7 (human TLR8) (respond to single-stranded RNA) and 9 (unmethylated CG motifs (CpG motifs) in DNA) in immune cells. However, in nonimmune cells, accumulated foreign nucleic acids are recognised in the cytosol by retinoic acid inducible gene 1 (RIG-I) and melanoma differentiation associated antigen 5 (MDA5), Nod-like receptors and C-type lectin receptors (Akira et al., 2006, Kawamura et al., 2014). RIG-I is a DEXH/D-containing RNA helicase which recognises 5' triphosphate moiety of foreign RNA in cytosol during the course of infection and subsequently mediates immune responses through type I interferons (IFNα/β) (Hwang et al., 2012). Since, cellular mRNA is modified at the 5' triphosphate by capping prior to nuclear export. Therefore, only molecules containing a 5' triphosphate in cytosol would be foreign, such as viral RNA. RIG-I is predominantly expressed in fibroblasts, epithelial cells, hepatocytes, and conventional dendritic cells (cDCs) (Kato et al., 2006). RNA molecules that are capable of triggering RIG-I response might harbour a recognition sequence or be single-stranded (ss) or double-stranded (ds) RNA with 5' triphosphate (Cui et al., 2008, Hornung et al., 2006).

However, single-stranded 5' triphosphate oligoribonucleotides were shown to be unable to bind or activate RIG-I, unless the complementary strand was added (Schlee et al., 2009b). As it was indicated before, activation of MDA5 or RIG-I has been observed to be dependent on the length of RNA molecules. While long double-stranded RNAs (≥ 1 kbp) trigger innate immunity via MDA5, short double-stranded RNAs (~70bp – 1kbp) and shorter single-stranded RNA or DNA molecules with a 5' triphosphate group activate that through RIG-I (Kato et al., 2008, Schlee et al., 2009a). Unmodified RNA is highly sensitive to endogenous nucleases. However, 2'-Fluoro modification of ribose reduces unspecific immune responses mediated by TLRs, which causes most of the potential adverse effects of aptamers (Yu et al., 2009). However, presence of triphosphate moiety at the 5' end of the aptamer can also stimulate innate immunity. Aptamers can chemically be synthesised to consist of an alternative moiety at the 5' end in order to eliminate immune activation effects of triphosphate, if desired. For example, the aptamer bearing -OH instead of a triphosphate did not trigger interferon production in cervical cancer cell lines (Belyaeva et al., 2014).

1.3.3.4 Need for efficient delivery systems

Internalisation of ligands, extracellular molecules, plasma membrane proteins and lipids occurs through endocytosis. This can be grouped into these two mechanisms; clathrin-dependent and in-dependent as further introduced in section 5.1. Endocytosed cargo molecules are first delivered into the early endosomes, then move to the late endosomes and lysosomes for degradation, trans-golgi network (TGN) or recycling endosomes in order for the cargo to return back to the cell membrane (Grant and Donaldson, 2009). Most experimental approaches involve lipid-based transfection and electroporation to deliver nucleic acid molecules into the cells (see section 5.1.3). It was suggested that cargo was usually delivered into early endosomes regardless of the mechanism of internalisation (Grant and Donaldson, 2009). These cargo molecules accumulate in the endosomal compartments and later lysosomes for degradation unless they manage to escape. Such data have been mostly derived from siRNAs studies (Barreau et al., 2006, Gonzalez et al., 2007, Lu et al., 2009, Menager et al., 2014, Sioud, 2005). A G-rich DNA aptamer, AS1411 were shown to enter cancer cells via micropinocytosis, localising in the macropinosomes (Reyes-Reyes et al., 2010). Macropinocytosis is a dynamin-independent pathway for endocytosis (see section 5.1.4 for endocytosis pathways). Macropinocytosis might be an ideal way of delivery due to the fact that they can form large vesicles varying in size and shape, mediated by the formation of actin-dependent lamellipodia. Resulting

macropinosomes are leaky, giving them an advantage over other endosomal vesicles (Wadia et al., 2004). These vesicles are also non-digestive non-acidic in contrast to lysosomes (Conner and Schmid, 2003). Macropinocytosis is also thought to be a good means of delivery mechanisms of a range of different cargos including peptides, intact proteins, bacterial virulence factors and viruses into cells (Reyes-Reyes et al., 2010). Macropinocytosis have been shown to be involved in the uptake of siRNAs (Love et al., 2010) and also naked DNA plasmids (Basner-Tschakarjan et al., 2004, Fumoto et al., 2009, Wittrup et al., 2007). However, there is little data in the literature regarding the uptake and localisation of RNA aptamers.

1.3.4 Aptamers in clinical trials and approved by FDA

Unlike therapeutic antisense oligonucleotides or siRNAs which target intracellular compartments, aptamers can target intracellular (i.e. β-catenin, thyroid transcription factor 1 (TTF-1), HPV E6 and E7) and extracellular molecules (i.e. VEGF and Tenascin-C) as well as cell surface components (i.e. PSMA, EGFR, Mucin-1 and gp120) (Figure 1.7). This broad application of aptamers provides them such properties that make their systemic administration feasible i.e. against targets in the bloodstream, such as thrombin (NU172), factor IXa (REG1) and von Willebrand factor (ARC1779), or on the surface of cells such as growth factor receptors (Table 1.1). Aptamers can also access targets inside cells. However, non-toxic delivery methods are required for their administration *in vivo* (section 1.3.3.4). Different types of aptamers i.e. agonists and antagonists have been generated and characterised to date since they were first discovered. Aptamers with therapeutic potential mostly tend to inhibit protein–protein interactions (i.e. receptor–ligand and oncoprotein–cellular protein target), functioning as antagonists. However, aptamers have also been observed to function as agonists. For instance, aptamers selected against the extracellular domain of the human epidermal growth factor receptor 3 (HER3) (or known as ERBB3) can promote oligomerisation without affecting its downstream phosphorylation (Chen et al., 2003). Therapeutic effects of antagonist aptamers are dependent on the binding affinity. If aptamer binds the target molecule with a high affinity, its therapeutic use will last longer and be more relevant. However, aptamers with higher binding affinity do not necessarily bind their ligands more specifically. Binding specificities of RNA aptamers selected against guanosine triphosphate (GTP) with K_d values ranging between 8 µM and 9 nM were examined by competition binding studies using several chemical analogues of GTP (Carothers et al., 2006). This study failed to show that higher affinity binders were more specific for GTP. Thus, potential therapeutic aptamers should present strong specificity and high affinity for their

targets and be modified in order to increase their nuclease resistance and bioavailability (sections 1.3.3.1 and 1.3.3.2). There is currently one aptamer, termed “pegaptanib (Macugen; Pfizer/Eyetech)”, previously known as anti-VEGF (vascular endothelial growth factor) aptamer “EYE001”, in clinical use that is approved by Food and Drug Administration (FDA) in 2004 (Table 1.1). VEGF regulates the pathological angiogenesis in cancer, ocular and inflammatory diseases (Keefe et al., 2010). Pegaptanib is a modified RNA aptamer (truncated to 27, originally ~70 nucleotides) selected against VEGF and used to treat age-related macular degeneration (AMD), a disease leading to vision loss of elderly caused by enhanced expression of VEGF, damaging the retina. Modification was accomplished by the incorporation of 2'- fluoro pyrimidines and 2'-O-Methyl purines to the RNA transcript and also capping the 3' end with an inverted deoxythymidine (dT) (for alternative modifications see section 1.3.3.1 and 1.3.3.2) (Ng and Adamis, 2006). In addition, bioavailability of this aptamer was enhanced by a 40 kDa polyethylene glycol (PEG) conjugation to the 5' position.

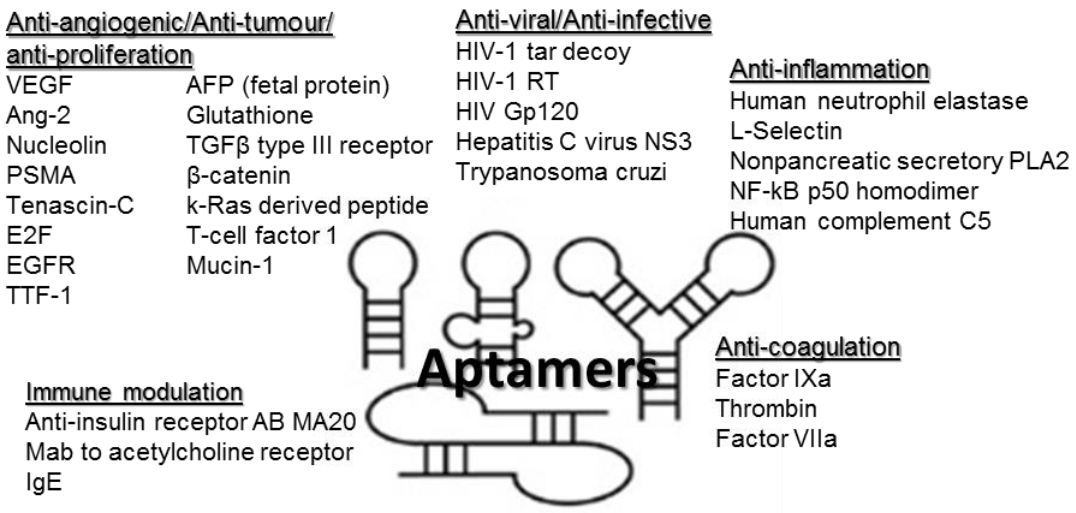

Figure 1.7 Aptamers have been selected against a wide range of target molecules. Modified from (Que-Gewirth and Sullenger, 2007, Santosh and Yadava, 2014).

Apart from their therapeutic potential, aptamers possess a wide range of applications such as in disease diagnosis (Barfod et al., 2009, Wan et al., 2010), as imaging tools (Kim et al., 2010) and in biomarker discovery (Mi et al., 2010). Moreover, aptamers generated against cell surface receptor proteins found an alternative utility on the delivery of therapeutic and diagnostic substances including small siRNAs, drugs, toxins, enzymes, photodynamic molecules and nanoparticles into target cells as “escort molecules” (Hicke and Stephens, 2000). Aptamers selected against cell surface receptors may be internalised along with target receptors themselves,

carrying the cargo inside the cells. To ensure the selective delivery of aptamers into the target cells (but not healthy cells), the receptor protein should be overexpressed only in the disease condition i.e. cancer which can be considered as a tumour biomarker. Examples will be given in the below section. Aptamers targeting proteins that are cancer- or virus- related, of interest, will be further introduced in the following section.

Name (Company)	Composition	Target	Medical indication	Current phase (Trial registration number)	Ref
Pegaptanib sodium/ Macugen/ EYE001 (Pfizer/ Eyetech)	2' -O-methyl purine/2'-fluoro pyrimidine with two 2' -ribo purines conjugated to 40 kDa PEG, 3'inverted dT	Vascular endothelial growth factor	Age-related macular degeneration	Approved in the US and the EU	(Ng et al., 2006)
AS1411/ AGRO001 (Antisoma)	G-rich DNA	Nucleolin	Acute Myeloid Leukemia, Metastatic Renal Cell Carcinoma	Phase II completed (NCT00512083) Phase II status unknown (NCT00740441)	(Bates et al., 2009, Teng et al., 2007)
REG1/RB006 plus RB007 (Regado Biosciences)	2' -ribo purine/2' -fluoro pyrimidine (RB006)/40 kDa PEG plus 2'-O-methyl antidote (RB007)	Coagulation factor IXa	Coronary artery disease	Phase III (NCT00715455)	(Becker and Chan, 2009)
ARC1779 (Archemix)	DNA and 2'-*O*-methyl with a single phosphorothioate linkage conjugated to 20kDa PEG, 3' inverted dT	A1 domain of von Willebrand factor	Thrombotic microangiopathy	Phase II closed (NCT00726544)	(Diener et al., 2009, Gilbert et al., 2007)
ARC19499 (Baxter Healthcare)	2'-ribocytidine/2'-*O*-methyl Adenine/Guanine/Uracil conjugated to 40 kDa PEG, 3' inverted dT	TFPI	Hemophilia	Phase I closed (NCT01191372)	(Waters et al., 2011)
NU172 (ARCA biopharma)	Unmodified DNA aptamer	Thrombin	Cardio-pulmonary bypass to maintain steady state of anticoagulation	Phase II status unknown (NCT00808964)	(Gomez-Outes et al., 2011)
ARC1905 (Ophthotech)	2'-ribo purine/2'-fluoro pyrimidine conjugated to 40 kDa PEG, 3' inverted dT	Complement component 5	Dry age-related macular degeneration	Phase I completed (NCT00950638)	(Biesecker et al., 1999)
E10030 (Ophthotech)	DNA and 2'-*O*-methyl 5'-conjugated to 40 kDa PEG, 3' inverted dT	Platelet-derived growth factor	Wet age-related macular degeneration	Phase III recruiting participants (NCT01089517)	(Green et al., 1996)
NOX-A12 (NOXXON Pharma)	L-RNA with 3'-PEG	CXCL12	Chronic Lymphocytic Leukemia (CLL), Multiple Myeloma (MM)	Phase IIa ongoing (NCT01486797), (NCT01521533)	(Sayyed et al., 2009)
NOX-E36 (NOXXON Pharma)	L-RNA with 3'-PEG	CCL2	Type 2 diabetes and albuminuria, diabetic nephropathy	Phase IIa completed (NCT01547897), (NCT01372124)	(Kulkarni et al., 2009, Kulkarni et al., 2007, Maasch et al., 2008)
NOX-H94 (NOXXON Pharma)	L-RNA with 3'-PEG	Hepcidin	Anemia of chronic disease	Phase II completed (NCT01691040) (NCT02079896) (NCT01372137)	(Schwoebel et al., 2013)

Table 1.1 The list of aptamers undergoing clinical trials updated from (Keefe et al., 2010, Sun et al., 2014). CXCL12, chemokine (C-X-C motif) ligand 12 (or SDF-

1α); CCL2, chemokine (C-C motif) ligand 2 (or MCP1); EU, European Union; US, United States; PEG, polyethylene glycol; TFPI, tissue factor pathway inhibitor.

1.3.5 Aptamers in cancer and virology

Some of the best characterised aptamers (in particular for targeted delivery) are the aptamers identified against prostate specific membrane antigen (PSMA). PSMA is a transmembrane glycoprotein that is aberrantly expressed in human prostate cancer cells and vascular endothelium. PSMA plays a major role in the internalisation of certain ligands and in the enzymatic processes i.e. glutamate carboxypeptidase (Pei et al., 2014). It can be used as a potential cell surface target for prostate cancer cells. In 2002, 2'-fluoropyrimidine RNA aptamers, A9 and A10, against extracellular domain of PSMA were generated and shown to inhibit the enzymatic activity of PSMA (Lupold et al., 2002). These aptamers have been utilised as tools to deliver nanoparticles, toxins, therapeutics and siRNAs in cells. Cell-type specific delivery of siRNAs is the main problem in their therapeutic applications. This can potentially be accomplished by creating chimeras with aptamers. PSMA specific aptamer-siRNA chimeras were constructed to consist of the aptamer sequence, A10, and a siRNA against cell survival factors polo-like kinase 1 (Plk-1) or B-cell lymphoma 2 (Bcl-2) (McNamara et al., 2006). Both are anti-apoptotic oncoproteins overexpressed in cancer. In order to generate these chimeras, the sense strand of the siRNA was covalently linked to the 3` end of the aptamer. Subsequently, complementary anti-sense strand was annealed to generate double-stranded siRNA molecules. An alternative approach to create chimeras is the non-covalent conjugation of siRNAs and aptamers, that are both biotinylated, through a streptavidin linker (Chu et al., 2006). Upon intratumoural injection, these chimeras were reported to induce apoptosis in PSMA-expressing cells and reduce the prostate tumour size in a xenograft model (McNamara et al., 2006). PSMA aptamer-siRNA chimeras were also used to increase tumour immunity. Aptamer A10 was used to deliver siRNAs against Upf2 and Smg1, which are involved in nonsense-mediated mRNA decay (NMD) pathway, in to PSMA expressing tumour cells (Pastor et al., 2010). NMD pathway is a post-transcriptional RNA surveillance process that eliminates mRNAs with premature termination codons. Interference with this pathway results in the production of antigens, leading to the stimulation of the immune system. It was shown that Upf2 or Smg1 siRNA-A10 chimeras (siRNA was conjugated to the 3' end of the aptamer) inhibited the tumour cell growth in *in vivo* xenograft models as well as in cultured cells (Pastor et al., 2010). Another example was that a short hairpin RNA (shRNA) was linked to the 3' end of the truncated PSMA-targeted aptamer and used to enhance the radio-sensitivity of prostate cancer cells

(but not neighbouring tissues) to ionizing radiation (IR) therapy (Ni et al., 2011). This aptamer-shRNA chimera was selectively targeting the catalytic subunit of the DNA protein kinase (DNAPK) in cancer cells, resulting in the attenuation of DNA repair mechanisms leading to reduced cancer cell survival following ionising radiation treatment.

Cell surface specific aptamers can also be conjugated to the surface of nanoparticles, formulated with poly D,L-lactic-co-glycolic acid poly ethylene glycol (PLGA-bPEG) copolymer, containing chemotherapeutics (Farokhzad et al., 2006). A truncation of PSMA aptamer A10 (A10-3) conjugated to these nanoparticles containing docetaxel (Dtxl), an anti-mitotic chemotherapy drug, was shown to deliver the drug into PSMA-expressing tumour cells and reduce the tumour volume following intratumoural injection in mouse models of prostate cancer (Farokhzad et al., 2006). The targeted uptake of these nanoparticles modified with PSMA aptamer into PSMA-expressing prostate cancer cells can reduce the side-effects and toxicity of chemotherapy drugs such as docetaxel.

NOX-A12, a Spiegelmer and AS1411 aptamer are the only aptamers in clinical trials for cancer treatment (Table 1.1). AS1411 is a 26-mer guanosine-rich DNA oligonucleotide (GRO) that can form G-quadruplex structures. G-quadruplex-forming sequences have been identified in the genome for example in telomeric repeats and promoter regions of some oncogenes in addition to DNA and RNA aptamers (Cogoi and Xodo, 2006, Oganesian and Bryan, 2007, Reyes-Reyes et al., 2010, Huang et al., 2014). AS1411 (AGRO100) was discovered while several G-rich oligonucleotides were being tested in numerous cancer cell lines for anti-proliferative activity (Bates et al., 1999). In this study, radiolabelled oligonucleotides were incubated with cancer cell extracts, resulting protein complexes were analysed by electrophoretic mobility shift assays (EMSAs). One of the protein complexes was hypothesised to be nucleolin due to its apparent molecular weight of around ~110 kDa (Bates et al., 1999). Nucleolin was later confirmed as the major interacting protein for AS1411 by western blotting (using biotinylated aptamer to pull-down interacting proteins thorough streptavidin magnetic beads from cell extracts or whole cells) and mass spectrometry fingerprinting (Girvan et al., 2006, Teng et al., 2007). Nucleolin is a Bcl-2 mRNA-binding protein that is overexpressed on the surface of cancer cells. *In vitro* and *in vivo* studies showed that AS1411 aptamer causes apoptosis in several cancer cell lines and a reduction in tumour size, respectively (Mongelard and Bouvet, 2010). The induction of apoptosis and the S-phase arrest by AS1411 was shown to be through interference with DNA replication and stabilisation of Bcl-2 mRNA (an apoptosis

inhibitor), respectively (Ireson and Kelland, 2006, Soundararajan et al., 2008). A phase II clinical trial with AS1411 in combination with cytarabine to treat acute myeloid leukemia (AML) was completed (Table 1.1); and response rate in patients was found to be considerably higher (21%) when compared to the treatment with cytarabine alone (5%) (Mongelard and Bouvet, 2010). Another phase II trial with AS1411 was performed in metastatic renal cell carcinoma (Table 1.1), however, only 1 out of 35 patients responded the treatment (Rosenberg et al., 2014). The current status of this trial is unknown.

Recently, AS1411 was utilised for targeted delivery of therapeutic molecules into cancer cells overexpressing nucleolin on the cell surface. Targeted delivery of drugs and siRNAs was accomplished using liposome-aptamer conjugates in MCF-7 breast cancer (Cao et al., 2009) and A375 melanoma cells (Li et al., 2014), respectively. Moreover, same aptamer was also used for the labelling of cancer cells. U87MG glioblastoma cells was efficiently labelled using cadmium telluride (CdTe) quantum dot-AS1411 conjugates (Alibolandi et al., 2014).

NOX-A12 is a 45-nucleotide L-RNA aptamer or Spiegelmer (section 1.3.3.1), binds stromal cell-derived factor-1 (SDF-1) also known as chemokine (C-X-C motif) ligand 12 (CXCL12) with an affinity of less than 1 nM (Keefe et al., 2010). This aptamer does not contain any further modifications apart from being made using L-nucleotides and conjugated to a PEG polymer. Inhibition of the chemokine, involved in tissue generation, angiogenesis, tumour metastasis and cell homing, by NOX-A12 aptamer can be useful to treat some cancers. NOX-A12 is currently in a phase II clinical trial for the treatment of multiple myeloma and chronic lymphocytic leukemia (CLL) (Table 1.1) in combination with bortezomib and dexamethasone; and bendamustine and Rituximab, respectively.

There are several more therapeutic and diagnostic aptamers selected against cancer-related proteins or biomarkers. For example, an aptamer (SQ-2) identified by cell-based selection to specifically recognise pancreatic cancer cells (Dua et al., 2013). The target of this aptamer was shown to the alkaline phosphatase placental-like 2 (ALPPL-2) protein by pull down assays and also genome-wide microarrays (to identify target mRNAs in the aptamer transfected or untransfected cells) (Dua et al., 2013). Further characterisation of this protein showed tumour-associated functions such as inhibiton of cell proliferation and invasion in pancreatic cells (Dua et al., 2013).

As described above, many aptamers have been identified with anti-tumour activity (Figure 1.7). However, there are aptamers used to inhibit virus replication, viral entry,

transcription and translation. 2'-fluoro-pyrimidine modified aptamers were selected against R5-strain of HIV-1 glycoprotein 120 (gp120), an envelope glycoprotein involved in the attachment of HIV to cell surface receptor CD4 (Khati et al., 2003). This aptamer competes with highly conserved N-terminus region of HIV co-receptor, CCR5 for binding to gp120 and prevents the entry of the virus into helper T-cells (Dey et al., 2005a, Dey et al., 2005b), reducing the infectivity of HIV-1 as well as some other R5 viruses (Khati et al., 2003) The minimal region of the aptamer involved in binding to gp120 were identified by RNAase footprinting analysis (nuclease protection mapping) and mutagenesis (Dey et al., 2005a). Although clinical trials were not pursued, gp120 aptamer was used for the development of aptamer-siRNA chimeras. These chimeras, generated by base-pairing of one strand of a 27-mer anti-tat/rev siRNA that is covalently attached to the 3' end of the aptamer to the complemetry strand, dual-function to inhibit virus replication (aptamer) and downregulate the expression of the target gene (siRNA) (Zhou et al., 2008). Same group was later coupled the siRNA and anti-gp120 aptamer through packaging RNA (pRNA), one of the components of the bacteriophage phi29 DNA-packaging motor, and used it as potential HIV-1 inhibitor as well as a vehicle for cell-type specific delivery of siRNAs (Zhou et al., 2011).

Influenza virus entry was also targeted using DNA aptamers, A22, generated against H3 type haemagglutinin (HA) which mediates the attachment of the virus to target cells via the sialic acid-containing oligosaccharide receptors (Jeon et al., 2004). A22 was shown to prevent binding of virus to host cells, therefore reducing virus titres (Jeon et al., 2004). However, this aptamer was cross-reacting with H1N1, H3N2 and H2N2 strains. Subtype specific RNA aptamers were generated against influenza virus H3N3 HA (Gopinath et al., 2006). These aptamers were shown to recognise the target virus, A/Panama/2007/99 and also A/Wyoming/3/2003 by surface plasmon resonance (SPR) analysis at 20 and 50 nM, concentrations, however fail to bind other closely related H3 strains even at higher concentrations (500 nM). Moreover, the selected aptamer showed higher binding affinity to HA (15-fold) than currently available monoclonal antibodies. These studies showed the possibility of using aptamers as biosensors for rapid genotyping of influenza virus strains and also for the development of diagnostic tools for influenza infection.

Aptamers can interfere with the assembly of the viral nucleocapsid (NC). An aptamer generated against HIV NC inhibited the proper packaging of the viral genome by competing with the HIV-1 packaging signal, psi sequence (Kim et al., 2002). Another

NC aptamer against HIV-1 Gag protein reduced the replication of HIV in cells by downregulating the Gag protein or mRNA (Ramalingam et al., 2011).

Viral polymerases are some of the earliest targets for aptamer selection. HIV reverse transcriptase (RT) produces double stranded DNA (dsDNA) from single stranded RNA genome (ssRNA). RNA aptamers were identified against HIV-RT, inhibiting cDNA synthesis (Tuerk et al., 1992). These aptamers were only effective against RT of HIV but no other retroviruses. HIV RT is a heterodimeric and multifunctional enzyme with an RNase H activity, mediating the cleavage of replication intermediates, DNA/RNA hybrids. Therefore, its RNAse activity was also targeted with aptamers (Andreola et al., 2001). Some of these selected aptamers, with G-quadruplex structures, were shown to inhibit both RNase H and DNA polymerase activities, therefore HIV infection with an IC_{50} values of 10 nM in a tat transactivation reporter assay when applied on the cells without transfection. Another virus polymerase to be a target for aptamer studies was RNA-dependent RNA polymerase (RdRp) of hepatitis C virus (HCV), non-structural protein 5B (NS5B). Both DNA and RNA aptamers were generated against NS5B, inhibiting its polymerase activity (Bellecave et al., 2008, Biroccio et al., 2002). The RNA aptamer, B.2 was shown to bind to NS5B with a K_d value of 1.5±0.2 nM by filter-binding assays (Biroccio et al., 2002). The use of point mutagenesis of deletion mutants of the aptamer indicated the requirement of a GC bulge and a stem loop for aptamer binding to NS5B (Biroccio et al., 2002). Aptamers were also identified against the RdRp of FMDV termed, $3D^{pol}$ as introduced above (Ellingham et al., 2006). Some of these aptamers, 47tr and 52tr, with 2'-fluoro Cy3 modifications were recently shown to inhibit the replication of FMDV sub-genomic replicon, monitoring green fluorescent protein (GFP) reporter expression over time (Forrest et al., 2014). Same study also showed that aptamers had an effect on replication but not translation (through binding to 5' untranslated region, UTR) by luciferase reporter assays using reporter genes under the control of either cap- or IRES dependent translation. IRES is an internal ribosome entry site located in the 5' UTR of the mRNA. This structured region mediates the attachment to the ribosome and initiates the cap-independent (IRES-dependent) translation. There are aptamers targeting IRES such as HCV anti-IRES aptamers inhibiting IRES-dependent translation (Kikuchi et al., 2005). These aptamers have a potential therapeutic value with reduced side effects. Since, aptamers recognises the secondary structures in the viral mRNA which does not exist in the host mRNA. These anti-IRES aptamers are also modified with conjugation to other aptamers targeting different regions in the IRES in order to enhance the inhibitory activities of aptamers (Kikuchi et al., 2009).

1.3.5.1 Aptamers against HPV proteins

There are few studies explained the identification and characterisation of aptamers against HPV proteins. High level expression of high-risk HPV E6 and E7 oncoproteins in cervical cancer tumours led to the development of aptamers for potential diagnostic and therapeutic applications (Belyaeva et al., 2014, Gourronc et al., 2013, Graham and Zarbl, 2012, Nicol et al., 2011, Nicol et al., 2013, Toscano-Garibay et al., 2011). HPV16 E7 aptamers described by (Toscano-Garibay et al., 2011) was shown, using deletion mutants of E7, to bind first on the N-terminus CR1 and then CR3 in a two-step mechanism through a stem-loop structure on the aptamer. However, these aptamers were not tested in terms of their function and effects in cells or *in vivo*. However, an HPV16 E7 aptamer used in this study, possibly binding the LXCXE motif in the CR2 of E7 where pRb binding occurs, was shown to induce apoptosis in HPV positive cervical cancer cells (Nicol et al., 2013). This was suggested to probably be due to the loss of E7 and accompanying recovery of pRb following aptamer transfection. Another study described aptamers against HPV L1 virus-like particles produced in a baculovirus expression system (Leija-Montoya et al., 2014). HPV L1 aptamers may help the development of an effective diagnostic tool for the diagnosis of the HPV infection. There are examples of aptamers that can be used for early detection of virus infected cells. For example, a fluorescently labelled aptamer HBs-A22, selected against the Hepatitis B virus (HBV) surface antigen (HBsAg) which locates on the cell surface of HBV-infected hepatocytes, was used to discriminate HBsAg positive cells (HepG2.2.15) from HBsAg negative cells (HepG2) by fluorescence microscopy (Liu et al., 2010).

In the work described here, HPV16 E7 aptamers were used for further characterisation. These aptamers were selected using GST-E7 by SELEX. Negative selection was performed to eliminate GST-binding aptamers (Nicol et al., 2011). Negative selection against closely related targets or affinity tags can both reduce cross-reactivity and increase target specificity. RNA aptamers synthesised by *in vitro* transcription using 2'-Fluoro modified (CTP and UTP) and unmodified (GTP and ATP) nucleotides by a mutant T7 RNA polymerase in an “optimised” reaction conditions. A mutation (Y639F) in T7 RNA polymerase was identified to cause an approximately 20- fold decrease in the ability of enzyme to discriminate between rNTPs and dNTPs, retaining its wild type activity (Padilla and Sousa, 1999).

The sequence alignment using ClustalW2 multiple sequence alignment tool (EMBL-EBI) of identified monoclonal HPV16 E7 aptamers after 10 rounds of SELEX was

published previously (Nicol et al., 2011). While some of these aptamers were grouped into families i.e. A, B, C, D and E, some others were outliers F1, G1, H1, I1 and J1. Apparent binding affinities (K_{Dapp}) of HPV16 E7 aptamers were determined as the concentration of GST-E7 at which 50% binding by aptamer was observed by a bead-binding assay through scintillation counting (Nicol et al., 2011). Values for A-series aptamers were also published (Nicol et al., 2011). After 10 rounds of SELEX process, the K_{Dapp} for the naïve pool was shown to be decreased from 333 nM to 58 nM. Amongst A-series aptamers, A3 (K_{Dapp} = 251 nM) differs from A2 (K_{Dapp} = 107 nM) by 1 nucleotide and from A1 (K_{Dapp} = 87 nM) by 2 nucleotide deletions. These few nucleotide changes were shown to affect binding affinities of aptamers as indicated in brackets, above. A-series aptamers especially A2 were the focus for this study.

1.4 Aims of the project

One of the aims of this project was to characterise previously selected aptamers to HPV16 E7. These aptamers were used to analyse their effects on the steady state levels of E7 and also in the induction of apoptosis in HPV positive cells. There were several questions. Are these aptamers cross-reacting with E7 from other HPV types? Does the 5' triphosphate group of the aptamer trigger an interferon response and if so, could this be partly responsible for the induction of apoptosis in cervical cancer cells?

If E7 is lost from the cells after aptamer treatment, is this degraded? If so, how does E7 degradation occur? Was this through general protein degradation pathways or were there some other mechanisms also involved?

Did aptamer transfection alter the localisation of E7 in cells?

For an aptamer to be used as a therapeutic reagent, an efficient delivery system needs to be generated. For this, several questions were asked. Can we deliver aptamers into cells without the need for transfection? If so, can we block this by using endocytosis inhibitors? Can we analyse the efficiency of the uptake? Do the molecules enter cells through passive or active internalisation? Which endosomal compartments do aptamers localise? Can we use alternative delivery methods such as nanoparticles to introduce aptamers into cells?

The outcome of this study should therefore aid to the further characterisation of HPV16 E7 aptamers and also to understand internalisation and localisation of aptamers in cells.

2 MATERIALS AND METHODS

2.1 General Buffers, Media and Reagents

2.1.1 Luria-Bertani (LB) broth

10 g NaCl

10 g Tryptone

5 g Yeast extract

1 L dH_2O

For LB agar, add 1 g Bactoagar

2.1.2 10xTBE (Tris-borate-EDTA) buffer pH 8.3

100 g Tris base

55 g Boric acid

9.3 g Na_4EDTA

1L dH2O

For 1x TBE buffer, dilute 100 ml in 1L dH2O

2.1.3 6x DNA loading buffer

0.03% bromophenol blue

0.03% xylene cyanol FF

30% glycerol

10 mM Tris-HCL (pH 7.5)

50 mM EDTA (pH 8.0)

2.1.4 Protein extraction buffer

20 mM Tris-HCl (pH 7.5)

250 mM NaCl

0.5% Nonidet P40 (NP40)

2.1.5 SDS-PAGE resolving gel

0.4 M Tris-HCl (pH 8.8)

8, 10, 12 or 15% 29:1 Acrylamide: bisacrylamide

10% SDS

10% Ammonium persulphate (APS)

1% NNNN-tetramethyl-ethane-1, 2-diamine (TEMED)

2.1.6 SDS-PAGE stacking gel

0.2 mM Tris-HCl (pH 6.8)

5% 29:1 Acrylamide: bisacrylamide

10% SDS

10% APS

1% TEMED

2.1.7 Laemmli SDS-PAGE loading buffer

4% SDS

20% glycerol

10% 2-mercaptoethanol

0.004% bromphenol blue

25 mM Tris-HCl (pH 6.8)

2.1.8 10x SDS-PAGE running buffer

10 g SDS

30.3 g Tris-HCl

144.1 g Glycine

1L dH_2O

For 1x SDS-PAGE running buffer, dilute 100 ml in 1L dH_2O

2.1.9 Coomassie blue protein stain

2.5 g Coomassie brilliant blue

300 ml methanol

100 ml acetic acid

400 ml dH_20

Mix and adjust to 1L with dH_2O

2.1.10 Coomassie destain solution

300 ml methanol

100 ml acetic acid

400 ml dH_20

Mix and adjust to 1L with dH_2O

2.1.11 10x PBS

1.4 M NaCl

27 mM KCl

100 mM Na_2HPO_4

18 mM KH_2PO_4

For 1 x PBS, dilute 100 ml in 1L dH_2O

2.1.12 TE buffer

10 mM Tris-HCl (pH 7.5)

1 mM Ethylenediamine tetra-acetic acid (EDTA)

2.1.13 Eukaryotic cell growth medium

Dulbecco`s Modified Eagle`s Medium (DMEM)

10% (v/v) Foetal bovine serum

100 units/ml penicillin

0.1 mg/ml streptomycin

1% (w/v) glutamine

2.1.14 Propidium iodide (PI) stain

50 µg/ml PI

50 units/ml RNase A

Diluted in PBS

2.1.15 10 x Annexin V buffer

100 mM HEPES (pH 7.4)

1.4 M NaCl

25 mM $CaCl_2$

For 1x Annexin V buffer, dilute 1 ml in 10 ml dH_2O

2.1.16 Radio-immunoprecipitation assay (RIPA) buffer

50 mM Tris-HCl (pH 8.0)

150 mM NaCl

1% (v/v) Nonidet P-40

0.5% (w/v) Sodium deoxycholate

0.1% (w/v) SDS

2.1.17 10x Transfer buffer

30.3 g Tris-base

144.1 g Glycine

1L dH_2O

For 1 x transfer buffer, dilute 100 ml in 200 ml methanol and 700 ml dH_2O

2.1.18 10x TBS-T

500 mM Tris-HCl (pH 7.5)

1.5 M NaCl

1% (v/v) Tween-20

For 1x TBS-T, dilute 100 ml in 1L dH_2O

2.1.19 Chemiluminescence reagent

Solution 1:

2.5 mM luminol

400 µM p-coumaric acid

100 mM Tris-HCl (pH 8.5)

Solution 2:

0.018% (v/v) H_2O_2

100 mM Tris-HCl (pH 8.5)

Immediately prior to use, mix solution 1 and 2 in a 1:1 ratio

2.1.20 10x T7 RNA polymerase buffer

10 x Tris-acetate buffer

400 mM Tris-acetate

10 mM EDTA

100 mM MgAc

5 mM $MnCl_2$

Titrate with 5M NaOH to pH 8.0

Sterilise by autoclaving

To make 10 x T7 polymerase buffer, take 100 ml of 10 x Tris-acetate buffer and add 80 mM spermidine.

Titrate again with 5 M NaOH to pH 8.0

Filter sterilise and keep at -20°C

2.1.21 Acidic wash buffer

0.2 M Glycine

0.15 M NaCl

Adjust to pH 3.0 with HCl

2.2 Oligonucleotides

Cy3 – Apt21-2 (2' F-U and C)
5' Cy3 – GGUCUAGCCGGAGGAGUCAGUAAUCGGUAGACC – 3'

Cy5 – Apt21-2 – Cy3 (2' F-U and C)
5' Cy5 – GGUCUAGCCGGAGGAGUCAGUAAUCGGUAGACC – Cy3 3'

Cy3 – 47tr (2' F-C)
5' Cy3 – GGGUUAACAGAAAACCUCAGUUGCUGGGUUGU – 3'

Control aptamer SF1 template DNA sequence:
5' – GGGAATGGATCCACATCTACGAATTCGGCTCAAAAATACGTCCGC
ACCATACATTCACTGCAGACTTGACGAAGCTT – 3'

HPV16 E7 aptamer template DNA sequences:
A1:
5' – GGGAATGGATCCACATCTACGAATTCCCTTCATTAACCCGTCCACGC
GCTTCACTGCAGACTTGACGAAGCTT – 3'
A2:
5' – GGGAATGGATCCACATCTACGAATCCCTTCATTAACCCGTCCACGC
GCTTCACTGCAGACTTGACGAAGCTT – 3'
A3:
5' – GGGAATGGATCCACATCTACGAATCCTTCATTAACCCGTCCACGC
GCTTCACTGCAGACTTGACGAAGCTT – 3'
J1:
5' – GGGAATGGATCCACATCTACGAATCACGTTGAGGCCGTCGGGCTG
TTCGGAGCACCCTTCACTGCAGACTTGACAGAAGCTT – 3'

HPV18 E7 forward primer

5' – TATATAGGATCCATGCATGGACCTAAGGC – 3'

HPV18 E7 reverse primer

5' – TATATAGAATTCTTACTGCTGGGATGC – 3'

HPV11 E7 forward primer
5' – TATATAGGATCCATGCATGGAAGAC – 3'
HPV11 E7 reverse primer
5' – TATATAGAATTCTGGTTTTGGTGCGC – 3'

pGEX sequencing primers:
pGEX5' (Forward)
5' – GGGCTGGCAAGCCACGTTTGGTG – 3'
pGEX3' (Reverse)
5' – CCGGGAGCTGCATGTGTCAGAGG – 3'

Aptamer template primers:
N30P1 (Forward)

5' – TGATAATACGACTCACTATAGGGAATGGATCCACATCTACGAAT – 3′

N30P2 (Reverse)

5' – AAGCTTCGTCAAGTCTGCAGTGAA – 3'

U6 qPCR primer sequences

Forward (5' – 3') CTCGCTTCGGCAGCACA

Reverse (5' – 3') GCAAATTCGTGAAGCGTT

2.3 Antibodies

Mouse monoclonal HPV16 anti-E7; clone NM2, Santa Cruz Biotechnology, Inc., USA (1:200)

Mouse monoclonal HPV16 anti-E7; clone 289-17013, AbCam, UK (1:2000)

Mouse monoclonal HPV18 anti-E7; clone 8E2, AbCam, UK (1:2000)

Rabbit anti-GAPDH, Sigma-Aldrich, USA (1:6000)

Mouse monoclonal anti-pRb, clone 1F8, AbCam, UK (1:2000)

Rabbit polyclonal anti-pRb, Clone Ab-2, Calbiochem, Merck Millipore, USA (1:1000)

Mouse monoclonal anti-Rb2, clone 10/Rb2, BD Biosciences, USA (1:1000)

Alexaluor 568 F (ab`) 2 fraqment of goat anti-mouse IgG (H+L), Invitrogen (Life Technologies), UK (1:500)

Alexafluor 488 chicken anti-mouse IgG (H+L), Invitrogen (Life Technologies), UK (1:500)

Alexafluor 488 goat anti-rabbit IgG (H+L), Invitrogen (Life Technologies), UK (1:500)

Alexafluor 488 donkey anti-goat IgG (H+L), Invitrogen (Life Technologies), UK (1:500)

Rabbit polyclonal anti-EEA1, Millipore, USA (1:500)

Rabbit polyclonal anti-LAMP-1 (CD107a), Millipore, USA (1:500)

Sheep anti-TGN46 (1/500), a gift from Dr Vas Ponnambalam, University of Leeds, Leeds, UK

Donkey anti-sheep 488, Invitrogen (Life Technologies), UK (1:500)

Goat anti-mouse IgG peroxidase conjugate, Sigma, USA (1:2000)

Goat anti- rabbit IgG peroxidase, Sigma, USA (1:1000)

Mouse monoclonal acetylated anti-tubulin (6-11B-1), Sigma-Aldrich, USA (1:500)

Mouse purified anti-GST, BioLegend, Inc., USA (1:1000)

Rabbit monoclonal anti-calreticulin (D3E6), Cell Signalling, USA (1:200)

Rabbit polyclonal anti-LC3, (1:2000) was provided by Prof Mark Harris, University of Leeds, Leeds, UK

2.4 Enzymes

Terminal deoxynucleoside transferase, stored at – 20°C (New England Biolabs (NEB), USA)

Yeast inorganic pyrophosphatase, stored at – 20°C (YIP, Sigma Aldrich, USA)

T7 RNA polymerase (Y639F), stored at – 20°C (Padilla and Sousa, 1999) (a kind gift from Dr David Bunka, University of Leeds)

RNaseOut, stored at – 20°C (Invitrogen [Life Technologies], UK)

pfu DNA polymerase, stored at – 20°C (Promega, USA)

Taq DNA polymerase, stored at – 20°C (New England Biolabs, USA)

DNase, stored at – 20°C (Promega, USA)

DNase I, stored at – 20°C (Thermo Scientific, USA)

2.5 Cell lines

SiHa (ATCC No. HTB-35), derived from a human squamous cell carcinoma of the cervix, contains 1 copy of the HPV16 genome integrated into chromosome 13 (Baker et al., 1987, el Awady et al., 1987).

CaSki (ATCC No. CRL-1550), derived from a human epidermoid carcinoma of the cervix, contains approximately 600 copies of the HPV16 genome arranged as tandem repeats distributed across 11 chromosomes (Baker et al., 1987, Mincheva et al., 1987).

HaCaT, spontaneously immortalised human keratinocyte cell line (Boukamp et al., 1988).

HaCaT HPV16 and HPV18 E6/E7 expressing stable cell lines were generated by Kat Richards (University of Leeds, Leeds, UK) (Richards et al., 2014).

HeLa (ATCC No. CCL-2), derived from a human adenocarcinoma of the cervix, contains approximately 10-50 copies of HPV18 genome (Scherer et al., 1953).

C33A (ATCC No. HTB-31), derived from a human epidermoid carcinoma of the cervix, expresses abnormal size retinoblastoma protein (pRb) and elevated levels of p53 with a point mutation at codon 273 resulting in an Arg to Cys substitution. These cells are negative for HPV DNA (Yee et al., 1985).

HEK293T (CTCC no. CRL-3216) (formerly known as 293tsA1609neo), a derivative of human embryonic kidney 293 cells. It contains the SV40 T-antigen and is highly transfectable.

SaOS-2(ATCC No. HTB-85), derived from primary osteosarcoma (Fogh et al., 1977, Rodan et al., 1987).

2.6 Electrophoresis methods

2.6.1 Agarose gel electrophoresis

DNA samples were mixed with 6 x DNA loading buffer (Promega, USA) and resolved by using agarose gels with the concentrations of 0.8 (≥1kb DNA) – 2 (≤300bp DNA)% (w/v) depending on the sizes of DNA fragments. 1 x TBE buffer and 1xSYBR safe (Invitrogen, Life Technologies) were used as running buffer and DNA stain, respectively. Current was applied to electrophoresis unit at 8 – 10 V/cm for 45 min until the blue dye reaches the bottom of the gel. DNA was visualised under UV light using a GeneDoc system (Syngene).

2.6.2 RNA gel electrophoresis

RNA samples were electrophoresed using 12% (w/v) 19:1 acrylamide/bis-acrylamide gel containing 7M urea in 1X TBE (Severn Biotech, UK). RNA samples and marker (RiboRuler, Fermentas, Thermo Fisher Scientific, USA) were denatured in RNA loading buffer containing 95% (v/v) formamide, 0.025% (w/v) SDS, 0.025% (w/v) bromophenol blue, 0.025% (w/v) xylene cyanol FF, 0.025% (w/v) ethidium bromide and 0.5 mM EDTA (Fermentas,Thermo Fisher Scientific) at 95° C for 10 min. Gel was preheated at 12 W for at least 30 min before loading the samples. Electrophoresis was performed at 10 W for between 30-45 min. Gel was stained in 1 x SYBR safe/TBE for 15 min to allow visualisation of RNA.

2.6.3 SDS-polyacrylamide gel electrophoresis (SDS-PAGE)

Proteins were analysed on 8, 10, 12 or 15% (w/v) 29:1 acrylamide/bisacrylamide gels (Severn Biotech, UK) containing 375 mM Tris (pH 8.8) and 0.1% (w/v) SDS with a 5% (w/v) acrylamide stacking layer containing 187.5 mM Tris (pH 6.8) and 0.1% (w/v) SDS. Samples were denatured by incubation in Laemmli SDS-PAGE loading buffer (Sigma, USA) at 95°C for 5 min. Electrophoresis was performed in 1 x SDS-PAGE running buffer at 150-200 V. Proteins were visualized by staining in InstantBlue (Expedeon, Inc., USA) or Coomasie blue stain for 15 min – 1 h.

2.6.4 Western blotting

SDS-PAGE gels were soaked in 1 x ice-cold transfer buffer for 5 min before assembly in a vertical rig for transfer to nitrocellulose membrane (Whatman) or PVDF (Millipore,

USA). Vertical electrophoretic transfer was performed at 30 V at room temperature for 1.5-2 hrs. Membranes were washed in 1 x TBS-T and blocked in 5% (w/v) milk/TBS-T for at least 1 h prior to incubation with primary antibodies diluted in 5% (w/v) milk/TBS-T overnight at 4°C. Membranes were washed for 4 x 15 min in 1 x TBST prior to incubation with secondary antibodies diluted in 5% (w/v) milk/TBS-T for 1 h at room temperature. Membranes were again washed for 4 x 15 min in 1 x TBS-T. Membranes were incubated with ECL (Thermo Scientific, USA) for 1 min and exposed to X-ray films (Hyperfilm ECL, GE Healthcare, USA) and developed manually or automatically (Konica film processor, Srx-101A). Densitometry analysis of western blots was perfomed using Aida image analyser software (Raytest) and levels of protein expressions were normalised against the level of housekeeping protein GAPDH.

2.7 Preparation of plasmid DNA

The HPV16 E7 open reading frame (ORF) had previously been cloned from a plasmid containing the HPV16 ORFs, pEF3.99 (obtained from Dr P. Lambert, University of Wisconsin-Madison, GenBank Accession Number AF125673) into the BamHI and EcoRI restriction sites of pGEX-2T expression vector (GE Healthcare, USA). Resulting pGEX-2T-E7 plasmid was transformed into *E. coli* (DH5α) and (BL21) (Invitrogen, Life Technologies, UK) cells and sequence analysis was performed using the pGEX 5' and 3' standard sequencing primers. Sequencing analysis was performed by DNA sequencing unit of Beckman Coultier Genomics. PCR amplification of HPV 11 and 18 E7 fragments were performed from pBabepuro constructs containing whole HPV11 or 18 genomes (kindly provided by Dr Andrew Macdonald, University of Leeds, Leeds). HPV11 and 18E7 were amplified from these plasmid templates using specific primers by *Pfu* DNA polymerase (NEB, USA). pGEX-6P-1 plasmid were double digested with EcoRI (NEB, USA) and BamHI (NEB, USA) restriction enzymes at 37°C for 2 h. PCR products and linearised vector were analysed on agarose gels and gel purification was performed to recover the DNA. Ligation reaction was performed 3:1 vector: insert molar ratios using T4 DNA ligase 1 h at room temperature. *E. coli* DH5α cells were transformed with ligation reactions and spread on LB/amp (100 µg/ml ampicillin) plates. Following overnight incubation at 37°C, several colonies were picked to perform colony PCR and diagnostic digestion. Positive clones were sent for sequencing to confirm the presence of inserts. Sequencing primers were pGEX 5' and 3' (section 2.2).

2.8 Transformation of competent cells

Stocks of transformation competent *E. Coli* DH5a were produced using calcium chloride ($CaCl_2$) in the lab (by research technicians; Susan Matthews and Rajni Bhardwaj). Transformation of plasmid DNA into *E. coli* DH5α was performed using heat shock method. 650 µl LB was added onto the transformants and incubated at 37°C with shaking. Serial dilutions (50 µl, 100 µl and 200 µl) were spread onto LB/Amp plates (100 µg/ml ampicillin) and plates were left overnight at 37°C. A colony was picked from plates and inoculated into LB/amp broth (100 µg/ml ampicillin) to grow overnight. Next day, glycerol stocks of BL21 (DE3)-pGEX-2T-16E7, pGEX-6P-1-11E7 and pGEX-6P-1-18E7 were prepared by mixing equal volumes of 80% glycerol and cell suspension, and stored at – 70°C.

2.9 Recombinant protein expression

2.9.1 Expression in *E. coli* BL21 (DE3) cells

pGEX-2T-16E7, pGEX-6P-1-11 and pGEX-6P-1-18E7 transformed *E. coli* BL21 (DE3) from glycerol stocks were inoculated into 20 ml LB broth supplemented with 100 µg/ml ampicillin and incubated with shaking at 37°C overnight. 5 ml of this starter culture was used to inoculate 500 ml LB broth supplemented with 100 µg/ml ampicillin and incubated with shaking at 37°C until OD600 reached 0.6 – 0.7. GST-11E7, GST-16E7 and GST-18E7 expressions were induced by the addition of 1mM isopropyl β-D-1-thiogalactopyranoside (IPTG) (Fisher Scientific, USA) overnight at 16°C, 3 hrs at 37°C and 6 hrs at 30°C, respectively. Cells were pelleted by centrifugation at 18,600 x g (Avanti® J-26xp centrifuge), 4°C for 20 min and re-suspended in 20 ml protein extraction buffer containing 1 mg/ml lysozyme (Calbiochem [Merck Millipore], USA) and 5 µg/ml DNase I (Thermo Scientific, UK, stored at – 20°C). Cells were lysed on ice by sonication for 6 x 20 seconds with 30 seconds intervals (Soniprep 150, Sanyo). The soluble protein fraction was obtained by centrifugation at 16,100 x g at 4°C for 2 min (Centrifuge 5415 R, Eppendorf). A 20 µl aliquot of the soluble fraction and 2 ml pellet (as insoluble fraction) was reserved for SDS-PAGE analysis.

2.9.2 Purification of GST-E7 via a glutathione sepharose column

A few millilitres of Glutathione sepharose 4b (GE Healthcare, USA) was placed into a column followed by a wash with 1 x PBS. Supernatant of the cell lysate obtained by centrifugation after sonication was filtered using 0.22 µm filters and applied to the glutathione column. Column was then washed with 0.5% Triton X-100/PBS. Proteins were eluted from glutathione beads with 50 mM reduced glutathione, pH 8.0. Proteins

in the flow through, wash and elution fractions were analysed by SDS-PAGE. Protein samples might be stored in 10% glycerol at – 20°C.

2.9.3 Buffer exchange by dialysis of protein

Appropriate length of dialysis membrane (Spectrum Laboratories, Inc., UK) with a molecular weight cut-off (MWCO) of 6-8 kDa was left in the dialysis buffer (e.g. 1 x phosphate buffered saline) for 10 – 15 min. Elution fractions was collected in the membrane and stirred in the dialysis buffer overnight at 4°C. PBS buffer was changed twice in order to remove the elution buffer from protein solution.

2.9.4 Binding of GST-E7 protein to glutathione sepharose beads

To bind GST-E7 to glutathione sepharose (GE Healthcare, USA) beads, sepharose first washed with 1 x PBS three times. Dialysed protein was then mixed with glutathione sepharose and incubated for 1 hour at 4°C on a mixing platform. Glutathione sepharose beads were recovered via centrifugation, supernatant was also used for SDS-PAGE analysis. Beads were then washed with 1 x PBS, washes were also used for SDS-PAGE analysis.

2.10 Methods used in cell culture

2.10.1 Maintenance of the cell culture

Maintenance of HEK293T, SaOS-2, CaSki, HeLa, C33A and HaCat cells was managed in DMEM containing 1% L-glutamine (GE Healthcare, USA) supplemented with 10% foetal bovine serum (FBS) (PAA, Austria), 100 units/ml penicillin (Lonza, Slough, UK), 0.1 mg/ ml streptomycin (Lonza, Slough UK) in T-25 flasks. Cells were observed using a light microscope. Cell passages were performed every 3 – 4 days before they became 80 – 90% confluent. Old medium was removed from the flask and the cells were washed with 1 x PBS before addition of 2 x Trypsin. When cells were detached from the surface of the flask, they were transferred into sterile falcon tubes. $1/10^{th}$ of the cell suspension were transferred back into the flask to maintain the cell culture. Growth medium (maximum 15 ml for T-25 flasks) was added onto cells. Flasks were then placed in the horizontal position in the humidified incubator (37°C; 5% CO_2). HaCat stable cells expressing HPV 16 and HPV 18 E7 (provided by Dr Kat Richards, University of Leeds, Leeds) were maintained as described above with the addition of 0.5 µg/ml puromycin. Generally, 0.4 x 10^6 cells/well were seeded in 6-well plates 24-hour prior to transfection to be used in experiments. Cells were

counted using a Neubauer hemocytometer (Assistant, Germany). Tryptan blue solution (0.4 %) (Sigma, USA) was used to screen out dead cells.

2.10.2 Culture of primary keratinocytes

Human primary keratinocytes (HPK) were cultured in Keratinocyte Growth Media (KGM) Kit II (PromoCell, Heidelberg, Germany). Culture medium was changed every second to third day. On stimulation keratinocytes were placed in Keratinocyte Growth Media with all supplements apart from epidermal growth factor and hydrocortisone. When the HPK cells reached 60-70% confluency the cells were passaged. Cells were washed with sterile phosphate buffered saline (PBS) (Gibco, Life technologies, UK) and then EDTA (Versen) 1% (Pan Biotech, Germany) for 2 min at 37°C, 5% CO_2. Trypsin (170.000U/L)-EDTA (200mg/ml) (Lonza, Slough, UK) was added and placed in the incubator for 2 minutes at 37°C, 5% CO2. An equal amount of trypsin neutralising solution (Lonza, Slough, UK) was added to the trypsinised cells in order to neutralise the enzyme. The cells were then centrifuged at 230 x g and then re-seeded. Cells were cultured at 37°C with 5% CO2.

2.10.3 Bringing up frozen cells

A vial of cells from liquid nitrogen or – 70°C freezer was removed and thawed quickly in a water bath. Cells were then mixed with 5 ml DMEM (GE Healtcare, USA) and centrifuge in order to remove DMSO (Sigma, USA). Pellet was re-suspended in appropriate amount of media and placed in a T-25 flask in a total volume of 5 ml growth medium. Flask was maintained in a CO_2 cabinet at 37°C. Media was changed in 24 hours with the fresh medium.

2.10.4 Preparation of freezer stocks

Cells were collected from the flask and transferred into a 15 ml falcon tube. The falcon tube was then centrifuged at 230 x g for 5 min to pellet the cells. Media was removed and cells were re-suspended in 1 ml of freezing mixture (10% DMSO, 90% FBS). Cells were frozen gradually with 1°C per minute in isopropanol at – 70°C.

2.10.5 Transfection of cells

2.10.5.1 Polyethylenimine (PEI) transfection

2 – 3 µg of plasmids was diluted in 200 µl of serum-free media (DMEM, GE Healtcare, USA) and mixed by vortexing. 10 µl of PEI (1 µg/µl) reagent was added to plasmid suspension, and incubated at room temperature for 10 – 15 min. PEI-plasmid mixture

was applied onto HEK293T cells in a drop wise manner and cells were allowed to express proteins in the humidified CO_2 incubator at 37°C for 24 hrs.

2.10.5.2 Introducing aptamers into cells by Oligofectamine

Cells were transfected with aptamers to a final RNA concentration of 100 nM using Oligofectamine (Invitrogen, Life Technologies, UK). 3 µl of Oligofectamine and 12 µl of serum-free medium (DMEM, GE Healtcare, USA) were mixed and incubated at room temperature for 5 min. 100 nM of RNA was diluted in 185 µl serum free DMEM. Oligofectamine (15 µl) and RNA diluents (185 µl) were mixed and incubated for 20 min at room temperature. Meantime, cells were removed from the incubator, old medium was aspirated and they were washed with 1 x PBS. 800 µl of serum free DMEM was added onto 70% confluent cells. Oligofectamine – RNA mixture was then added onto cells in a drop wise manner and plates were placed in the humidified CO_2 incubator (37°C) for 4 hrs. When this period is over, cells were returned to 10% serum-media by adding 500 µl of 30% FBS/DMEM, and left to grow overnight.

2.10.5.3 Introducing aptamers into cell by HappyFect (Nanocin)™

Cells were transfected with aptamers to a final RNA concentration of 100 nM using HappyFect™ (Nanocin) (Tecrea, UK). Aptamer was diluted in 50 µl serum-free media (DMEM, GE Healthcare). 4 µl of nanocin was added into the aptamer mixture and incubated for 15 min at room temperature. Meantime, cells were removed from incubator, old medium was aspirated and cells were washed with 1 x PBS. 450 µl of serum free DMEM was added onto 70% confluent cells in a 12-well plate. HappyFect – RNA mixture was then added onto cells in a drop wise manner and plates were placed in the humidified CO_2 incubator (37°C) for 4 hours. When this period is over, cells were returned to 10% serum-media by adding 250 µl of 30% FBS/DMEM, and left to grow overnight.

2.10.6 Collection of cells and protein extraction

Media was removed into 15 ml tubes and cells were collected after 2 x trypsin treatment for 5 – 10 min. Tubes were centrifuged to obtain the pellet. Cells were washed with 1 x PBS and transferred into 1.5 ml Eppendorf tubes. Cell suspension was then centrifuged again in the chilled centrifuge at 4°C at 16,100 x g for 2 min. Cell pellet was re-suspended in appropriate volume of RIPA buffer containing EDTA free protease inhibitor tablet (Roche, Penzberg, Germany) (1 tablet for 10 ml buffer), DNase (5 µg/ ml) and 10 mM $MgCl_2$, and incubated on ice for 30 min, vortexing every 10 min. Protein sample was mixed with 2 x Laemmli buffer and boiled to denature at

95°C for 5 min. Protein samples were loaded in the SDS-acrylamide gel for separation after 1 min centrifugation at 16,100 x g.

2.11 Generation and labelling of 2'-fluoro-modified RNA molecules

A library for templates of RNA aptamers selected against GST-E7 is available (Nicol et al., 2011). Sequences of some of the aptamers are listed in Section 2.2.

2.11.1 PCR amplification of DNA template for in *in vitro* transcription

DNA template below which harbours a T7 recognition site at the 5' – end was utilized to generate RNA aptamers by *in vitro* transcription. T7 enzyme recognises the sequence below underlined in order to initiate RNA synthesis starting from nucleotides, GGG. N_{30} region is specific to each aptamer molecules while constant region is shared between different aptamers to enable primer binding to initiate the PCR amplification.

TGATAATACGACTCACTATAGGGAATGGATCCACATACTACGAAT

-N_{30}-TTCACTGCAGACTTGACGAAGCTT

Amplification of double stranded DNA template was achieved using N30P1 (Forward) and N30P2 (Reverse) primers. *Pfu* DNA polymerase (2.5 U) (Promega, USA) and 10 x *Pfu* DNA polymerase buffer (Promega, USA) [200mM Tris-HCl (pH 8.8), 100mM KCl, 100mM $(NH_4)_2SO_4$, 20mM $MgSO_4$, 1mg/ml nuclease-free BSA and 1% Triton® X-100], 0.2 mM of each dNTPs, 0.5 µM each primers (N30P1 and N30P2) and 20-40 ng aptamer DNA template were used for 50 µl of PCR reaction.

PCR was performed in the conditions below:

1 cycle	
Initial denaturation	95°C for 5 min
25 cycles	
Denaturation	95°C for 30 sec
Primer annealing	52°C for 30 sec
Extention	72°C for 1 min
1 cycle	

Final extension 72°C for 5 min

PCR fragments were then recovered from an agarose gel using gel purification kit (Qiagen, USA). Another PCR reaction was performed using templates obtained from gel purification step. Resulting PCR product was cleaned up by using PCR purification kit (Qiagen, USA).

2.11.2 *In vitro* transcription of 2`-fluoro-modified RNA

In vitro transcription was achieved using 1 µg of template DNA, 20 units of mutant T7 RNA polymerase, 10 x T7 RNA polymerase buffer, 10 mM dithiothreitol (DTT), 2 units of yeast inorganic pyrophosphatase (YIP, Sigma Aldrich, USA), 0.2 mM ATP and 0.2 mM GTP (Fermentas [Thermo Fisher Scientific], USA), 0.2 mM 2'-fluoro-UTP and 0.2 mM 2'-fluoro-CTP (TriLink Biotechnologies, USA) for 3 hrs at 37°C. After incubation, DNA template was removed by 5 units of RNase free DNase (Promega, USA) treatment for 30 min at 37°C. This enzyme was inactivated by incubating at 65°C for 10 min, alternatively EDTA to 1 mM would stop the reaction. Excess nucleotides were removed using a spin column (NucAway spin column, Ambion Inc., Life Technologies, UK) which retains free nucleotides while eluting the RNA into the solution. Neutral phenol: chloroform extraction was performed to purify RNA from proteins. An equal volume of cold phenol: chloroform: isoamyl alcohol (25: 24: 1) was added to the RNA sample and mixed by vortexing followed by centrifugation at top speed for 2 min to separate the phases, the aqueous phase was removed and this step was repeated three times. Additional step was performed in chloroform only to remove phenol. The aqueous phase was removed and 1/10 volume of 3M sodium acetate and 2.5 volume of ice cold 100% ethanol were added into the tube. The sample was left at – 20°C to precipitate for 1 h or overnight followed by centrifugation at 16,100 x g for 20 min. RNA pellet was then mixed with 70% ice cold ethanol and centrifuged to the pellet at 16,100 x g for 10 min. Ethanol was removed, and the pellet was left to dry for 5 min at room temperature prior to re-suspending in RNase-free dH_2O (Severn Biotech, UK).

2.11.3 Quantitation of aptamers

Following removal of excess nucleotides using a NucAway column, aptamers were quantified by NanoDrop (Thermo Scientific, USA). An A_{260} value of 1 was estimated to be equivalent to 40 µg/ml RNA. The A_{260}/A_{280} ratio around ~2.0 was indicative of purified RNA (low contamination by proteins, phenol and other contaminants).

2.11.4 De-phosphorylation of aptamers

De-phosphorylation of *in vitro* transcribed A2 and SF1 RNA (section 2.11.2) was performed using 4 µM of aptamer, 10 x reaction buffer, 20 units of RNaseOut (Invitrogen, Life technologies, UK) and 10 units of Antarctic phosphatase (New England BioLabs, UK) for 45 min at 37°C. Reaction was inactivated at 70°C for 10 min. Mixture was phenol: chloroform extracted and ethanol precipitated overnight. RNA was eluted in nuclease-free dH_2O to obtain 10 µM aptamer solutions.

2.11.5 Fluorescent labelling of aptamer

In order to label 5' end of aptamers with fluorescein maleimide, aptamer RNAs were de-phosphorylated, phenol: chloroform extracted and ethanol precipitated before labelling performed. All were performed according to the manufacturer`s instructions by Vector Laboratories. Up to around ~10 µg RNA (0.6 nmols of 5' ends) was incubated with 1 µl universal reaction buffer and 1 µl alkaline phosphatase (Vector Laboratories, USA) in a total reaction volume of 10 µl (with dH_2O). Reaction was incubated for 30 min at 37°C. The entire dephosphorylation reaction mixture were then treated with 2 µl universal reaction buffer, 1 µl ATPγS, 2 µl T4 polynucleotide kinase in a total reaction volume of 20 µl (with dH_2O). Mixture was incubated for 30 min at 37°C. Then 10 µl (135 µg) of thiol-reactive label [Fluorescein Maleimide, ($C_{27}H_{18}N_2O_8$)] (Vector Laboratories, USA) was added in to the reaction mixture for additional 30 min at 65°C in order to allow labelling of 5' end of RNA. The RNA was again phenol: chloroform extracted and ethanol precipitated to remove excess label (Section 2.11.2).

2.12 RNA extraction, cDNA synthesis and Quantitative PCR (qPCR)

SiHa and C33A cells were transfected with 100 nM A2, SF1 or 21-2 and de-phosphorylated A2 and SF1 along with mock transfection and Poly I:C (InvivoGen, France) incubations as negative and positive controls, respectively. Poly I:C was used at 1 µg/ml from the stock of 1 mg/ml. Cells were maintained at 37°C for 24 h. Cells were harvested and RNA was extracted using Quick RNA Mini-prep kit (Zymo Research, USA) according to the manufacturer`s instructions. RNA was eluted in 35 µl of $dH_2O$. cDNA synthesis were performed using First-strand cDNA synthesis kit (Thermo Fisher Scientific, UK), following manufacturer`s instructions. Around ~1 µg of RNA (~10 µl) was pre-incubated with 0.5 µg (1 µl) oligo $(dT)_{18}$ for 5 min at 65°C. Then, reaction buffer, 20 units of RiboLock RNAase inhibitor, 2 mM dNTP mix, 20

units of M-MuLV Reverse Transcriptase were added for 60 min at 42°C. Enzyme was inactivated by incubating at 70°C for 10 min. Quantitative real-time PCR (qPCR) was performed using the Quantifast SYBR Green PCR kit (Qiagen, Germany) by a Corbett Rotor-Gene 6000 (Qiagen, Germany). Around ~ 80 ng of cDNA, 1 µM from forward and reverse primers and 2 x Quantifast SYBR Green PCR master mix were combined in a 25 µl of total reaction. Primers utilised were MX1, IFNβ, which were purchased from Qiagen. U6 forward and reverse primers were purchased from Sigma and sequences were as listed in Section 2.2. Conditions for PCR reactions were as follows: initial activation step and two-step cycle of denaturation, for 5 min at 95°C and 10 sec at 95°C, respectively, followed by 40 x repeats of combined annealing and extension steps for 30 sec at 60°C. A melting curve from 60°C to 95°C with 5 sec at every 1°C interval was performed at the end of last cycle. Data was analysed according to the ΔΔ C_t method described previously (Livak and Schmittgen, 2001) using the Rotor-Gene 6000 software.

2.13 Analysis of apoptosis by flow cytometry using Annexin V

Cells were transfected with up to 200 nM of aptamer RNA (section 2.10.5.2) and maintained at 37°C for 24 h. Cells were washed with 1 x PBS and incubated with trypsin (section 2.10.6). Cells were collected in 5 ml flow cytometry tubes and pelleted by centrifugation at 230 x g. Pellets were washed 3 times with 1 x PBS and re-suspended in 100 µl ice cold Annexin V buffer. 3 µl of FITC – conjugated Annexin V (BD Biosciences) was added and incubated on ice for 15 min. Cells were co-stained with 5 µl of 50 µg/ml propidium iodide/PBS. Analysis was performed using the FACSCalibur (Becton Dickinson) software. Cells were treated with staurosporine (Cell Signalling, USA) at 1 µM for 24 hrs as a positive control for apoptosis.

2.14 Immunostaining of cells

Cells on coverslips were washed three times with 1 x PBS for 5 min each. Cells were fixed with 4% (v/v) formaldehyde/PBS for 10 min at room temperature. Cells were washed 3 x with PBS in order to remove formaldehyde. Permeabilisation of cells was performed by incubation in 0.1% (v/v) TritonX-100/PBS for 10 min. Cells were again washed with 1 x PBS, and incubated in blocking solution [1% BSA/Triton X-100 in 1 x PBS (w/v)] for 1 h at room temperature. Primary antibodies were added onto cells with appropriate dilutions and incubated overnight at 4°C on a rotating platform. Cells were washed three times with 1 x PBS for 5 min each and incubated with flurochrome-conjugated secondary antibodies at a dilution of 1/500 in 1% BSA/Triton X-100 for 2

h at room temperature and kept in dark. Cells were washed in 1 x PBS three times and mounted on microscope slides in Vectashield containing DAPI stain (Vector laboratories, USA). Cells were imaged on the Zeiss LSM 510 upright or LSM 700 inverted confocal microscopes. In order to image fluoro labelled aptamers per se, above was performed until permeabilisation step. Then glass coverslips were mounted on microscope slides and imaged as described above.

2.15 GST- pull down assay

HaCat cells were used as a pRb source for pull down assays. Cells were lysed in radio-immunoprecipitation assay (RIPA) buffer. Lysates were pre-cleared by incubation with GST coated magnetic beads for 30 min at 4°C on a rotating platform. 10 µg of GST-E7 bound to sepharose (Section 2.9.4) was pre-incubated with aptamer RNA in 100 µl 1 x PBS at 4°C for 30 min with mixing. 600 µg of protein from the pre-cleared HaCat cell lysate was then added and incubated at 4°C for 1 h with mixing. Sepharose was recovered by centrifugation at 1200 x g and washed 3 times in RIPA buffer. Beads were re-suspended in 2 x Laemmli sample buffer, boiled at 95°C for 5 min and analysed by SDS-PAGE and Western blot (sections 2.6.3 and 2.6.4).

2.16 Use of Inhibitors to investigate the mode of protein degradation

In order to analyse the pathway of E7 degradation in the presence or absence of aptamers, inhibitors of the 26S proteasome/lysosome (MG132), 20S and 26S proteasome (lactacystin), lysosomal degradation pathway (chloroquine), HDAC6 mediated misfolded protein degradation pathway (tubacin) and ER-associated protein degradation pathway (eeyarestatin I) were utilised for treatment of CaSki cells. MG132 (Cayman Chemicals, USA), lactacystin (Tocris Bioscience, Bristol, UK), chloroquine (Sigma Aldrich, USA), tubacin (Sigma, USA) and eeyarestatin I (Calbiochem, Merck Millipore, USA) were used at concentrations of 100 µM, 20 µM, 30 µM, 25 µM and 8 µM for up to 6 h.

2.17 Detection of transfection efficiency by Flow Cytometry

Primary or SiHa cells were incubated with up to 100 nM of cy5 labelled aptamer 21-2 or transfected using oligofectamine or HappyFect-] (Nanocin) (section 2.10.5.2 and 2.10.5.3) with the aptamer. Cells were maintained at 37°C for 5 hrs and then washed with 1 x PBS and incubated with 2 x trypsin (Sections 2.10.1 and 2.10.6). Cells were collected in 5 ml flow cytometry tubes and pelleted by centrifugation at 230 x g. Pellets were washed 3 times with 1 x PBS and once with an acidic wash buffer (Section

2.1.21) (Kameyama et al., 2007), and re-suspended in 100 µl of 1 x PBS. Cells were stained with 5 µl of 50 µg/ml propidium iodide/PBS for 5 min. 10, 000 cells were counted for each sample. Analysis on flow cytometer was performed using APC (allophycocyanin) (Excitation at 633 nm, emission at 660 nm) and PI (Propidium Iodide) (Excitation at 488 nm, emission at 617 nm) channels by counting 10, 000 cells. Results were represented as percentage of cells that are positive for cy5. Data was analysed using the FACSCalibur (Becton Dickinson) software.

2.18 Treatment of cells with endocytosis inhibitors

In order to determine the pathway of uptake of aptamers, inhibitors of dynamin-mediated uptake (dynasore) and macropinocytosis (amiloride) were used in SiHa cells. Dynasore (Sigma, USA) and amiloride (Sigma, USA) were used at concentrations of 80 µM and 75 µM, respectively for up to 2 hrs treatments.

3 EFFECTS OF APTAMERS IN CELLS

3.1 Introduction

Cervical cancer is the second most common cancer in women worldwide. Nearly all cases have been linked to persistent infection with one of the approximately 15 genotypes of high risk human papillomavirus (HPVs) (Cogliano et al., 2005). Each HPV genotype could result in an independent infection. Current knowledge in the field aided the development of strategies for prevention of the disease, such as screening tests and vaccines as well as clinical management for cancer patients. High-risk HPV16 and 18 are known to be the most carcinogenic HPV genotypes, responsible for more than 70% of cervical carcinoma and almost 50% of cervical intraepithelial neoplasia (CIN) grade 3 (CIN3), whereas low-risk HPV6 and 11 have been shown to be the cause of approximately 90% of genital warts (Smith et al., 2007). The HPV genome encodes only eight genes, with E6 and E7 the major transforming HPV oncoproteins. These oncoproteins have a variety of cellular target proteins, most importantly retinoblastoma tumour suppressor protein (pRb) for E7, and p53 for E6. These interactions result in cell cycle progression and inhibiton of apoptosis, respectively, leading the transformation of infected cells. As well as pRb, E7 also target the other members of pocket protein family, p107 and p130 for degradation (Helt and Galloway, 2003, Jones and Wells, 2006). C-terminal region are highly conserved amongst all pRb family members, which is known as “pocket domain”. This region is where E2F transcription factors bind. However, E7 could also bind tightly this pocket region in order to abrogate their association with cellular targets (Chellappan et al., 1992, Liu et al., 2006). The major function of pRb is to interact with the E2F family transcription factors in order to stop cells entering into the S-phase of the cell cycle by acting as transcriptional co-repressor. Therefore inactivation and degradation of pRb by E7 leads to disruption of pRb tumour suppressor activity, causing uncontrolled division of cells (Bartek et al., 1997, Dyson, 1998).

A library of HPV16 E7 aptamers which were selected previously by a process called systematic evolution of ligands by exponential enrichment (SELEX) was available (Nicol et al., 2011). This technology has been widely used for the isolation of RNA and DNA molecules that bind a specific target with a high affinity and strong specificity from a large pool (approximately 10^{14} molecules) of random nucleotide sequences. Sequence similarity of HPV16 E7 aptamers were analysed by multiple alignment of random regions (each aptamer also contains constant region harbouring T7 polymerase and primer binding sites) and classified in to the groups that were named

A, B, C, D and E (Nicol et al., 2011). There were also other molecules that could not be grouped together due to sharing less than 65% similarity. Therefore, these outlier molecules were classified into F, G, H, I and J families. Sequence similarity of aptamers in the random region that were grouped into A and D families were 82.4% - 96.9% (Nicol et al., 2011). Although the A-family of aptamers only differed in 1-2 nucleotides, they had quite different effects on the pRb-E7 interaction as well as steady state levels of E7. It was shown previously by bead binding assays that from the A-family, only A2 disrupted the pRb-E7 interaction probably due to tertiary structures of the aptamers especially when in a complex with the target protein, E7 (Nicol et al., 2011). Bead binding assays using several mutant forms of E7 and radio-labelled A2 also suggested that disruption of pRb-E7 interaction could possibly be due to the fact that A2 might also be binding a region around LXCXE motif of E7 where pRb binding occurs (Nicol et al., 2013). SF1, selected against an unrelated protein, RNA-dependent RNA polymerase (3Dpol) of foot-and-mouth disease virus (FMDV) was included in all experiments as a control aptamer (Nicol et al., 2013). In addition, SF1 is similar to E7 aptamers in their length and constant regions (2.2). These aptamers were used in cancer cells/HPV16 E7 positive cells in order to determine their apoptotic potentials as well as the abilty to degrade E7 oncoprotein. HPV16 E7 aptamer synthesis was performed by *in vitro* transcription using chemically modified 2'-fluoro pyrimidines (U and C) and natural purine nucleotides (A and G). Modification of ribose groups with 2'-fluoro increases the stability of aptamers in cells (Kong and Byun, 2013).

Two main immune receptors, RIG-I and MDA5, have been shown to detect viral RNA in the cytosol. RIG-I like receptors (RLRs) play an important role in the inflammatory response against infection. RIG-I recognises short double stranded RNA ligands or single stranded RNA with 5' triphosphate moiety. Whereas, longer genomic RNA and replication intermediates are recognised by MDA5 (Reikine et al., 2014). When aptamers are introduced into cells, being foreign nucleic acid molecules harbouring 5' triphosphate moiety, they are recognised by host cell innate immunity through canonical pattern recognition receptors, mostly RIG-I. Some viruses such as influenza A virus and vesicular stomatitis virus (VSV) single-stranded RNA are not capped and contain a 5' triphosphate, therefore they are likely to be recognised by RIG-I receptors. Treatment of these viruses with calf intestinal phosphatase was shown to stop their stimulatory effects (Pichlmair et al., 2006). In addition, influenza virus A non-structured NS1 protein was found in a complex with RIG-I following infection, resulting in abrogation of RIG-I recognition (Pichlmair et al., 2006). In addition, some viruses

which bear 5' triphosphate such as encephalomyocarditis virus (EMCV) from the picornavirus family escapes RIG-I recognition with a different mechanism by the linkage of viral RNA to the small viral protein VPg (Gitlin et al., 2006, Kato et al., 2006, Pichlmair et al., 2006).

Non-self nucleic acids with 5' triphosphate could therefore result in the production of interferons and pro-inflammatory cytokines by downstream activation of IRF and NFκB transcription families (Chi and Flavell, 2008). There was a possibility that HPV16 E7 aptamers were triggering these responses in transfected cells, leading to apoptosis due to the presence of triphosphate on the 5' end of the aptamer following their *in vitro* transcription. Therefore, this was also investigated here.

Another objective of this chapter was to determine the cross-specificity of HPV16 E7 aptamers with E7 from other HPV types such as high-risk HPV18 and low-risk HPV11. E7 oncoproteins share a sequence similarity amongst several HPV types, such as some conserved motifs like LXCXE in CR 1 and CXXC in the C-terminal zinc finger (McLaughlin-Drubin and Munger, 2009). Aptamers are known to be highly specific to their target molecules. For instance, in a recent study, an aptamer that can specifically bind to avian influenza virus (AIV) H5N1 was utilised for the detection of AIV H5N1 in chicken swab samples with no interference detected from other AIV subtypes, such as H5N9, H7N2, H2N2, H9N2 and H1N1 (Wang et al., 2013). However, there are some other cases in the literature where an aptamer selected against a specific molecules were also shown to be targeting closely related species. One example of this is the aptamer selected against 40-residue form of Aβ (Aβ40) oligomers (Rahimi et al., 2009). This aptamer was also observed to recognise fibrils of Aβ40, Aβ42, and several other amyloidogenic proteins. Another example is the single-stranded DNA aptamer RT1t49 selected against reverse transcriptase (RT) of a subtype B strain of HIV-1 (Kissel et al., 2007). This aptamer was also demonstrated to inhibit the recombinant RT clones amongst various members of lentivirus family such as HIV-2 and SIV RTs.

In order to determine cross-specificity of HPV16 E7 aptamers *in vitro* with HPV11 and 18 E7, GST-tagged E7 constructs were generated and expressed in *E. coli* BL21 cells. Recombinant proteins were utilised in GST-pull down experiment to analyse whether HPV11 or 18 E7 – pRb interactions were affected in the presence of some of the HPV16 aptamers. In addition, some of the HPV16 aptamers were transfected in to HPV18 positive HeLa cell in order to determine and quantitate the steady state levels of 18E7, observing any degradation following addition of aptamers.

3.2 Effects of aptamers on HPV E7 levels

3.2.1 Steady state levels of E7, pRb and p130 in CaSki, SiHa and HeLa cells

p130 and pRb are cellular proteins, whereas E7 is expressed only in HPV transformed cell lines. In the first instance the steady state levels of p130, pRb and E7 expression in the cervical cancer cell lines CaSki, SiHa and HeLa cells was analysed. The cervical cancer cell lines studied here have different copy numbers of HPV DNA per cell (CaSki with 600 copies of HPV 16 and some HPV18 related sequences, SiHa with 1 – 2 copies of HPV 16, HeLa with 10 – 50 copies of HPV 18 (Chardonnet et al., 1995). Human Embryonic Kidney 293T (HEK293T) cells were used as a positive control for p130 and pRb; and a negative control for proteins related to HPV such as E7. The HEK293T cell line was generated from embryonic tissue by transformation with sheared adenovirus 5 DNA as well as transformation with the simian virus 40 (SV40) large T antigen. This cell line could be easily and efficiently transfected with plasmid DNA and therefore it has been widely used for transient protein expression. Therefore, we decided to determine the level of expression of E7 oncoprotein as well as that of pRb and p130 in cervical cancer cell lines and HEK293T cells. As shown in Figure 3.1 CaSki cells expressed the highest amounts of HPV16 E7 oncoprotein even when quite small number of cells was used (3×10^5). SiHa cells were also found to express HPV16 E7, however to be able to detect this, at least 6×10^5 cells were needed to be lysed for analysis. Likewise, HPV18 E7 was also well expressed in HeLa cells. pRb (key target for E7 oncoprotein) was well expressed in all cervical cancer cell lines. The expression of pRb in HEK293T cells seemed to be greater than cervical cancer cells. HEK293T cell contains large T antigen, ~100 kDa oncoprotein derived from polyomavirus SV40, which inhibits the functions of p53 and Rb-family tumour suppressor proteins, resulting in the cellular transformation (Ahuja et al., 2005). Another finding was that levels of p130 detected in CaSki and SiHa cells were quite low compared to that in HEK293T cells even in the case when a large number of cells were utilised for analysis.

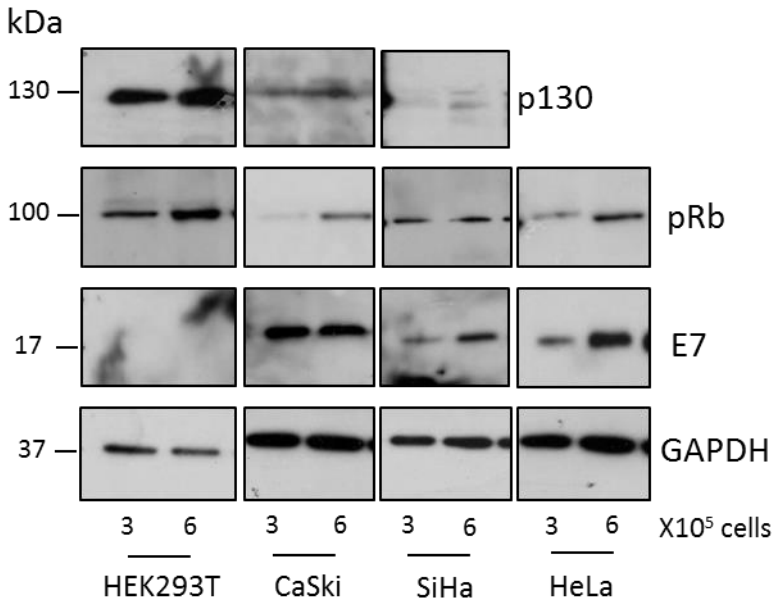

Figure 3.1 Steady state level expression of p130, pRb, E7 in cervical cell lines CaSki, SiHa (both HPV16+), HeLa (HPV18+) and HEK293T cells (HPV negative, pRb and p130+). 3 and 6 x 10^5 cells from each cell line were analysed by SDS-PAGE and western blotting. A housekeeping protein, GAPDH was used as a loading control for E7. Separation of p130 and pRb was performed using a 10% acrylamide gel whereas that of E7 and GAPDH was using a 15% acrylamide gel. Membranes were blocked in 5% milk/TBS-T solution for at least 1 h prior to primary antibody incubations overnight. Anti-p130, anti-pRb, anti-HPV16E7, anti-HPV18E7 and anti-GAPDH were used as primary antibodies). Image shown is representative of two independent experiments (n = 2).

3.2.2 Effects of HPV16 E7 aptamers on the steady state levels of E7, pRb and p130 in CaSki cells.

Here, we have examined the levels of E7 oncoprotein as well as some of its major cellular targets, pRb and p130 in the presence and absence of HPV16 E7 aptamers. For this experiment, CaSki cells were utilised due to the fact that their E7 expression was considerably higher and easily detectable in small number of cells by immunoblotting in comparison with SiHa cells. CaSki cells were transfected with A-series aptamers A1, A2 and A3 as well as an outlier E7 aptamer J1 (see Figure 3.3 for Mfold structures and section 2.2 for aptamer sequences) for 24 hrs. SF1, selected against an unrelated protein, was used as a control. Levels of E7, pRb and p130 were then analysed by immunoblotting. Relative levels of protein expression were quantified by densitometry analysis (Figure 3.2A and C). Results were normalised against the level of GAPDH from at least three independent experiment and represented as graphs with standard errors (Figure 3.2B and D). Looking at the data

obtained at Section 3.2.1, 3 x 10^5 cells were seeded on to experimental plates 24-hours prior to transfection with aptamers.

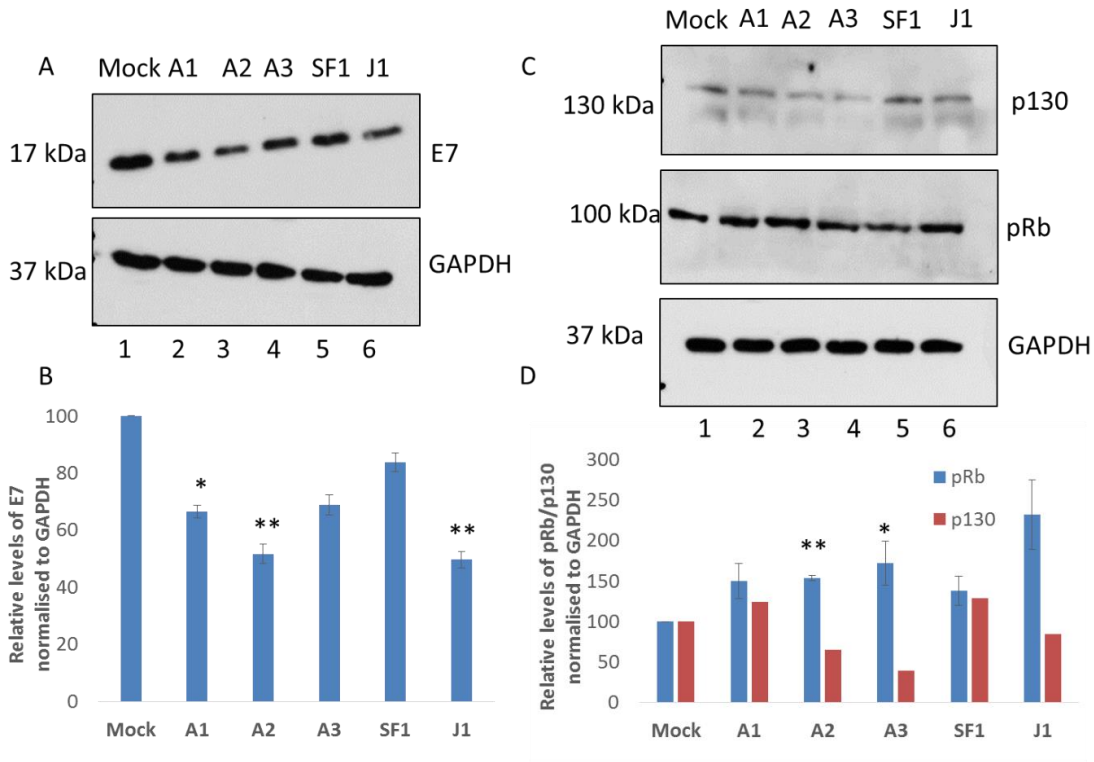

Figure 3.2 Effects of HPV16 E7 aptamers on the steady state levels of HPV16 E7 (A, B) and pRb and p130 (C, D) in HPV16 positive CaSki cells. Cells were mock transfected or transfected with 100 nM A1, A2, A3, SF1 and J1 for 24 hrs using oligofectamine transfection reagent (A, C). Cells were lysed in RIPA and Laemmli buffer. Immunoblot analysis was then performed to detect HPV16 E7, pRb, p130 and GAPDH. (B) Graph shows the data from eight independent experiments (n = 8), with E7 levels shown as % mock together with standard errors (*p = 0.05, **p = 0.008). Significance was calculated over SF1 transfection. (D) Graph shows the data from four independent experiments (n = 4) for pRb and two independent experiments for p130 (n = 2), with pRb and p130 levels shown as % mock in blue, together with standard errors (*p = 0.039, **p =4.5991E-05). Significance was calculated over mock treatment.

Figure 3.2 showed that A2 (Lane 3) caused a considerable amount of decrease in the levels of E7 in CaSki cells. In addition, some other aptamers also affected E7 levels especially A1 and J1, but not A3. Aptamer A1, A2 and A3 differ only by 1-2 nucleotide change, whereas aptamer J1 is one of the HPV16 aptamers classified as an outlier (Nicol et al., 2011). Although the sequences of the A-series aptamers are almost

identical, a single nucleotide change is the cause for the prediction of different secondary structures of these aptamers by Mfold (Figure 3.3). pRb levels, however, seemed to increase slightly following A1, A2 and J1 transfections but not control aptamer SF1 or other E7 aptamer A3. p130 levels were observed to be unaffected by aptamers.

When E7 levels were analysed by densitometry analysis from three independent experiments and presented as a percentage relative to mock treatment Figure 3.2B, A1, A2 and J1 resulted in a significant decrease in the levels of HPV 16 E7 (33.5 ± 2.20%, 48.3 ± 3.37% and 50.3 ± 3.87%, respectively). In addition, reduction in the E7 levels was significant over mock transfection with corresponding p values of 0.05, 0.008 and 0.0083. However, only 31.15 ± 3.58% and 16.32 ± 3.24% decrease in E7 levels following A3 and SF1 transfections, respectively, were observed.

Levels of pRb and p130 tumour suppressor proteins following aptamer transfections were also quantitated by densitometry analysis. It was shown in Figure 3.2D that there was a 53.42 ± 3.31% increase in pRb in A2 transfected cells. Although recovery of pRb with A2 transfection did not seem significant over that of SF1, pRb levels were significantly increased over mock transfection with **p = 4.5991E-05. Similarly A1, A3 and J1 transfections also resulted in a similar increase in the levels of pRb. However, p130 as demonstrated by western blot (Figure 3.2C), seemed unaffected by aptamers.

Computational RNA folding secondary structures of some of the HPV16 E7 aptamers were determined using the RNA mFold web server (Zuker, 2003). This software performs the prediction of RNA secondary structures according to the free energy (ΔG) minimisation and based on a dynamic programming algorithm using several energy parameters for example from Watson-Crick and GU base pairing, loop structures and mismatching or unpaired nucleotides (Mathews et al., 1999). However, it does not take in to account the 3D interactions and protein-RNA interactions, which could make suboptimal folding favourable. In addition, it does not always represent accurate folding of RNA in the biological environment.

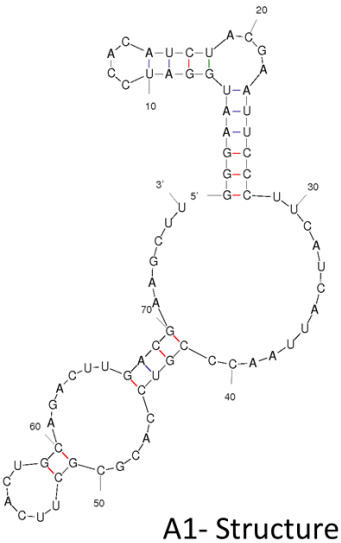

A1- Structure 1

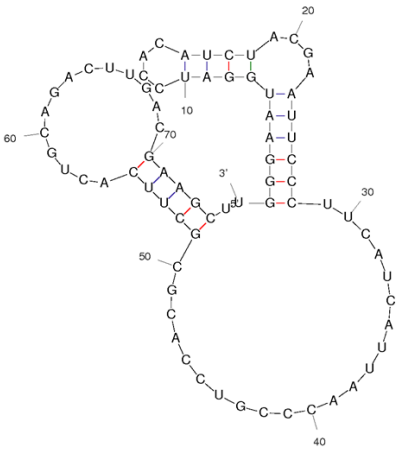

A1- Structure 2

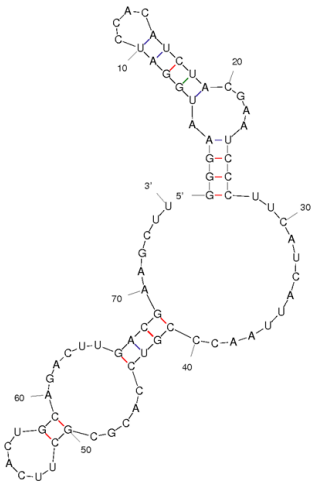

A2- Structure 1

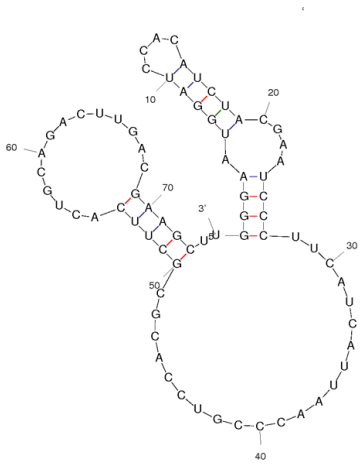

A2- Structure 2

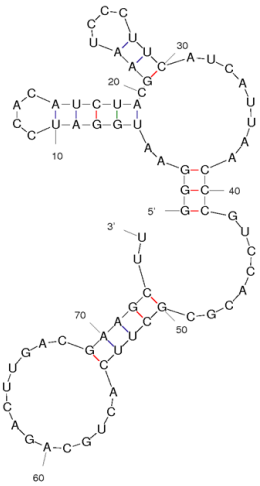

A2- Structure 3

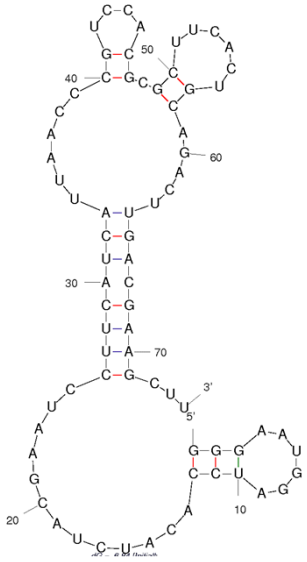

A3- Structure 1

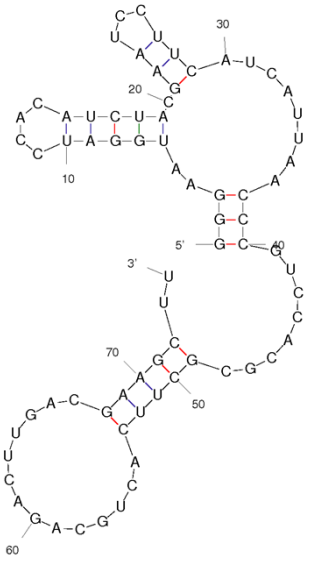

A3- Structure 2

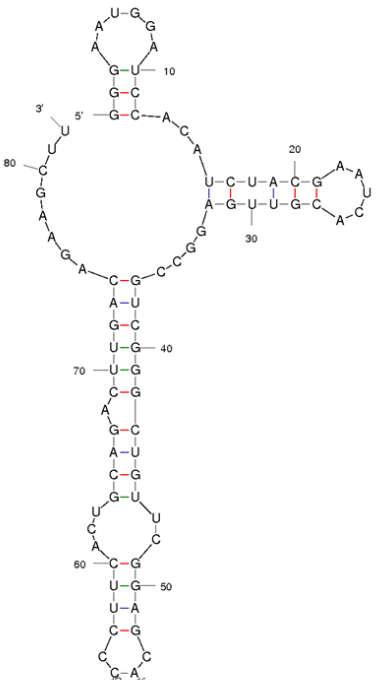

J1

Figure 3.3 Predicted secondary structures of aptamers, A1, A2, A3 and J1. ΔG values for these aptamers are as indicated in brackets [structure 1 (ΔG = -13.00) and 2 (ΔG = -12.60)], A2 [structure 1 (ΔG = -11.9), 2 (ΔG = -12.6) and 3 (ΔG = -7.73)], A3 [structure 1 (ΔG = -6.84) and 2 (ΔG = 6.83)] and J1 (ΔG = -19.7) using Mfold (Zuker, 2003).

Mfold predicted two different lowest energy secondary structures for aptamers A1, A2 and A3 with the lowest –ΔG structure being more stable and more likely to be formed. Although A1, A2 and A3 are almost identical in RNA sequence with only 2 nucleotide difference (Nicol et al., 2011), slightly different structures were predicted. A2 was previously shown to have an effect on E7 steady state level in CaSki cells (Nicol et al., 2013). Predictions for A1 and A2 were similar but the predicted structures for A3 were quite different, possibly reflecting the differences in the effects of aptamers on E7 levels observed here. Interestingly, there was only one structure predicted for J1 with a quite low ΔG (-19.7), indicating a very stable RNA structure. However, it should be noted that some parameters during the course of in vitro transcription such as pH, temperature and the local composition bias of RNA as well as intracellular conditions when RNA was delivered in cells are also important in determining the secondary structures.

3.2.3 Dose dependence and time course for effect of A2 in CaSki cells

HPV16 E7 aptamer A2 has been shown to cause a reduction in the levels of E7 oncoprotein when used at 100 nM (Figure 3.2). Here a dose-dependence experiment was performed in order to determine the effects of A2 transfections in CaSki cell when used at lower and higher concentrations. Figure 3.4 shows that loss of E7 was dramatic even at lowest concentrations. In contrast control aptamer SF1 (at 100 and 200 nM) was shown not to have an effect on the levels of E7. In addition, Following A2 transfections, pRb levels seemed to recover, whereas pRb levels were not affected by SF1 transfections similar to that of mock treatment. Finally, an increase in p130 expression was also shown if cells were transfected with A2 at concentrations of 200 nM or higher. However, the result was inconclusive due to the detection of the recovery of p130 in SF1 transfected cells.

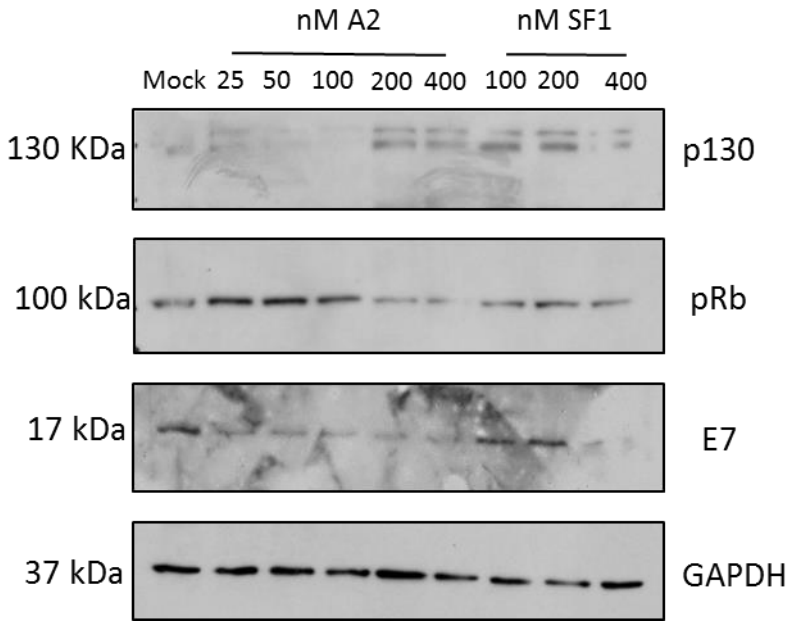

Figure 3.4 Dose-dependence of A2 in CaSki cells. CaSki cells were seeded on to 6-well plates and incubated 24 hrs prior to the aptamer transfection. An increasing concentration of A2 and control aptamer SF1 (from 25 to 400 nM) was used for transfections. Transfections were performed in a serum-free medium for 4 hrs, followed by returning the cells into the media containing 10% of foetal bovine serum. Proteins were analysed by SDS-PAGE and Western blotting. Anti-p130, anti-pRb, and anti-HPV16E7 and anti-GAPDH were used as primary antibodies. A housekeeping protein, GAPDH was used as a loading control for E7. A representative blot was shown (n = 2).

In order to understand better and determine the time point when A2 starts affecting the E7 levels, a time course experiment was employed. Following 100 nM A2 transfections, cells were collected at different time points; 6, 14 and 20 hrs post-transfection. Figure 3.5 shows that A2 caused a considerable reduction in E7 levels as early as 14 hrs post-transfection. However, no difference was detected in the levels of pRb during 20 hrs time course.

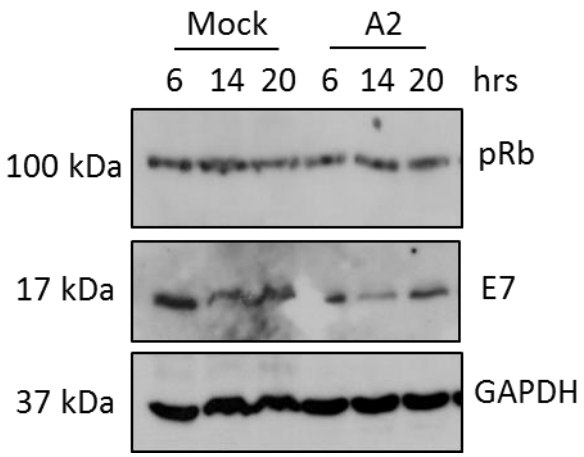

Figure 3.5 Effects of A2 transfections on E7 and pRb levels in CaSki cells. Cells were transfected with 100 nM A2 for 6, 14 and 20 hrs, collected and lysed prior to analysis by SDS-PAGE and Western blotting in order to determine the levels of E7 and pRb. GAPDH was used as a loading control for E7. A representative blot was shown (n = 2).

3.3 Cross-specificity of HPV16 E7 aptamers with other HPV E7 proteins

3.3.1 Using several HPV E7 types in *in vitro* assays

3.3.1.1 Cloning and E.coli expressions of GST-tagged HPV11 and 18 E7

The aim of this section was to design GST – tagged expression vectors of several high- and low- risk HPV E7 oncoproteins for use with the existing aptamers. PCR fragments were obtained from plasmids containing HPV11 and 18 open reading frames (ORFs) (see methods section 2.7). HPV11 and 18 E7 fragments were cloned into the *BamH*I/*EcoR*I restriction sites of the pGEX-6P-1 expression vector. The integrity of the plasmids was analysed by sequencing and the data indicated that E7 ORFs were in-frame downstream of the GST ORFs. Vectors were transformed into *E. coli* BL21 (DE3) Rosetta-competent cells. BL21 cells are deficient in the expression of Ion proteases and outer membrane protease, ompT in order to prevent the degradation of heterologous proteins. These cells contain a T7 RNA promoter and Lambda DE3 phage for expression of T7 RNA polymerase under the control of a lacUV5 promoter. IPTG was used to induce the expression of recombinant proteins cloned downstream of the T7 RNA promoter in these BL21 (DE3) cells. Rosetta™ host strains have been designed to enhance the expression of eukaryotic proteins that contain codons rarely used in *E. coli*. Expression of GST- 11E7 and 18 E7 was optimised (20, 30 and 37°C for 3, 6hrs or overnight) and conducted at 20°C overnight and 30°C for 6 hrs, respectively following 1 mM IPTG inductions. The results of the

successful expression using conditions of 30°C for 6 hrs for GST-18E7 and 37° overnight for GST-11E7 are shown in Figure 3.6 and 3.7, respectively. The predicted molecular weights (MW) of GST, 11E7 and 18E7 are 26.62 kDa, 11 and 12 kDa, respectively. However, MW of GST-11 and 18E7 were detected to be around ~40 kDa as oppose to calculated predicted molecular weights of 37.6 and 38.6 kDa, respectively.

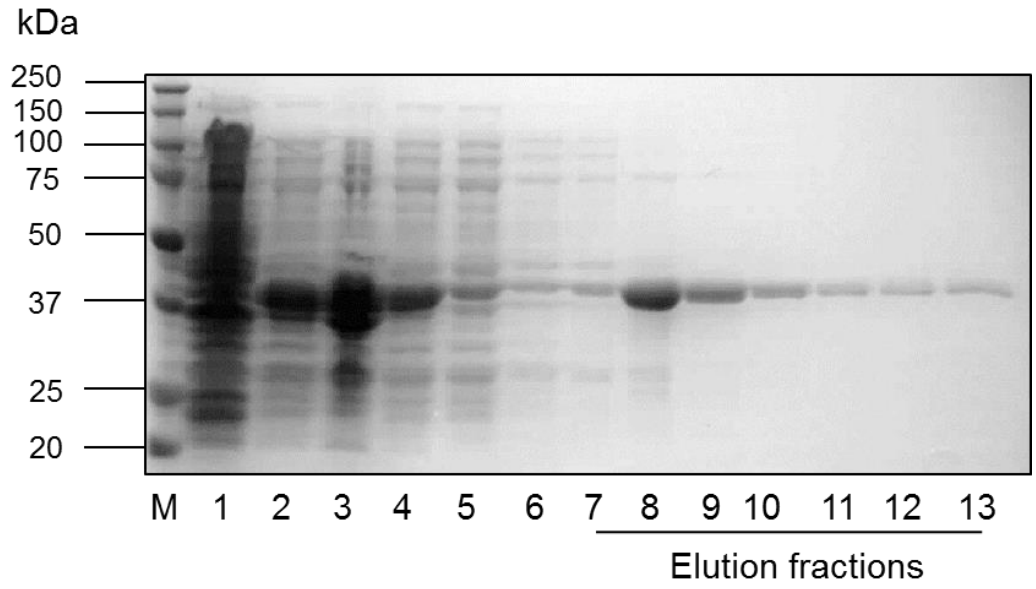

Figure 3.6 GST- HPV18 E7 was successfully expressed in *E. coli* BL21 (DE3) Rosetta cells and purified on glutathione sepharose (GS) beads. Protein expression was performed at 30° C for 6 h with 220 rpm shaking following 1 mM IPTG induction. Samples were kept before and after induction for gel analysis. Cells were pelleted by centrifugation and lysed in protein extraction buffer containing DNase (5 µg/ml) and lysosyme (1 mg/ml) by sonication. Protein was purified from soluble fraction of the cell lysate on the glutathione sepharose column by gravity flow. Insoluble protein fraction, column flow through and wash were all kept for gel electrophoresis. Elution fractions were collected in 50 mM glutathione/PBS pH 8.0. Samples from each purification steps were analysed on a 12% SDS-PAGE. Gel stained with Coomassie blue [M: marker (Precision Plus Protein™ Dual Colour, BioRad), 1: Un-induced, 2: Induced, 3: Soluble, 4: Insoluble, 5: Flow Through, 6: Wash, 7-13: Elution Fractions 1-7]. A representative blot is shown from three independent protein expression (n = 3).

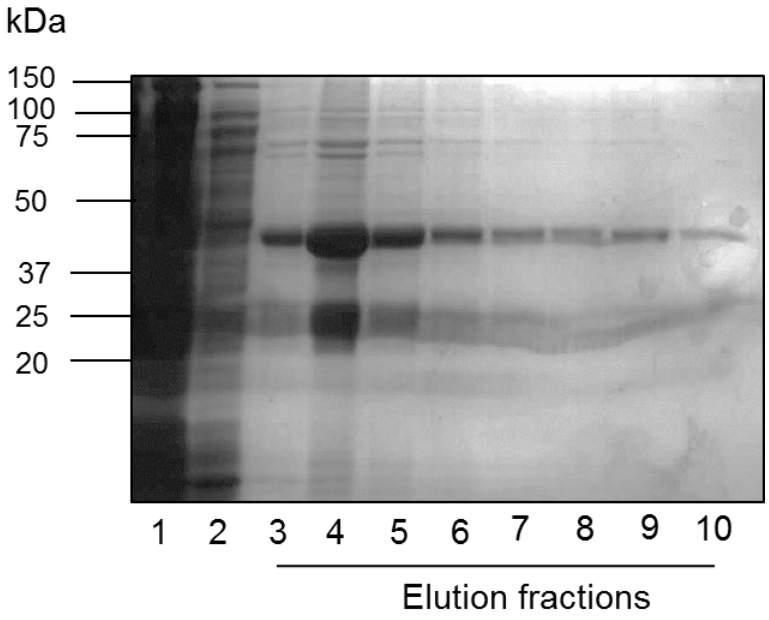

Figure 3.7 GST- HPV11 E7 was successfully expressed in *E. coli* BL21 (DE3) Rosetta cells and purified on Glutathione sepharose (GS) beads. Protein expression was performed at 20°C overnight with 220 rpm shaking following 1 mM IPTG induction. Cells were pelleted by centrifugation and lysed in protein extraction buffer containing DNase (5 µg/ml) and lysosyme (1 mg/ml) by sonication. Protein was purified from soluble fraction of the cell lysate on the glutathione sepharose column by gravity flow. Elution fractions were collected in 50 mM glutathione/PBS pH 8.0. Samples were analysed on a 12% SDS-PAGE. Gel stained with Coomassie blue (1: Flow Through, 2: Wash, 3-10: Elution Fractions 1-8). Molecular weight was as indicated. A representative blot is shown from two independent protein expression (n = 2).

Following the expression and purifications of GST- tagged 11 and 18 E7, recombinant GST-E7 was successfully bound to GS-beads (Figures 3.8 and 3.9). Binding of the protein to beads was performed at 4°C for 1 h. Almost all of the protein was observed to bind an equal volume of GS-beads, since levels of GST-11 and 18E7 level detected from samples of unbound and several washes were quite low. Molecular weights of these recombinant proteins were around ~43 kDa (26 kDa GST + 17 kDa E7). GST alone as well as some degradation products were also detected by SDS-PAGE seen as bands between molecular weights of 43 – 26 kDa. These proteins bound to GS-beads were subsequently used in GST – pull down experiments where pRb and E7 interactions were studied *in vitro* in the presence and absence of HPV16 E7 aptamers in order to determine their cross-specificity for E7 from other HPV types (section 3.3.1.2).

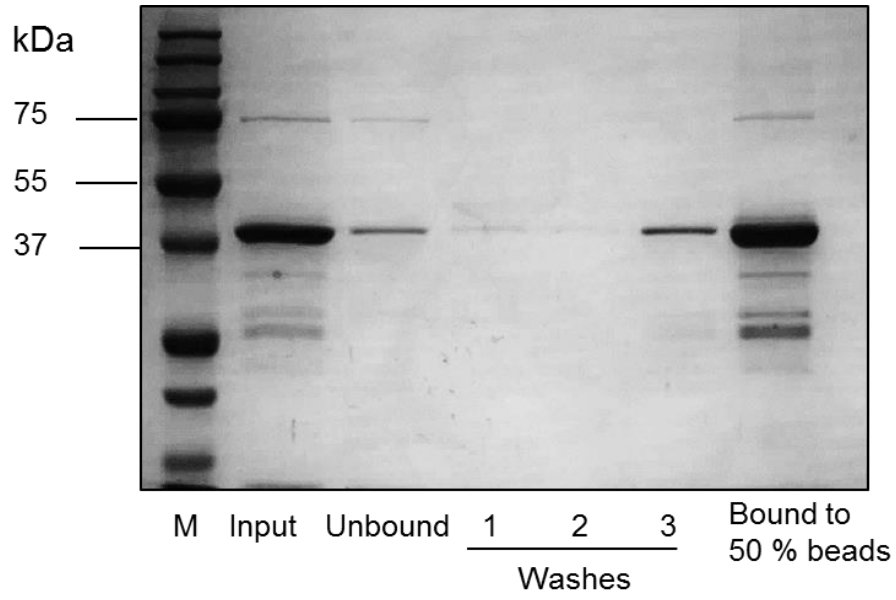

Figure 3.8 GST-18 E7 was bound to glutathione sepharose beads. The input and unbound lanes shows the amount of protein incubated with beads and the amount of protein did not bound to the beads, respectively. Bound beads were than washed with 0.5% Triton-X100/PBS three times. The last lane is the amount of protein bound an equal amount of glutathione sepharose beads. M= marker (Precision Plus Protein™ Dual Colour, BioRad). 20 µl of each sample was loaded on to the each well. Gel was Coomassie stained.

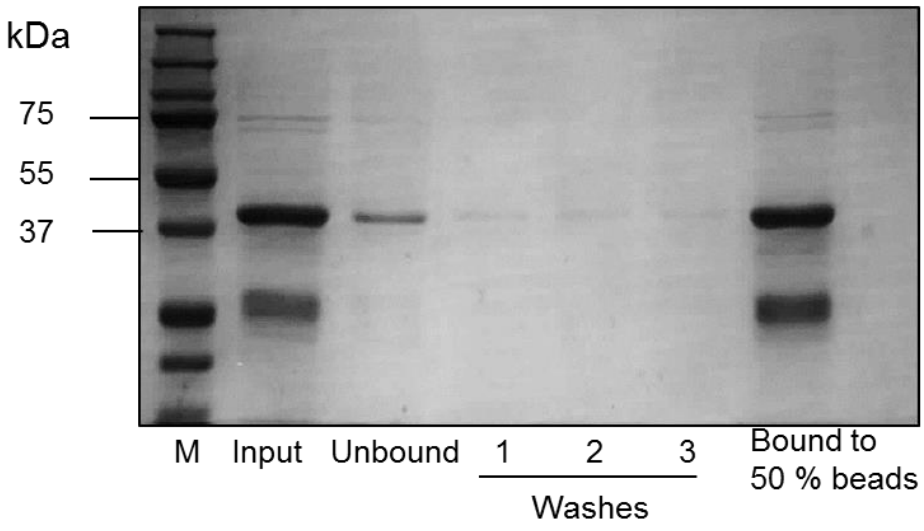

Figure 3.9 GST-11 E7 was bound to glutathione sepharose beads. The input and unbound lanes shows the amount of protein incubated with beads and the amount of protein did not bound to the beads, respectively. Bound beads were than washed with 0.5% Triton-X100/PBS three times. The last lane is the amount of protein bound an equal amount glutathione sepharose beads. M= marker (Precision Plus Protein™ Dual Colour, BioRad). 20 µl of each sample was loaded on to the each well. Gel was Coomassie stained.

3.3.1.2 GST-pull down experiments

GST-pull down experiments were designed in order to study the effects of HPV16 E7 aptamers on E7 – pRb binding using E7 from other HPV types. HaCaT cell (immortalised keratinocytes) lysate was used as a source for pRb and p130. GST-E7 (from HPV11, 16 or 18) immobilised onto GS-beads (from 3.3.1.1) was incubated with 600 µg protein from HaCaT cell lysate. GST-immobilised GS-beads and GS-beads alone were also incubated with the lysate as controls. Figure 3.10 shows that pRb and p130 were precipitated by GST11, 16 and 18 E7. However, there was some nonspecific binding of the beads to pRb and p130. Several washes and different washing buffers were used to optimise the conditions for pull-down. However, attempts to remove nonspecific binding were unsuccessful. Therefore, aptamers could not be included in the experiments to investigate if these HPV16 E7 aptamers were also effective in disrupting pRb interaction with HPV 11 and 18 E7.

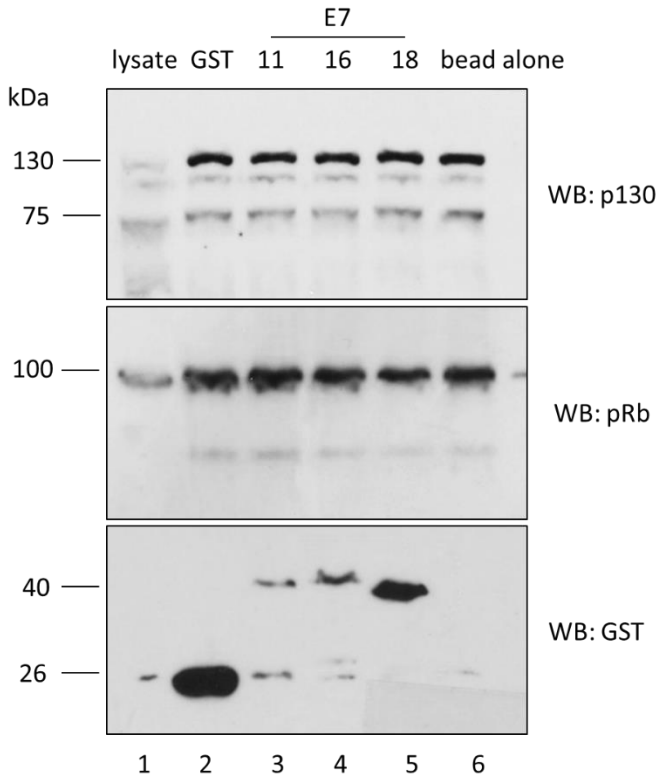

Figure 3.10 GST pull-down assay in order to study interaction of pRb and p130 with E7 from HPV11, 16 and 18. 10 µg of GST-E7 bound to GM-beads was incubated with 600 µg of protein from a HaCaT cell lysate (as a source of pRb) for 1 hour at 4°C. Bead-bound GST was also incubated with cell lysate. GST proteins and interacting proteins were isolated from the reaction and analysed by immunoblotting using antibodies to pRb, p130 and GST. A representative blot was shown (n = 2).

3.3.2 Effects of HPV16 E7 aptamers on the steady state levels of 18 E7 in HPV18 positive HeLa cells

In order to determine if HPV16 E7 aptamers had an effect on 18 E7 as well as 16 E7, HeLa cells were transfected with these aptamers for 24 hrs followed by immunoblotting. As it was seen from the Figure 3.11A, some of the aptamers were likely to be active against HPV18 E7, possibly due to amino acid conservation around the pRb binding site (as discussed in section 3.2).

Observations in CaSki cells (Figure 3.2) indicated that A2 was the most effective aptamer in the reduction of E7 levels of those tested. However, in HeLa cells A1 and J1 resulted in the largest reductions of E7 levels (Figure 3.11). In addition, A2 also seemed to cause a moderate decrease in the levels of 18 E7 oncoprotein in HeLa cells (Figure 3.11). Several independent experiments were conducted and densitometry analysis using Aida image analyser was performed from each transfections. Mean E7 levels from three different experiments were then showed as a percentage relative to mock treatment Figure 3.11B. Transfections with A1, A2 and J1 resulted in a significant decrease in the levels of HPV 18 E7 (to 54.78 ± 5.44%, 72.18 ± 6.22% and 48.33 ± 6.5%, respectively). In addition, reduction in the E7 levels were significant over mock transfection with $p = 0.034$ for A2 and $p = 0.003$ for A1 and J1 transfections. However, transfections with A3 and SF1 caused only approximately 20% decrease in 18 E7 which was smaller than that observed for the other aptamers tested.

As well as determining the effects of aptamers on E7 levels in HeLa cell, steady state levels of pRb was also examined following aptamer transfections. According to Figure 3.11C and D, transfection with aptamers resulted in an increase in pRb levels when compared to mock treatment. pRb levels following A1, A2, A3, SF1 and J1 transfection presented as percentage of mock, indicated a 35, 57, 69, 51 and 39% increase, respectively (Nicol et al., 2013). Further aptamers were also tested in HeLa cells (B1, C4 and D1) (data not shown), however E7 levels did not seem to be affected by transfection with these aptamers.

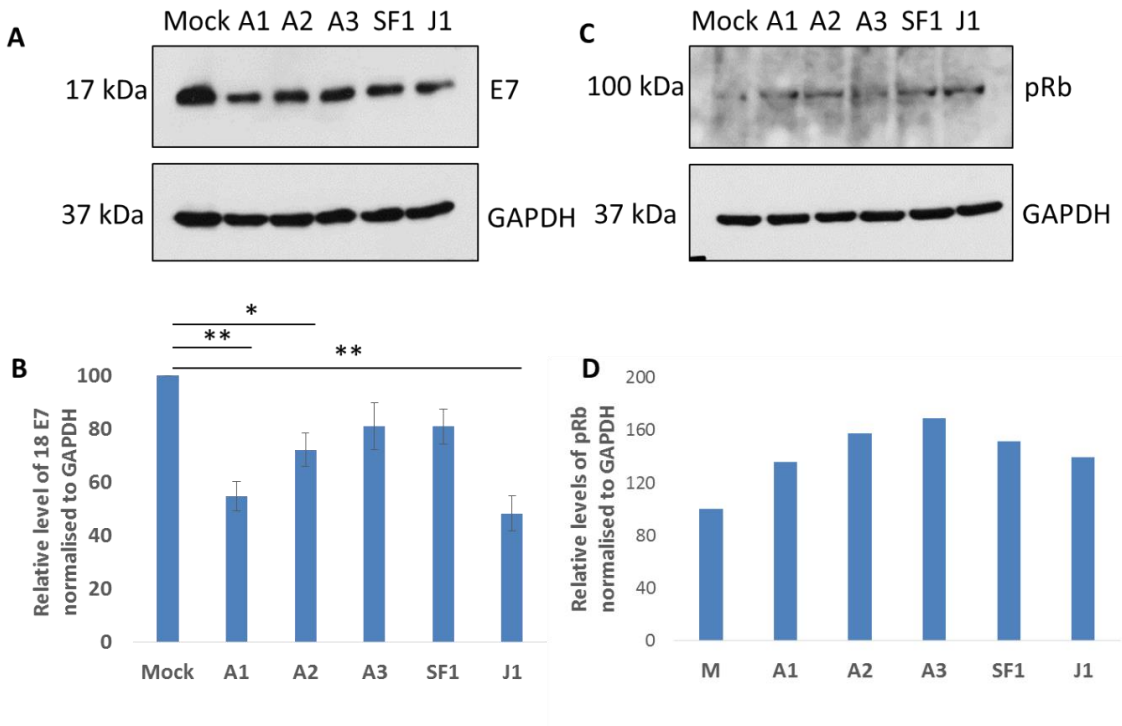

Figure 3.11 Effects of HPV16 E7 aptamers on the steady state levels of HPV18 E7 and pRb in HPV18 positive HeLa cells. (A, C) HeLa cells were transfected with 100 nM A1, A2, A3, SF1 and J1 for 24 hrs using oligofectamine transfection reagent. Cells were lysed in RIPA then Laemmli buffer. Immunoblot analysis was then performed to detect HPV18 E7, pRb and GAPDH. (B) Graph shows the data from six independent experiments (n = 6), with E7 levels shown as % mock, together with standard errors. *p = 0.034, **p = 0.003. (C). Graph shows the data from three independent experiment (n = 3), with pRb levels shown as % mock.

3.4 Effects of 5` tri or monophosphate aptamers on the induction of apoptosis and interferon response

3.4.1 Effect of *in vitro* transcribed HPV16 E7 aptamers on apoptosis

3.4.1.1 Annexin V apoptosis assays in SiHa, HeLa and C33A cervical cancer cell lines

It could be proposed that reduction of E7 levels in the cervical cancer cell lines should result in an induction of apoptosis. To detect apoptotic cells followed by aptamer transfection, Annexin V apoptosis assays were utilised. This assay is sensitive, easy to perform and offers the possibility of detection of early stages of apoptosis. The method is based on the detection of apoptotic cells via Annexin V-phosphatidyl serine (PS) interaction on the cell membrane. During apoptosis PS translocates to the outer layer of membrane from the inner layer. When Ca^{2+} is present in the environment, Annexin V can bind negatively charged phospholipids such as PS. Therefore, Annexin V with a flurorescent tag has been widely used for the detection of apoptosis by flow

cytometry. This protocol should be performed with extra care to avoid damaging the plasma membrane integrity which might result in the false positive Annexin V readings. Another dye such as PI is included in the assay to assess the integrity of plasma membrane to detect necrotic and dead cells.

SiHa, C33A and HeLa cells were used in apoptosis experiments. Information about the cell lines has already given at sections 2.5 and 3.2.1. C33A and HeLa cells were used as controls in order to determine any cross-specificity of the HPV16 E7 aptamer A2. These cell lines were transfected with up to 200 nM A2 and also SF1 as a control against non-specific effects of transfection with aptamers. Staurosporine was used as a positive control since it is a known inducer of apoptosis possibly via activation of caspase-3 (Feng and Kaplowitz, 2002) (Chae et al., 2000) in addition to caspase-independent mechanisms (Belmokhtar et al., 2001, Zhang et al., 2004).

To perform the assay, samples were dual-stained with fluorescein isothiocyanate (FITC)-labelled Annexin V (green fluorescence) and propidium iodide (PI) (red fluorescence) (Vermes et al., 1995) and analysed by flow cytometry. The staining pattern indicates if cells are intact/healthy (FITC-/PI-), early apoptotic (FITC+/PI-), late apoptotic (necrotic) (FITC+/PI+) or dead (FITC-/PI+). Results were presented as % of early and late apoptosis in the three different cervical cancer cell lines. Figure 3.12 shows that A2 induced apoptosis in SiHa cells but not in the control cells, C33A and HeLa. Total (combined early and late) apoptosis was found to be increased in SiHa cells (Figure 3.12A) transfected with 50, 100 and 200 nM of A2 with 30.6 ± 1.64%, 18.01 ± 1.28% and 23.67 ± 0.63% apoptosis, respectively, over mock transfected cells (3.34 ± 0.176%). The effect of A2 transfection on the induction of apoptosis was significant over that of SF1 transfections. 50, 100 and 200 nM of SF1 transfections resulted in 17.73 ± 0.42%, 5.22 ± 0.93% and 11.15 ± 1.01% , which was significantly lower compared to A2 transfections with $p = 0.006$, $p = 0.03$ and $p = 0.0005$, respectively. Staurosporine treatment caused an increase up to 34.16 ± 1.45% apoptosis. The percentage of early (FITC+/PI-) and late apoptotic cells (FITC+/PI+), were analysed separately in Figure 3.12. The percentage of early: late apoptotic cells following 100 and 200 nM A2 transfections were 11%: 9% and 14%: 12%, respectively.

In C33A cells (Figure 3.12B), although apoptosis was increased by A2 6.4 ± 1.2%, 5 ± 1.2% and 6.5 ± 1.2% for 50, 100 and 200 nM, respectively) and by transfection with SF1 (9.36 ± 0.83%, 5.3 ± 1.2% and 5.2 ± 0.58%, respectively) over mock-transfection (2.16 ± 0.62%), the level of apoptosis caused by control aptamer was similar to the

E7 aptamer A2. There was no significant difference between aptamer transfections. Staurosporine, as a positive control, found to increase the percentage of apoptosis up to 32.9 ± 6.77%. When the effect of A2 was compared between SiHa and C33A cells, induction of apoptosis in SiHa cells with 100 and 200 nM of A2 were significantly greater than that of C33A cells with p values of 0.022 and 0.0002, respectively. Therefore, we suggest that A2 induces apoptosis in HPV16 positive SiHa cells but not HPV negative control cell line, C33A (Nicol et al., 2013).

HeLa cells were also utilised to check if there was any cross-specificity of HPV16 E7 aptamers on a HPV18 positive cell line (Figure 3.12C). These cells were also transfected with 50, 100 and 200 nM of A2, which resulted in 6.26 ± 1.05%, 7.6 ± 0.29% and 8.03 ± 1.25% of apoptosis, respectively, and SF1, which resulted in 6.26 ± 0.82%, 6.23 ± 0.86% and 7.46 ± 0.83% of apoptosis, respectively (Nicol et al., 2013). Although A2 and SF1 transfections enhanced the percentage of apoptosis in HeLa cells over mock transfection (2.23 ± 0.18%), there was no significant difference observed between A2 and SF1 transfection.

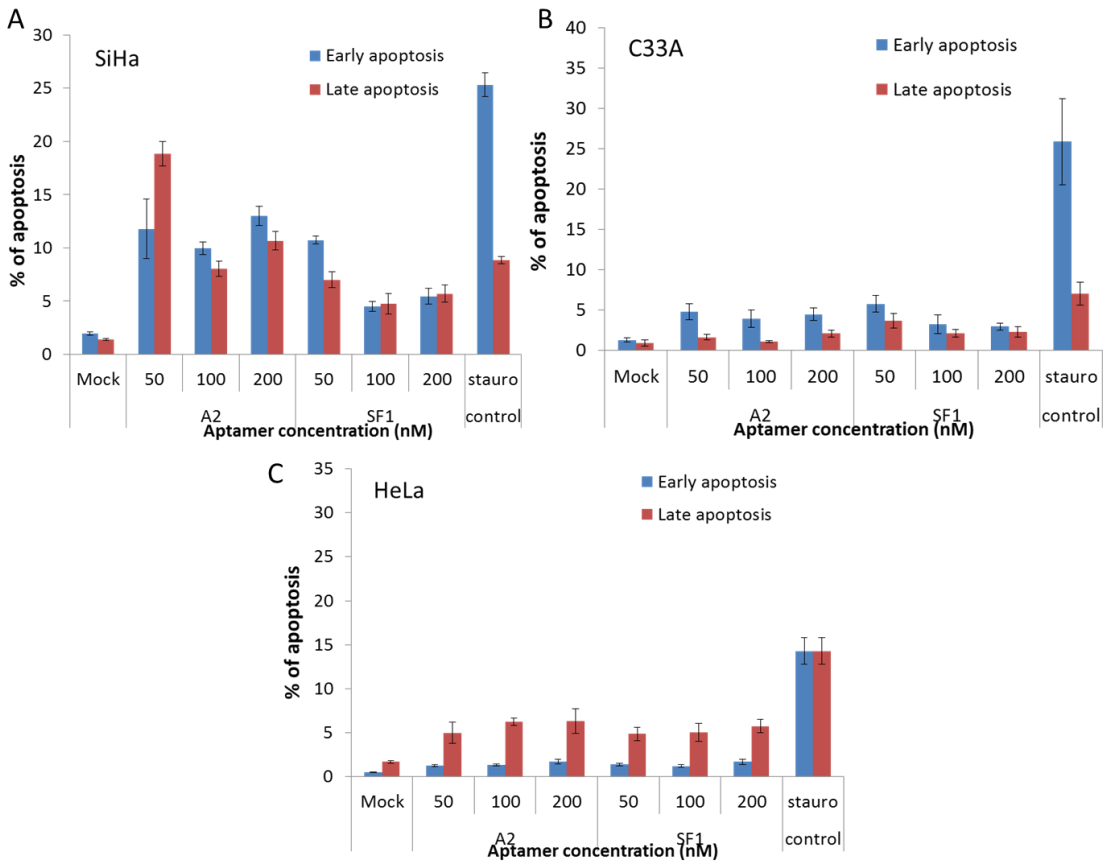

Figure 3.12 HPV16 E7 aptamer A2 is inducing apoptosis in HPV16 positive cervical carcinoma derived cell line (SiHa), however not in control cell lines which are derived from HPV negative and HPV18 positive cervical carcinomas. SiHa (A), C33A (B) and HeLa (C) cells were seeded on to 12-well plates at 1.5 x 10^5 cells/ ml per well and incubated for 24 hrs at 37°C with 5% CO_2. Cells were mock transfected or transfected with *in vitro* transcribed aptamer A2 and SF1 up to 200 nM. Staurosporine was also used as a positive control due to its high potency of causing apoptosis. Cells were analysed for apoptosis 24 hrs later. Cells were collected and washed several times with PBS. Cell pellets were dual-stained with FITC-conjugated annexin V and propidium iodide followed by analysis on the flow cytometer. Graph shows early and late apoptosis data from seven independent experiments for SiHa (n = 6) and three independent experiments from HeLa and C33A (n = 3), together with standard errors. P values (by student`s t-test) were calculated to determine the significance of A2 treatments over that of control aptamer SF1 within SiHa cells as well as the significance of A2 treatments in comparison to control cell lines, C33A and HeLa.

A1, A2 and A3 are quite similar in sequence, differing only by a single nucleotide change (Nicol et al., 2011). Therefore, the effects of these aptamers were tested in SiHa cells as well as C33A cells as a negative control (Figure 3.13). It seemed as if all of these aptamers induced apoptosis in SiHa cells. The total percentage (early and late) of apoptosis caused by A1, A2 and A3 was 26.22 (± 0.59), 24.41 (± 0.53) and

24.11 (± 0.51)%, respectively. These aptamers caused apoptosis in SiHa cells which was significantly higher than that observed for C33A cells with corresponding p values of 0.0001, 3.01E-05 and 8.39E-06, respectively.

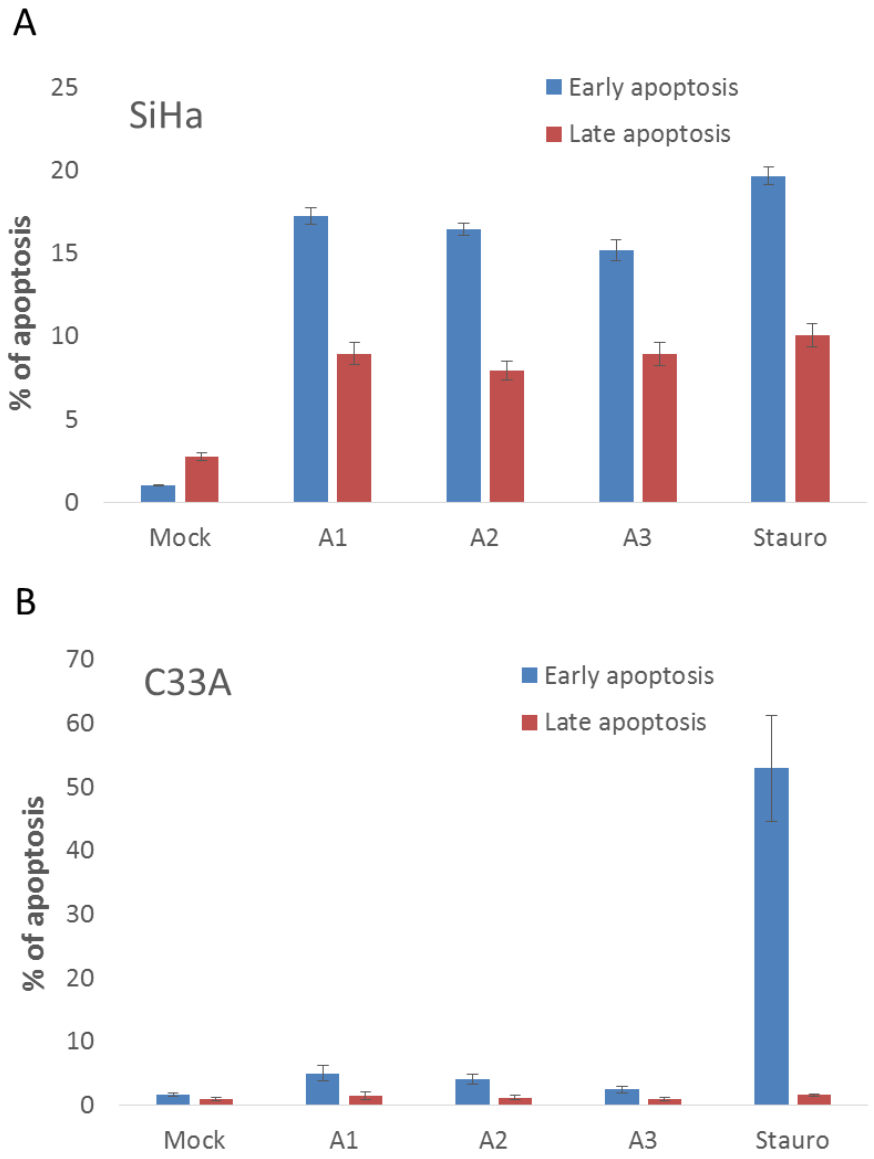

Figure 3.13 Induction of apoptosis by HPV16 E7 aptamers A1, A2 and A3, which differs only one nucleotide in sequences. 100 nM aptamer was used for transfections of SiHa (A) and C33A (B) cells for 24 hrs prior to the assay using Annexin V/Propidium iodide. Staurosporine was used as a positive control. Percentages of early and late apoptotic cells induced by aptamers were presented in the graphs from three independent experiments (n = 3), together with standard errors.

3.4.1.2 Annexin V apoptosis assays in HaCaT, HaCaT 16 and 18E7 stable cells

HPV16 E7 aptamer A2 as well as control aptamer SF1 was also used for transfection of HaCaT, HaCaT HPV16 E7 and HaCaT HPV18 E7 stable cell lines to detemine the apoptotic effects of aptamers. HaCaT cells are from an immortalised (>140 passages), long-term primary culture of human adult skin keratinocytes (Boukamp et al., 1988). HaCaT E7 stable cell lines were generated by Kat Richards (University of Leeds, Leeds, UK). Figure 3.14 shows that percentage of apoptosis with 50, 100 and 200 nM A2 was 10.86 (± 1.43), 14.63 (± 1.05) and 14.33 (± 1.0), respectively in HaCaT cells; and 18.8 (± 0.41), 19.93 (± 0.66) and 17.03 (± 1.04), respectively, in HaCaT 16 E7 stable cell line. Therefore, transfection with 50 and 100 nM A2 was significantly induced apoptosis in HaCaT 16 E7 expressing cells compared to HaCaT cells ($p = 0.0185$ and $p = 0.034$, respectively). Staurosporine treatment of both cell lines resulted in a similar level of apoptosis [for HaCat 30.23 (± 2.39)% and for HaCaT 16 E7 stable cells 32.03 (± 3.24)%]. However, SF1 seemed to be apoptotic in the HaCaT 16 E7 expressing cell, therefore only significant difference between A2 and SF1 transfection was detected when 100 nM of aptamer was used ($p = 0.02$). There was no significant difference in apoptosis between A2 and SF1 transfection in HaCaT 18 E7 stable cells. However, apoptosis was increased significantly by A2 in HaCaT 18 E7 stable cells when compared to that in HaCaT cells.

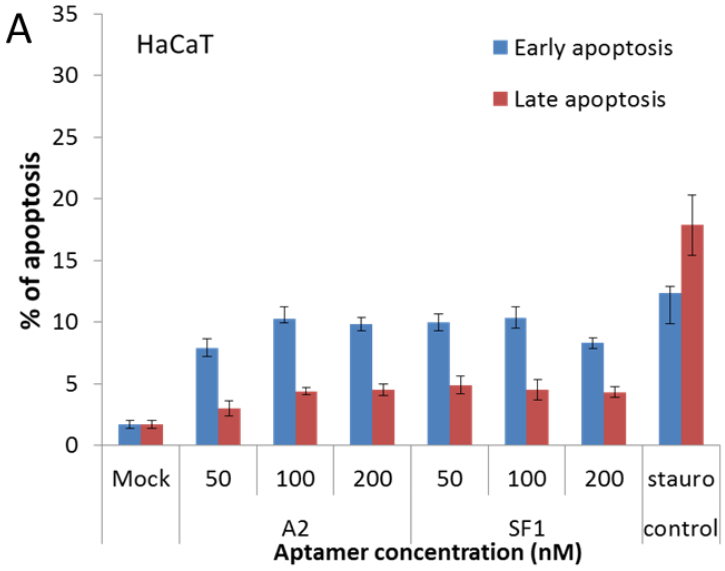
A
HaCaT
Early apoptosis
Late apoptosis
% of apoptosis
35
30
25
20
15
10
5
0
Mock
50
100
200
50
100
200
stauro
A2
SF1
control
Aptamer concentration (nM)

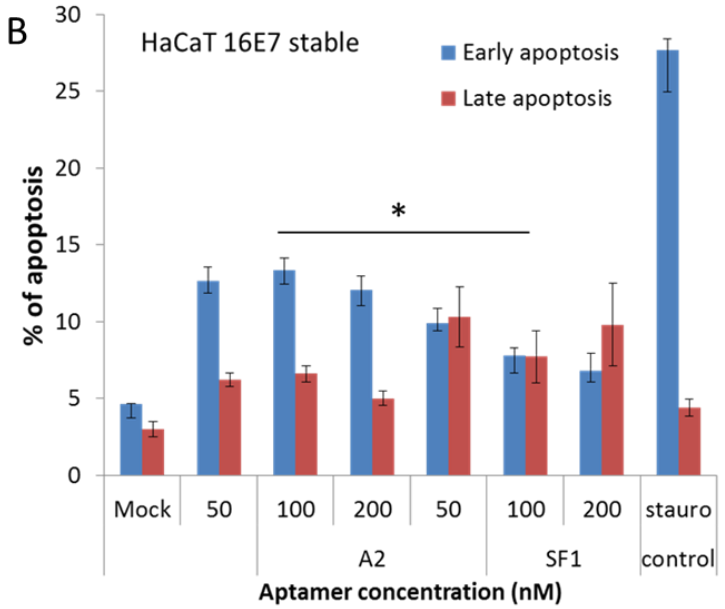
B
HaCaT 16E7 stable
Early apoptosis
Late apoptosis
*
% of apoptosis
30
25
20
15
10
5
0
Mock
50
100
200
50
100
200
stauro
A2
SF1
control
Aptamer concentration (nM)

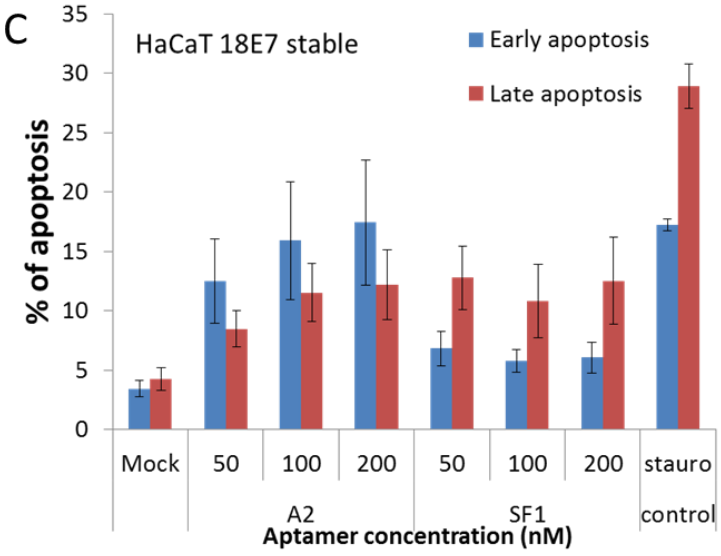
C
HaCaT 18E7 stable
Early apoptosis
Late apoptosis
% of apoptosis
35
30
25
20
15
10
5
0
Mock
50
100
200
50
100
200
stauro
A2
SF1
control
Aptamer concentration (nM)

Figure 3.14 Effects of HPV16 E7 aptamer A2 and a control aptamer SF1 on inducing apoptosis in the immortalised human keratinocyte HaCat cells and as well as HaCat cells stably expressing HPV16 and 18E7. HaCaT stable cells were maintained in the regular DMEM plus 0.5 µg/ ml puromycin. Cells were seeded on to 12-well plates at 1.5 x 10^5 cells/ ml per well and incubated for 24 hrs at 37°C with 5% CO_2. Cells were mock transfected or transfected with *in vitro* transcribed aptamer A2 and SF1 up to 200 nM. Staurosporine was also used as a positive control. Cells were analysed for apoptosis 24 hrs later. Cells were collected and washed several times with PBS. Cell pellets were dual-stained with FITC-conjugated annexin V and propidium iodide followed by analysis on the flow cytometer. Graph shows the total percentage of apoptosis, analysed from three independent experiments (n = 3), together with standard errors. P* = 0.02.

3.4.2 Use of 5` triphosphate and monophosphate (dephosphorylated) aptamers in apoptosis assays and quantitative real-time PCR (qPCR) for detection of expression of interferon responsive genes

3.4.2.1 Introduction

Since the recognition of ds/ss RNA is mostly dependent on the presence of 5' triphosphate, aptamers such as HPV16 E7 aptamer A2 could also activate innate immunity by triggering RIG-I, resulting in the expressions of interferon genes. Although E7 aptamers are single-stranded without extensive double-stranded regions, they are able to form secondary structures with complementary base-pairing. These lowest energy secondary structures could be predicted by Mfold software (section 3.2.2). Hence, we hypothesised that although these aptamers will probably not have enough double-stranded regions, they have 5' triphosphate moiety which could induce RIG-I. One could consider this as a non-specific effect of an aptamer. However, this property of aptamer can also provide potential advantages as discussed in section 1.3.4 especially for induction of apoptosis by interferon stimulation in HPV-transformed cancer cells. Since, some toll-like receptors and interferon stimulating genes (ISGs) were reported as being down-regulated in HPV positive cervical cancer cells with different oncogenic types (CaSki and HeLa) rather than HPV negative cervical cancer cells (C33A), subsequently leading to the reduced interferon levels (Yu et al., 2012). There is little data on the effects of aptamers, however, siRNA molecules modified with 5' triphosphate group in the RIG-I activation have been studied (Chen et al., 2013, Poeck et al., 2008). For example, use of an 5' triphosphate siRNA for anti-apoptotic gene Bcl2 (B-cell lymphoma 2) was shown to simultanously knock down Bcl2, resulting in an increased susceptibility to apoptosis

and activate RIG-I, leading to type I interferon response with anti-tumour activity in B16 melanoma cells (Poeck et al., 2008).

3.4.2.2 Interferon response to mono or tri-phosphate aptamers

HPV negative C33A and HPV16 positive SiHa cells were utilised to determine if aptamers were triggering expression of interferon response genes, MX1 and IFNβ and also how dephosphorylation of aptamers would affect this response. After 24 hrs incubation with aptamers, RNA levels for MX1 and IFNβ were analysed by quantitative real-time PCR (qPCR) following RNA extraction and cDNA synthesis (Figure 3.15). Resulting data was analysed according to the ΔΔ Ct method by Corbett Rotor-Gene 6000 software (Livak and Schmittgen, 2001). The level of gene expression in A2 and SF1, dephosphorylated A2 and SF1, 21-2 and Poly I:C transfection was compared with that of the mock transfection after normalization of the expression level to the small nuclear RNA (snRNA), U6. Poly I:C was used as a positive control, since has been shown to increase the expression of interferon response genes (Magee and Griffith, 1972, Manetti et al., 1995). 21-2 is a 33 nucleotide oligomer, chemically synthesised aptamer selected against human IL-17A (Ishiguro A., 2011). This aptamer has a 5' OH group instead of triphosphate, therefore could be used as a good control to study 5' immune stimulatory effects of aptamers in cells.

First, effect of aptamers in the upregulation of some interferon response genes was determined in SiHa cells (Figure 3.15A). MX1 and IFNβ gene expressions were enhanced following Poly I:C treatment by up to 87.69 (± 16.13) and 265.75 (± 229.59) fold, respectively. A2 transfection resulted in the up-regulation of MX1 and IFNβ gene expressions with 111.47 (± 46.80) and 628.62 (± 475.0) fold, respectively. De-phosphorylation of A2 resulted in decreased levels of corresponding gene expression by 35 (± 12.48) and 204.52 (± 170.22) fold, respectively. However, a student`s t-test did not show a significant difference between 5' triphosphate and de-phosphorylated (5' monophosphate) A2 transfections in the up-regulation of interferon response genes. When aptamer 21-2, which has 5' OH instead of 5' triphosphate, was used for transfection of SiHa cells, up-regulation of MX1 and IFNβ was relatively low with (4.28 (± 1.46) and 1.78 (± 0.54) fold, respectively, compared to A2 and SF1 transfection. 5' triphosphate and de-phosphorylated SF1 were also used to determine the interferon response. MX1 and IFNβ gene expression were observed as being enhanced in SiHa cells by up to 115.32 (± 40.09) and 1602.69 (± 1440) fold by 5' triphosphate SF1 transfection and 51.85 (± 15.23) and 435.75 (± 366.19) fold, respectively, by de-

phosphorylated SF1 transfection (Belyaeva et al., 2014). There was no significant difference between 5' triphosphate and de-phosphorylated SF1 both in MX1 and IFNβ gene expression (Belyaeva et al., 2014).

Secondly, quantitative real-time PCR (qPCR) technique was also employed in a HPV-negative cervical cancer cell line, C33A (Figure 3.15B). This allowed investigation of the changes in interferon gene expression followed by aptamer transfection +/- de-phosphorylation, as a result of non-specific innate immune sensing. It was shown that MX1 and IFNβ expressions were up-regulated by the Poly IC treatments by 1645.01 (± 762.04) and 2923.28 (± 237.51) fold, respectively. Similar to the results presented above for SiHa cells, 21-2 did not seem to enhance the expressions of MX1 and IFNβ genes [1.41 (± 0.18) and 2.85 (± 0.53) fold, respectively]. Whereas, expression of those genes were up-regulated by 14.33 (± 3.29) and 39.01 (± 2.30) fold, respectively, by transfections with 5' triphosphate A2, and a 3.56 (± 1.48) and 3.23 (± 0.54) fold increase, respectively, by de-phosphorylated A2. Likewise, transfection with 5' triphosphate and de-phosphorylated SF1 resulted in 50.00 (± 21.52) and 7.34 (± 3.37) fold increase, respectively, in MX1; and a 20.23 (± 2.38) and 4.16 (± 0.65) fold increase in IFNβ gene expression (Belyaeva et al., 2014). With reference to the p values calculated by student t-tests, it was indicated that 5' triphosphate A2 and 5' triphosphate SF1 enhanced the expression of IFNβ in C33A cells. Furthermore, it was seemed to be significant compared to the corresponding de-phosphorylated aptamers ($p = 0.0005$ and $p = 0.01$, respectively). It should also be noted that transfections with 5' triphosphate A2 seemed to cause an up-regulation of IFNβ gene significantly higher than that with 5' triphosphate SF1 ($p = 0.015$).

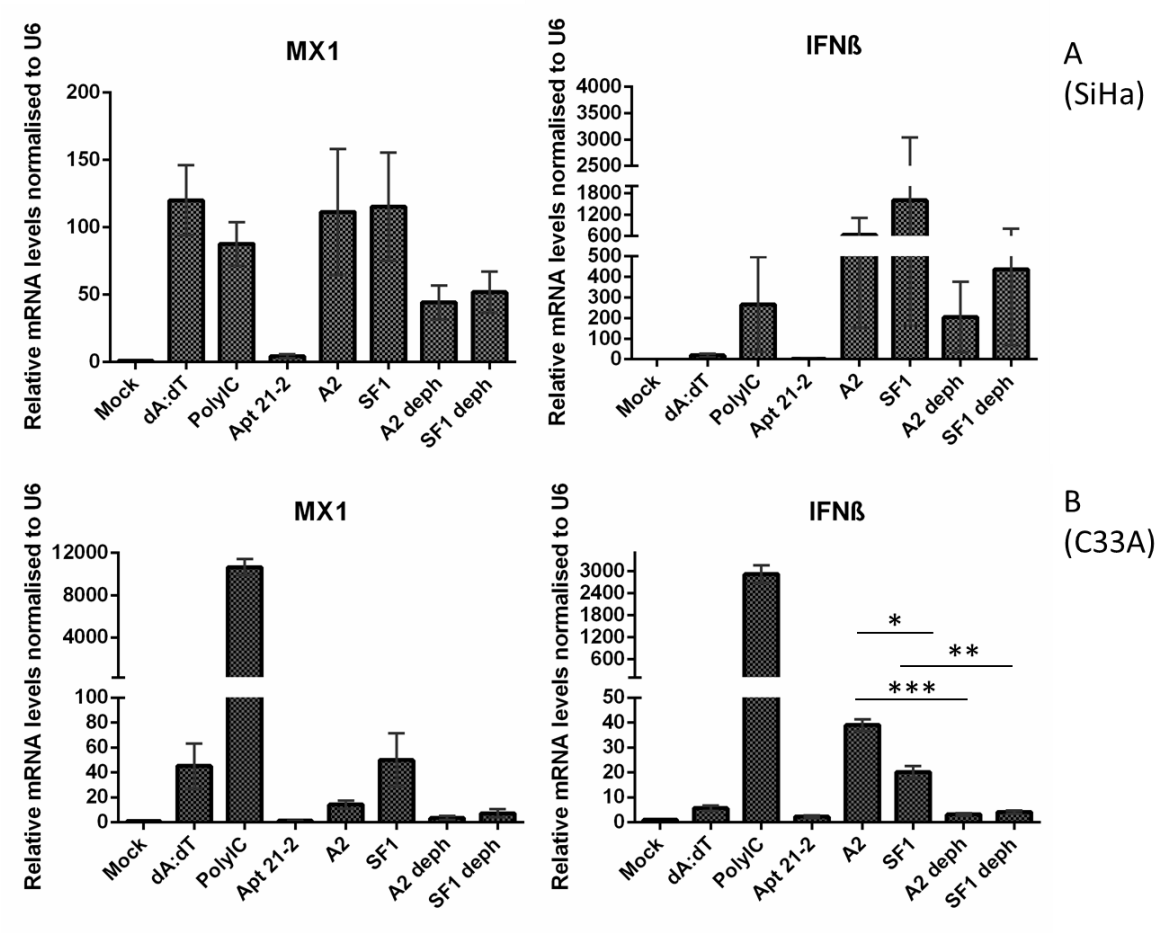

Figure 3.15 Effects of the 5' de-phosphorylation of the RNA on the expressions of interferone response genes; MX1 and IFNβ. SiHa (A) and C33A (B) cells were transfected with either 5' triphosphate or de-phosphorylated A2 and SF1 aptamers. Mock transfections and Poly IC incubations were also included as negative and positive controls, respectively. Aptamer 21-2 was also included as a control due to the presence of –OH groups (a chemically synthesised aptamer) at the 5' end instead of a triphosphate. Cells were incubated at 37°C for 24 hrs, followed by RNA extraction and cDNA synthesis according to the manufacturer`s instructions. Quantitative real-time PCR (qPCR) was performed using Quantifast SYBR Green PCR mix, synthesised cDNA from each transfections and primers (MX1, IFNβ and U6. Gene expression was measured by Corbett Rotor-Gene 6000. Resulting data was analysed according to the ΔΔ C_t method by Corbett Rotor-Gene 6000 software. The level of gene expression in A2 and SF1, dephosphorylated A2 and SF1, 21-2 and Poly IC transfected wells was compared with that of the mock transfected (control) after normalization of the expression level to U6. The data was obtained from three independent experiments (n = 3), shown together with standard errors. p* = 0.015, p = 0.01, p*** = 0.0005 (student`s t-test). Only significant values were represented in the graph.**

Some of the effects on apoptosis could be due to non-specific effects of the 5' triphosphate. To investigate this, apoptosis assays was repeated by using de-phosphorylated aptamers in SiHa cells (section 3.4.2.3).

3.4.2.3 Effects of de-phosphorylation of aptamers on apoptosis in SiHa cells

In order to study whether the 5' triphosphate groups of aptamers were involved in the induction of apoptosis in SiHa cells, *in vitro* transcribed aptamers as well as de-phosphorylated aptamers were utilised. SiHa cells were transfected with A2 and SF1 +/- de-phosphorylation as well as 21-2 (Figure 3.16). Transfection of SiHa cells with 50, 100 and 200 nM A2 resulted in an induction of apoptosis by up to 26.7 (± 3.09)%, 29.3 (± 1.33)% and 30.3 (± 1.51)%, respectively. The corresponding percentage of apoptosis with dephosphorylated A2 was 16.26 (± 0.98)%, 16.96 (± 2.66)% and 18.06 (± 1.79)%, respectively. When A2 was de-phosphorylated, apoptosis was found to be decreased with $p = 0.0162$, $p = 0.00735$ and $p = 0.003221$ for 50, 100 and 200 nM of aptamer, respectively. Transfection with control aptamer SF1 +/- de-phosphorylation was also shown to induce apoptosis in SiHa cells. Apoptosis was found to be 16.6 (± 0.45)%, 19.8 (± 2.47)% and 18.4 (±1.97)% for 5' triphosphate SF1 and 11.86 (± 0.33)%, 12.83 (± 0.82)% and 14.3 (± 0.65)% for de-phosphorylated SF1, respectively, when SiHa cells were transfected with 50, 100 and 200 nM of the aptamer. 5' OH aptamer 21-2 and mock treatment were similar in the apoptosis ratio with 5.66 (± 0.35)% and 5.1 (± 0.92)%, respectively, whereas staurosporine treatment, as a positive control, induced apoptosis by up to 55.23 (± 10.62)% in SiHa cells. The significance between 5' triphosphate and dephosphorylated SF1 was $p = 0.000573$, $p = 0.0275$ and $p = 0.058$ for 50, 100 and 200 nM aptamer transfections, respectively. Although, there was a decrease in apoptosis following de-phosphorylation of both A2 and control aptamer SF1, induction of apoptosis was significantly enhanced in cells transfected with 50 nM de-phosphorylated A2 compared to that of SF1 with $p = 0.0066$. 5' triphosphate A2, as shown in section 3.4.1.1, induced apoptosis in SiHa cells and it was significant over SF1 transfection with p values of 0.016, 0.014 and 0.004 for 50, 100 and 200 nM aptamer transfection, respectively.

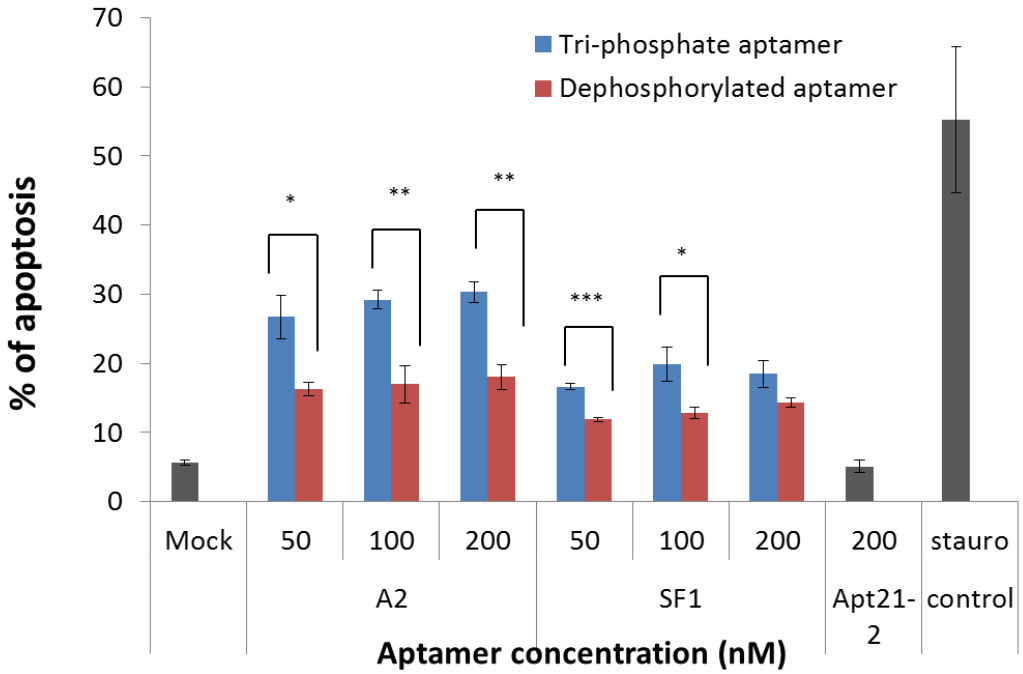

Figure 3.16 Effects of de-phosphorylation on the total apoptosis (early+late) triggered by aptamers. Aptamer A2 and SF1 (4 µM each) were de-phosphorylated using 10 u of Antarctic phosphatase, reaction buffer and 20 u RNase for 45 min at 37°C, followed by enzyme inactivation at 70°C for 10 min. After phenol: chloroform extraction and ethanol precipitations, aptamers were re-suspended in nuclease-free dH_2O to obtain 10 µM solutions. SiHa cells were seeded on to 12-well plates at 1.5 x 10^5 cells/ ml per well and incubated for 24 hrs at 37°C with 5% CO_2. Cells were mock transfected or transfected up to 200 nM with either tri-phosphate (*in vitro* transcribed) or de-phosphorylated aptamers as well as 21-2 (5' OH) as a control. Staurosporine was also used as a positive control due to its high potency of causing apoptosis. Cells were analysed for apoptosis 24 hours later. Cells were collected and washed several times with PBS. Cell pellets were dual-stained with FITC-conjugated annexin V and propidium iodide followed by analysis on the flow cytometer. Graph shows the total percentage of apoptosis, analysed from three independent experiments (n = 3), together with standard errors. P values were calculated for each concentrations in the same aptamer, tri-phosphate or de-phosphorylated. p* <0.05, p <0.01 and p*** <0.001.**

3.5 Chapter Discussion

Tumour formation in HPV positive cervical cancers is initiated by uncontrolled proliferation of cells due to abrogation of cell cycle control by HPV oncoproteins. pRb and its related proteins, p107 and p130 are major tumour suppressor proteins that prevents uncontrolled proliferation by preventing cells to enter S-phase of cell cycle (Nevins, 2001). pRb is a key target for inactivation by the viral oncoproteins E1A, E7 and T-antigen from adenovirus, HPV and simian 40 (SV40), respectively (Felsani et al., 2006) E7 from other high- and low- risk HPVs are able to target these tumour

suppressor proteins for degradation, resulting in the release of E2Fs therefore leading to transcription of downstream S-phase genes (Davies et al., 1993, Felsani et al., 2006, Zhang et al., 2006). In this chapter, the levels of E7 and pRb expression in three different cervical cancer cell lines; CasKi, SiHa and HeLa cells were studied and compared to levels in HEK293T cells. 16E7 from CaSki and SiHa cells and 18E7 from HeLa cells were detected, however levels were higher in CaSki cells (Figure 3.1). pRb expression levels in SiHa and HeLa cells were higher than in CaSki cells which is consistent with having lower levels of E7 present in these cells. Both phosphorylated and unphosphorylated forms of p130 from CaSki and SiHa cells were also detected despite the fact that their levels were also reduced in comparison to 293T cells possibly due to E7 oncoprotein expression. Attempts in order to detect p130 from HeLa cells were not successful. Due to the high level of E7 expression, CaSki cells were selected for further experiments.

The effects of HPV16 E7 aptamers especially A2 on pRb and E7 levels was then investigated (Figure 3.2). Following the transfection of CaSki cells with A2, steady state levels of E7 decreased with an accompanied increase in pRb levels (Nicol et al., 2013). This was consistent with the hypothesis that A2 was binding to LXCXE motif of E7, therefore preventing its binding to pRb (Nicol et al., 2011, Nicol et al., 2013). Recovery of pRb, especially the hypophosphorylated active form, might lead to cell cycle arrest and apoptosis of cervical cancer cells, since, it was shown that expression of constitutively active ectopic pRb alleles (PSM-Rb) suppress cell proliferation by arresting the cell cycle (Angus et al., 2002). Depletion of E7 following A2 treatment in SiHa cells might have resulted in the reactivation of mechanisms that are involved in the cell cycle control, indicating that although HPV positive cells are highly transformed they are still very much dependent on the functions of E7 for cell viability (Goodwin and DiMaio, 2000, Magaldi et al., 2012). Elevated levels of active pRb might have also been the trigger for apoptosis that was observed in HaCaT-HPV16 E7 stable cells (Figure 3.14B). However, some pRb-independent mechanisms could also result in cell proliferation in cervical cancer cells. Some antibodies that were identified against E7 were shown to bind to the amino terminus but not pRb binding site by epitope mapping and inhibit cell proliferation in SiHa cells possibly via pRb-independent mechanisms (Accardi et al., 2011). The region upstream of the LXCXE pocket of E7 at the amino terminus was also shown to be involved in the degradation of pRb and its related proteins although it does not play a role in E7-pRb binding (Gonzalez et al., 2001). Non-pRb targets of E7 have also been studied and demonstrated to be important in development of invasive cervical carcinoma (Balsitis

et al., 2003). In addition, E7 could also destabilise pRb via other cellular proteins (Huh et al., 2005).

Rb is the first gene from Rb family, however, subsequently two other related proteins from same family were identified as p130 (Rb2) and p107 (Rbl2) (Felsani et al., 2006). These family of proteins share a considerable structural and functional homology, primarily at the level of the 'pocket' domain (see section 1.2.4.2) (Felsani et al., 2006). HPV16 E7 and other DNA tumour viruses such as polyomavirus Large T antigen and adenovirus E1A, which contains an LXCXE motif could also bind other Rb related-proteins, p107 and p130 (DeCaprio, 2014). Therefore, steady state level of p130 was also investigated in the presence and absence of aptamers (Figure 3.2C). Levels of p130, however, seemed unaffected following aptamer transfection with A2 (Figure 3.2D). In addition to A2, transfection with A1 and J1 seemed to slightly decrease E7 levels. Mfold software predicts a very similar, and quite stable secondary structures for aptamers A1 and A2, having a stemloop containing a CCAC motif (Figure 3.3). However, both secondary structures predicted for A3 by Mfold were less stable than for other A-series aptamers although there is only 1-2 nucleotide difference in sequence. This structure prediction seemed to be consisted with data presented here where A1 and A2 had an effect on E7 degradation but not A3 (Figure 3.2A, B). One reason for this could be the lower affinity binding of A3 (KD_{app} = 251 nM), to GST-E7 in comparison with A1 and A2 (KD_{app} = 87 and 107 nM, respectively) (Nicol et al., 2011). J1 was also demonstrated as being effective on E7 oncoprotein degradation (Figure 3.2A, B).

The amino terminus of E7 is “intrinsically disordered” or “natively unfolded” which may present conformational plasticity to E7 in order to optimise their binding to multiple cellular components by conformational change (α-helix and β-sheet transition) depending on the conditions of intracellular environment such as pH (Garcia-Alai et al., 2007, Uversky et al., 2006). Therefore, we could hypothesise that an HPV16 E7 aptamer, especially A2 binding to amino terminus, could result in a conformational shift of the E7 oncoprotein, preventing its interactions with other cellular target proteins as well as pRb. Therefore, in addition to preventing pRb binding via occupying LXCXE pocket with aptamers, A2 could affect E7 conformational change, therefore effecting other interactions leading to unstability and subsequently degradation of E7. E7 is a highly unstable protein with a half-life of around ~30 min (Smotkin and Wettstein, 1987). Prevention of E7 oncoprotein binding pRb by A2 could therefore be resulting in the gradual depletion of E7 from CaSki cells.

The model above predicts that E7 loss could be accompanied by apoptosis. This was investigated in SiHa cells (HPV16 positive) as well as HeLa and C33A cells (HPV18 positive and HPV negative, respectively) (Figure 3.12). Apoptosis assays indicated that HPV16 E7 aptamer A2 induced apoptosis in SiHa cells but not in HeLa or C33A cells. It was not possible to demonstrate the same experiments in CaSki cell cells due to higher levels of E7 expression. In addition, it was not possible to increase the amount of transfected RNA (Nicol et al., 2013, personal communication). It was shown that CaSki cells were highly resistant to the overexpression or recovery of pRb compared to SiHa and HeLa cells (Bourgo et al., 2009). One explanation could be that CaSki cells could also bear additional mutations preventing responses to ectopic expressions or recovery of pRb.

Apoptosis induced by A2 was significantly higher than that by control aptamer SF1 in HPV positive SiHa cells (Figure 3.12A). Other A-series aptamers A1 and A3, similarly, seemed capable of inducing apoptosis in SiHa cells (Figure 3.13A). However, they did not cause a decrease in the levels of E7 oncoprotein as good as A2 (as discussed above). Although A1 and A3 might not be as effective in disrupting E7-pRb interactions (Nicol et al., 2013), they could still change the conformation of E7 oncoprotein which might be affecting its interactions with other cellular proteins, resulting in non-pRb mediated apoptosis in HPV positive cells.

HPV16 and HPV18 only share around ~ 50% homology at the nucleotide level (Corden et al., 1999) and they result in similar disease although HPV16 and 18 differs in malignant transformation. HPV18 might be more aggressive than HPV16 (Badaracco et al., 2002, Fernandes et al., 2005). This could be due to the full integration of HPV18 into the host genome even in pre-invasive lesions (Badaracco et al., 2002).There are, however, conserved sequences between HPV16 and 18 E7. Therefore, cross-reactivity of the E7 aptamers with HPV18 E7 was investigated (Figure 3.11). Our main observation was that aptamer A2 seemed to have relatively smaller effect on HPV18 E7 when compared to another A-series aptamer A1 and also an outlier aptamer J1. These aptamers (especially A1 and J1) resulted in a decrease in the levels of HPV18 E7 in HeLa cells. When pRb levels were analysed, there was an accompanying increase in its steady state level (figure 3.11C, D). However, this was not correlated with the degree of reduction of HPV18 E7 following aptamer transfections. Therefore, the interaction of A1 and J1 with HPV18 E7 could be via other regions of oncoprotein than the pRb binding site, LXCXE in conserved region 2.

RNA polymerases, including phage polymerase, leave a triphosphorylated end at the 5' end of RNA molecules transcribed *in vitro* from 5' – to 3' – using a template DNA (Kim et al., 2004). Due to possessing this 5' triphosphate moiety, aptamers might trigger RIG-I induced upregulation of interferon genes. The recognition of 5' triphosphate RNA by RIG-I is known to be independent of the RNA sequence (Hornung et al., 2006). In addition to RIG-I, interferon-induced proteins with tetratricopeptide repeats (IFITs) were recently discovered and shown to directly engage with 5' triphosphate RNAs in a non-sequence specific manner via their tetratricopeptide repeat domains (TPRs), resulting in the reduction of viral replication in HEK cells (Abbas et al., 2013). RIG-I, however, has been studied extensively well and shown to require recoginition by base-pairing to some extent (10 bp) and/or a 5' triphosphate group to induce antiviral signaling (Schlee et al., 2009b, Schmidt et al., 2009).

Interferon production was observed to be enhanced by poly I:C treatment in both SiHa and C33A cells (Figure 3.15). Since, RIG-I can be activated by poly I:C (Yoneyama et al., 2004), in particular by shorter size fractions (300 bp) (Kato et al., 2008), which is a dsRNA polymer generated by polynucleotide phosphorylase and harbours 5`monophosphates (Grunberg-Manago, 1967). However, 21-2 bearing a 2' – OH at the 5' end of RNA did not induce upregulation of interferon genes (Figure 3.15A, B).

Aptamer A2 and SF1 (control aptamer) as well as dephosphorylated A2 and SF1 were used for transfection of SiHa (HPV positive) and C33A (HPV negative) cells in order to analyse by RT-qPCR whether some interferon response genes, MX1 and IFNβ, were upregulated (Figure 3.15). A2 and SF1 were both found to induce production of MX1 and IFNβ in SiHa and C33A cells. Dephosphorylation of aptamers did not result in a significant decrease in interferon production in SiHa cells although mean values were indicating that dephosphorylation did reduce the response. However, IFNβ expression were found to be significantly downregulated by transfection with dephosphorylated aptamers compared to 5`triphosphate aptamers in C33A cells although overall production of interferon were higher in SiHa cells than C33A cells. This could be due to the difference in localisation of aptamer/RIG-I complexes in different cells.

Modifications of bases (pseudouridine, 2-thio-uridine) and backbone (2'-O-methyl-uridine, 2'-fluoro-uridine) have been shown to abolish innate immune signalling via both TLR7/8 and RIG-I by triphosphate RNA (Hornung et al., 2006, Uzri and Gehrke,

2009, Morrissey et al., 2005). HCV 3 - UTR and poly (U/UC) RNAs transcribed with 2'- fluoro-dUTP, 2'-fluoro- dCTP and pseudouridine were demonstrated to be impaired in their immunostimulatory effects (Uzri and Gehrke, 2009) although they were still able to bind RIG-I, suggesting that these modifications might be inhibiting the subsequent conformational change, dimerisation or ATPase activation of RIG-I. Conversely, HPV16 aptamers as well as control aptamer SF1 with 5' triphosphate triggered an interferon response, especially IFNβ production despite incorporation of 2'-deoxy-2'-fluoro-UTP or CTP (in order to increase the stability against endonucleases).

Dephosphorylated aptamers seemed also to induce IFNβ and MX1 gene expression although the average fold activation of the response were slightly lower than for 5' triphosphate aptamers. This could have resulted from the fact that dephosphorylation might not be 100% efficient. Similar studies have been perfomed using siRNAs. These molecules were treated with RNase T1 or phosphatase which abolised the interferon production triggered by transcribed RNA molecules (Kim et al., 2004). These dephosphorylated (mono-phosphate) aptamers could be activating innate immunity via some other pathways such as TLR3. Since, synthetic mono-phosphate 2' fluoro modified siRNA molecules were shown to induce type I interferon (IFNα and β), IL-8 and TNF-α production through TLR3 (Kariko et al., 2004). It has been shown that although TLR expression was reduced in HPV positive cells when compared to HPV negative (C33A) cells, TLR3 however was found to be expressed relatively better among other TLRs in HPV positive cells (Yu et al., 2012). Activation of TLR3 triggers intracellular pathways mediated by NFκB and MAPK, resulting in the upregulation of IFNβ and TNF-α gene expression (Alexopoulou et al., 2001, Kenny and O'Neill, 2008). NFκB will then result in the expression of pro-inflammatory cytokines (e.g. IL-1) which induces senesence and apoptosis along with IFN-β (Chiantore et al., 2012, Duan et al., 2011). This could be one of the reasons why relatively higher background of induction of apoptosis in cells by 5' triphosphate aptamer transfection was observed. Therefore, the effect of 5' triphosphate as well as dephosphorylated aptamers in the induction of apoptosis was analysed by Annexin V apoptosis assays (Figure 3.15). Although apoptosis induced by A2 was significantly higher than that by control aptamer SF1, dephosphorylation of aptamers also resulted in a decrease in apoptosis. Therefore, we could suggest that some of the apoptosis reported might be due to the 5' triphosphate moiety.

4 PATHWAYS OF E7 DEGRADATION BY APTAMER TRANSFECTION

4.1 Use of inhibitors to study the degradation of E7 in the presence or absence of aptamers

4.1.1 Introduction

In eukaryotes, protein degradation occurs via four different mechanisms (Ryhanen et al., 2009). Proteasomes are the major pathway which is responsible for the degradation of normal or mis-folded long- or short- lived proteins. Second is mitochondrial proteases that are responsible for degradation of mitochondrial proteins. Third is the degradation of membrane associated proteins or enzymes as well as cytoskeletal proteins via calcium-activated calpains (cysteine proteases). Last is lysosomal degradation/autophagy where membrane proteins, endocytosed proteins and organelles are degraded.

Proteasomes are located both in the nucleus and cytosol of all cells both free or attached to the endoplasmic reticulum. They are responsible for the ATP-ubiquitin-dependent protein degradation. This means that proteasomes recognise and digest proteins that targeted for degradation with an ubiquitin group. The proteasome is a large 26S multicatalytic complex which is responsible for degradation of polyubiquitinated substrates generated by the polyubiquitinating enzymatic machinery (Ciechanover, 2005). It consists of two subcomplexes one of which is ATP-dependent 19S regulatory particle responsible for recognition of polyubiquitinated substrates (Ciechanover, 2005). The 20S subcomplex is the core of the proteasome which harbours multiple peptidase activities including chymotryptic, tryptic-, and peptidylglutamyl-like activity (Bochtler et al., 1999). 20S proteasome has a cylindrical shape with four rings. Two rings with seven α-subunits are located on the outer sides and other two rings with seven β-subunits are both located on the inner side (Craiu et al., 1997). Centre of this 20S particle somewhere in β-subnuits functions as a proteolytic core. There are also a variety of protein substrates which can be degraded by proteasomes in a ubiquitin-independent manner such as Rpn4, thymidylate synthase and ornithine decarboxylase which functions as a transcriptional regulator of proteasome homeostasis, an enzyme in DNA replication and polyamine biosynthesis, respectively (Erales and Coffino, 2014).

The other mechanism for protein degradation is through lysosomes which are membraneous organelles containing digestive enzymes such as aspartin, cysteine and serine proteases (Craiu et al., 1997). They can metabolise cytoplasmic proteins and organelles as well as endocytosed extra cellular proteins, nucleic acids or other substances. In order to be able to degrade cellular proteins, proteins need to be internalised by lysosomes. This could happen via “autophagy” where vesicles termed “autophagosomes” are formed in the cytoplasm which originates from endoplasmic reticulum, mitochondria, glycogen bodies and other cytoplasmic materials (Ciechanover, 2005). These vesicles are then fused with lysosomes and degradation of their contents occurs by lysosomal enzymes. Uptake by lysosomes is not completely nonselective. In the case of starvation, for instance, some cellular proteins could be internalised and broken down by lysosomes. These proteins have been suggested to contain a consensus amino acid sequence, KFERQ, possibly involved in targeting to the lysosomes (Ciechanover, 2005). Molecular chaperons such as Hsp70 family could also play a role in the internalisation of proteins into lysosomes by unfolding the proteins in order to ensure their transport across the lysosomal membrane (Ryhanen et al., 2009).

As shown in section 3.2, HPV16 E7 aptamers, especially A2, were found to reduce the steady state level of E7 in CaSki cells. To further analyse E7 degradation induced by A2, several proteasomal and lysosomal inhibitors as well as inhibitors against endoplasmic reticulum associated and HDAC6 mediated (for mis-folded proteins) degradations were used to look for differences in degradation patterns in the presence or absence of aptamer. Levels of E7 oncoprotein and cellular proteins were determined by immunoblot analysis and results were also represented as graphs obtained by densitometry analysis.

4.1.2 Effects of MG132 (an inhibitor for proteasomes/lysosomes) on E7 degradation

The peptide-aldehyde proteasome inhibitor, MG132 (carbobenzoxyl-L-leucyl-L-leucyl-L-leucinal) (a natural triterpene) is derived from a Chinese medicinal plant, which inhibits 20S proteasome activity by a covalent association with the active site of the beta subunits and effectively interrupt the proteolytic function of the 26S proteasome complex, which is the most commonly used mammalian cytosolic proteasome, reversibly (Guo and Peng, 2013). In order to determine the toxicity of this inhibitor in CaSki cells, the concentration of MG132 for use was optimised by treatments of 50, 100 and 200 µM. At 100 µM, protein translation was not completely

abolished but degradation was inhibited (data not shown). CaSki cells that were transfected with aptamers for 16 hours were treated with MG132 for 0, 3 and 6 hrs. Treatments were performed for 16 hours which should allow enough time to A2 to bind E7 without completely depleting E7 levels (Figures 3.4 and 3.5).

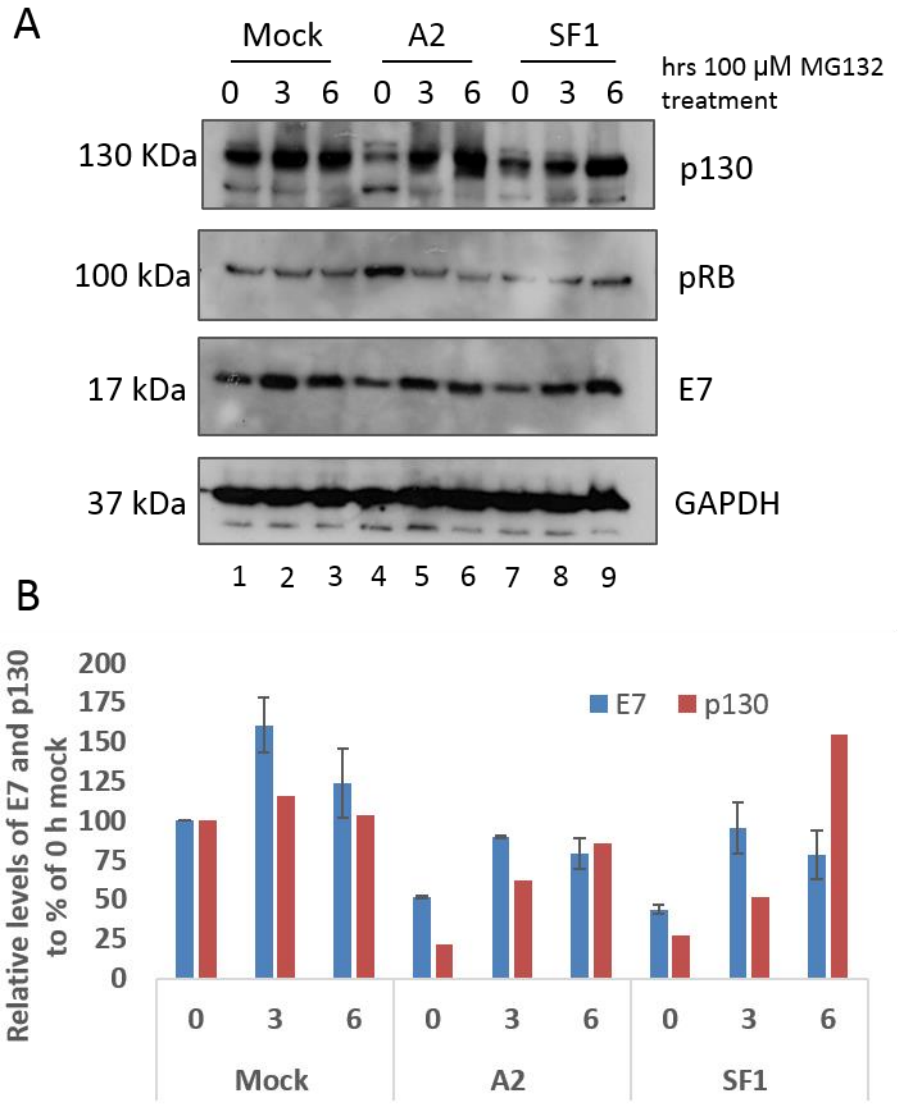

Figure 4.1 Treatment of CaSki cells with 100 µM MG132 for 0, 3 and 6 hrs to analyse E7 degradation following aptamer transfection. CaSki cells were seeded on 6-well plates 24 hrs prior to transfection with aptamers. Cells were then mock transfected (Lane 1-3) or transfected with 100 nM A2 (Lanes 4-6) or SF1 (Lanes 7-9) for 16 hrs. Each transfection was subjected to 0 (Lanes 1, 4, 7), 3 (Lanes 2, 5, 8) and 6 (Lanes 3, 6, 9) hrs incubation with 100 µM MG132 at 37°C. Samples were collected, lysed in RIPA (containing protease inhibitors, DNase I, $MgCl_2$) and Laemli SDS-loading buffer. Immunoblot analysis was performed

to detect p130, pRb, E7 and GAPDH (loading control for E7). Densitometry analysis of band intensities were performed and presented as a graph, together with standard errors (B) following normalisation against GAPDH relative to % of 0 h mock treatment. The result shown is a representative of three (n = 3) and two (n = 2) independent experiments, respectively for E7 and, pRb and p130.

Figure 4.1 showed an increase in E7 levels following MG132 treatment in the presence or absence of the aptamer, suggesting that E7 degradation in general occurs via proteasomal degradation. The levels of E7 did not appear to be affected by MG132 treatment. Therefore, proteasomal pathways might not be responsible for A2-mediated effects. In addition, p130 levels were enhanced following MG132 treatment in a time dependent manner, suggesting that this protein was also degraded by the proteasomal pathway. When 0 h MG132 treatments from mock (Lane 1), A2 and SF1 (Lanes 4 and 7, respectively) were compared in Figure 4.1A, A2 transfection was shown to result in the recovery of pRb as expected (section 3.2.2). However, overall the effects of MG132 treatment on pRb levels were clouded by possible E7 build up. An interesting observation from both western blot and densitometry data was that 0 h MG132 treatment of aptamer transfected CaSki cells (Figure 4.1A, Lanes 4 and 7) showed less p130 expression when compared to mock treated cells (Figure 4.1A, Lane 1). This was not consistent with the increase seen in pRb levels following A2 transfections.

4.1.3 Effects of lactacystin (a proteasome inhibitor) on E7 degradation

Lactacystin, an antibiotic isolated from *Streptomyces*, inhibits protein degradation irreversibly by covalently modifying chymotryptic, tryptic and peptydylglutamyl peptide hydrolysing activities of 20S and 26S proteasomes (Craiu et al., 1997). It is a highly specific inhibitor showing no effects on cysteine or serine proteases which belong to lysosomal proteases located within all vesicles of the endocytic pathway (Craiu et al., 1997).

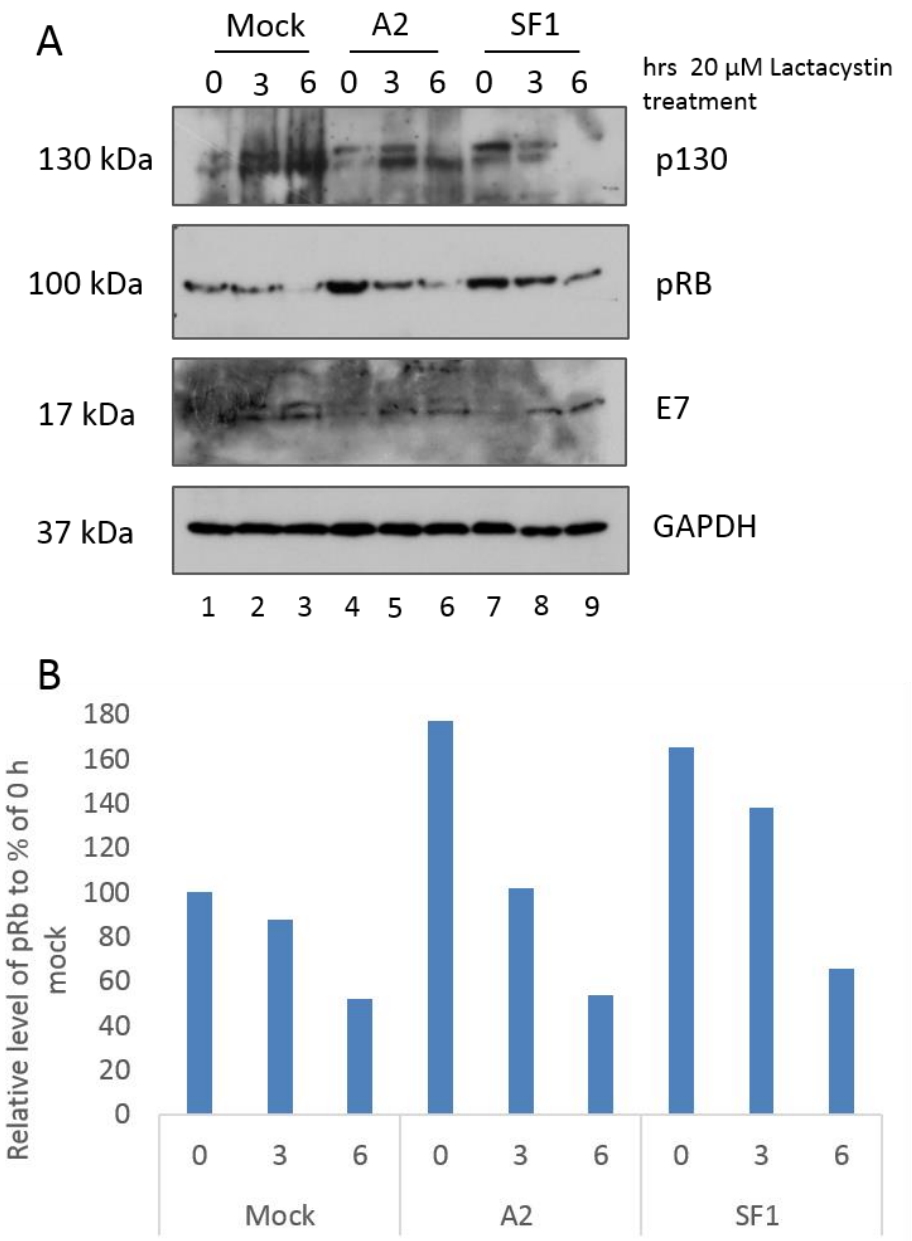

Figure 4.2 Treatment of CaSki cells with 20 µM lactacystin for 0, 3 and 6 hrs to analyse E7 degradation following aptamer transfection. CaSki cells were seeded on 6-well plates 24 hrs prior to transfection with aptamers. Cells were then mock transfected (Lanes 1-3) or transfected with 100 nM A2 (Lanes 4-6) or SF1 (Lanes 7-9) for 16 hrs. Each transfection was subjected to 0 (Lanes 1, 4 and 7), 3 (Lanes 2, 5 and 8) and 6 (Lanes 3, 6 and 9) hrs incubation with 20 µM Lactacystin at 37°C. Samples were collected, lysed in RIPA (containing protease inhibitors, DNase I, $MgCl_2$) and Laemli SDS-loading buffer. Immunoblot analysis was performed to detect p130, pRb, E7 and GAPDH (housekeeping control for E7). Densitometry analysis of band intensities were performed and presented (B) following normalisation against GAPDH relative to % of 0 h mock treatment. The result shown is a representative of two independent experiments (n = 2) for E7 and single experiment for pRb and p130 (n = 1).

E7 and pRb and p130 degradation with or without aptamers were also investigated with the more specific proteasome inhibitor, lactacystin (Figure 4.2). Treatment of mock (Lanes 2 and 3) or aptamer transfected (Lanes 5 and 6 for A2; Lanes 8 and 9 for SF1) CaSki cells with lactacystin resulted in accumulation of E7 oncoprotein (Figure 4.2A), indicating that degradation of E7 occurred via proteasomal pathway with no difference between mock or aptamer transfections. Figure 4.2A also showed the detection of both hypo- and hyper- phosphorylated forms of p130. Inhibitor treatment seemed to result in an increase in the hypo-phosphorylated form and a decrease in the hyper-phosphorylated p130 with A2 transfected cells (Figure 4.2A, Lanes 4, 5 and 6). Whereas, both forms of p130 seemed to increase in mock treated cells following incubation with the inhibitor (Lanes 1, 2 and 3). Detection of p130 for SF1 treated cells were poor (Lanes 7, 8 and 9), therefore results for the effect of SF1 on p130 were inconclusive. E7 and p130 protein bands were difficult to quantitate, therefore only western blot data is presented here.

However, pRb was detected by immunoblotting and densitometry analysis was also performed (Figure 2.4A and B). Both demonstrated that inhibitor treatment resulted in a decrease in pRb levels in mock and aptamer transfected cells despite expectation of an increase instead. This could result from accumulation of E7 which could be targeting pRb and preventing its build-up. However, the densitometry graph (Figure 2.4B) was generated from n = 1 data.

4.1.4 Effects of chloroquine (a lysosomal inhibitor) on E7 degradation

Chloroquine (well-known as anti-malarial drug) as a weakly basic compound could accumulate in acidic organelles such as endosomes and lysosomes, therefore prevents lysosomal acidification. Accumulation of this inhibitor in lysosomes results in the inhibition of enzymes which are highly dependent on the acidic pH, and enlargement of lysosomes (Nujic et al., 2012). Consequently, many cellular functions including receptor–mediated endocytosis, autophagy, apoptosis and protein degradation could be affected due to inhibition of autophagosome–lysosome fusion (Shintani and Klionsky, 2004). Chloroquine seemed to be highly toxic to cells, resulting in a dramatic decrease in protein levels possibly by affecting translation of proteins including E7 oncoprotein (data not shown). Therefore, first, working and nontoxic concentrations of chloroquine were determined and optimised by treating CaSki cells with a series of concentrations (10 – 200 µM) for several time points (0 – 6 hrs), and analysing cell lysates by immunoblotting. Treatment of cells with 30 µM of chloroquine, concentration was selected for further experiments due to the lowest

toxicity, was performed in CaSki cells in the presence and absence of aptamer (Figure 4.3).

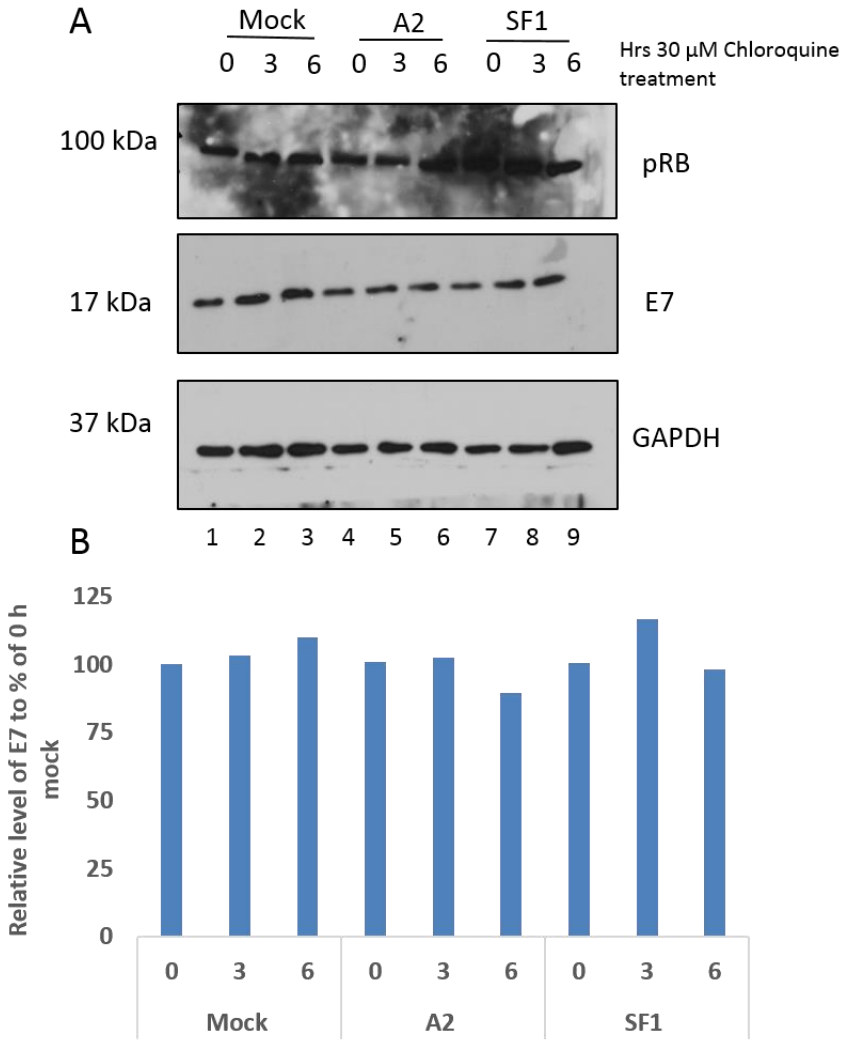

Figure 4.3 Treatment of CaSki cells with 30 µM chloroquine for 0, 3 and 6 h to analyse E7 degradation following aptamer transfection. CaSki cells were seeded on 6-well plates 24 h prior to transfection with aptamers. Cells were then mock transfected (Lanes 1-3) or transfected with 100 nM A2 (Lanes 4-6) or SF1 (Lanes 7-9) for 16 h. Each transfection was subjected to 0 (Lanes 1, 4 and 7), 3 (Lanes 2, 5 and 8) and 6 (Lanes 3, 6 and 9) hrs incubation with 30 µM chloroquine at 37° C. Samples were collected, lysed in RIPA (containing protease inhibitors, DNase I, $MgCl_2$) and Laemli SDS-loading buffer. Immunoblot analysis was performed to detect p130, pRb, E7 and GAPDH (loading control used for E7). Densitometry analysis of band intensities were performed and presented (B) following normalisation against GAPDH relative to % of 0 h mock treatment. The result shown is one of two independent experiments (n = 2).

Figure 4.3 A and B showed that there was a slight increase in the levels of E7 with mock (Lanes 2 and 3) and SF1 (Lanes 8 and 9) transfection following chloroquine

treatment, suggesting that E7 could also be degraded via lysosomes. There was no A2-mediated build-up of E7 detected (Lanes 5 and 6), however, this was n = 1. pRb levels were shown in Figure 4.3A as unaffected by chloroquine treatment, possibly due to the fact that pRb degradation could not be mediated by lysosomes. Densitometry analysis of pRb could not be performed owing to the poor quality of the pRb blot.

4.1.5 Effects of Tubacin (an inhibitor of HDAC6 which is required for degradation of mis-folded proteins) on E7 degradation

As discussed in section 3.5, E7 oncoprotein might have had a conformational change as a result of aptamer binding, therefore resulting in the degradation of the protein via pathways involved in mis-folded protein degradation such as HDAC6. Histone deacetylase 6 (HDAC6) is a cytoplasmic deacetylase involved in the catalysis of alpha-tubulin deacetylation, which result in cell motility (Gao et al., 2007). Data obtained from co-localisation experiments of HDAC6 with some aggresome markers showed that HDAC6 could translocate to aggresomes in response to stress or potent agent that induce mis-folding of proteins such as DTT and tunicamycin (Kawaguchi et al., 2003). The same report also indicated by immunoprecipitation of HDAC6 with polyubiquitinated and unubiquinated species of the same protein that HDAC6 selectively co-precipitates with polyubiquitinated proteins, and therefore facilitates the formation of polyubiquitinated mis-folded proteins in aggresomes (Kawaguchi et al., 2003). Inhibition of HDAC6 diminishes the recruitment of polyubiquitinated proteins to dynein, the clearance of mis-folded protein aggregates from the cytoplasm, and aggresome formation (Kawaguchi et al., 2003). Therefore, an inhibitor against HDAC6, Tubacin was utilised in order to disrupt HDAC6-mediated protein degradation. Due to the fact that tubacin has been reported to induce tubulin acetylation (Chou and Chen, 2008), an acetylated tubulin antibody were also included in immunoblotting in order to confirm the efficiency of tubacin treatments as a positive control (Figure 4.4).

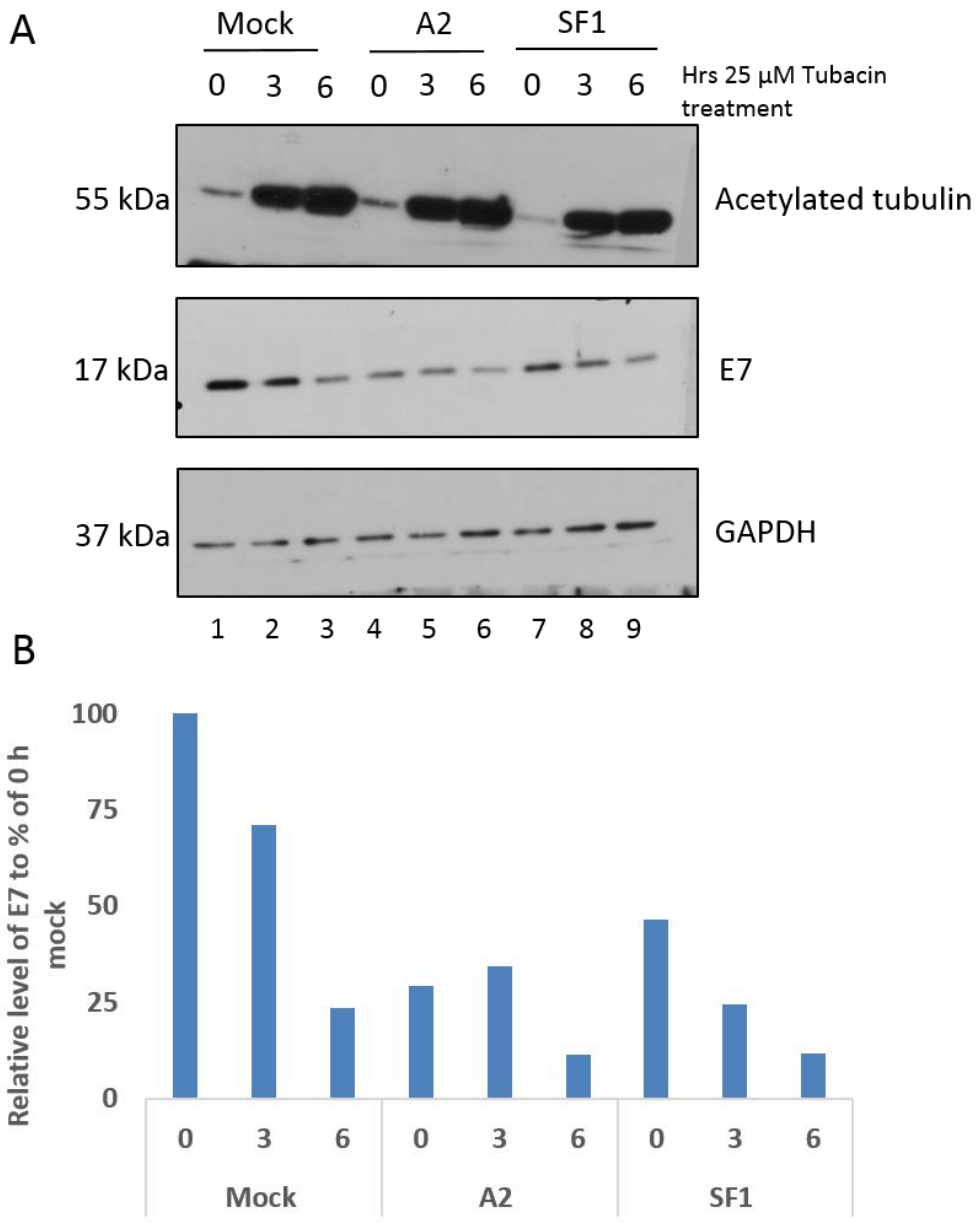

Figure 4.4 Treatment of CaSki cells with 25 µM tubacin for 0, 3 and 6 hrs to analyse E7 degradation following aptamer transfection. CaSki cells were seeded on 6-well plates 24 hrs prior to transfection with aptamers. Cells were then mock transfected (Lanes 1-3) or transfected with 100 nM A2 (Lanes 4-6) or SF1 (Lanes 7-9) for 16 hrs. Each transfection was subjected to 0 (Lanes 1, 4 and 7), 3 (Lanes 2, 5 and 8) and 6 (Lanes 3, 6 and 9) hrs incubation with 25 µM Tubacin at 37°C. Samples were collected, lysed in RIPA (containing protease inhibitors, DNase I, $MgCl_2$) and Laemli SDS-loading buffer. Immunoblot analysis was performed to detect p130, pRb, E7 and GAPDH (loading control used for E7). Densitometry analysis of band intensities were performed and presented (B) following normalisation against GAPDH relative to % of 0 h mock treatment. The result shown is a representative of two independent experiments (n = 2).

Figure 4.4A showed that tubacin treatment resulted in a dramatic increase in acetylated tubulin (~55 kDa) in a time-dependent manner. Conversely, E7 levels seemed unaffected or slightly decreased with inhibitor treatment, suggesting that mis-folded protein response is not responsible for normal E7 degradation (Figure 4.4 A, B). Even if A2 causes conformational change of E7, it does not seem to trigger this pathway. pRb and p130 data could not be obtained for tubacin treatment.

4.1.6 Effects of Eeyarestatin I (an inhibitor for ER-associated protein degradation) on E7 degradation

The ER-associated degradation (ERAD) pathway is responsible for ubiquitin-mediated degradation of several ER-associated mis-folded as well as normal proteins in cytosol by proteasome. This pathway requires AAA ATPase p97, which is a cytosolic ATPase and its function is to carry polyubiquitinated mis-folded proteins from the ER membranes in to the proteasome for degradation (Wang et al., 2008). ERAD can be inhibited by Eeyarestatin I in mammalian cells. This inhibitor was shown to form complexes with p97 (Wang et al., 2008). These complexes were detected to emit higher fluorescence from eeyarestatin I treated cells when compared to untreated cells or complexes formed by another cytosolic protein, heat shock protein 90 (Hsp90) (Wang et al., 2008). Formation of eeyarestatin I and p97 complexes were later indicated by surface plasmon resonance (SPR) analysis as a result of a direct interaction (Wang et al., 2010). This inhibitor, eeyarestatin I was employed so as to investigate E7 degradation in CaSki cells in the presence or absence of aptamers (Figure 4.5).

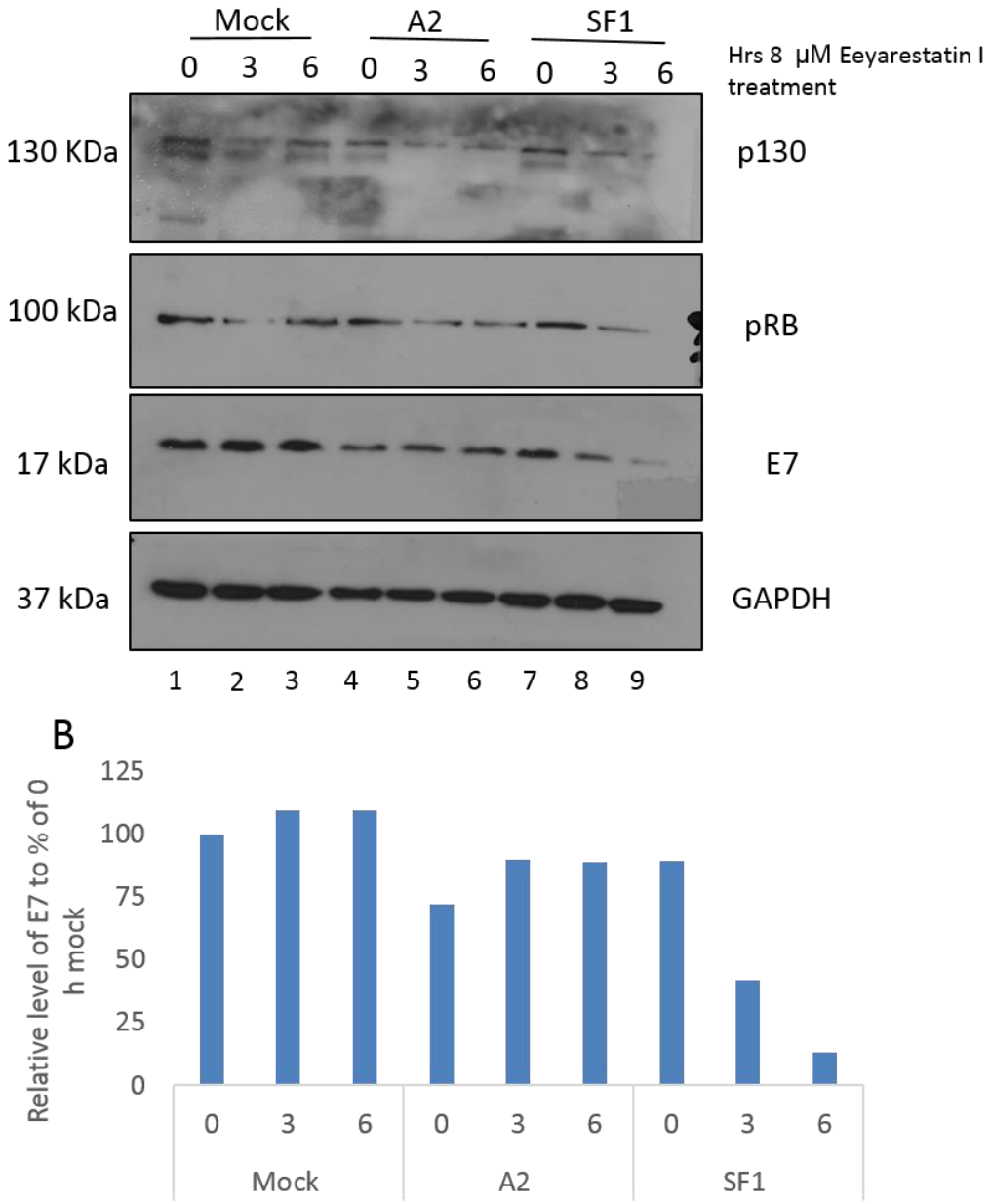

Figure 4.5 Treatment of CaSki cells with 8 μM eeyarestatin I for 0, 3 and 6 hrs to analyse E7 degradation following aptamer transfection. CaSki cells were seeded on 6-well plates 24 hrs prior to transfection with aptamers. Cells were then mock transfected (Lanes 1-3) or transfected with 100 nM A2 (Lanes 4-6) or SF1 (Lanes 7-9) for 16 hrs. Each transfection was subjected to 0 (Lanes 1, 4 and 7), 3 (Lanes 2, 5 and 8) and 6 (Lanes 3, 6 and 9) hrs incubation with 8 μM eeyarestatin I at 37°C. Samples were collected, lysed in RIPA (containing protease inhibitors, DNase I, $MgCl_2$) and Laemli SDS-loading buffer. Immunoblot analysis was performed to detect p130, pRb, E7 and GAPDH (loading control for E7). Densitometry analysis of band intensities were performed and presented (B) following normalisation against GAPDH relative to % of 0 h mock treatment. The result shown is a representative of two independent experiments (n = 2).

Figure 5.5A and B demonstrated that E7 levels from mock (Lanes 1, 2 and 3) and A2 (Lanes 4, 5 and 6) transfected cells slightly increased with eeyarestatin I treatment, suggesting that this pathway might be involved in normal E7 degradation. However, SF1 transfected cells showed a decrease in E7 levels with inhibitor (Lanes 7, 8 and 9). This could be related to toxicity issues of the inhibitor or issues with poor quality of western blot. Levels of pRb as well as p130 seemed to decrease with inhibitor treatment, and protein bands were difficult to quantitate.

4.2 Investigation of the E7 cellular localisation in the presence and absence of aptamers

4.2.1 Introduction

E7 localisation in CaSki cells has shown previously in soluble cytoplasmic fraction by subcellular fractionation using a radioactively labelled cysteine, L – [^{35}S] cysteine (Smotkin and Wettstein, 1987). Immunofluorescence studies indicated that E7 also localised in the nucleus (Smith-McCune et al., 1999). In addition, HPV16 E7 was reported to be associated with nucleolus of HPV16 positive CaSki cells by immunofluorescence and electron microscopy immuno-gold labelling (Zatsepina et al., 1997). There is a discrepancy in the literature regarding the localisation of E7 in cells. It appears to be cytoplasmic by subcellular fractionation, however it was shown also to be nuclear by immunofluorescence staining and immunocytochemistry. This was explained by the assumption that cell fractionation disrupts E7 – nuclear associations due to a broken cell structure (Sato et al., 1989). Another explanation could be the fact that E7 has been shown to exist as dimers in the nucleus, therefore it might easily escape into the cytoplasmic fraction during subcellular fractionation. It was shown using antibodies with high discrimination capacity against monomeric, dimeric as well as oligomeric forms of E7 in immunofluorescence that E7 exist as a dimer in the nucleus but as in an oligomeric form in the cytoplasm of CaSki cells (Dantur et al., 2009). HPV16 E7 contains nuclear localisation and export sequences, therefore could shuttle between cytoplasm and nucleus (Knapp et al., 2009). When nuclear export was blocked by treatment of cells with Leptomycin B, accumulation of E7 was detected in the nucleus (Knapp et al., 2009, Laurson and Raj, 2011). With the use of an rabbit monoclonal antibody raised against conformational epitope (86 – TLGIVCPICSQK – 97) in the carboxyl-terminal domain of the HPV16 E7, it was shown that E7 is less homogenously distributed in both cytoplasm and nucleus of HPV16 positive CaSki cells as well as tumour cells (Dreier et al., 2011). Confluency of cell culture was also shown by immunocytochemistry to have an effect on E7 localisation,

being predominantly cytoplasmic in confluent cells whereas locating to both nucleus and cytoplasm in sub-confluent cells (Laurson and Raj, 2011).

E7 localisation was investigated in SiHa cells by an antibody raised against full-length HPV16 E7. Fluorescent signal could be seen visible throughout the cell membrane in surface of non-permeabilised cells, however permeabilisation allows staining detected in the cytoplasm (Shrimal et al., 2012). Therefore, permeabilised and non-permeabilised cells were used in order to be able to detect E7 on the plasma membrane of HPV16 positive SiHa cells.

4.2.2 Localisation of E7 on cellular membrane and co-localisation with Cell Mask-Orange (a membrane stain)

HPV16 E7 were analysed by immunofluorescence using an HPV16 E7 specific antibody as well as a fluoro-labelled secondary antibody for microscopic detection. SiHa (HPV16 E7 expressing), SaOS-2 (derived from osteosarcoma, an HPV negative cell line) and HaCaT (immortalised human keratinocytes, an HPV negative cell line) cells were utilised. Both permeabilised and non-permeabilised cells were employed in order to investigate both intracellular protein as well as possible membrane localised E7.

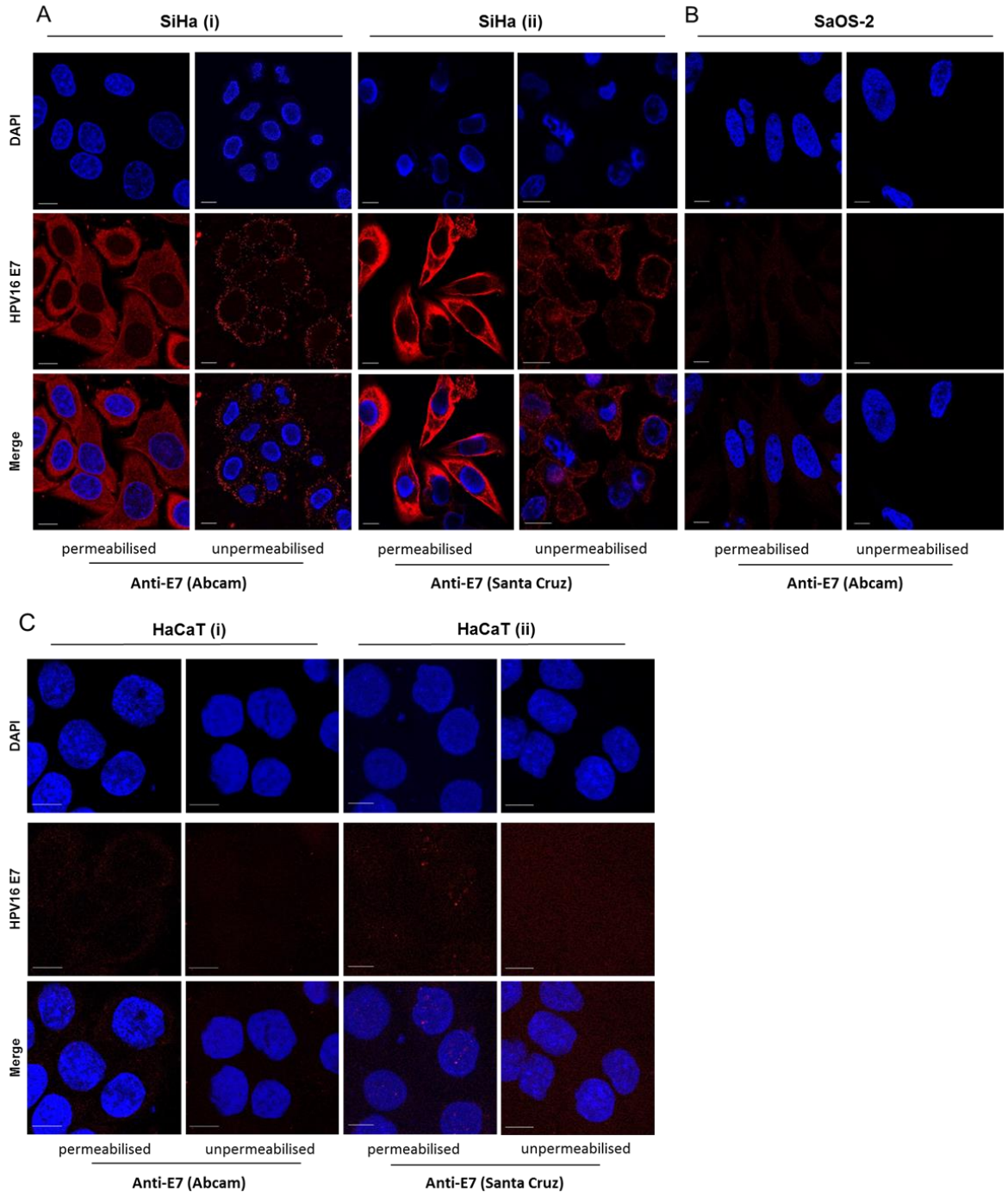

Figure 4.6 E7 distributes to the plasma membrane of HPV-transformed cells. HPV16 E7+ SiHa cells (i and ii) (A), SaOS-2 and (B) HaCaT cells (C) (as negative controls, containing no E7) were fixed, permeabilised and incubated with antibodies recognising full-length HPV16 E7 (A-i, C-i) and (B), and residues 35-56 (A-ii) and (C-ii). A comparable group of live cells was incubated with these antibodies in parallel. Incubation with anti-E7 antibody was performed for 1 h at 4°C. Cells were fixed with 4% formaldehyde and stained with AlexaFluor568 anti-mouse antibodies. Fluorescent imaging was performed using either a Zeiss LSM700 or LSM510 inverted microscope. Blue and red are DAPI (nucleus) and

E7, respectively. The scale bar is 10 µm. Representative images are shown for SiHa, SaOS-2 and HaCaT cells, respectively with n = 3, n = 2 and n = 2.

Permeabilised SiHa cells showed that E7 oncoprotein were predominantly localised to the cytoplasm of the cells (Figure 4.6A). However, when these cells were left non-permeabilised and unfixed, E7 antibody was able to recognise E7 located on the outer layer of plasma membrane (Figure 4.6A). Same antibody was used in SaOS-2 and HaCaT cells (Figure 4.6B anc C) as a negative controls to check specificity of the antibody and showed no E7 detection as expected.

In order to confirm the localisation of E7 on the plasma membrane, a cell membrane marker, CellMask Orange was used for co-localisation experiment. This stain is an amphipathic molecule, consisting of a lipophilic region for membrane loading and a negatively charged hydrophilic dye for attachment of the probe in the plasma membrane. It can be seen from Figure 4.7A that E7 seemed to be co-distributed with the CellMask Orange, indicating possible membrane localisation of E7 oncoprotein. Cell-mask is not suitable for experiments where an intracellular target also needs to be probed with an antibody due to the fact that it cannot survive membrane permeabilisation. However, E7 on the surface was also detected in non-permeabilised cells without the need for permeabilisation.

Since E7 fluorescence was observed on the cell membrane in non-permeabilised cells, an internalisation experiment were also performed by incubating these cells with an anti-E7 antibody (abcam), which were kept at 4°C (to minimise the temperature related internalisation). These cells were then moved onto 37°C water bath and fixed at different time points in order to investigate whether E7 on the cell surface was taken up via endocytic vesicles in to the cytoplasm in a time and temperature-dependent manner. Results from 0 min and 30 min incubation were shown in Figure 4.7B, indicating surface distribution of E7 and localisation of E7 at peri-nuclear area, respectively. E7 could not be detected in the cytoplasm after incubation at 37°C at earlier time points such as 1, 2, 5 and 10 min possibly due to the dispersion of E7 punctate inside the cytoplasm which does not allow detection of weak signals by confocal imaging (data not shown).

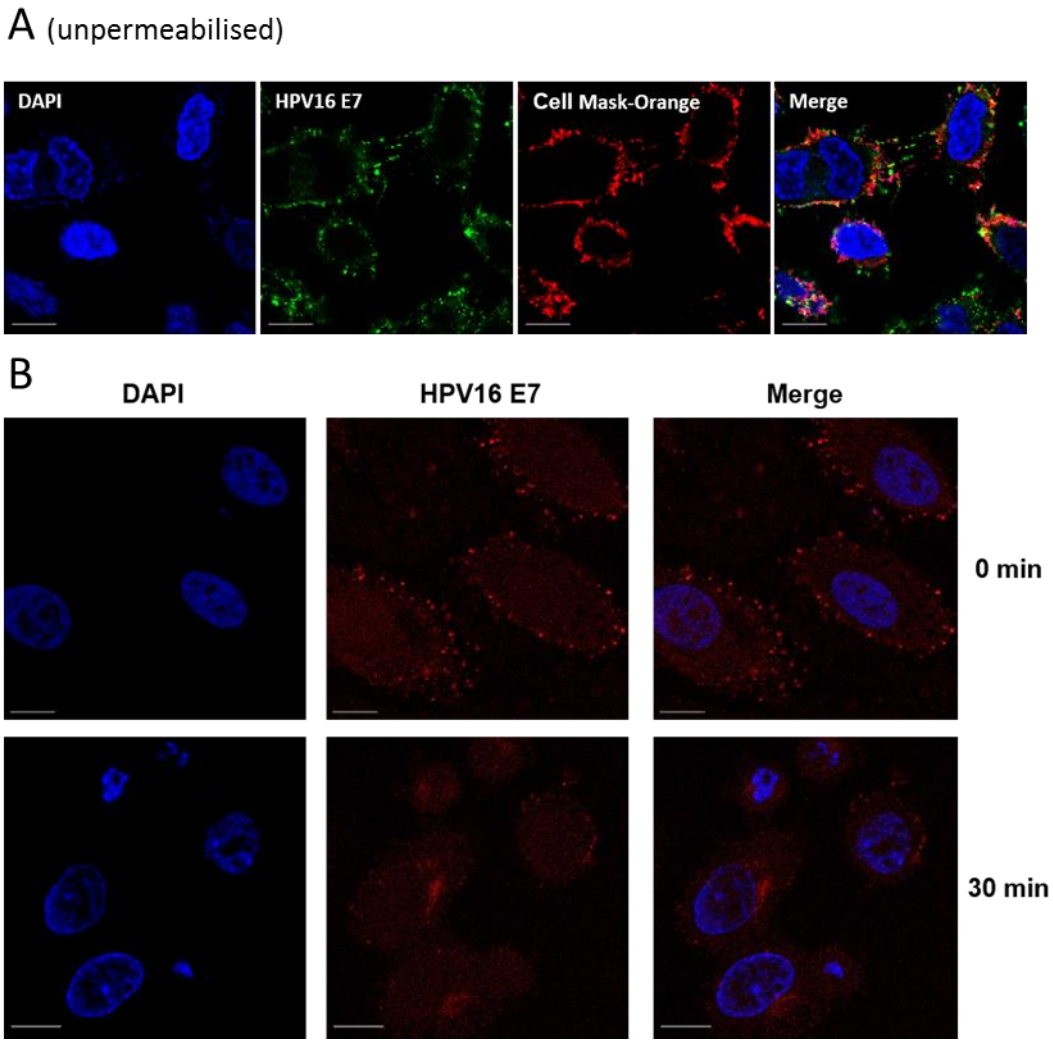

Figure 4.7 (A) Co-distribution of E7 with the cell membrane marker CellMask-Orange (red) in unpermeabilised SiHa cells. Cells were grown on glass coverslips for 48 hrs. Live cells were dual-stained with anti-E7 (Abcam) and CellMask Orange (1:2000) for 1 h at 4°C. Cells were washed at least 3 x with PBS, fixed with 4% formaldehyde and stained with AlexaFluor568 anti-mouse antibodies. Representative images are shown from three independent experiments (n = 3) (B) Time and temperature-dependent internalisation of cell surface E7, chased by anti-E7 antibody (Abcam). SiHa cells were incubated with the anti-E7 antibody for 1 h at 4°C and incubated at 37°C for 30 min to allow E7 internalisation. Cells were fixed, permeabilised and stained with AlexaFluor568 anti-mouse antibodies. Fluorescent imaging was performed using either a Zeiss LSM700 or LSM510 inverted microscope. Blue, green and red are DAPI (nucleus) and E7 and cell membrane, respectively. Images are from single experiment (n = 1). The scale bar is 10 µm.

4.2.3 Co-localisation of E7 in cellular compartments

Internalisation of ligands, extracellular molecules, plasma membrane proteins and lipids occurs through endocytosis. This can be grouped into these two mechanisms; clathrin-dependent and in-dependent as discussed in the chapter 5. First, an endocytosed cargo molecule is delivered into the early endosomes, then it moves to late endosomes and lysosomes for degradation, trans-golgi network (TGN) or recycling endosomes in order to return the cargo back to the cell membrane (Grant and Donaldson, 2009). It was suggested that cargo usually is delivered into early endosomes regardless of the mechanism of internalisation (Grant and Donaldson, 2009). Early endosomal markers are a small GTPase Rab5, phosphatidylinositol 3-kinase (PI3K) and its product phosphatidylinositol-3-phosphate (PtdIns3P), which are required for its activity (Grant and Donaldson, 2009). When late endosomes are fused with lysosomes, it becomes a degradative compartment (Russell et al., 2006). The lysosome is generally considered the end point of the endocytic pathway. Marker could be used for late endosomes is Rab7 GTPase (Russell et al., 2006). Lysosome-associated membrane protein 1 (LAMP1, also known as CD107a) was utilised for the detection of lysosomes/late endosomes.

E7 localisation throughout the plasma membrane (Figures 4.6 and 4.7) suggested a new hypothesis for how E7 aptamers might be affecting E7 degradation. That would be due to binding of aptamers to cell surface E7 leading to internalisation of aptamer along with the protein through transfection or endocytosis. Degradation of E7 caused by aptamers (Section 3.2.2), especially A2, therefore could be via endosomal/lysosomal pathways. In order to investigate this, co-localisation studies with E7 and endosomal markers were performed by immunofluorescence. Since autophagosomes could fuse with lysosomes and generate autolysosomes in order to play a role in degradation using lysosomal hydrolases, an autophagosomal marker LC3 was also utilised in co-localisation experiments with E7 oncoprotein in the presence or absence of A2. LC3 (microtubule-associated protein 1A/1B-light chain 3) is a 17 kDa soluble protein that is ubiquitously expressed in mammalian cells (Tanida et al., 2008). During autophagy, a cytosolic form of LC3 (LC3-I) conjugates to phosphatidylethanolamine forming LC3-phosphatidylethanolamine conjugate (LC3-II), which localises to the membranes of autophagosomes (Tanida et al., 2008). Calreticulin are components of the quality control system that promotes correct folding of proteins that enter the secretory pathway and targets misfolded proteins for degradation. Due to low efficiency of labelling A2 *in vitro* (Figure 5.3), this could not be included in the co-localisation experiments.

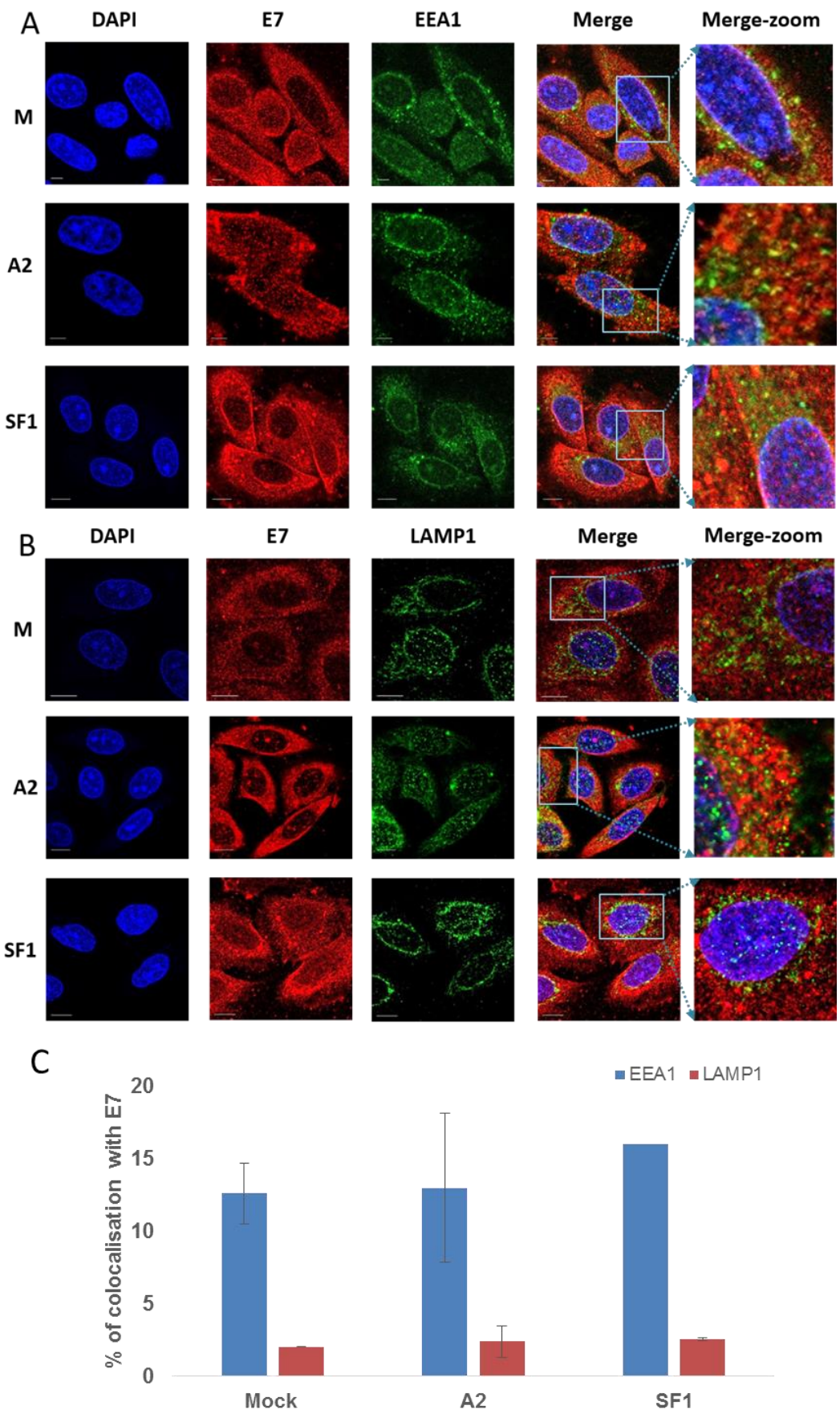
A
DAPI
E7
EEA1
Merge
Merge-zoom
M
A2
SF1
B
DAPI
E7
LAMP1
Merge
Merge-zoom
M
A2
SF1
C
EEA1
LAMP1
% of colocalisation with E7
20
15
10
5
0
Mock
A2
SF1

Figure 4.8 E7 does not co-localise with the early endosomal marker, EEA1 (A) or the late endosomal (lysosomal) marker, LAMP1 (B). SiHa cells were mock-transfected (M) or transfected with 100 nM A2 or SF1 using Oligofectamine. At 14 h post-transfection, cells were washed with PBS, fixed with 4% formaldehyde, permeabilised with 0.1% Triton-X100 and co-stained with either anti-EEA1 or anti-LAMP1 (staining early and late endosomes, respectively) (1:400) prior to incubation with AlexaFluor488 goat anti-rabbit secondary antibody. Cells were then incubated with anti-E7 antibody (Abcam) (1:2000) followed by AlexaFluor568 rabbit anti-mouse secondary antibody. Confocal imaging was performed using the Zeiss LSM700. Red, green and blue are E7, FITC (early or late endosomes) and DAPI (nucleus), respectively. The last panel is a zoom of merged images. The scale bar is 10 µm. E7/EEA1 and E7/LAMP1 colocalisation were analysed using Bitplane: Imeris image analysis software based on the calculation of Pearson`s correlation coefficient values and presented as percentage co-localisation, together with standard errors (C). Number of of cells analysed were n = 27, 23 and 4 for E7/EEA1 and n = 12, 24 and 9 for E7/LAMP-1 in mock-, A2- and SFI-treated SiHa cells, respectively.

E7 colocalisation with both EEA1 and LAMP was analysed using Bitplane: Imeris image analysis software based on the calculation of Pearson`s correlation coefficient values. Data were presented as percentage co-localisation. It was shown in Figure 4.8 that only minimal co-localisation of E7 with the endosomal marker EEA1 (Figure 4.8A and C) was observed with values of 12.6, 13.0 and 16.0 % for mock-, A2- and SF1-transfected SiHa cells, respectively. No statistical significant differences were detected between the three treatments. There was no colocalisation of E7 with LAMP1 (Figure 4.8B and C), and colocalisation values were very similar for the three treatments (ranged between 2.0 and 2.5 %) with no significance. The level of colocalisation between the autophagosomal marker LC3 (Figure 4.9A and C) and E7 also showed no difference between the three treatments (12.7, 10.2, 11.6 %, no significance). In contrast, there was an increased colocalisation of E7 with the ER marker, calreticulin, upon transfection with A2 (Figure 4.9B and C). Colocalisation in mock- and SF1-transfected cells was 15.1 and 15.1 %, but significantly higher at 32.3 % in A2-transfected cells ($p \leq 0.01$). Taken together, these data suggest that A2 perturbs normal E7 trafficking and cellular distribution through enhancing E7 ER retention following E7 binding.

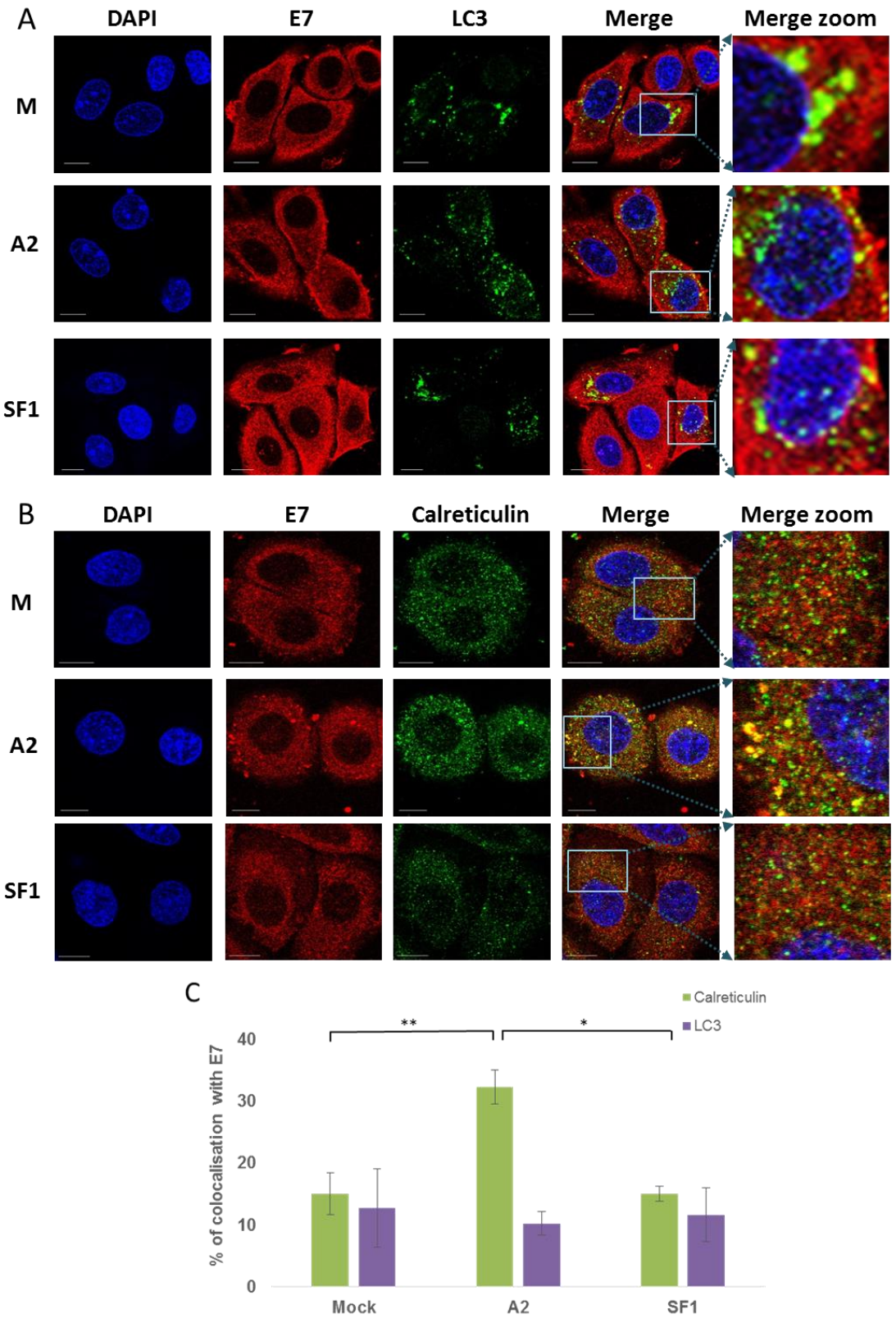

Figure 4.9 E7 does not co-localise with an autophagosome marker, LC3 (A) but appears to co-localise with endoplasmic reticulum marker calreticulin (B) in the presence of A2. SiHa cells were mock-transfected (M) or transfected with 100 nM A2 or SF1 using Oligofectamine. At 14 h post-transfection, cells were co-stained with anti-E7 (Abcam) and either anti-LC3 (an autophagosomal marker)

(1:2000) or anti-calreticulin (an ER marker) (1:200) overnight at 4°C prior to incubation with either AlexaFluor568 rabbit anti-mouse or AlexaFluor488 goat anti-rabbit secondary antibodies for 1 h at room temperature. Red, Green and Blue are E7, FITC (LC3, autophagosome or calreticulin, ER) and DAPI (nucleus), respectively. The last panel is a zoom of merged images. Images were taken using the Zeiss LSM700. The scale bar is 10 µm. E7/LC3 and E7/calreticulin colocalisation was analysed using Bitplane: Imeris image analysis software based on the calculation of Pearson`s correlation coefficient values and presented as percentage co-localisation, together with standard errors (C). Number of cells were analysed was n = 21, 23 and 17 for E7/LC3 and n = 19, 39 and 20 for E7/calreticulin with mock-, A2- and SF1-treatment, respectively. p* ≤ 0.0005, p ≤ 0.002.**

4.3 Chapter Discussion

Genetic mutations, presence of excessive amounts of protein subunits and several enviromental denaturing stress conditions causes proteins to misfold and nonfunction (Goldberg, 2003). In addition, a good deal of newly synthesized proteins contains misfolded products and accumulates as nonfunctional proteins in cells (Schubert et al., 2000). These misfolded proteins potentially assemble into aggregates (Kawaguchi et al., 2003, Sherman and Goldberg, 2001) and several mechanisms operates in order to eleminate their cytotoxic effects for example via degradation. The proteasome/ubiquitin system is mostly responsible for clearance of cellular misfolded proteins. One of the hyphotheses was that if binding of the HPV16 E7 aptamer A2 to E7 preventing its major interaction with (pRb or possible other cellular targets), E7 could be destabilised and/or conformationally changed, resulting in its degradation. In order to investigate this, proteasome, lysosome inhibitors as well as inhibitors against mis-folded protein degradation were utilised to determine their involvement in the degradation of E7 in the presence or absence of aptamers. It was shown in section 3.2.2 that transfection of CaSki cells with HPV16 E7 aptamer A2 resulted in a decrease of E7 levels. Therefore, mechanism of E7 degradation following A2 transfections were further studied by treating mock or aptamer transfected cells with several inhibitors. E7 is a short – lived protein with a 30 – 40 min half-life (Smotkin and Wettstein, 1987), allowing detection of protein accumulation at early time points such as 3 and 6 hrs following addition of inhibitors. It was demonstrated here that treatment of cells with a peptide aldehyde, MG132 resulted in the accumulation of E7 oncoprotein in mock and aptamer-transfected cells. Peptide aldehydes are not a very specific inhibitors for proteasomes, they could also inhibit cysteine (thiol) proteases in lysosomes (Craiu et al., 1997), therefore inhibiting degradation of endocytosed proteins. In order to ensure the degradation was proteasomal, cells were also treated

with another inhibitor for lysosomes, chloroquine (blocking H^+ ion, resulting in dysfunction of lysosomal enzymes). Inhibition of lysosomal protein degradation by chloroquine did not result in the accumulation of E7 as much as it was detected with MG132 treatment. However, there was a slight increase in the E7 level with chloroquine, suggesting possible involvement of lysosomes for E7 degradation in addition to proteasomes. In order to confirm, E7 degradation in the presence and absence of aptamers is most likely proteasomal, a more specific inhibitor of β-subunit of the proteasome, lactacystin was utilised. Treatment of CaSki cells with lactacystin was shown to result in accumulation of E7 oncoprotein both in the presence or absense of aptamer. Together with data from MG132 treatment, it can be concluded that degradation of E7 oncoprotein is possibly via proteasomes which is the major protein degradation pathway in mammalian cells. Aptamer A2 did not seem to alter the mode of normal degradation pathway of E7.

HDAC6 plays an important role in clearance of misfolded protein aggregates. Co-localisation experiments of HDAC6 with some aggresome markers showed that HDAC6 could translocate to aggresomes in the case of stress or treatment with potent agents, inducing protein mis-folding (Kawaguchi et al., 2003). In addition, HDAC6 was shown that selectively co-precipitates with polyubiquitinated proteins, therefore facilitates the formation of polyubiquitinated mis-folded proteins in aggresomes (Kawaguchi et al., 2003). Inhibition of HDAC6 found to be distrupting the transport of polyubiquitinated proteins to dynein motor, therefore aggresome formation (Kawaguchi et al., 2003). When proteasomes are not adequate in degradation of misfolded proteins accumulated in aggresomes (Hao et al., 2013), they could be cleared by autophagic machinery mediated by HDAC6 (Iwata et al., 2005). HDAC6 inhibitor, tubacin was used in this study in order to determine whether misfolded protein response is also involved in the degradation of E7 oncoprotin with aptamer A2. Acetylated tubulin levels seemed to increase with tubacin treatment in a time-dependent manner, indicating that the inhibitor is functioning properly. Treatment of CaSki cells with tubacin showed that E7 levels were either not affected or decreased possibly due to cytotoxic effects of the inhibitor. Accumulation of E7 with tubacin was not detected in the A2 transfected cells, suggesting that degradation of E7 oncoprotein in A2 transfected cells was not likely to be due to HDAC6-mediated misfolded protein degradation. Decrease in E7 levels with inhibitor treatment could result from depletion of HDAC6 and reactivation of cellular anti-tumour response. Histone deacetylases (HDACs), which removes acetyl groups from histones, were indicated to be upregulated in various tumours (Bolden et al., 2006). Threfore,

inhibitors of HDAC lead to histone hyperacetylation and could be reactivating tumour-suppressor genes such as p21 (a cyclin-dependent kinase inhibitor), inducing apoptotic pathways (Peart et al., 2005, Rocchi et al., 2005). Tubacin treatment was performed at 25 µM for 0, 3 and 6 hrs. However, lower doses could also be tried in order to minimise its cytotoxic effects. Tubacin is specific for HDAC6 inhibition, however another inhibitor trichostatin A could also be used to inhibit HDAC1-11 (Kawada et al., 2009).

Eeyarestatin I treatment caused a slight increase of E7 in mock and A2 transfected cell. However, the level of protein seemed to decrease in SF1 transfected cells. It is possible that A2 is affecting endoplasmic reticulum-associated protein degreadation. The increase in E7 levels with eeyarestatin I might be indicating accumulation of the newly synthesised and incorrectly folded nonfunctional E7. Decrease in E7 in SF1 transfected cells could be dose-related. Since higher doses could result in ER stress, leading to reduced protein translation or translocation into the ER (Harding et al., 1999, Kang et al., 2006). Therefore, inhibition studies was mostly performed by using 5 – 10 µM of the inhibitor in cells, however higher concentrations were utilised *in vitro* protein translocation experiments with around ~70 µM (Cross et al., 2009). Another alternative to eeyarestatin I is DBeQ, N2,N4-dibenzylquinazoline-2,4-diamine, which is a selective, potent and reversible p97 inhibitor. DBeQ has been shown to inhibit multiple pathways which requires p97 (by RNAi) including degradation of ubiquitin fusion proteins, endoplasmic reticulum-associated degradation (using α-chain of T-cell receptor-GFP reporter in a reporter assay due to the fact that overexpression of this reporter in non-T cells locates in the ER as an unfolded protein and degradation occurs in a p97-dependent manner) and autophagasome maturation (using autophagasome markers along with siRNA to p97 or expression of dominant-negative mutants to inhibit p97) (Chou et al., 2011).

It was shown here by the use of several inhibitors on HPV 16 E7 positive CaSki cells that degradation of E7 in general is proteasome-mediated, and could partly be lysosomal. In addition, tranfection of cells with A2 did not seem to change this pathway of degradation. However, inhibitors used here were limited, therefore using several other inhibitors for protein degradation could enable to determine the exact pathway of E7 degradation following aptamer transfections. In order to investigate the degradation pathway of E7, HPV 16 positive SiHa cells were utilised for co-staining with several endosomal markers and E7 oncoprotein in the presence and absence of A2 and a control aptamer SF1. This experiment was perfomed due to the fact that E7 was detected on the cell surface of SiHa cells using non-permeabilised and non-

fixed cell by imaging and shown to co-localised with a cell surface marker. It was hypothysised here that E7 on the cell surface might be internalising along with the bound aptamer and resulting in the accumulation in endosomes and then late endosomes/lysosomes or autophagosomes for degradation. Immuno co-staining with E7 and several endosomal markers showed that A2 transfection did not increase the localisation of E7 in early/late endosomes or autophagasomes. However, E7 localisation in ER (using Calreticulin as a marker) seemed to increase significantly in cells transfected with A2. Interestingly, E7 localisation to the ER has been demonstrated previously in CaSki cells (using calnexin as a marker) (Valdovinos-Torres et al., 2008). These data suggest that a possible conformational change of E7, mediated by A2 binding, may lead to an accumulation in the ER. This would be predicted to perturb normal biosynthetic delivery of E7 to the plasma membrane or other organelles (Figure 4.10). As E7 does not possess common peptide ER retention motifs such as [K/H]DEL, KKXXX, KXKXXX and PL[Y/F][F/Y]XXN, it is therefore likely that A2 binding prevents correct E7 folding or oligomerisation leading to its accumulation in an unfolded/aberrant state. This accumulation of unfolded E7 and subsequent stimulation of related stress responses may contribute to the stimulation of apoptosis previously observed in HPV+ cells (Casagrande et al., 2000, Liu and Kaufman, 2003, Nicol et al., 2013, Travers et al., 2000).

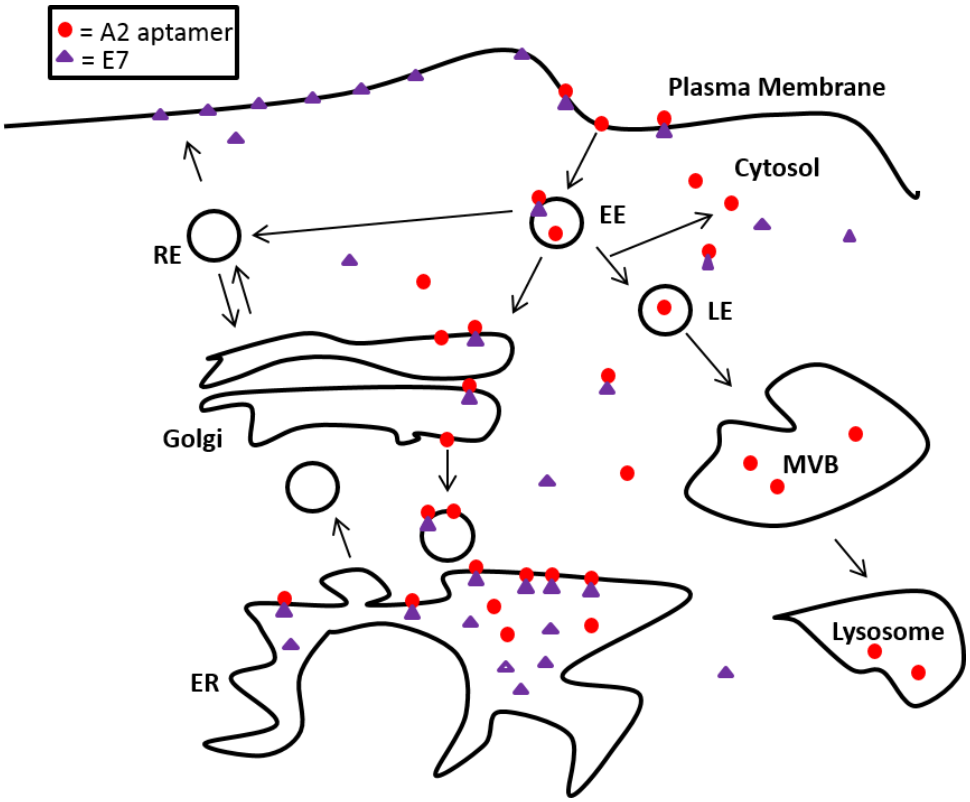

Figure 4.10 The schematic shows the model proposed for A2-mediated E7 degradation. A2 can enter the cells alone or via the endosomal system. Upon contact with E7; either at the plasma membrane or intracellularly, A2 enhances E7 retention in the ER. This would be predicted to reduce E7 delivery to the plasma membrane via its normal biosynthetic route. ER: endoplasmic reticulum, EE: early endosome, LE: late endosome, MVB: multivesicular bodies, RE: recycling endosome.

5 APTAMER DELIVERY

5.1 Introduction

Structured single-stranded DNA and RNA molecules known as aptamers are a viable and promising alternative to antibody and small drug-based therapies. They can be potent biological agonists or antagonists (Section 1.3.4). Several aptamers have been selected to date against a wide range of targets from membrane proteins to whole living cells, intracellular or extracellular proteins, etc. (see Section 1.3.1).

5.1.1 Advantages and disadvantages of using aptamers in therapy

Aptamers adopt a three-dimensional, globular-structure and possess excellent therapeutic potential. This is partly because of binding target molecules with high affinity and specificity (Huang et al., 2003). In addition, they are non-toxic and non-immunogenic. They have great potential to replace monoclonal antibodies in therapy due to the fact that they can be made synthetically in large scale and modified to improve their stability and bioavailability. Use of first generation aptamers in therapy was limited until several modifications were applied to the molecule such as incorporation of modified or unnatural locked nucleotides, dT cap at 3 end and conjugation of a polymer to the 5' end of the aptamer (see section 1.3.2 for generation of aptamers and 1.3.3.1 for aptamer modification). Aptamers are small (approx. 5 – 25 kDa). Therefore can relatively easily be internalised by cells and tissues. One shortcoming is that aptamers selected against human proteins might not be effective in animal models. This could be a particular problem when considering possible therapeutic applications, which need to be tested in animal systems before moving onto human clinical trials. The problem can be overcome by generating aptamers to recognise common and conserved motifs in both human and prospective animal models.

5.1.2 Importance of reagent-free uptake

Aptamers can be selected to bind intracellular or extracellular proteins. The aptamers that bind to the latter hold great therapeutic potential owing to the fact that their administration could be done intravenously or subcutaneously (see section 1.3.4 for aptamers in clinical trials). For an aptamer to be used as a delivery vehicle, the aptamer must be efficiently internalised following binding to its target receptor molecules (Shigdar et al., 2011). A great number of aptamers have been identified against cell-surface/receptor proteins which do not require intracellular delivery

(Lupold et al., 2002). Several aptamers have been used as promising tools for drug delivery by incorporating them on the surface of a virus vector or a nanoparticle in order to recognise a specific cell type (Que-Gewirth and Sullenger, 2007) . These delivery cargos might be internalised by cells along with the bound receptor, or cargos might be further modified by conjugation to cell penetrating peptides to facilitate their entry.

5.1.3 Techniques used in RNA delivery

Most of the literature in this area relates to the delivery of siRNAs. There are two predominant techniques which have been used to introduce siRNA into primary cells. One of these is transient transfection, where cationic lipids that interact with negatively charged DNA or RNA form liposome complexes and are taken up by electrostatic forces via endocytic routes. The second is electroporation which involves the use of an external electric field in order to increase membrane permeability, resulting in pore formation on cell membranes, allowing DNA and RNA molecules to enter cells directly (Neumann et al., 1982, Zuhorn et al., 2007). Non-lipid, nanoparticle-forming transfection reagents can also be used for transfection of small oligonucleotides into a wide range of cell types with low toxicity. Nanoparticles can be classified into inorganic NPs including gold NPs, Qdots, superparamagnetic iron oxide NPs, paramagnetic lanthanide ions and organic NPs including dendrimers, micelles, liposomes and ferritin. For example, hydrophobic hyaluronic acid–spermine conjugates (HHSC) self-aggregate in water to form nanoparticles, which can be used for efficient delivery of siRNA molecules (Shen et al., 2011).

5.1.4 Pathways of endocytosis

Understanding the mechanism of uptake of small RNAs with therapeutic potential is clearly very important, but not yet fully understood (Meade and Dowdy, 2009). Different pathways may be used by different molecules in different cell types. Dynamin-dependent, dynamin-independent and phagocytosis are known pathways of endocytosis. Dynamin-dependent endocytosis (which can be blocked by dynasore) can be clathrin-mediated or caveolar-mediated. These subtypes of endocytosis can be inhibited by cholorpromazine, and genistein, nystatin and filipin III, respectively. Dynamin-independent pathways are non-clathrin/non-caveolar, lipid-raft mediated and macropinocytosis. Inhibitors used to block lipid-raft mediated endocytosis and macropinocytosis are genistein and amiloride, respectively (Doherty and McMahon, 2009, Kotula et al., 2012).

Uptake of plasmid DNA was found to require surface proteoglycans and also some proteins or peptides such as antimicrobial Peptide LL-37. This is secreted from mammalian cells and is able to bind the DNA and carry it in to the cytosol or nucleus (Sandgren et al., 2004, Wittrup et al., 2007). It was shown that full length 70-kDa heat shock protein Hsp70, which is an ATP-dependent chaperone that is involved in protein folding, assembly and transport of proteins across cellular membranes, was able to deliver bound RNA molecules into the cytoplasm of mammalian cells (Henics and Zimmer, 2006).

Macropinocytosis presents advantages over other mechanisms of endocytosis due to the nature of resulting macropinosome vesicles, facilitating the escape of cargo molecules (see section 1.3.3.4). Macropinocytosis can be enhanced by several compunds including fetuin, PMA and epidermal growth factor (EGF) and exogenous factors such as G-rich nucleic acids. These treatments could be cell-type specific. EGF (but not fetuin) treatment increased the expression of naked plasmid DNA in stomach of mice following administration onto cells of the gastric surface (Fumoto et al., 2009). Hyperstimulation of macropinocytosis by continuous uptake of molecules results in a novel form of apoptosis defined by vacuolisation, irregular nuclei and swollen cells (Overmeyer et al., 2008). However, although enhancers could increase the uptake of plasmid DNA, some other critical factors might be involved in the reduced expression of transgenes such as endosome/macropinosome escape of vectors (Reyes-Reyes et al., 2010). In addition, these enhancers should be applied with caution due to their tumorigenicity or tumour promoting activity (such as PMA and EGF), and also their ability to trigger inflammation (such as zymosan and leukotriene B4). However, stable and non-immunogenic G-rich nucleic acids have been shown to increase macropinocytosis followed by enhanced cellular uptake in mono layer cell culture with anti-proliferative effects (Reyes-Reyes et al., 2010).

Internalisation of RNA has been well-studied in *C. elegans.* A multispan transmembrane protein, SID-1 (systemic RNAi deficient-1) mediates the internalisation of RNA in *C. elegans*, possibly functioning as a membrane channel to transport RNA molecules into cells (Feinberg and Hunter, 2003). In addition, overexpression of FLJ20174, the mammalian homologue of SID-1, facilitates the internalisation of RNA (Duxbury et al., 2005) and due to the fact that uptake was not affected by incubation in the or ATP depletion (using an ATPase inhibitor, oligomycin), the mechanism involved was suggested to be a passive, not a receptor-mediated uptake. Another channel forming protein, SID-2, is an apical intestinal membrane

protein, which is not as well-studied as SID-1. *C. elegans S*ID-2 mutants are unable to deliver RNA from the intestinal lumen of the nematode to the cytoplasm (McEwan et al., 2012). Therefore, uptake in *C. elegans* requires both of these channel forming membrane proteins sequentially. Cellular entry of RNA via the SID-2 channel is highly dependent on the acidity of the extracellular environment which reflects the intestinal lumen conditions (McEwan et al., 2012). Structure-function analysis revealed that three positively charged extracellular histidine residues (at low pH) might be interacting with negatively charged RNA to facilitate its internalisation. In addition, uptake was found to be significantly decreased following treatment with oligomycin, latrunculin A (an actin polymerisation inhibitor) or bafilomycin A1 (an endosome maturation inhibitor), suggesting an energy-dependent endocytosis, which is totally opposite to that of SID-1 forming a receptor or pump in order to passively internalise the RNA (McEwan et al., 2012). Vertebrates also possess SID-1 homologues called SID transmembrane protein 1 (SIDT1) and 2 (SIDT2), which are involved in RNA transport.

Aptamer 21-2, selected against human IL-17A, binds IL-17A, blocking its interaction with its receptor IL-17R which results in the inhibition of IL-17A-induced production of IL-6 cytokine (Ishiguro et al., 2011). Neutralising effects of aptamer 21-2 was investigated in fibroblast T cell co-culture systems which represent a psoriatic inflammation as well as fibroblasts alone (Doble et al., 2014). However, these suggested effects of the aptamer were absent in keratinocytes. It was suggested to be due to reduced levels of the aptamer in extracellular matrix upon non-specific internalisation of the aptamer into keratinocytes (Doble et al., 2014). Thus, the conclusion was that this aptamer may not be used as a neutralising agent for extracellular inflammatory mediators. However, it can be a valuable tool to understand the uptake mechanism of some of the aptamers as model molecules and could also be used as a drug delivery agents.

There is relatively little data on the uptake of RNA aptamers in the literature. In this chapter, labelled 21-2 and a model aptamer of a similar size 47tr, selected against FMDV RNA-dependent RNA polymerase (Ellingham et al., 2006) were used to study uptake mechanisms and cellular localisation of aptamers with or without lipofection.

5.2 Delivery of aptamers into cells

5.2.1 Reagent-free uptake of aptamers (47tr and 21-2) into primary cells

In order to study if aptamers can be delivered in to cells without the need for a transfection reagent, primary cells and a HPV16 positive cervical cancer cell line SiHa cells were used for confocal imaging. Cells were grown until they reach at a confluency of around 60% prior to incubation with aptamers. Chemically synthesised Cy3 and Cy3/Cy5 labelled aptamer 21-2 and Cy3 labelled 47tr were used. 21-2 and 47tr contain 33 and 32 nucleotides, respectively. Single-labelled aptamers were 5' Cy3 labelled 21-2 and 47tr (Cy3 21-2 and Cy3 47tr) and double-labelled aptamer was 5' Cy5 and 3' Cy3 labelled (Cy5 21-2 Cy3). Cells were incubated with aptamers in the absence of foetal bovine serum (10%). Following the incubation at 37°C for 4-6 hrs, confocal images were taken using a LSM510 upright and LSM700 inverted confocal microscopes.

First, primary cells were used to study internalisation of aptamers Cy5 21-2 Cy3, Cy3 21-2 and Cy3 47tr. Interestingly, uptake of both aptamers (red) were detected by confocal microscopy in primary cells (Figure 5.1). These cells were able to internalise Cy3 21-2 and Cy3 47tr, presumably in the absence of their ligand/receptor or target protein (Doble et al., 2014).

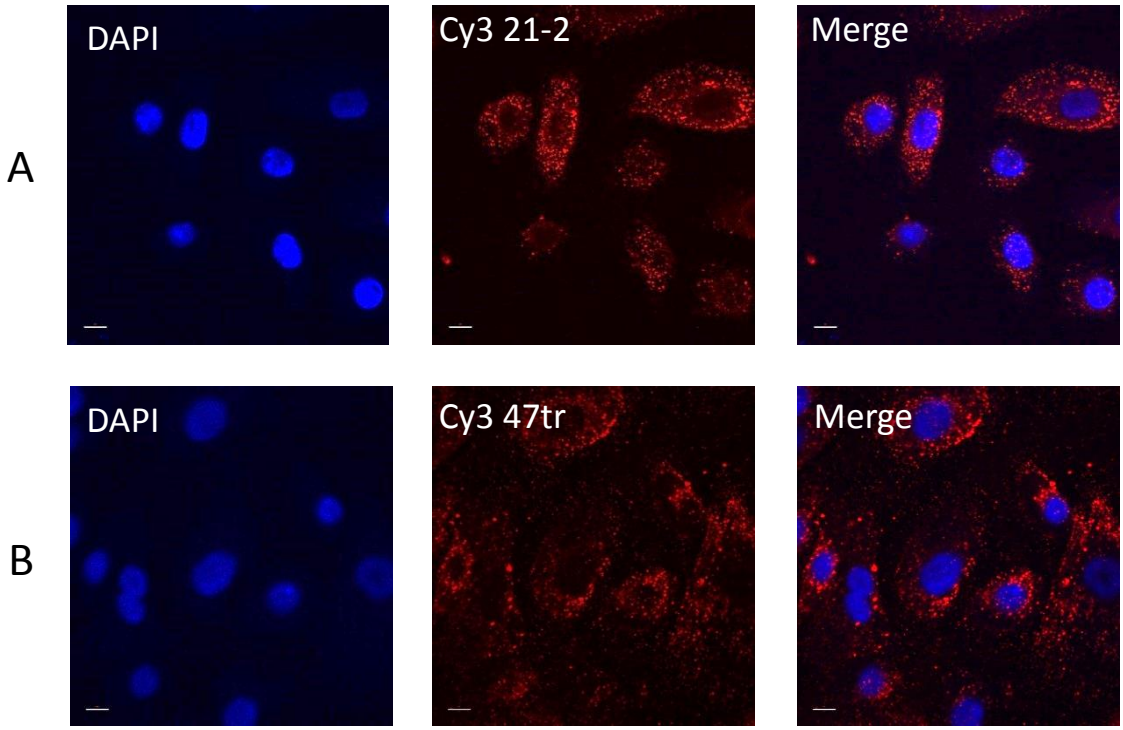

Figure 5.1 Reagent-free uptake of Cy3 21-2 (A) and Cy3 47tr (B) was detected in primary cells. Primary cells were plated on coverslips on 12-well tissue culture plates 24 hrs prior to incubation with aptamers. Cells were maintained in the keratinocyte growth medium lacking serum to prevent cell differentiation. Aptamers were added at 80 nM (final concentration) for 5 hrs. Coverslips were then washed with PBS, fixed with 4% formaldehyde for 10 min followed by mounting on microscope slides using a glycerol-based mounting media containing DAPI. Nuclear staining with DAPI and aptamers with Cy3-label, are blue and red, respectively. Images are representatives of three independent experiments (n =3). The scale bar is 10 µm.

HPV18+ primary keratinocytes (Figure 5.2A) and HeLa (HPV18+) (Figure 5.2B) cells were also tested for their ability to internalise these aptamers as well as SiHa (HPV16+). HPV18 positive keratinocytes were also able to internalise the double-labelled aptamer 21-2. According to our observations, all cell types except HeLa cells were able to internalise both the 47tr and 21-2 aptamers. HeLa and SiHa cells are both cervical cancer cell lines, however HeLa is derived from adenocarcinoma whereas SiHa is derived from grade II, squamous cell carcinoma. Having originated from different cell types might explain the results seen.

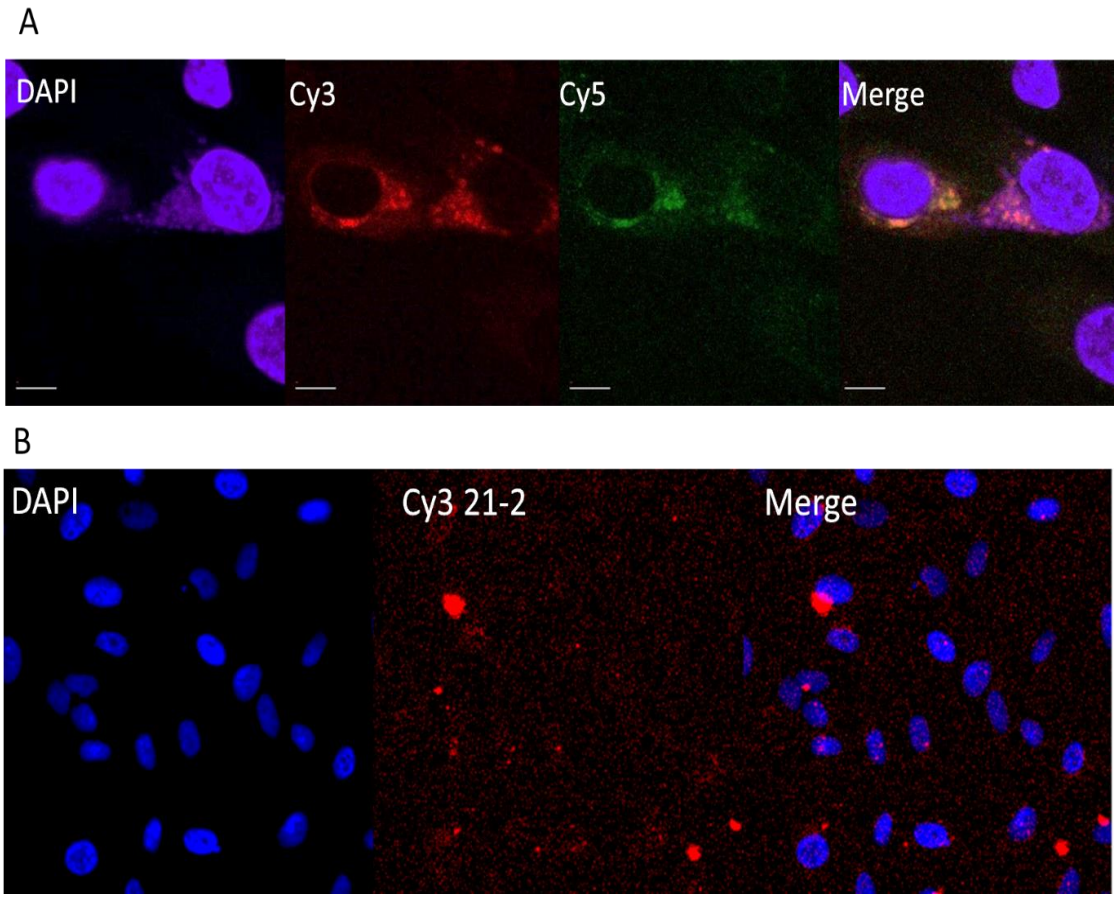

Figure 5.2 Reagent-free uptake of (A) Cy3 21-2 Cy5 in HPV18 + primary keratinocytes and (B) Cy3 21-2 in HeLa cells. Primary and HeLa cells were plated on coverslips on 12-well tissue culture plates 24 hrs prior to incubation with aptamers. Cells were maintained in the keratinocyte growth medium lacking serum to prevent cell differentiation for primary cells and DMEM for HeLa cells. Aptamers were added at 80 nM (final concentration) for 5 hours. Coverslips were washed with PBS, fixed with 4% formaldehyde for 10 min followed by mounting on microscope slides using a glycerol-based mounting media containing DAPI. Nuclear staining with DAPI (blue) and aptamers with both Cy3 (red) and Cy5 (green) - labelled. Images are representatives of two independent experiments (n = 2) for Panel A and a single experiment (n = 1) for Panel B.The scale bar is 10 µm.

The uptake experiment was repeated using a fluorescently labelled HPV16 E7 aptamer, A2 in SiHa cells (Figure 5.3). When Fl-A2 (75 nucleotides in size) was used for reagent-free uptake experiments, the amount of aptamer detected in intracellular compartments was much lower compared to those of 21-2 and 47tr (Figure 5.3A). However, increased levels of Fl-A2 were detected in cells when it was introduced by oligofectamine transfection (Figure 5.3B). However, the labelling efficiency of the A2 with fluorescein was not sufficient for it to be used for further uptake experiments.

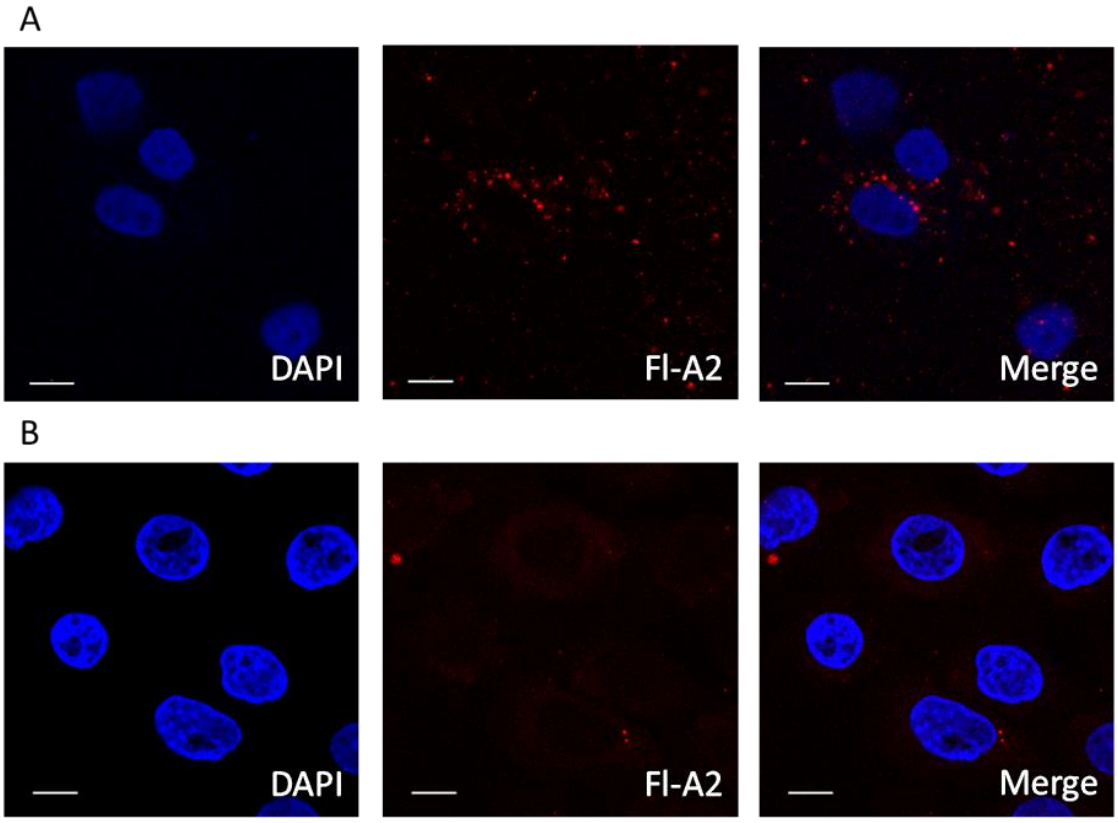

Figure 5.3 Internalisation of Fl-A2 in transfected (A) and non-transfected (B) keratinocytes. 5' end of the aptamer was re-modified using 5' EndTag™ Nucleic Acid Labeling system (Vector Laboratories). Aptamer (0.6 nM) was incubated with alkaline phosphatase at 37°C for 30 min to obtain 5' hydroxyl group. Fluorescein maleimide was incorporated into the 5' hydroxyl position using ATPγS and T4 polynucleotide kinase according to manufacturer`s instructions. The resulting labelled aptamer was with phenol: chloroform and precipitated with ethanol. Primary cells were plated on coverslips on 12-well tissue culture plates 24 hrs prior to incubation with aptamers. Cells were maintained in the keratinocyte growth medium lacking serum to prevent cell differentiation. Fl-A2 was added at 80 nM (final concentration) for 5 hrs in the presence (A) or absence (B) of lipofection (using Oligofectamine). Cells were fixed and mounted on microscope slides prior to imaging using the Zeiss LSM510 upright confocal microscope. Nuclear staining with DAPI and aptamers with fluorescein maleimide (excitation and emission wavelengths are 494nm and 518 nm, respectively), are blue and red, respectively. Data is a representative of two independent experiments (n = 2). The scale bar is 10 µm.

Aptamers were detected in primary cells for the first time following a passive or receptor-mediated uptake mechanism that is not yet known (Figure 5.1). To determine whether the aptamers were still intact, a double-labelled, chemically synthesised aptamer 21-2 was used. This aptamer had Cy5 and Cy3 at the 5' and 3' ends, respectively. The formation of secondary structures should bring both ends to a very close proximity so that co-localisation could be detected by confocal imaging.

Incubation of primary cells with double labelled aptamer 21-2 in the absence of any transfection reagent resulted in internalisation of the aptamer as an intact molecule with the demonstration of red and green referring to 3' and 5' ends, respectively co-localisation (Figure 5.4A). Oligofectamine transfection of Cy3-5 labelled 21-2 into primary cells was used as a positive control to show the co-localisation of both ends of the aptamer (Figure 5.4C).

Pearson`s co-localisation coefficient values were calculated for reagent-free and Oligofectamine-transfected aptamers. The aim was to determine the degree of correlative variation as well as the overlap between Cy3-labelled 3' and Cy5' labelled 5' ends of the aptamer upon internalisation using confocal images and software called Imaris. It gives values closer to 1, are indicative of a high level co-localisation. Values between 0 and -1 are indicative of random localisation ranging to perfect exclusion, respectively. Pearson`s coefficient values for Oligofectamine-transfected and reagent-free internalised Cy5 21-2 Cy3 were found to be 0.9448 (Figure 5.4D) and 0.732 (+/-0.03) (Figure 5.4B), respectively, showing a strong co-localisation of Cy3 and Cy5 channels indicating that both ends of the aptamer are co-localising together in the cells. Other parameters indicating the co-localisation were percentage volumes of Cy3 co-localising with Cy5 or vice versa. Although these values were slightly higher when Oligofectamine transfection was utilised to deliver the aptamer into cells, they also showed a strong overlap between red and green channels indicating that a large proportion of RNA in cells was still intact upon internalisation.

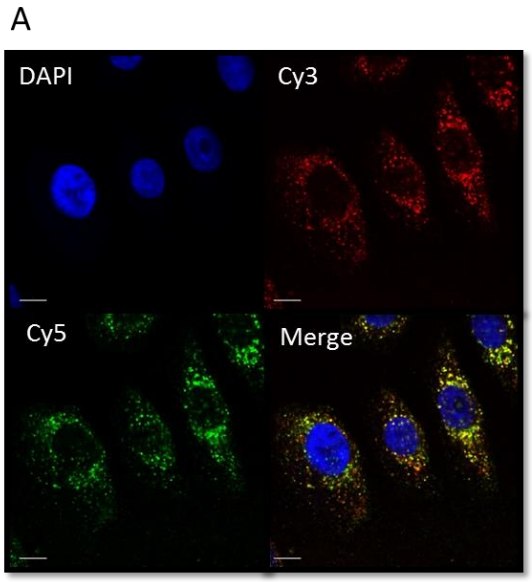

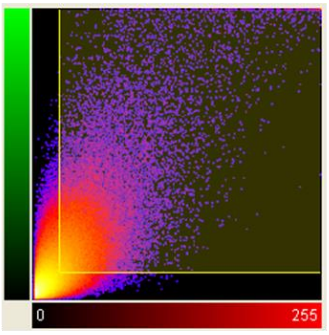

Pearson`s coefficient	0.732 (+/- 0.03)
% volume of Cy3	61.43 (+/-5.23)
% volume of Cy5	72.62 (+/-5.76)

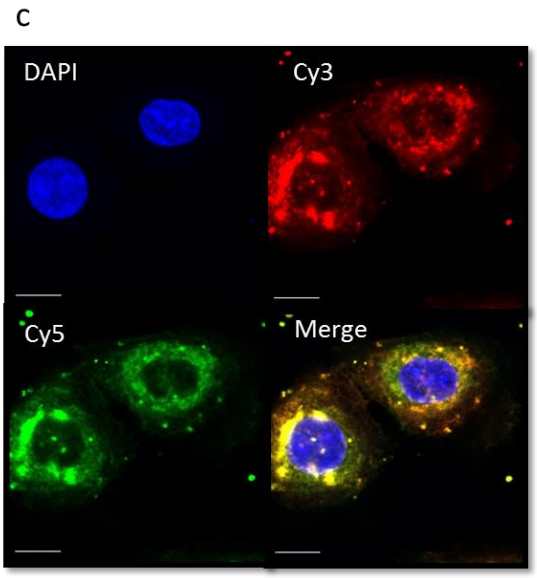

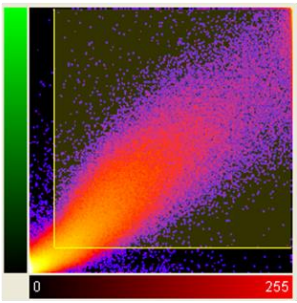

Pearson`s coefficient	0.9448
% volume of Cy3	80.79
% volume of Cy5	95.58

Figure 5.4 Co-localisation of 3' and 5' ends of aptamer 21-2 double-labelled with Cy3 and Cy5 in keratinocytes.The confocal image shows the co-localisation of both channels when a reagent-free delivery approach (A) or oligofectamine transfection (C) was performed for delivery of the aptamer. Co-localised pixel scatter plots B and D were analysed from images A and C, respectively using Imaris software in order to calculate the Pearson`s coefficient and % co-localisation of Cy3 with Cy5 or vice versa (+/- standard erros, from three (n = 3) and two (n = 2) independent experiments for A, B and C, D, respectively). For the analysis on Imaris, thresholds for each channels were set to 25%. DAPI was used to stain the nucleus. The scale bar is 10µm.

5.2.2 Delivery of aptamers in SiHa cells using a nanoparticle-based transfection reagent, Nanocin™

Nanocin is invented as a clinically safe polymer which can spontaneously form nanoparticles with nucleic acids, protein and peptides and mediate their uptake into a

wide range of cells including those of mammalian, fungal, bacterial and parasitic origin. Use of nanoparticles as delivery agents for aptamers could be advantageous over lipofection due to the drawbacks of using lipid-based transfection reagents (see chapter discussion 5.4). When cargo molecules, in this case aptamers, are mixed with Nanocin, particles are formed, which then facilitate the delivery of molecules into the cytoplasm of target cells.

SiHa cells were grown for 48 hrs on glass coverslips and used for Nanocin transfection. Double-labelled aptamer Cy5 21-2 Cy3 was used as a model aptamer for transfections. Aptamer at 80 nM final concentration was mixed with Nanocin and applied to cells. Following incubation at 37°C for 5 hrs, cells were washed, fixed and mounted onto microscope slides prior to imaging by confocal microscopy, followed by co-localisation analysis (as above). Analysis of co-localisation by Imeris showed a Pearson`s value of 0.82, indicating that both ends were mostly co-localising.

A further aptamer, Cy3 47tr, was also used for transfection of SiHa cells with Nanocin, with similar results. Nanocin could be used as apossible delivery reagents for aptamers although the pathway of entry into cells is yet unknown.

A

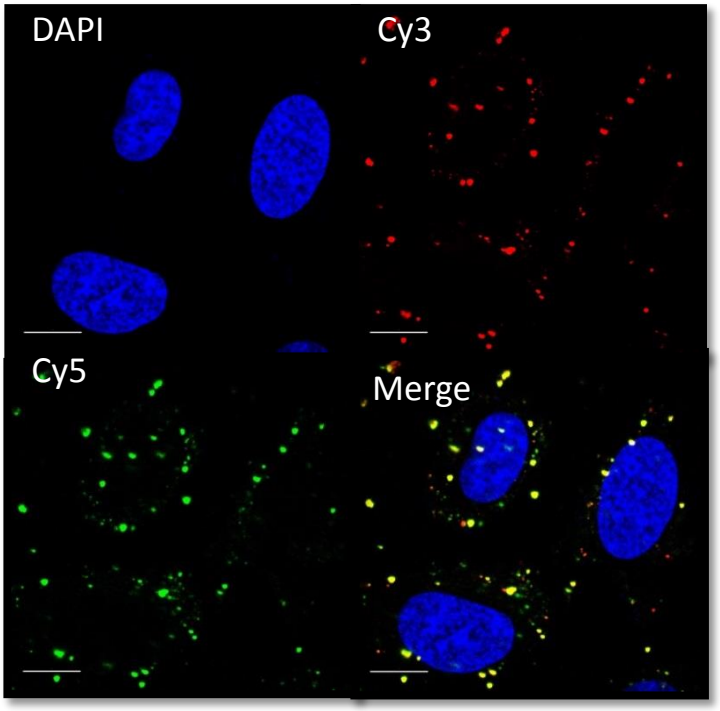

B

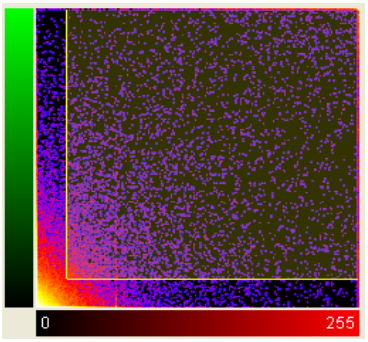

Pearson`s coefficient	0.82
% volume of Cy3	65.44
% volume of Cy5	41.38

C

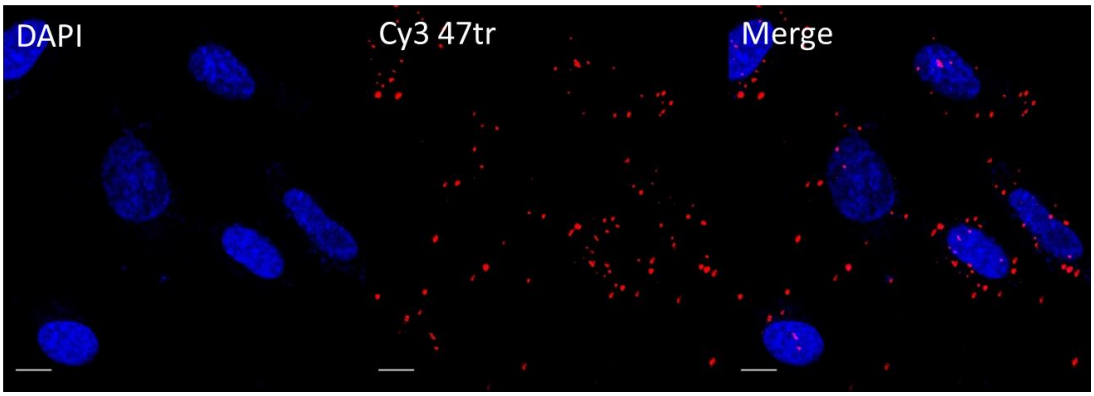

Figure 5.5 Use of Nanocin as a transfection reagent to deliver aptamers into SiHa cells. Double labelled Cy5 21-2 Cy3 (80 nM) (A, B) or single labelled Cy3 47tr (80 nM) (C) was mixed with 4 µl of Nanocin (trade name HappyFect™) in a total volume 50 µl of serum-free medium. The medium of SiHa cells grown for 48 hrs was replaced with serum-free media and the Nanocin-aptamer mixture was applied to cells. Internalisation and/or co-localisation 21-2 and 47tr was analysed by confocal microscopy (Panels A and B, respectively) and a scatter plot of co-localised pixels from (Panel A) was shown in Panel B along with the

calculated Pearson`s coefficient and the % volume of co-localised pixels which was analysed by Imeris. Results are representatives of two independent experiments (n = 2). For the analysis on Imaris, thresholds for each channel were set to 25%. DAPI was used as a nuclear stain. The scale bar is 10µm.

5.2.3 Effects of dynasore (dynamin-dependent endocytosis inhibitor) and amiloride (macropinocytosis inhibitor) on the uptake of aptamers 21-2 and 47tr

In order to study if the uptake of aptamers 21-2 and 47tr was via macropinocytosis and/or dynamin-mediated endocytosis, inhibitors of each processes were used. First, SiHa cells were treated with Dynasore, a dynamin-dependent uptake inhibitor, at a final concentration of 80 µM or (0.04% DMSO, the control vehicle) for 2 hrs at 37°C. The aptamers, 47tr (Cy3-labelled) and 21-2 (double-labelled) were added to cells at a final concentration of 80 nM for a further 5 hrs. Cells from each treatment were then imaged, and approximately 30 cells were analysed from different focal planes. The percentage of cells with internalised aptamer was determined and represented as a graph for DMSO or dynasore treatment of cells exposed to Cy3 47tr or Cy5 21-2 Cy3 uptake (Figure 5.6).

Dynasore treatment seemed to reduce the internalisation of aptamers, Cy3 47tr and Cy5 21-2 Cy3 up by 35 and 20%, respectively (Figure 5.6C). However, there was still a relatively high proportion of cells with internalised aptamers. Therefore, although dynamin-mediated endocytosis may be involved in uptake, there may be further pathways. The ring-like pattern of aptamers around the cell membrane that was observed following inhibitor treatment might be an indication of receptor-mediated endocytosis (Figure 5.6A, B).

FITC-Transferrin was used as a marker for endocytosis (Figure 5.7). When cells were treated with DMSO, transferrin was taken up and transported to the peri-nuclear region of the cell, whereas dynasore treatment caused the accumulation of transferrin on the outside of the cell membrane. 47tr co-localised with transferrin in both DMSO-treated (where transferrin was perinuclear) and dynasore-treated cells (where transferrin localised on the plasma membrane), indicating a receptor-mediated uptake of the aptamer (Figure 5.7). However, 21-2 was not detected in an association with transferrin in DMSO-treated cells (Figure 5.7B). When endocytosis was blocked by dynasore treatment, transferrin and only small amounts of 21-2 co-localised on the plasma membrane, suggesting that an alternative pathway (such as macropinocytosis) might be involved in the internalisation of 21-2.

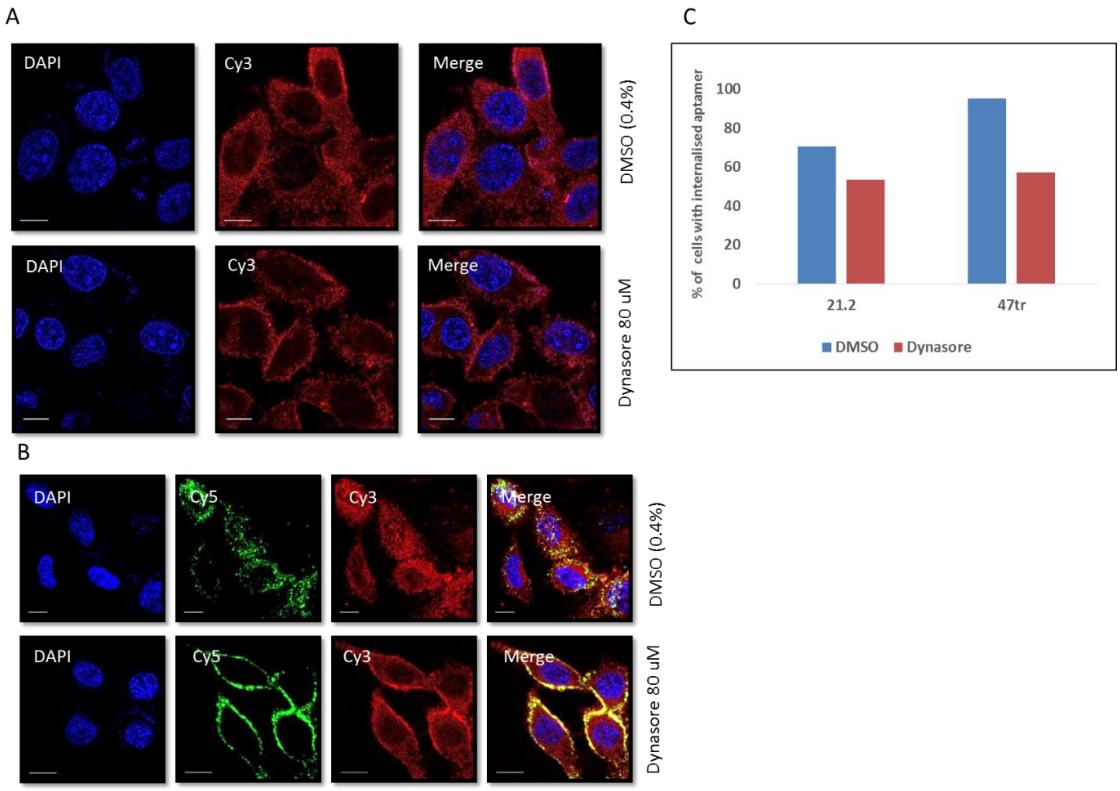

Figure 5.6 Internalisation of aptamers in the presence or absence of dynasore (an inhibitor of dynamin-dependent endocytosis). Cy3 47tr (Panel A) and Cy5 21-2 Cy3 (Panel B) were used for transfection and a representative graph showed the percentage of cells in which aptamers were internalised (Panel C), in the presence or absence of the inhibitor. SiHa cells were grown on glass coverslips for 48 hrs. Prior to incubation with Cy3 47tr (A) and Cy5 21-2 Cy3 aptamers (80 nM final concentration), cells were subjected to 0.4% DMSO or 80 µM dynasore treatment for 2 hrs at 37°C. Following addition of aptamer, cells were incubated for a further 5 hrs to allow uptake. Coverslips were washed with PBS and fixed with 4% formaldehyde followed by mounting on microscope slides. Images were taken using the Zeiss LSM510 upright microscope. Cy3, Cy5 and DAPI were visualised as red, green and blue, respectively. N = 30 cells were counted for each aptamer for Dynasore or control treatments and represented as a percentage of cells with internalised aptamers in the presence or absence of dynasore (Panel C). The scale bar is 10 µm.

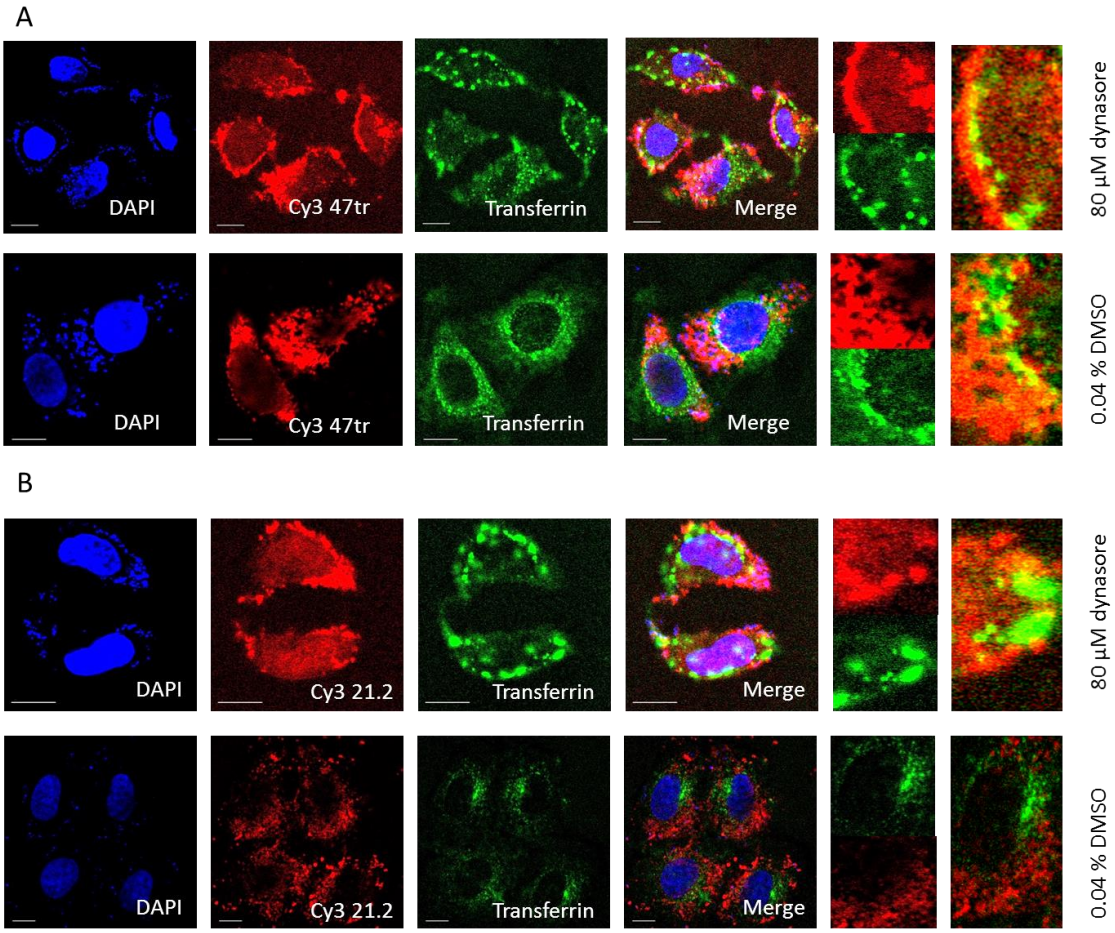

Figure 5.7 Inhibition of uptake of Cy3 47tr (A) and Cy3 21-2 (B) by dynasore and co-localisation of aptamers with a labelled marker for endocytic pathway (Transferrin). Cy3-labelled aptamers were incubated with SiHa cells, which were pre-treated with 80 µM dynasore or DMSO (0.04%) for 2 hrs at 37°C, in the presence of FITC-Transferrin as a marker for dynamin-dependent endocytosis. Images were taken using the Zeiss LSM510 upright microscope. Cy3 (aptamer 47tr or 21-2, Red), transferrin (green) and DAPI (blue, nucleus) were detected as red, green and blue, respectively. The last panel showed red and green co-localisation. The scale bar is 10 µm. N = 2.

Second, SiHa cells were treated with an inhibitor of micropinocytosis, amiloride. Amiloride treatment, but not DMSO (as negative control) caused a reduction in the internalisation of the uptake of both aptamers, but preferentially 21-2 (Figure 5.8A and B). The number of cells that were with or without internalised aptamer was counted from several focal planes and percentage of decrease in the number of cells still bearing the signals was calculated (Figure 5.8C). Amiloride treatment resulted in a 40% and 10% decrease in the number of aptamer positive cells in SiHa cells incubated with aptamer 21-2 and 47tr, respectively.

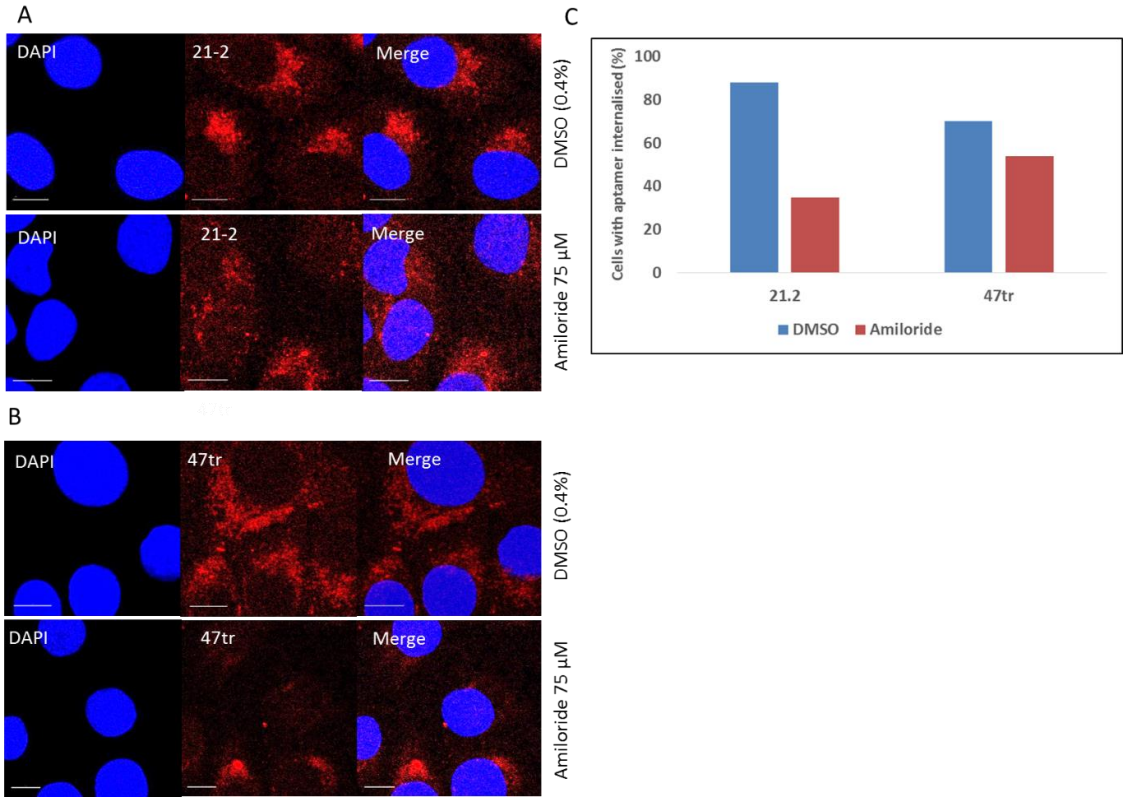

Figure 5.8 Effect of an inhibitor of micropinocytosis, amiloride, on aptamer internalisation. SiHa cells were grown on glass coverslips for 48 hrs. Prior to incubation with aptamers Cy3 47tr (A) and Cy3 21-2 (B) (80 nM), cell were subjected to 0.4% DMSO and 75 µM Amiloride treatments for 2 hrs at 37°C. Cells were incubated with aptamers for 5 hrs. Coverslips were washed with PBS and fixed with 4% Formaldehyde followed by mounting on microscope slides. Images were taken using LSM510 upright microscope. Cy3 and DAPI were visualised as red and blue, respectively. The scale bar is 10 µm. N = 30 cells were counted for each aptamer for Amiloride and control treatments and represented as percentage of cells with internalised aptamers in the presence or absence of the inhibitor (C).

Receptor-mediated uptake can be blocked by cold incubation of aptamers with cells. Therefore, cells were incubated with aptamers 21-2 and 47tr at 4°C for 6 hrs. It was shown in the Figure 5.9 that internalisation of 47tr did not appear to be as efficient as that of 21-2. Transfection efficiency for 21-2 was 73.91% at 4°C, whilst that for 47tr was 12.50% when n = 46 and n = 40 cells were counted, respectively. This may indicate that 21-2 internalised by such mechanisms that do not require energy (e.g. micropinocytosis), while internalisation of 47tr requires energy-dependent mechanisms.

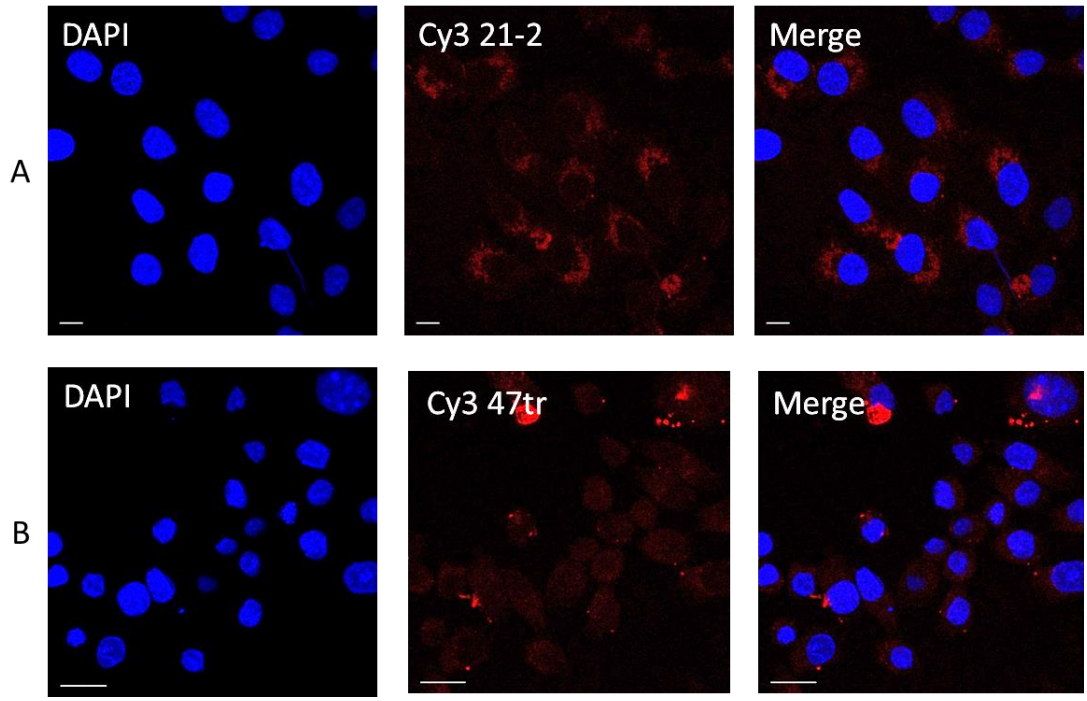

Figure 5.9 Uptake of aptamers into SiHa cells at 4°C. Cells were plated on glass coverslips on 12-well tissue culture plates 48 hour prior to incubation with aptamers. Aptamers Cy3 21-2 (A) and Cy3 47tr (B) were added at 80 nM (final concentration) in serum-free medium for 5 hrs and plates were kept at 4°C. Coverslips were then washed with PBS, fixed with 4% formaldehyde for 10 min followed by mounting on microscope slides using a glycerol-based mounting media containing DAPI. Nuclear staining with DAPI and aptamers with Cy3-label, are blue and red, respectively. Number of cells were counted was n = 46 and n = 40 respectively, for 21-2 and 47tr. The scale bar is 10 µm.

5.2.4 Prediction of G-quadruplex structure in aptamers

Guanine-rich phosphodiester oligonucleotide sequences (more than 25% G-content) that can form quadruplex structures (G-quartets) (Dapic et al., 2003) are thought to be internalised more efficiently compared to non- guanine-rich sequences via micropinocytosis in cells grown in monolayer culture (Reyes-Reyes et al., 2010). The G-contents (%) of 21-2 and 47tr were 36 and 28, respectively. In order to reveal whether 21-2 and 47tr were forming G-quadruplexes, the sequences of these aptamers were analysed using QGRS software which calculates G-scores. Sequences with higher score`s would form more stable structures. The highest possible G-score for a maximum 30-nucleotide sequence is 105. Here is an example of such sequences: GGGGGGTGGGGGGTGGGGGGTGGGGGG. G-scores have been devised to evaluate the likelihood of a sequence to form stable G-quadruplexes Figure 5.10 showed that there was one possible predicted structure for 21-2 with a G-

score of 11. No G-quadruplex structure was predicted for 47tr although it contained ~28% of guanine.

Aptamer	Position	Length	QGRS prediction	G-content (%)	G-score
21-2	1	33	**GGUCUAGCCGGAGGAGU CAGUAAUCGG**UAGACC	36	11
47tr	N/A	32	**GGGUUAACAGAAAACCU CAGUUGCUGGGUUGU**	28	N/A

Figure 5.10 G-quadruplex structure predictions of 21-2 and 47tr by using QGRS software. 21-2 and 47tr aptamer sequences with G-contents of 36% and 28% respectively were analysed using the software. There was one G-quadruplex prediction for 21-2 with a G-score of 11. A similar size aptamer, 47tr was not suggested to form these structures according to the software (Kikin et al., 2006).

5.2.5 Transfection efficiency of aptamers as measured by flow cytometry

The levels of aptamer uptake into primary keratinocytes and SiHa cells were determined by flow cytomery using aptamer cy5 21-2. Keratinocytes and SiHa cells were plated on 12-well plates at 24 or 48 hrs prior to incubation with aptamers, respectively. Incubation of cells with aptamers was performed in the presence or absence of transfection reagents for 5 hrs, followed by cell harvesting and several washes of the cell pellets in PBS, including an acidic wash to remove the surface bound RNA molecules. Cells were stained with propidium iodide and analysed by flow cytometer using the APC (allophycocyanin) channel (Excitation at 633 nm, emission at 660 nm) (Cy5 and APC have the same excitation) and PI (Propidium Iodide) (Excitation at 488 nm, emission at 617 nm) channels by counting 10, 000 cells. The results are represented as percentage of cells that are positive for Cy5.

5.2.5.1 Uptake in primary cells

Primary cells were grown in keratinocyte growth medium lacking serum to prevent cell differentiation. Cells were incubated with aptamers in the same medium conditions prior to flow cytometry analysis to measure the efficiency of uptake.

The Sample	The percentage of Cy5 positive keratinocytes under different conditions	
	Oligofectamine transfection	Incubation in media
Mock	3.5	6.2
5 nM 21-1	27.4	4.0
80 nM 21-2	99.2	19.3

Figure 5.11 Flow cytometric analysis to detect percentage of primary cells with aptamer 21-2 internalised in the presence/absence of Oligofectamine transfection. Primary cells were plated onto 12-well plates 24 hrs prior to incubation or transfection with aptamer 21-2. Primary cells were either incubated or transfected with 5 or 80 nM cy3-5 double labelled aptamer 21-2. At 5 hrs post-transfection, cells were washed with PBS and trypsinised. Cells were pelleted and washed with PBS twice followed by an additional wash with an acidic wash buffer to remove surface-bound RNA molecules. Flow cytometry was performed following staining the cells with propidium iodide (PI). 10, 000 cells were counted for each transfection. Results are shown as percentage of Cy5-positive and therefore aptamer positive cells from a single experiment (n = 1).

Figure 5.11 showed the percentage of keratinocytes containing a Cy5 signal from mock-transfected, cells transfected with 5 or 80 nM cy5-21-2 in the presence/absence of oligofectamine (a cationic transfection reagent). Oligofectamine transfection was reported to deliver 5nM and 80 nM cy5-21-2 to up to 27 and 99% of primary cells, respectively. The transfection efficiency of Oligofectamine was found to be quite high even when as little as 5 nM of aptamer was used. Therefore, 80 nM aptamer was sufficient to target almost all of the cells in the culture. As propidium iodide was used to distinguish dead cells, the percentage of Cy5 positive cells represented only living cells. Another set of cells were not transfected but only incubated with Cy5-21-2 without replacing the growth medium. Although the use of low concentrations of 21-2 (5 nM) was not adequate to obtain a detectable signal, 80 nM of 21-2 was delivered to delivered approximately 20% of cells that were counted by flow cytometry.

5.2.5.2 Uptake in SiHa cells

Reagent-free uptake was also studied in a cervical cancer cell line, SiHa, derived from grade II, squamous cell carcinoma which contains 1 or 2 copies of HPV16 integrated into the host genome. Nanocin was evaluated together with Oligofectamine.

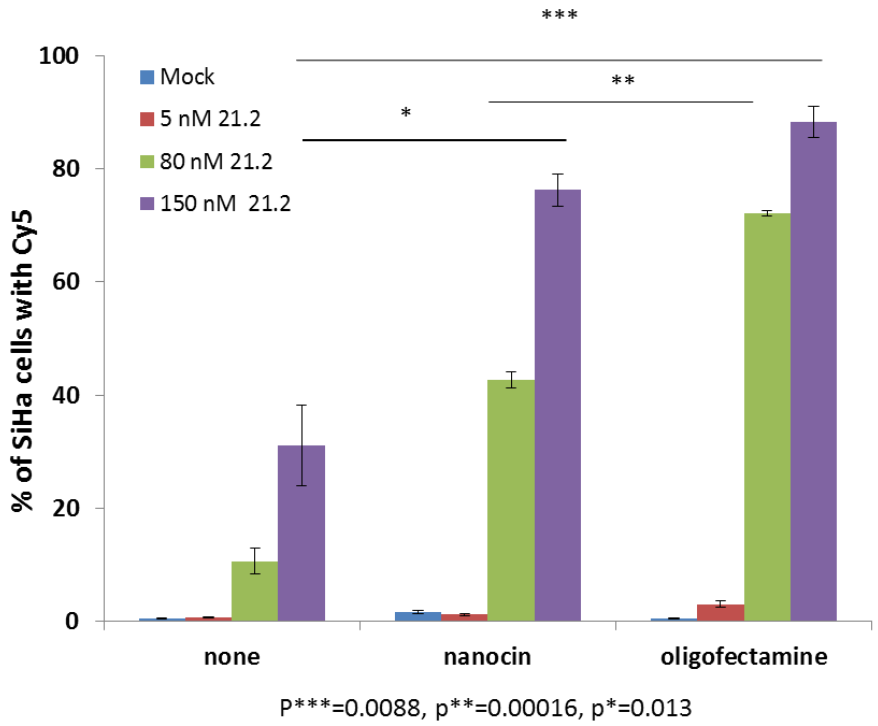

Figure 5.12 Uptake of aptamer 21-2 by SiHa cells in the presence or absence of transfection reagents (Nanocin and Oligofectamine) detected by flow cytometry. Cells were plated onto 12-well plates 48 hrs prior to transfection or incubation with double labelled aptamer 21-2 (Cy5 21-2 Cy3). Cells were either incubated or transfected with 5, 80 or 150 nM Cy5- labelled aptamer 21-2 with (oligofectamine or nanocin). At 5 hrs post-transfection, cells were collected and washed with PBS twice followed by an additional wash with an acidic wash buffer to remove surface-bound RNA molecules. Flow cytometry was performed following staining the cells with propidium iodide (PI) to remove dead cells from the analysis. 10, 000 cells were counted for each transfection. Results were presented as percentage of Cy5-positive cells, therefore aptamer positive cells. The data was obtained from three independent experiments (n = 3), shown together with standard errors.

SiHa cells were incubated or transfected (using either nanocin or oligofectamine) with 5, 80 or 150 nM of Cy5 21-2 Cy3. Similar to primary keratinocytes, SiHa cells were also able to internalise aptamer without the need for a transfection reagent, with up to around 40% of cells being detected aptamer positive when 150 nM of Cy5 21-2 Cy3 was used. The use of 80 nM of aptamer resulted in ~20%, which seemed similar to the data from keratinocytes (section 5.2.5.1). Oligofectamine and nanocin transfections with the highest concentration of aptamer (150 nM) significantly increased the uptake up to 95 and 80 %, with p values of ***0.008 and *0.013, respectively. Although the difference between nanocin and oligofectamine transfections was not significant with 150 nM aptamer transfections, when lower

concentrations of aptamer such as 80 nM were used, oligofectamine delivered the aptamer into more cells than that of nanocin ($p^{**} = 0.00016$). Nanocin had little toxicity, resulting in only up to 20-30% cell death detected by PI staining (data not shown). In addition, use of nanocin as a delivery agent will require more cells to avoid cytotoxicity and more RNA molecules to be able to target all cells present, although reagent was used at very small amounts which could be advantages over other transfection reagents to economise on its excessive use.

5.3 Co-localisation of aptamers in cellular compartments upon internalisation

In common with keratinocytes, SiHa cells were shown to be internalising 21-2 and also 47tr without the need for transfection. There is little published data on cellular localisation of RNA aptamers upon internalisation (Homann and Goringer, 2001). Therefore localisations of aptamers were studied with or without lipofection looking at the co-localisation with some of the endosomal markers such as EEA1 for early endosomes and LAMP1 for late endosomes/lysosomes.

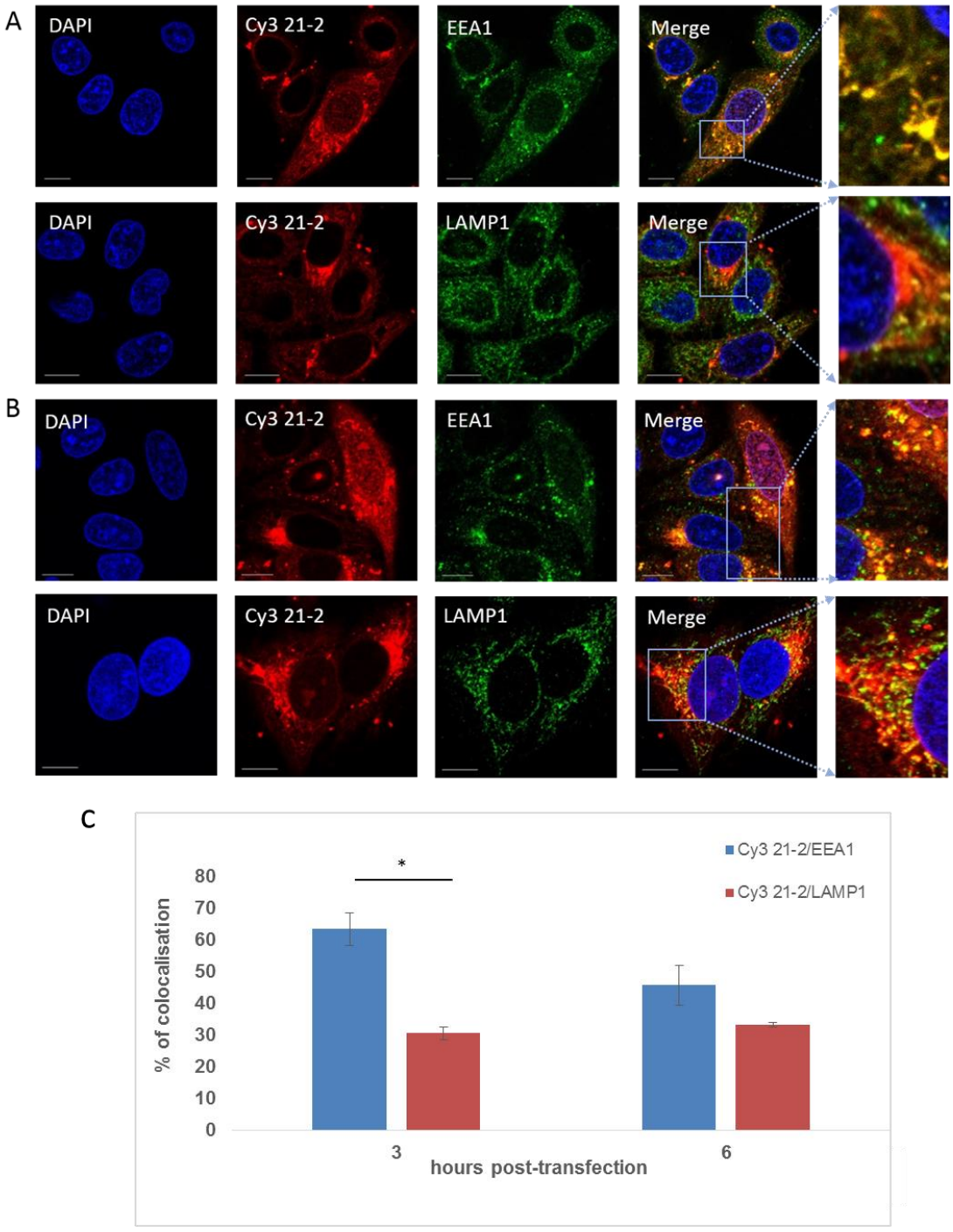

Figure 5.13 Cellular localisation of aptamer 21-2 in SiHa cells predominantly in early and late endosomes following Oligofectamine transfection. Cells were plated onto glass coverslips in 12-well plates and grown for 48 hrs. Then, cells were transfected with 80 nM Cy3 labelled 21-2 using Oligofectamine. At 3 (Panel A) or 6 hrs (Panel B) post-transfection, cells were washed with PBS, fixed with 4% formaldehyde and permeabilised with 0. 01% Triton-X100. Cells on coverslips were blocked with BSA for 30 min at room temperature. Primary antibodies anti-EEA1 (early endosomes) (1:400) and anti- LAMP1 (late endosomes) (1:400) were added onto cells and left at 4°C overnight on a shaking platform. Coverslips were washed on the following day with PBS and

AlexaFluor488 goat anti-Rabbit secondary was added in BSA for 1 h at room temperature. Secondary antibody was washed and coverslips were mounted on microscope slides. Images were taken using the Zeiss LSM700. The level of co-localisation was analysed by Bitplane: Imeris image analysis software (Panel C). For EEA1 and LAMP1 colocalisation respectively, n = 8 and 29 at 3 h and n = 30 and 19 at 6 h ($p^* \leq 0.003$). Red, Green and Blue are Cy3 (21-2), FITC (early or late endosomes) and DAPI (nucleus), respectively. The last panel is a zoom of merged images. The scale bar is 10 µm.

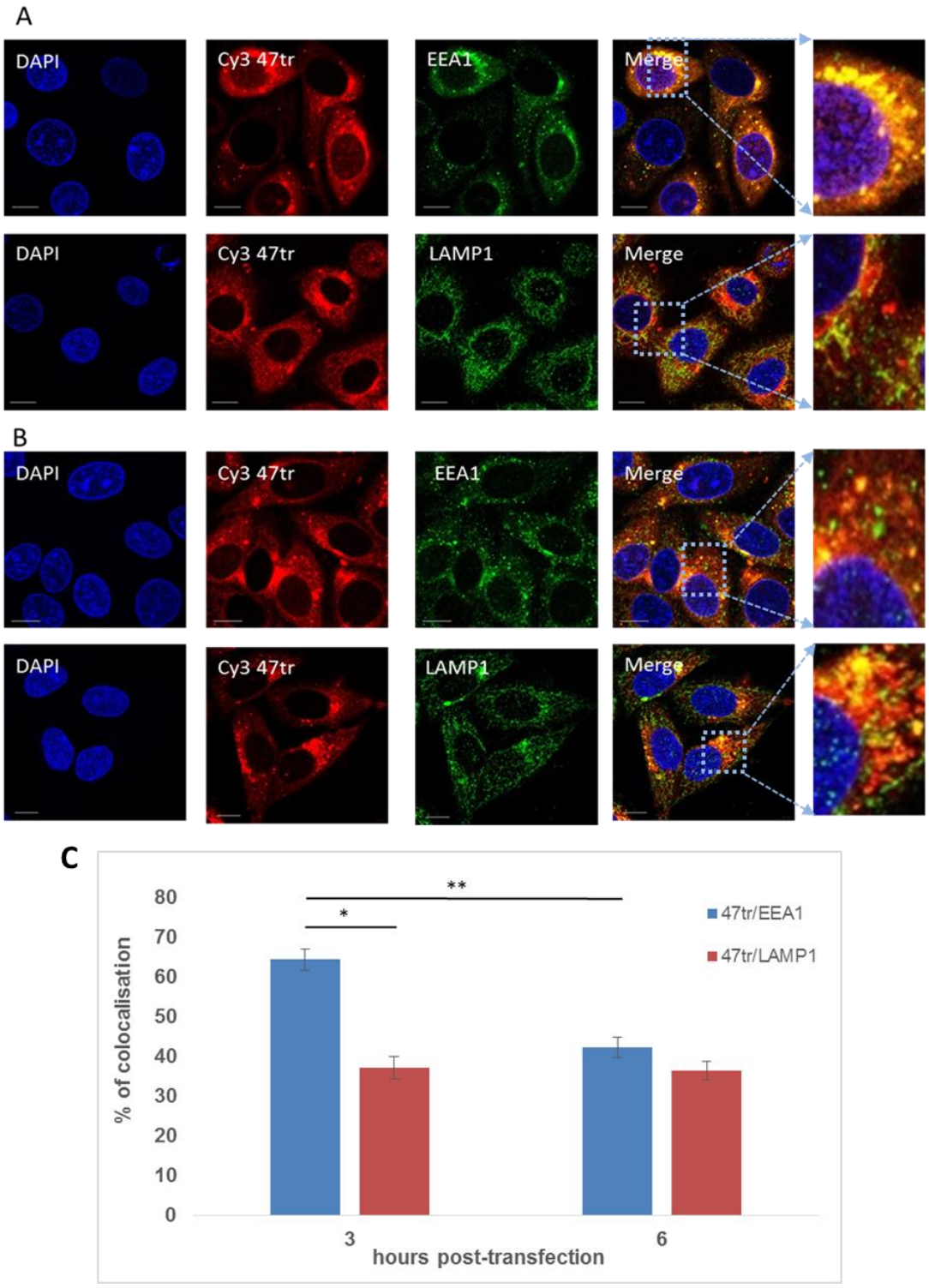

Figure 5.14 Cellular localisation of aptamer 47tr in SiHa cells predominantly in early and late endosomes following Oligofectamine transfection. Cells were plated onto glass coverslips in 12-well plates and grown for 48 hrs. Cells were transfected with 80 nM Cy3-labelled 47tr using Oligofectamine. At 3 (Panel A) or 6 hrs (Panel B) post-transfection, cells were washed with PBS, fixed with 4% formaldehyde and permeabilised with 0. 01% Triton-X100. Cells on coverslips were blocked with BSA for 30 min at room temperature. Primary antibodies anti-EEA1 (early endosomes) (1:400) and anti- LAMP1 (late endosomes) (1:400) were

added onto cells and left at 4°C overnight on a shaking platform. Coverslips were washed on the following day with PBS and AlexaFluor488 goat anti-Rabbit secondary was added in BSA for 1 h at room temperature. Secondary antibody was washed and coverslips were mounted on microscope slides. Images were taken using the Zeiss LSM700. The level of co-localisation was analysed by Bitplane: Imeris image analysis software (Panel C). For EEA1 and LAMP1 colocalisation respectively, n = 25 and 48 at 3 h and n = 24 and 23 at 6 h ($p^* \leq 9.308E-05$, $p^{**} \leq 0.001$). Red, Green and Blue are Cy3 (47tr), FITC (early or late endosomes) and DAPI (nucleus), respectively. The last panel is a zoom of merged images. The scale bar is 10 µm.

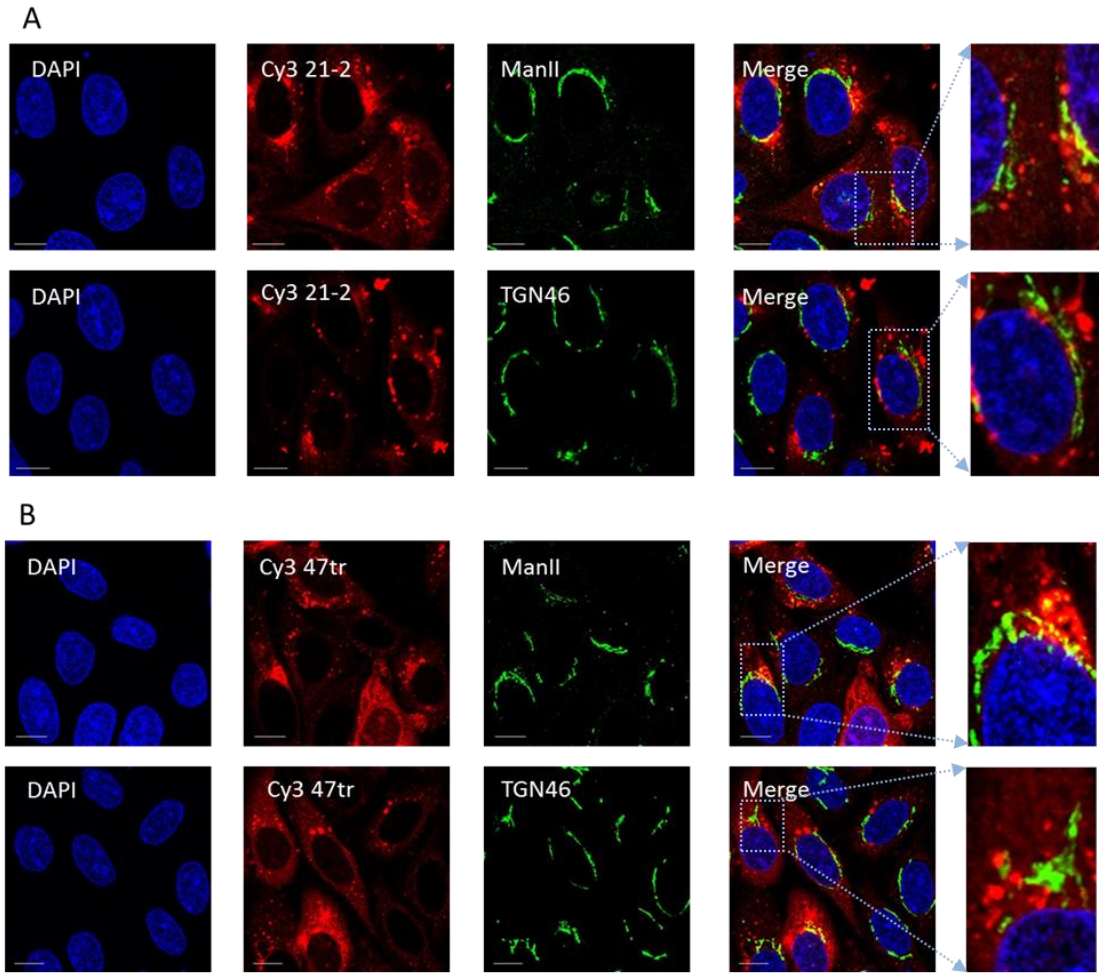

Figure 5.15 Cellular localisation of aptamer with Cis and Trans-golgi markers, ManII and TGN46. Cells were plated onto glass coverslips in 12-well plates and grown for 48 hrs. Then, cells were transfected either with 80 nM Cy3 21-2 (Panel A) or Cy3 47tr (Panel B) using Oligofectamine. At 6 hrs post-transfection, cells were washed with PBS, fixed with 4% formaldehyde and permeabilised with 0. 01% Triton-X100. Cells on coverslips were blocked with BSA for 30 min at room temperature. Primary antibodies anti-ManII (Cis-golgi) (1:400) and anti-TGN46 (Trans-golgi) (1:400) were added onto cells and left at 4°C overnight on a shaking platform. Coverslips were washed on the following day with PBS, and AlexaFluor488 goat anti-rabbit or Alexafluor488 donkey anti-sheep secondary was added in BSA for 1 at room temperature. Secondary antibody was washed and coverslips were mounted on microscope slides. Images were taken using the Zeiss LSM700. Red, Green and Blue are Cy3 (21-2 or 47tr), FITC (Cis- or Trans- golgi) and DAPI (nucleus), respectively. Images are representatives of two independent experiments (n = 2). The last panel is a zoom of merged images. The scale bar is 10 µm.

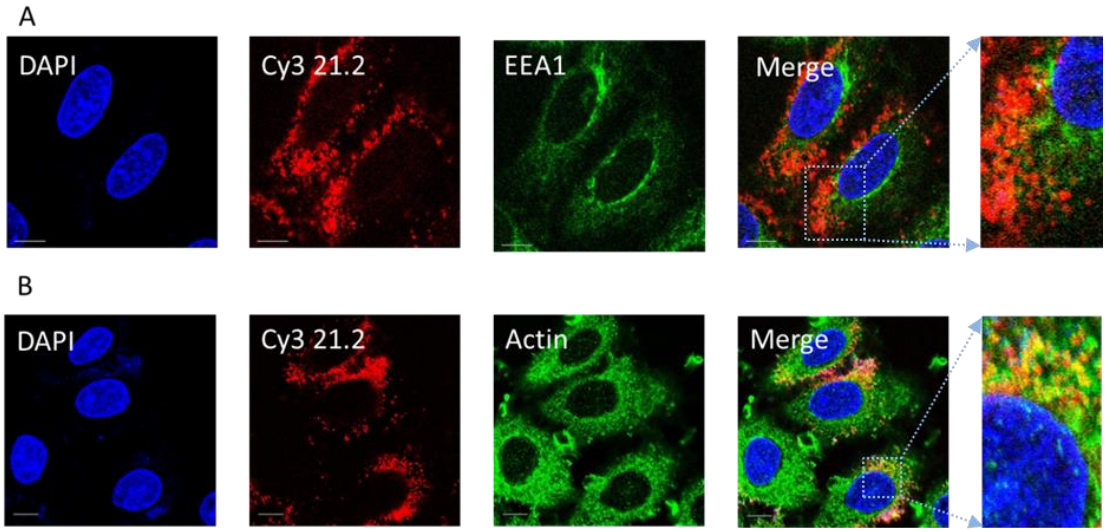

Figure 5.16 Co-localisation of aptamer 21-2 in SiHa cells following reagent free uptake with actin but not early endosomes. SiHa cells were incubated with 80 nM Cy3 labelled 21-2 for 6 hrs followed by fixation and permeabilisation of cells. Primary antibodies anti-EEA1 (early endosomes) (1:400) (Panel A) and anti-actin (:/200) (Panel B) were added in BSA and left at 4°C overnight on a shaking platform. Incubation with alexaFluor488 goat anti-Rabbit and donkey anti-Goat secondary antibodies was performed in BSA for 1 h at room temperature. Images were taken by the Zeiss LSM510 upright confocal microscope. Red, Green and Blue are Cy3 (21-2), FITC (early endosomes or actin) and DAPI (nucleus), respectively. Images are from a single experiment (n = 1). The last panel is a zoom of merged images. The scale bar is 10 µm.

SiHa cells were seeded on glass coverslips in a 12-well tissue culture plate, and grown for 48 hrs prior to incubation or tranfection with the aptamers for 3 hrs and 6 hrs. Cells were then incubated with primary antibodies for early and late endosomes, and FITC-secondary antibodies, overnight at 4°C and room temperature for 1 h, respectively.

In Oligofectamine-transfected cells, most of the aptamer was found to be localised predominantly in early and late endosomes. Transfection efficiency for both aptamers, 21-2 and 47tr was around 87% (number of cells counted was n = 91 and n = 121, for 21-2 and 47tr). At three hrs post transfection, 21-2 was mostly localised in early (63.36%) rather than late endosomes (30.54%) ($p^* \leq 0.003$) (Figure 5.13A,C). However, in cells transfected for 6 hrs, this co-localisation was reduced and the aptamer was localised to both early and late endosomes/lysosomes (45.66% and 33.21% respectively, Figure 5.13B,C) which may indicate the escape of the aptamer from endosomes. Aptamer was also detected in the nucleus of some of the cells following transfection (Figure 5.13B). Another aptamer, Cy3 47tr also showed a similar pattern of distribution to Cy3 21-2 in SiHa cell. At three hrs post transfection,

47tr was mostly localised in early (64.44%) rather than late endosomes (37.19%) ($p^* \leq 9.308E-05$) (Figure 5.14A,C). Whereas, in cells transfected for 6 hrs, this co-localisation was significantly reduced ($p^{**} \leq 0.003$) and the aptamer was localised to both early and late endosomes/lysosomes (42.32% and 36.47% respectively, Figure 5.14B,C). Data from both aptamers may indicate that RNA aptamers in transfected cells can be targeted to early/late endosomal/lysosomal pathways, in which they are degraded or manage to escape to complete their function in the cytosol. Markers for cis- and trans- Golgi, Man II and TGN46, respectively were also utilised to understand the localisation of aptamer (Cy3 21-2 and Cy3 47tr) (Figure 5.15). These aptamers did not appear to be localised in the Golgi compartments following transfection.

Localisation of aptamer 21-2 (Figure 5.16A), when introduced into SiHa cells without any transfection reagent, was not detected in endosomes, unlike in lipofection, suggesting a different uptake mechanism. In addition, when SiHa cells that had been incubated with aptamer 21-2 were reacted with anti-actin antibody, co-localisation of actin with aptamer 21-2 was observed. This may indicate the involvement of macropinocytosis for internalisation (Figure 5.16B). During micropinocytosis, actin-driven protrusions along the plasma membrane were formed upon exposure to an extracellular stimuli such as growth factors, nutrients and other signals. Extracellular fluid then becomes surrounded by these actin protrusions in order to form vesicles to “cargo” the content along the microtubules towards the perinuclear area.

5.4 Chapter Discussion

Understanding the mechanism of uptake of aptamers or other such molecules with therapeutic potential is very important due to the current problems in targeted-cellular delivery of small oligonucleotide-based therapeutics such as siRNAs and anti-sense oligonucleotides (Meade and Dowdy, 2009). For an aptamer to be used as a delivery vehicle, it must be efficiently internalised (Shigdar et al., 2011).

Reagent-free uptake of a DNA aptamer, AS1411, siRNA and also naked plasmids DNAs have been extensively studied, however literature on the uptake of RNA aptamers is not substantial. Here the uptake of labelled RNA aptamers, 21-2 and 47tr, in primary keratinocytes and also the cervical cancer cell line, SiHa was described. Internalisation of 21-2 and 47tr was studied in primary keratinocytes and it was shown that cells took up both aptamers.

To establish an effective and non-toxic delivery system is very important prior to clinical use of these molecules. Although, there are two main techniques that are used

to introduce foreign nucleic acid molecules such as siRNAs, DNA and aptamers into cells, namely lipofection and electroporation, both techniques have disadvantages (Barreau et al., 2006). When HeLa cells were transfected with hyper-unstable nonadenylated/non-capped mRNAs, these molecules were as equally stable in cells as control mRNAs, and were associated with membrane structures, indicating that mRNA could be sequestered in vesicles to protect them from the degradation machinery of cells. Therefore, the proportion of the functional RNA released in the cytoplasm may be low as opposed to RNAs trapped in membranous structures. In addition, large amounts of RNA molecules can be toxic to cells and trigger unwanted responses such as the stress response which could alter cell metabolism. Cationic liposomes and polymers might have toxic side effects such as liposome/plasmid DNA inducing haemagglutination and apoptosis in macrophages (Aramaki et al., 1999, Eliyahu et al., 2002).

In this Chapter, aptamer 21-2 was shown to be internalised into primary cells. When double-labelled 21-2 was used for confocal imaging, it was shown that both ends of the RNA were taken up and co-localised with each other. A computer program Imaris was used for quantitation of co-localisation, and measurement was represented as a Pearson`s coefficient value. Although this value is higher for Oligofectamine-transfected cells (0.9448), indicating that with lipofection, almost all of the aptamers appeared to be intact molecules. In reagent-free uptake of 21-2, this value was slightly lower but it was still indicated that most the molecules were intact.

As siRNAs enter cells by endocytosis following liposome delivery (Lu et al., 2009), this might result in RNA escaping from the complexes and being functional (Sioud, 2005, Yoo et al., 2006). In addition, the efficiency of liposome transfections varies amongst different cell types. Electroporation delivers the RNA directly to the cell cytoplasm, therefore off-target immune responses can be prevented. However, to introduce siRNA in to bovine monocytes with the use of electroporation caused cells to be more fragile compared to transiently-transfected cells, and more cell death was observed, although gene silencing effects were comparable with lipofection (Jensen et al., 2014). Drawbacks of electroporation include high cell death, requirement for serum-free transfection conditions, use of highly confluent cell monolayers and relatively large amounts of RNA (Gonzalez et al., 2007). However, cargo could still be subjected to lysosomal degradation due to accumulation in endosomes. Interestingly, when a 25 amino acid synthetic long peptide (SLP), which was designed from a melanoma associated antigen as an anti-tumour vaccination agent, was introduced

into human dentritic cells by electroporation, it was shown to co-localise in early and late endosomes (Menager et al., 2014).

Aptamer 21-2 and also 47tr were used for co-localisation experiments to understand their location after passive uptake or Oligofectamine transfection. Aptamer 21-2 and 47tr was predominantly localised to both early and late endosomes in Oligofectamine transfected SiHa cells. Localisation to early endosomes was particularly striking at early timepoints post-transfection (3 hrs). It is interesting to note that the reduction in co-localisation seen after 6 h did not correlate with an increase in co-localisation with the late endosomal marker. Further time points might be useful, however, this could be indicative of escape of aptamers from the endocytic pathway. While there is little data on the sub-cellular localisation of aptamers, transfection of siRNAs using cationic lipids, nanoparticles or cell-type-specific delivery reagents have shown that siRNAs are trafficked to the endosomal pathway (early and then late endosomes), reviewed in (Dominska and Dykxhoorn, 2010). When 21-2 was passively internalised by SiHa cells, aptamer was not co-localised with the endosomal marker, indicating that endocytosis may not be involved in its uptake. Other mechanisms such as micropinocytosis could be involved in the uptake of 21-2. In addition, aptamer 21-2 was found to be associated with actin, which could be due to the involvement of actin e.g. during macropinocytosis.

An alternative to lipid-based transfection, non-lipid, and nanoparticle-forming transfection reagents such as Nanocin can also be used for transfection of small oligonucleotides into a wide range of cell types with lower toxicity. Nanocin (HappyFect^{TM}) was used to test the effectiveness of the aptamer delivery and possibility of future use of this reagent for other aptamers such as the HPV16 E7 aptamer A2 to target intracellular proteins. SiHa cells were used for transfections. A simple protocol was used in which RNA molecules and the reagent were mixed and applied to the cells. Double-labelled 21-2 was used to transfect these cells, and images indicated that RNA was both efficiently internalised and was still intact (with a co-localisation of both ends of the RNA, calculated Pearson`s value was 0.82). Nano-particle forming transfection reagents have been used elsewhere for RNA delivery, such as hydrophobized hyaluronic acid–spermine conjugate (HHSC) self-aggregates in water to form nanoparticles, which could be used for efficient delivery of RNA molecules (Shen et al., 2011).

Macropinosomes may give aptamers a better chance to escape and avoid degradation (Conner and Schmid, 2003, Wadia et al., 2004) as they are non-acidic

and non-digestive vesicles and are potentially leaky compared to lysosomes. How these DNA or RNA molecules escape from macropinosomes in to cytosol are not yet known. Macropinocytosis is thought to be an efficient means of delivering a range of different cargos including peptides, intact proteins, bacterial virulence factors and viruses into cells (Reyes-Reyes et al., 2010). Reagent-free or passive uptake of aptamers could therefore also aid the development of new strategies for drug delivery. In fact, aptamers that are passively internalised might be better therapeutics if they enter the cells via alternative pathways rather than receptor-mediated endocytosis by which they localise in endosomes and lysosomes.

In order to understand the pathway that those two aptamers, 21-2 and 47tr were internalised, inhibitors for macropinocytosis (amiloride) and endocytosis (dynasore) were utilised in SiHa cells. Dynasore treatment of SiHa cells did not affect the uptake of 21-2 (15% decrease) as it did for 47-tr (30%), suggesting that alternative mechanisms could be involved such as macropinocytosis in the uptake of these aptamers especially for 21-2. Transferrin was used to test effectiveness of dynasore treatments. 47tr but not 21-2 was found to partly co-localise with transferrin around the peri-nuclear area and on the cell membrane of DMSO and dynasore treated cells, respectively. It is possible that 47tr may use receptor-mediated endocytosis, although it was not selected against a receptor protein. Another evidence for receptor-mediated endocytosis of 47tr was that uptake of 47tr in SiHa cells at 4°C was strongly inhibited, whereas 21-2 was still being internalised although as not efficiently as it was at 37°C. Aptamers internalised into cells via receptor-mediated uptake were identified before, however, they are mostly selected against plasma membrane proteins. For example, an RNA aptamer for cancer stem cell marker CD133, which is a transmembrane protein was found to be internalised via receptor-mediated endocytosis as aptamer was detected in a ring-like pattern outside the cells on the plasma membrane on potassium-depleted and hypertonic treated cells which are used as inhibitors of endocytosis (Shigdar et al., 2011).

Amiloride (an inhibitor to Na^+/H exchange and micropinocytosis), treatment of SiHa cells decreased the uptake of 21-2 and 47tr by around 40% and 10%, respectively (Figure 5.8C), indicating that 21-2 may possibly be internalising via macropinocytosis. It was described that a DNA plasmid could be internalised via macropinocytosis (Basner-Tschakarjan et al., 2004). However, they were not certain if naked plasmid DNA is taken up via constitutive macropinocytosis or binding of the plasmid DNA to certain membrane receptor molecules such as integrins, resulting in induction of downstream intracellular signalling pathways for macropinocytosis. Therefore, uptake

of 21-2 might also involve some membrane receptors to trigger macropinocytosis. Dextran-FITC needs to be utilised along with the aptamers especially 21-2 (since dextran is known to be internalised via macropinocytosis) and co-localisation of 21-2 with dextran in amiloride or DMSO treated cells could be studied to confirm that 21-2 is using macropinocytosis to enter the cells.

Uptake of 21-2 could be via macropinocytosis in SiHa cells. However aptamers could also enter a different cell type via another pathway. AS1411 appears to be internalised by non-malignant Hs27 cells predominantly by clathrin- or caveolae-dependent pathways whereas cancer cell line DU145 uses macropinocytosis to internalise the aptamer (Merit Reyes-Reyes E., et al., 2010). Amiloride treatment reduced the uptake of AS1411 in cancer cells, suggesting the involvement of macropinocytosis (Reyes-Reyes et al., 2010). Even if aptamer 21-2 was suggested to enter primary cells via macropinocytosis, downstream mechanisms and molecules involved could be different to those in SiHa cells. Mesothelial cells in mice were found to internalise plasmid DNA through macropinocytosis. Here, Rac (Rac inhibitor-NSC2376639 and p21-activated kinase (PAK, downstream molecule of Rac) inhibitor-PAK1840 inhibited the transgene expression significantly) but not Rho pathways (No significant difference between control and ROCK (a downstream molecule of Rho) inhibitor Y-27632 treatments) found to be involved in inducing actin dynamics for macropinocytosis of pDNA. Latrunculin B (an actin polymerization inhibitor) and ML-7 (myosin light chain kinase (MLCK) inhibitor) were found to inhibit the transgene expression, indicating the involvement of actin dynamics (Fumoto et al., 2009). Naked plasmid DNA can also be taken up by macropinocytosis in keratinocytes. Several proteins found to be involved such as ezrin and moesin (Basner-Tschakarjan et al., 2004) which are parts of downstream Rho pathways unlike the mechanism in mesothelial cells of mice (Fumoto et al., 2009). Thus, different pathways might be involved for macropinocytosis in different cell types. Another example to show that the uptake mechanism is dependent on cell types is that uptake of naked plasmid DNA was inhibited by scavenger receptors class A inhibitors (e.g. polyinosinic acid and dextran sulphate) in macrophages (Takagi et al., 1998), but not in gastric serosal surface cells (Fumoto et al., 2009).

Proteoglycan-dependent DNA uptake is mediated by macropinocytosis not caveole- or clathrin- mediated endocytosis. DNA was shown to form complexes with DNA-binding proteins that are secreted from cells in conditioned media and resulting protein-DNA complexes require cell surface proteoglycans to enter the cells. Proteoglycan deficient cells showed decreased levels of uptake (Wittrup et al., 2007).

An anti-microbial peptide which is highly expressed in bone marrow and epithelial cells is involved in protection of plasmid DNA from serum nucleases. This peptide targeted the plamid DNA to the nuclear compartment through non-caveolar lipid raft mediated endocytosis involving surface proteoglycans of mammalian cells where plasmid DNA was expressed (Sandgren et al., 2004).

Guanine-rich phosphodiester oligonucleotide sequences that can form quadruplex structures (G-quartets) (Dapic et al., 2003) are found to internalise more efficiently compared to non-quanine rich sequences (more than 25% G-content) via macropinocytosis on in cells grown in monolayer culture (Reyes-Reyes et al., 2010). 21-2 (with 36.3% G-content) may also form this inter- and intramolecular structures as the QGRS software predicted one possible quadruplex structure for 21-2. (Kikin et al., 2006). This structure may increase the uptake of 21-2. Another way to facilitate the uptake of aptamers can be the pre-treatment of cells with unlabelled 21-2 overnight prior to incubation with labelled 21-2. This can facilitate internalisation of aptamer caused by continuous uptake resulting in the stimulation in macropinocytosis.

SID-1 (systemic RNAi deficient-1 and 2) mediates energy-independent internalisation of RNA in *C. elegans*, possibly functioning as a membrane channel to transport RNA into cells (Duxbury et al., 2005). Their mammalian homologues, SID transmembrane protein 1 (SIDT1) and 2 (SIDT2), could be responsible for passive uptake of aptamers as well as RNAs. SID-2 (apical intestinal membrane protein) from *C. elegans* was not as well-studied as that of SID-1. Both of these channels are required for RNA uptake (McEwan et al., 2012). The difference between these channels is that unlike SID-1, SID-2 uses energy-dependent endocytosis to internalise RNA. Single-stranded RNA (ssRNA) molecules were also found to be internalised by these channels, possibly due to folding of the aptamer on itself to form small double-stranded regions (McEwan et al., 2012). These channels might also be involved in the escape of RNA molecules from endocytic vesicles in to the cytosol.

Dynasore treatment of SiHa cells, was found to partly inhibit the uptake of 21-2 and 47tr, indicating the involvement of receptor-mediated endocytosis as well as macropinocytosis. The same cells could be using two different mechanisms to internalise the same molecules although one of the mechanisms might be stronger and more efficient than the other. Expression of SID-1 in Drosophila S2 cells, which lack SID protein homologues, resulted in the formation of a RNA-selected channel which mediates the passive uptake of the RNA molecules through cellular membrane

(Feinberg and Hunter, 2003). However, S2 cells are able to partly internalise the RNA from surrounding growth medium via endocytosis using scavenger receptor SR-CL (Saleh et al., 2006) although the uptake is relatively slow and dependent on high concentrations of RNA present in the extracellular environment.

Full length 70-kDa heat shock protein Hsp70 was able to deliver bound RNA molecules into the cytoplasm of mammalian cells (Henics and Zimmer, 2006). However, uptake of 21-2 and 47tr is not likely to be mediated or facilitated by these proteins in SiHa, as well as primary cells. These proteins are over-expressed in several cancers including cervical cancer. Its over-expression was detected both in cervical cancer cells of different origin (HeLa, SiHa, C-33 A and CaSki) and clinical cervical SCC samples and was highly linked to cell growth, survival and tumour aggressiveness (Garg et al., 2010). If uptake was via these channel-forming chaperone proteins, then one would expect internalisation of aptamers into HeLa as well as SiHa cells due to the over-expression of Hsp-70 in HeLa cells. However, uptake was seen to be limited in HeLa cells compared to SiHa cells in our experiments.

Cy5-labelled aptamer 21-2 was used to study transfection efficiencies following lipofection or incubation in medium only in both primary keratinocytes (Section 5.2.5.1) and SiHa cells (Section 5.2.5.2). Cells were incubated or transfected with aptamer and Cy5 fluorescence was determined by flow cytometry. The percentage of aptamer positive primary cells detected was presented in Figure 5.11. Up to 20% of cells was found to have taken up the aptamer (at 80 nM) when cells were incubated without lipofection. However, when aptamer was introduced by Oligofectamine transfection, the percentage of positive cells was 99%, almost all cells having internalised the aptamer. Although the level of uptake without lipofection was relatively low, the mechanism of uptake could also be considered in determining the function of the internalised aptamer. It has been shown that (Reyes-Reyes et al., 2010) cancer and non-cancer cells can both internalise a DNA aptamer, AS1411, however it can only trigger apoptosis in cancer cells. This might be explained by the use of different uptake mechanisms, macropinocytosis in cancer cells and clathrin-dependent endocytosis in non-cancer cells. It has been shown that hyperstimulation of macropinocytosis by continuous uptake of molecules results in a novel form of apoptosis in cancer cells (Overmeyer et al., 2008). In addition, molecules entering by macropinosomes could escape from these vesicles and function in the cytosol, whereas molecules entering by endocytosis e.g. by lipofection would be accumulated in the endosomes/lysosomes for degradation unless they manage to escape e.g. by

pore formation in the endosomal membrane, molecules with pH-buffering effects and the use of fusogenic agents (Varkouhi et al., 2011).

Flow cytometry experiments were also performed in SiHa cells to test the efficiency of 21-2 uptake in the presence/absence of lipofection (Figure 5.12). SiHa cells were also able to internalise the aptamer in different conditions. Both Oligofectamine and Nanocin transfection introduced aptamers (150 nM) to significantly more cells than untransfected (where aptamers were simply incubated with cells) with p values of 0.0088 and 0.013. When aptamer concentration was dropped to 80 nM, Oligofectamine transfection was found to be better than Nanocin transfection ($p = 0.00016$). Therefore, Nanocin transfection might require the use of higher concentrations of aptamers. In addition, more cells may need to be used to reduce the cytotoxic effects of Nanocin in SiHa cells.

In summary, 21-2 has been shown to be internalised efficiently in primary cells and also in the cervical cancer cell line SiHa possibly by macropinocytosis. Therefore, it can have a potential for drug delivery, since it is internalised into cells without the need for lipofection and, it could be designed to carry cargos such as siRNA, nanoparticles or aptamers into the target cells as chimeras. The HPV16 E7 aptamer A2 could be used to create a chimera with 21-2 to facilitate its entry into cancer cells and also primary cells which could be useful to target those cells in *in vitro* skin raft systems. However, a drawback may be that engineering such chimeras could also diminish the fuction of aptamers.

6 GENERAL DISCUSSION AND FUTURE PROSPECTS

Human papillomaviruses are a necessary cause of cervical cancers. Current treatment strategies involve surgical removal of the HPV-infected lesions as well as the stimulation of the innate immune system to minimise symptoms. Great success has been achieved in terms of preventing infection since HPV vaccination was introduced. However HPV vaccines are expensive and need to be maintained in a stable cold chain, making vaccination in the developing world difficult. These vaccines are prophylactic, not therapeutic, therefore will not be effective on people who are already infected with HPV16/18 or with HPV types not covered by the vaccine. However, there are ongoing clinical trials for the use of therapeutic vaccines (Section 1.2.6) In this perspective, the generation of novel anti-viral agents targeting HPV oncoproteins helps to further elucidate protein-protein interactions *in vivo* and *in vitro* as well as offering a possible therapeutic approach (1.2.5 and 1.3.5.1).

The work described here employed a library of RNA aptamers identified against HPV16 E7 by SELEX (Nicol et al., 2011). A number of aptamers were selected for use in this work. They seemed to cause a decrease in E7 levels in addition to the induction of apoptosis in cervical cancer cells. Here, delivery mechanisms of aptamers and also co-localisation of aptamers with several cellular markers were studied. The results suggested the involvement of some potential mechanisms in the internalisation of aptamers.

HPV16 E7 aptamers were used for transfection of HPV16 transformed CaSki cells in order to analyse the effects of aptamers on steady state levels of E7 and cellular proteins, pRb and p130. In the work described here, HPV16 E7 aptamers, in particular A2 was shown to cause a significant decrease in the levels of E7 oncoprotein with an accompanying increase in the pRb levels. The N-terminus of E7 is a intrinsically disordered region, which may give flexibility and thus multiplicity of interaction partners to E7 (Section 1.2.4.2). HPV16 E7 may undergo binding-induced conformational change upon target binding. When E7 is liganded or bound, it may form more stable structures than unliganded or free E7. It can be hypothesised that upon A2-binding, E7 can be destabilised either through disruption of protein-protein interactions on the N-terminus, or through induction of a conformational change in E7. Future work could involve circular dichroism (CD) spectroscopy to determine whether a conformational change in E7 occurs upon A2-binding. Techniques such as SILAC

(stable isotope labelling of amino acids in cell culture) could also be performed to analyse whether HPV16 E7 aptamers, in particular A2, can disrupt multiple protein-protein interactions in cells. Several E7 aptamers were suggested to bind E7 at the C-teminus (Nicol et al., 2011). The C-terminus of E7 contains a conserved sequence motif, CXXC involved in dimerisation (Section 1.2.4.2). These aptamers may lead to a change in the multimerisation/oligomerisation status of E7. Future work could involve size exclusion chromatography (SEC), sedimentation equilibrium experiments (by analytical ultracentrifugation [AUC]) (Clements et al., 2000, McIntyre et al., 1993) or mass spectrometry in order to determine whether the oligomerisation status of E7 is altered upon aptamer-binding.

An N-terminal point mutant of GST-E7 was used in an *in vitro* binding assay, binding of an aptamer, termed A2, was reduced and thus A2 was suggested to require residues in the N-terminus for binding (Nicol, January 2011). Future work could involve characterisation of the minimal binding region of A2 or other E7 aptamers. Some information on aptamer-E7 interactions could be obtained e.g. by the use of deletion mutants or truncations of E7 in *in vitro* binding assays and by nuclease protection assays to determine the nucleotides of aptamers (especially A2) that are required for E7 binding.

E7 binds hypophosphorylated pRb and mediates its phosphorylation. The resulting hyperphosphorylated form of pRb is inactive and cannot function as a tumour suppressor. The effects of aptamer, especially of A2 on the level of hypo- or hyper-phosphorylated pRb could be tested using phosphorylation specific antibodies. In Chapter 4, studies with the use of several inhibitors for proteasomal and lysosomal degradation in CaSki cells showed that the pathway of E7 degradation induced by A2 transfection may possibly be through the 26S proteasome. In order to determine the E7 degradation, immunofluorescence experiments were performed using HPV16 transformed SiHa cells with anti-E7 antibodies and endosomal/lysosomal markers e.g. against early and late endosomes as well as a marker against ER in the presence or absence of A2 and a control aptamer SF1. Transfection of SiHa cells with A2 appeared to induce E7 localisation in the ER. It was suggested that this can perturb the normal biosynthetic delivery of E7 to the plasma membrane or other organelles. It is likely that upon A2 binding, E7 folding or oligomerisation results in its retention in ER in an unfolded/aberrant state. However, localisation of aptamer A2 in these cellular compartments needs also to be confirmed using fluorescently-labelled A2 in immunofluorescence experiments. Labelling A2 with fluorescein maleimide was found

to be problematic and inefficient. However, an alternative labelling method can be considered for this purpose or A2 can be chemically syntesised with a desired label for the use in co-localisation experiments. Furthermore, there are many other proteasomal inhibitors that could be used to further analyse the pathway of E7 degradation.

There are many alternative methods to study the interactions of E7 with other cellular proteins in the presence or absence of aptamers. For example, the mammalian two hybrid (M2H) system has been recognised as a powerful assay to study protein-protein interactions in cells (Luo et al., 1997). This system might be used to verify direct interactions of HPV16 E7 with pRb, and related proteins, p130 and p107; and the effects of E7 aptamers could be tested in this system. This system consists of plasmid constructs encoding the bait protein (e.g. Rb) and a prey protein (E7) fused to a DNA binding or a transcription activation domain, respectively. Another construct containing reporter genes e.g. chloramphenicol acetyltransferase (CAT) and green fluorescence protein (GFP) is included in this system. When the bait and a prey protein interacts, DNA binding and activation domains reunion and activate the expression of reporter genes that can be measued e.g. by fluoresence microscopy or CAT activity assays. An *in vitro* approach, rabbit reticulocyte lysate systems may also be used to study the effects of aptamers on E7 interactions (Belyaeva et al., 2014). This system is based on the production of ^{35}S [Methionine]-labelled cellular proteins such as pRb, p130 and p107 in rabbit reticulocyte lysates. These radio-labelled proteins can subsequently be used in pull-down experiments with affinity tagged E7 e.g. GST-E7 that is recombinantly expressed in *E. coli* in the presence or absence of HPV16 E7 aptamers. These samples can be analysed on SDS-PAGE followed by autoradiography. An alternative approach might be the use of GFP-Trap system where GFP tagged E7 is used to pull-down target of interest in the presence or absence of aptamer molecules using GFP-Trap beads.

Inactivation of tumor suppressor function by HPV infection alters the cell cycle regulatory mechanisms and suppresses the induction of apoptosis, causing the accumulation of mutations and favouring mutant cells in survival. Although cells accumulate mutations over the course of tumor progression which might provide an opportunity to survive without the need for E6/E7 expression, constitutive expression of E6 and E7 are still required for the viability of cancer cells. For example, E2 antisense expression or RNAi inhibits E6/E7 expression, resulting in growth inhibition of HPV positive cancer cells (Hall and Alexander, 2003). E2 expression in HeLa cells

result in senescence and a decrease in telomerase activity, and ability of E7 to inactivate the pRb pathway is significant in terms of the maintenance of HeLa cell proliferation and elevated levels of telomerase activity (Nishimura et al., 2006). Annexin V apoptosis assays showed that the transfection of HPV 16 transformed SiHa cells with HPV16 E7 aptamer A2 resulted in apoptosis, possibly due to the destabilisation of E7 oncoprotein and the recovery of pRb tumour suppressor pathway. Induction of apoptosis by aptamers can also be analysed by DNA fragmentation, *in situ* terminal deoxynucleotidyl transferase-mediated dUTP nick-end labeling (TUNEL) analysis and caspase activation assays. These are the first RNA aptamers to E7 with apoptotic effects. However, peptide aptamers have been previously shown to induce apoptosis in CaSki cells (Nauenburg et al., 2001). Peptide aptamers are generated by using the yeast two-hybrid system from a pool of molecules containing 10-20 random amino acids presented on a constant protein scaffold. Furthermore, an HPV16 E7 short hairpin RNA (shRNA) was successfully used to induce degradation of E6 and E7 and proteins. Silencing of E6 resulted in the accumulation of p53 and p21 and that of E7 led to an increase in the hypophosphorylated and active species of pRb. These effects of E6 and E7 ceased cell proliferation and induced apoptosis in HPV positive but not HPV negative cancer cells (Sima et al., 2008). p97 promoter-targeting small interfering RNA (siRNA) has also been used to successfully induce E6 and E7 gene silencing of HPV in cervical cancer cells as well as xenograft mouse models via an increase and accompanying decrease in p53 and p21 levels, respectively (Zhou et al., 2012). RNAi with E7 siRNA was seen to be more anti-proliferative when compared to the E6 siRNA in HPV16 positive cervical cancer cells, indicating that E7 might be more favourable therapeutic target for HPV16 positive cervical cancers (Jiang and Milner, 2002). HPV18 E7 siRNA was also shown to be more effective in the supression of cell proliferation and induction of apoptosis due to to inhibition of both both E6 and E7 transcriptions (Lea et al., 2007) . Whereas E6 siRNA was observed having little effect on E7 expression. However, use of RNAi technology has some drawback due to unspecific binding of siRNAs to non-target mRNAs as well as low efficiency of liposomes in carrying RNA molecules in to the nucleus. This could be overcome by using alternative ways of delivery such as virus-like particles or lentiviruses encoding for E7 shRNA, which was shown to be greatly inhibiting cell proliferation in HPV positive cervical cancer cells (Bousarghin et al., 2009). Alternatively, antisense gene expression for E7, cloned in a retrovirus, in CaSki cells was also shown to reduce tumourogenicity via reducing the level of E7 accompanied by up-regulation and downregulation of pRb and E2F-1, respectively (Choo et al., 2000).

The pRb family of proteins (pRb, p130 and p107) are involved in cell differentiation, growth and apoptosis (Zhang et al., 2006). pRb acts as inhibitor of activating E2F1-3 promoters, whereas p130 and p107 associate with the repressor promoters E2F5 and E2F4 (Section 1.2.4.2). HPV E7 protein binds pRb through LXCXE motif in the CR2 domain, leading to the release of E2F promoters followed by the activation of E2F-responsive genes (Section 1.2.4.2). It is suggested that the lack of pRb can cause an increase in E2F activity, resulting in the increased levels expression of p107, which might possibly be a compensation for the loss of pRb (Sage et al., 2003). It can be suggested that p107 may function as a back up when pRb is depleted. Therfore, p107 expression could also be analysed in cervical cancer cells in the presence or absence of aptamers. Effects of aptamers on the activation or inhibition of E2F-responsive genes can also be studied by luciferase assays using reporter plasmid constructs consisting of wild-type or mutant forms of E2F promoter (e.g. E2F1) region followed by a luciferase gene. Such construct was designed during this project and is available for future use.

In Chapter 3, western blot analysis of HeLa cells expressing HPV18 E7 transfected with HPV16 E7 aptamers showed that some of the aptamers (in particular A1 and J1) may be cross-reacting with HPV18 E7. In this perspective, HPV18 and also low-risk HPV11 E7 was succesfully cloned into GST plasmids and their expressions were achieved in *E. coli.* There were several attempts to use these recombinant E7 proteins in pull-down assays with pRb in the presence or absence of aptamers. However, this system needs to be optimised. Cross-specificity of HPV16 E7 aptamers to HPV11 or 18 E7 could be analysed by *in vitro* binding assays as previously described (Nicol et al., 2011, Robinson et al., 2006). This method involves the immobilization of GST-E7 onto GST-coated glutathione beads and incubation with [γ-^{32}P]-ATP radiolabeled-RNA aptamers. Scintillation counting is then performed to quantitate the amount of aptamer bound, and calculation of apparent binding affinity K_{Dapp} is as previously described (Ellingham et al., 2006, Nicol et al., 2011, Robinson et al., 2006). An alternative approach to the scintillation counting may be an electrophoreticmobility shift assay (EMSA) where electrophoretic separation of a protein-DNA or protein-RNA complexes was performed on an acrylamide or agarose gel. SELEX protocol can also be applied for the selection of aptamers against HPV18 E7 due to the fact that organotypic raft cultures are well-estabilished for the studies of HPV18 life-cycle. As a future prospect, primary keratinocytes transduced with HPV16 can be stratified into organotypic raft systems that better represent a skin model. Aptamers can be delivered to this systems passively as suggested in Chapter 5 or by e.g. particle-

mediated RNA transfer (gene gun). W12 cell line represents a model of early HPV16 infection. This cell line is immortalised by HPV16 and contains around 100 copies of HPV DNA as extrachromosomal episomes (Stanley et al., 1989). These cells can be used as a model system as they represent early stages of cervical cancer (CIN1).

The anatomical advantage of cervical cancer gives a great advantage to local treatments, such as intratumoral or topical applications of theraupetic agents (Sections 1.2.3 and 1.2.5). An example of this was the study where inhibition of tumour growth was observed following siRNA microinjection that was combined with atelocollagen (Fujii et al., 2006) which is a purified type I collagen obtained by pepsin treatment of calf dermis and used in order to enhance cellular uptake and nuclease resistance of siRNAs. There are therapeutic HPV E7 vaccines in clinical trials that are being administired by lipid based formulations or the use of gene guns into target tissues (Section 1.2.5). Therefore, HPV16 E7 targeting aptamer A2 with further modifications could also be utilised as potential therapeutic in order to abrogate the proliferation of cervical cancer cells by topical application. However, HPV16 E7 aptamer A2 produced by *in vitro* transcription was shown to stimulate the production of interferon probably by RIG-I activation in section 3.4.2.2. However, de-phosphorylation of the aptamer seemed to reduce this effect. The similar effect was observed when a control aptamer, SF1 was utilised (Belyaeva et al., 2014). Activation of RIG-I leads to apoptosis through interferon-dependent and independent pathways (Besch et al., 2009, Poeck et al., 2008), providing aptamers potentially with an additional anti-tumour activity. This needs to be considered if aptamers will be used in clinical trials. As stated above, having 5' immunostimulatory effects, as well as sequence specific silencing effects on protein levels, may be advantageous by inducing innate immunity especially production of type I IFNs as well as resulting in apoptosis of the target cells. This could also be disadvantageous due to possible systemic adverse effects when administered intravenously such as by chemotherapy. However, specific delivery of aptamers directly into tumours might overcome this serious side effects of aptamers. In addition, *in vitro* transcribed aptamers could be replaced by synthetic chemically synthesised aptamers which contains 5' – OH instead of 5' triphosphate group. In addition, chemically synthesised RNA may also have further advantages over RNA generated by *in vitro* transcription (Schlee et al., 2009b). These synthetic RNAs are purer, base composition at the 5` triphosphate can easily be modified with preferred nucleosides, adenosine or guanine, additional modifications could be performed and biological activity of these synthetic RNAs would possibly be higher than *in vitro* transcribed RNAs. Therefore, these synthetic

oligonucleotides might present better theraupetics for future treatments of cancers and viral infections.

Administration of aptamers for extracellular proteins or membrane proteins can be mediated intravenously or subcutaneously. These aptamers are of use in drug delivery experiments where vectors or nanoparticles are engineered to carry these molecules to target specific cell types such as cancer cells (Que-Gewirth and Sullenger, 2007). Aptamers can also target the dermis when applied onto skin topically. Such an example is that of a modified DNA aptamer to target an extracellular upstream mediator of psoriasis, called the LL37 peptide which has been shown to transport into the dermis following topical use on mouse murine skin model (Jackson and Gilliet, 2013). This modification of the aptamer was performed as previously described where they modified antisense oligonucleotides with the use of 5-propynyl-2'-deoxycytidine-5'-triphosphate, which facilitated the entry of the oligonucleotides into psoriatic but not normal skin after topical administration (White et al., 2002). Later studies (Dokka et al., 2005) suggested that the possible route of penetration could be through hair follicles upon topical application of fluoro-tagged 2'-O-methoxyethyl-modified oligonucleotides on hairless murine skin by cream-based formulations. In Chapter 5, it was shown that model aptamers can be internalised into keratinocytes without the need for lipofection. This novel ability of aptamers can be advantageous in terms of developing novel potential therapeutics. Reagent-free internalisation of aptamer may be passive (in the case of 21-2) or active (47tr) by micropinocytosis or receptor-mediated endocytosis, respectively. Although this needs to be verified with more experiments such as the use of other inhibitors including cytochalasin D (an inhibitor for actin polymerisation) and oligomycin (an inhibitor to ATPase) to determine if uptake of aptamers is dependent on actin movement (that is important in macropinocytosis) and is also energy-dependent (indicating the receptor-mediated uptake), respectively. Another way to inhibit energy-dependent endocytosis of molecules is the cold incubation. When the incubation of aptamers 21-2 and 47tr with cells was performed in cold (4°C) instead of 37°C, uptake of 21-2 appeared to be unaffected while that of 47tr appeared to be blocked, suggesting an energy-dependent uptake mechanism for the latter. A variety of non-cancer or cancer cell types can be tested to determine whether there is any preference for uptake of 21-2 into one cell type over others. Fluoro-labelled HPV16 E7 aptamer A2 can be used for future experiments to study the uptake mechanisms of aptamers in the presence or absence of transfection reagents. An alternative to lipofection, nanoparticle-based transfection e.g. using Nanocin can be used as apossible delivery reagents for

aptamers although the pathway of entry into cells by this method is unknown. Several inhibitors for endocytosis and also co-localisation with some endosomal markers can be performed to reveal the fate of aptamers following internalisation by Nanocin. If they use a different entry mechanism than lipofection, this mode of entry might be advantages over lipid-based transfection. Lipofection has some disadvantages as molecules can accumulate in endosomes or lysosomes, following the entry, with only small proportion of them can manage to escape from these compartments. Aptamers that can use different mechanisms for internalisation into cells could be better therapeutics. As a future prospect, aptamers such as 21-2 might be used to generate chimeric aptamers together with some of HPV16 E7 aptamers, which might facilitate the entry of E7 aptamers into cervical cancer cells and tissues.

This study showed that aptamers could be used as molecular tools in order to investigate protein-protein interactions *in vitro* and in cells. In particular, some of the HPV16 E7 aptamers were shown to result in a decrease in E7 levels and in the induction of apoptosis in HPV16 transformed cervical cancer cells probably in pRb-dependent pathways. In the work described here, an aptamer was shown to internalise into cells by passive uptake (possibly by macropinocytosis). Therefore, aptamers can be potential candidates for the development of novel therapeutics and diagnostics.

7 REFERENCES

ABBAS, Y. M., PICHLMAIR, A., GORNA, M. W., SUPERTI-FURGA, G. & NAGAR, B. 2013. Structural basis for viral 5'-PPP-RNA recognition by human IFIT proteins. *Nature,* 494**,** 60-4.

ABDULKARIM, B., SABRI, S., DEUTSCH, E., CHAGRAOUI, H., MAGGIORELLA, L., THIERRY, J., ESCHWEGE, F., VAINCHENKER, W., CHOUAIB, S. & BOURHIS, J. 2002. Antiviral agent Cidofovir restores p53 function and enhances the radiosensitivity in HPV-associated cancers. *Oncogene,* 21**,** 2334-46.

ACCARDI, L., DONA, M. G., MILEO, A. M., PAGGI, M. G., FEDERICO, A., TORRERI, P., PETRUCCI, T. C., ACCARDI, R., PIM, D., TOMMASINO, M., BANKS, L., CHIRULLO, B. & GIORGI, C. 2011. Retinoblastoma-independent antiproliferative activity of novel intracellular antibodies against the E7 oncoprotein in HPV 16-positive cells. *BMC Cancer,* 11**,** 17.

ACCARDI, L., PAOLINI, F., MANDARINO, A., PERCARIO, Z., DI BONITO, P., DI CARLO, V., AFFABRIS, E., GIORGI, C., AMICI, C. & VENUTI, A. 2014. In vivo antitumor effect of an intracellular single-chain antibody fragment against the E7 oncoprotein of human papillomavirus 16. *Int J Cancer,* 134**,** 2742-7.

AHUJA, D., SAENZ-ROBLES, M. T. & PIPAS, J. M. 2005. SV40 large T antigen targets multiple cellular pathways to elicit cellular transformation. *Oncogene,* 24**,** 7729-45.

AKIRA, S., UEMATSU, S. & TAKEUCHI, O. 2006. Pathogen recognition and innate immunity. *Cell,* 124**,** 783-801.

ALEXOPOULOU, L., HOLT, A. C., MEDZHITOV, R. & FLAVELL, R. A. 2001. Recognition of double-stranded RNA and activation of NF-kappaB by Toll-like receptor 3. *Nature,* 413**,** 732-8.

ALIBOLANDI, M., ABNOUS, K., RAMEZANI, M., HOSSEINKHANI, H. & HADIZADEH, F. 2014. Synthesis of AS1411-aptamer-conjugated CdTe quantum dots with high fluorescence strength for probe labeling tumor cells. *J Fluoresc,* 24**,** 1519-29.

ALONSO, L. G., GARCIA-ALAI, M. M., NADRA, A. D., LAPENA, A. N., ALMEIDA, F. L., GUALFETTI, P. & PRAT-GAY, G. D. 2002. High-risk (HPV16) human papillomavirus E7 oncoprotein is highly stable and extended, with conformational transitions that could explain its multiple cellular binding partners. *Biochemistry,* 41**,** 10510-8.

ALONSO, L. G., GARCIA-ALAI, M. M., SMAL, C., CENTENO, J. M., IACONO, R., CASTANO, E., GUALFETTI, P. & DE PRAT-GAY, G. 2004. The HPV16 E7 viral oncoprotein self-assembles into defined spherical oligomers. *Biochemistry,* 43**,** 3310-7.

ANDREI, G., SNOECK, R., PIETTE, J., DELVENNE, P. & DE CLERCQ, E. 1998. Antiproliferative effects of acyclic nucleoside phosphonates on human papillomavirus (HPV)-harboring cell lines compared with HPV-negative cell lines. *Oncol Res,* 10**,** 523-31.

ANDREOLA, M. L., PILEUR, F., CALMELS, C., VENTURA, M., TARRAGO-LITVAK, L., TOULME, J. J. & LITVAK, S. 2001. DNA aptamers selected against the HIV-1 RNase H display in vitro antiviral activity. *Biochemistry,* 40**,** 10087-94.

ANGELO, M. G., ZIMA, J., TAVARES DA SILVA, F., BARIL, L. & ARELLANO, F. 2014. Post-licensure safety surveillance for human papillomavirus-16/18-AS04-adjuvanted vaccine: more than 4 years of experience. *Pharmacoepidemiol Drug Saf,* 23**,** 456-65.

ARAMAKI, Y., TAKANO, S. & TSUCHIYA, S. 1999. Induction of apoptosis in macrophages by cationic liposomes. *FEBS Lett,* 460**,** 472-6.

ARMSTRONG, D. J. & ROMAN, A. 1993. The anomalous electrophoretic behavior of the human papillomavirus type 16 E7 protein is due to the high content of acidic amino acid residues. *Biochem Biophys Res Commun,* 192**,** 1380-7.

BADARACCO, G., VENUTI, A., SEDATI, A. & MARCANTE, M. L. 2002. HPV16 and HPV18 in genital tumors: Significantly different levels of viral integration and correlation to tumor invasiveness. *J Med Virol,* 67**,** 574-82.

BAKER, C. C., PHELPS, W. C., LINDGREN, V., BRAUN, M. J., GONDA, M. A. & HOWLEY, P. M. 1987. Structural and transcriptional analysis of human papillomavirus type 16 sequences in cervical carcinoma cell lines. *J Virol,* 61**,** 962-71.

BALSITIS, S. J., SAGE, J., DUENSING, S., MUNGER, K., JACKS, T. & LAMBERT, P. F. 2003. Recapitulation of the effects of the human papillomavirus type 16 E7 oncogene on mouse epithelium by somatic Rb deletion and detection of pRb-independent effects of E7 in vivo. *Mol Cell Biol,* 23**,** 9094-103.

BARBOSA, M. S., EDMONDS, C., FISHER, C., SCHILLER, J. T., LOWY, D. R. & VOUSDEN, K. H. 1990. The region of the HPV E7 oncoprotein homologous to adenovirus E1a and Sv40 large T antigen contains separate domains for Rb binding and casein kinase II phosphorylation. *EMBO J,* 9**,** 153-60.

BARFOD, A., PERSSON, T. & LINDH, J. 2009. In vitro selection of RNA aptamers against a conserved region of the Plasmodium falciparum erythrocyte membrane protein 1. *Parasitol Res,* 105**,** 1557-66.

BARREAU, C., DUTERTRE, S., PAILLARD, L. & OSBORNE, H. B. 2006. Liposome-mediated RNA transfection should be used with caution. *RNA,* 12**,** 1790-3.

BARROW-LAING, L., CHEN, W. & ROMAN, A. 2010. Low- and high-risk human papillomavirus E7 proteins regulate p130 differently. *Virology,* 400**,** 233-9.

BARTEK, J., BARTKOVA, J. & LUKAS, J. 1997. The retinoblastoma protein pathway in cell cycle control and cancer. *Exp Cell Res,* 237**,** 1-6.

BASNER-TSCHAKARJAN, E., MIRMOHAMMADSADEGH, A., BAER, A. & HENGGE, U. R. 2004. Uptake and trafficking of DNA in keratinocytes: evidence for DNA-binding proteins. *Gene Ther,* 11**,** 765-74.

BATES, P. J., KAHLON, J. B., THOMAS, S. D., TRENT, J. O. & MILLER, D. M. 1999. Antiproliferative activity of G-rich oligonucleotides correlates with protein binding. *J Biol Chem,* 274**,** 26369-77.

BATES, P. J., LABER, D. A., MILLER, D. M., THOMAS, S. D. & TRENT, J. O. 2009. Discovery and development of the G-rich oligonucleotide AS1411 as a novel treatment for cancer. *Exp Mol Pathol,* 86**,** 151-64.

BEASLEY, R. P., HWANG, L. Y., LIN, C. C. & CHIEN, C. S. 1981. Hepatocellular carcinoma and hepatitis B virus. A prospective study of 22 707 men in Taiwan. *Lancet,* 2**,** 1129-33.

BECKER, R. C. & CHAN, M. Y. 2009. REG-1, a regimen comprising RB-006, a Factor IXa antagonist, and its oligonucleotide active control agent RB-007 for the potential treatment of arterial thrombosis. *Curr Opin Mol Ther,* 11**,** 707-15.

BEIGELMAN, L., MATULIC-ADAMIC, J., HAEBERLI, P., USMAN, N., DONG, B., SILVERMAN, R. H., KHAMNEI, S. & TORRENCE, P. F. 1995. Synthesis and biological activities of a phosphorodithioate analog of 2',5'-oligoadenylate. *Nucleic Acids Res,* 23**,** 3989-94.

BELLECAVE, P., CAZENAVE, C., RUMI, J., STAEDEL, C., COSNEFROY, O., ANDREOLA, M. L., VENTURA, M., TARRAGO-LITVAK, L. & ASTIER-GIN, T. 2008. Inhibition of hepatitis C virus (HCV) RNA polymerase by DNA aptamers: mechanism of inhibition of in vitro RNA synthesis and effect on HCV-infected cells. *Antimicrob Agents Chemother,* 52**,** 2097-110.

BELMOKHTAR, C. A., HILLION, J. & SEGAL-BENDIRDJIAN, E. 2001. Staurosporine induces apoptosis through both caspase-dependent and caspase-independent mechanisms. *Oncogene,* 20**,** 3354-62.
BELYAEVA, T. A., NICOL, C., CESUR, O., TRAVE, G., BLAIR, G. E. & STONEHOUSE, N. J. 2014. An RNA Aptamer Targets the PDZ-Binding Motif of the HPV16 E6 Oncoprotein. *Cancers (Basel),* 6**,** 1553-69.
BERGANT MARUSIC, M., OZBUN, M. A., CAMPOS, S. K., MYERS, M. P. & BANKS, L. 2012. Human papillomavirus L2 facilitates viral escape from late endosomes via sorting nexin 17. *Traffic,* 13**,** 455-67.
BERNARD, H. U., BURK, R. D., CHEN, Z., VAN DOORSLAER, K., ZUR HAUSEN, H. & DE VILLIERS, E. M. 2010. Classification of papillomaviruses (PVs) based on 189 PV types and proposal of taxonomic amendments. *Virology,* 401**,** 70-9.
BESCH, R., POECK, H., HOHENAUER, T., SENFT, D., HACKER, G., BERKING, C., HORNUNG, V., ENDRES, S., RUZICKA, T., ROTHENFUSSER, S. & HARTMANN, G. 2009. Proapoptotic signaling induced by RIG-I and MDA-5 results in type I interferon-independent apoptosis in human melanoma cells. *J Clin Invest,* 119**,** 2399-411.
BIESECKER, G., DIHEL, L., ENNEY, K. & BENDELE, R. A. 1999. Derivation of RNA aptamer inhibitors of human complement C5. *Immunopharmacology,* 42**,** 219-30.
BIROCCIO, A., HAMM, J., INCITTI, I., DE FRANCESCO, R. & TOMEI, L. 2002. Selection of RNA aptamers that are specific and high-affinity ligands of the hepatitis C virus RNA-dependent RNA polymerase. *J Virol,* 76**,** 3688-96.
BLUMBERG, B. S., LAROUZE, B., LONDON, W. T., WERNER, B., HESSER, J. E., MILLMAN, I., SAIMOT, G. & PAYET, M. 1975. The relation of infection with the hepatitis B agent to primary hepatic carcinoma. *Am J Pathol,* 81**,** 669-82.
BOCHTLER, M., DITZEL, L., GROLL, M., HARTMANN, C. & HUBER, R. 1999. The proteasome. *Annu Rev Biophys Biomol Struct,* 28**,** 295-317.
BOCK, L. C., GRIFFIN, L. C., LATHAM, J. A., VERMAAS, E. H. & TOOLE, J. J. 1992. Selection of single-stranded DNA molecules that bind and inhibit human thrombin. *Nature,* 355**,** 564-6.
BOLDEN, J. E., PEART, M. J. & JOHNSTONE, R. W. 2006. Anticancer activities of histone deacetylase inhibitors. *Nat Rev Drug Discov,* 5**,** 769-84.
BOSCH, F. X., LORINCZ, A., MUNOZ, N., MEIJER, C. J. & SHAH, K. V. 2002. The causal relation between human papillomavirus and cervical cancer. *J Clin Pathol,* 55**,** 244-65.
BOUCHARD, P. R., HUTABARAT, R. M. & THOMPSON, K. M. 2010. Discovery and development of therapeutic aptamers. *Annu Rev Pharmacol Toxicol,* 50**,** 237-57.
BOUKAMP, P., PETRUSSEVSKA, R. T., BREITKREUTZ, D., HORNUNG, J., MARKHAM, A. & FUSENIG, N. E. 1988. Normal keratinization in a spontaneously immortalized aneuploid human keratinocyte cell line. *J Cell Biol,* 106**,** 761-71.
BOURGO, R. J., BRADEN, W. A., WELLS, S. I. & KNUDSEN, E. S. 2009. Activation of the retinoblastoma tumor suppressor mediates cell cycle inhibition and cell death in specific cervical cancer cell lines. *Mol Carcinog,* 48**,** 45-55.
BOUSARGHIN, L., TOUZE, A., GAUD, G., IOCHMANN, S., ALVAREZ, E., REVERDIAU, P., GAITAN, J., JOURDAN, M. L., SIZARET, P. Y. & COURSAGET, P. L. 2009. Inhibition of cervical cancer cell growth by human papillomavirus virus-like particles packaged with human papillomavirus oncoprotein short hairpin RNAs. *Mol Cancer Ther,* 8**,** 357-65.
BOUSARGHIN, L., TOUZE, A., SIZARET, P. Y. & COURSAGET, P. 2003. Human papillomavirus types 16, 31, and 58 use different endocytosis pathways to enter cells. *J Virol,* 77**,** 3846-50.

BOWIE, A. G. & UNTERHOLZNER, L. 2008. Viral evasion and subversion of pattern-recognition receptor signalling. *Nat Rev Immunol,* 8**,** 911-22.
BOYER, S. N., WAZER, D. E. & BAND, V. 1996. E7 protein of human papilloma virus-16 induces degradation of retinoblastoma protein through the ubiquitin-proteasome pathway. *Cancer Res,* 56**,** 4620-4.
BREHM, A., MISKA, E. A., MCCANCE, D. J., REID, J. L., BANNISTER, A. J. & KOUZARIDES, T. 1998. Retinoblastoma protein recruits histone deacetylase to repress transcription. *Nature,* 391**,** 597-601.
BREHM, A., NIELSEN, S. J., MISKA, E. A., MCCANCE, D. J., REID, J. L., BANNISTER, A. J. & KOUZARIDES, T. 1999. The E7 oncoprotein associates with Mi2 and histone deacetylase activity to promote cell growth. *EMBO J,* 18**,** 2449-58.
BUCK, C. B., CHENG, N., THOMPSON, C. D., LOWY, D. R., STEVEN, A. C., SCHILLER, J. T. & TRUS, B. L. 2008. Arrangement of L2 within the papillomavirus capsid. *J Virol,* 82**,** 5190-7.
BURMEISTER, P. E., LEWIS, S. D., SILVA, R. F., PREISS, J. R., HORWITZ, L. R., PENDERGRAST, P. S., MCCAULEY, T. G., KURZ, J. C., EPSTEIN, D. M., WILSON, C. & KEEFE, A. D. 2005. Direct in vitro selection of a 2'-O-methyl aptamer to VEGF. *Chem Biol,* 12**,** 25-33.
BUTEL, J. S. 2000. Viral carcinogenesis: revelation of molecular mechanisms and etiology of human disease. *Carcinogenesis,* 21**,** 405-26.
CAMPO, M. S., GRAHAM, S. V., CORTESE, M. S., ASHRAFI, G. H., ARAIBI, E. H., DORNAN, E. S., MINERS, K., NUNES, C. & MAN, S. 2010. HPV-16 E5 down-regulates expression of surface HLA class I and reduces recognition by CD8 T cells. *Virology,* 407**,** 137-42.
CAO, Z., TONG, R., MISHRA, A., XU, W., WONG, G. C., CHENG, J. & LU, Y. 2009. Reversible cell-specific drug delivery with aptamer-functionalized liposomes. *Angew Chem Int Ed Engl,* 48**,** 6494-8.
CAROTHERS, J. M., OESTREICH, S. C. & SZOSTAK, J. W. 2006. Aptamers selected for higher-affinity binding are not more specific for the target ligand. *J Am Chem Soc,* 128**,** 7929-37.
CASAGRANDE, R., STERN, P., DIEHN, M., SHAMU, C., OSARIO, M., ZUNIGA, M., BROWN, P. O. & PLOEGH, H. 2000. Degradation of proteins from the ER of S. cerevisiae requires an intact unfolded protein response pathway. *Mol Cell,* 5**,** 729-35.
CHAE, H. J., KANG, J. S., BYUN, J. O., HAN, K. S., KIM, D. U., OH, S. M., KIM, H. M., CHAE, S. W. & KIM, H. R. 2000. Molecular mechanism of staurosporine-induced apoptosis in osteoblasts. *Pharmacol Res,* 42**,** 373-81.
CHAN, H. M., SMITH, L. & LA THANGUE, N. B. 2001. Role of LXCXE motif-dependent interactions in the activity of the retinoblastoma protein. *Oncogene,* 20**,** 6152-63.
CHANG, J. T., KUO, T. F., CHEN, Y. J., CHIU, C. C., LU, Y. C., LI, H. F., SHEN, C. R. & CHENG, A. J. 2010. Highly potent and specific siRNAs against E6 or E7 genes of HPV16- or HPV18-infected cervical cancers. *Cancer Gene Ther,* 17**,** 827-36.
CHANG, Y., CESARMAN, E., PESSIN, M. S., LEE, F., CULPEPPER, J., KNOWLES, D. M. & MOORE, P. S. 1994. Identification of herpesvirus-like DNA sequences in AIDS-associated Kaposi's sarcoma. *Science,* 266**,** 1865-9.
CHARDONNET, Y., LIZARD, G., CHIGNOL, M. C. & SCHMITT, D. 1995. Analytical methods for evaluation on whole cells of human papillomavirus infection. *Bull Cancer,* 82**,** 107-13.
CHELLAPPAN, S., KRAUS, V. B., KROGER, B., MUNGER, K., HOWLEY, P. M., PHELPS, W. C. & NEVINS, J. R. 1992. Adenovirus E1A, simian virus 40 tumor antigen, and human papillomavirus E7 protein share the capacity to

disrupt the interaction between transcription factor E2F and the retinoblastoma gene product. *Proc Natl Acad Sci U S A,* 89**,** 4549-53.
CHELLISERRYKATTIL, J. & ELLINGTON, A. D. 2004. Evolution of a T7 RNA polymerase variant that transcribes 2'-O-methyl RNA. *Nat Biotechnol,* 22**,** 1155-60.
CHEN, C. H., CHERNIS, G. A., HOANG, V. Q. & LANDGRAF, R. 2003. Inhibition of heregulin signaling by an aptamer that preferentially binds to the oligomeric form of human epidermal growth factor receptor-3. *Proc Natl Acad Sci U S A,* 100**,** 9226-31.
CHEN, X., QIAN, Y., YAN, F., TU, J., YANG, X., XING, Y. & CHEN, Z. 2013. 5'-triphosphate-siRNA activates RIG-I-dependent type I interferon production and enhances inhibition of hepatitis B virus replication in HepG2.2.15 cells. *Eur J Pharmacol,* 721**,** 86-95.
CHI, H. & FLAVELL, R. A. 2008. Innate recognition of non-self nucleic acids. *Genome Biol,* 9**,** 211.
CHIANTORE, M. V., VANNUCCHI, S., ACCARDI, R., TOMMASINO, M., PERCARIO, Z. A., VACCARI, G., AFFABRIS, E., FIORUCCI, G. & ROMEO, G. 2012. Interferon-beta induces cellular senescence in cutaneous human papilloma virus-transformed human keratinocytes by affecting p53 transactivating activity. *PLoS One,* 7**,** e36909.
CHOO, C. K., LING, M. T., SUEN, C. K., CHAN, K. W. & KWONG, Y. L. 2000. Retrovirus-mediated delivery of HPV16 E7 antisense RNA inhibited tumorigenicity of CaSki cells. *Gynecol Oncol,* 78**,** 293-301.
CHOU, C. W. & CHEN, C. C. 2008. HDAC inhibition upregulates the expression of angiostatic ADAMTS1. *FEBS Lett,* 582**,** 4059-65.
CHOU, T. F., BROWN, S. J., MINOND, D., NORDIN, B. E., LI, K., JONES, A. C., CHASE, P., PORUBSKY, P. R., STOLTZ, B. M., SCHOENEN, F. J., PATRICELLI, M. P., HODDER, P., ROSEN, H. & DESHAIES, R. J. 2011. Reversible inhibitor of p97, DBeQ, impairs both ubiquitin-dependent and autophagic protein clearance pathways. *Proc Natl Acad Sci U S A,* 108**,** 4834-9.
CHU, T. C., TWU, K. Y., ELLINGTON, A. D. & LEVY, M. 2006. Aptamer mediated siRNA delivery. *Nucleic Acids Res,* 34**,** e73.
CIBIEL, A., PESTOURIE, C. & DUCONGE, F. 2012. In vivo uses of aptamers selected against cell surface biomarkers for therapy and molecular imaging. *Biochimie,* 94**,** 1595-606.
CIECHANOVER, A. 2005. Proteolysis: from the lysosome to ubiquitin and the proteasome. *Nat Rev Mol Cell Biol,* 6**,** 79-87.
CLASSON, M. & DYSON, N. 2001. p107 and p130: versatile proteins with interesting pockets. *Exp Cell Res,* 264**,** 135-47.
CLEMENTS, A., JOHNSTON, K., MAZZARELLI, J. M., RICCIARDI, R. P. & MARMORSTEIN, R. 2000. Oligomerization properties of the viral oncoproteins adenovirus E1A and human papillomavirus E7 and their complexes with the retinoblastoma protein. *Biochemistry,* 39**,** 16033-45.
CLIFFORD, G., FRANCESCHI, S., DIAZ, M., MUNOZ, N. & VILLA, L. L. 2006. Chapter 3: HPV type-distribution in women with and without cervical neoplastic diseases. *Vaccine,* 24 Suppl 3**,** S3/26-34.
CLOUTIER, N. & FLAMAND, L. 2010. Kaposi sarcoma-associated herpesvirus latency-associated nuclear antigen inhibits interferon (IFN) beta expression by competing with IFN regulatory factor-3 for binding to IFNB promoter. *J Biol Chem,* 285**,** 7208-21.
COGLIANO, V., BAAN, R., STRAIF, K., GROSSE, Y., SECRETAN, B., EL GHISSASSI, F. & CANCER, W. H. O. I. A. F. R. O. 2005. Carcinogenicity of human papillomaviruses. *Lancet Oncol,* 6**,** 204.

COGOI, S. & XODO, L. E. 2006. G-quadruplex formation within the promoter of the KRAS proto-oncogene and its effect on transcription. *Nucleic Acids Res,* 34**,** 2536-49.
CONNER, S. D. & SCHMID, S. L. 2003. Regulated portals of entry into the cell. *Nature,* 422**,** 37-44.
CORDEN, S. A., SANT-CASSIA, L. J., EASTON, A. J. & MORRIS, A. G. 1999. The integration of HPV-18 DNA in cervical carcinoma. *Mol Pathol,* 52**,** 275-82.
CRAIU, A., GACZYNSKA, M., AKOPIAN, T., GRAMM, C. F., FENTEANY, G., GOLDBERG, A. L. & ROCK, K. L. 1997. Lactacystin and clasto-lactacystin beta-lactone modify multiple proteasome beta-subunits and inhibit intracellular protein degradation and major histocompatibility complex class I antigen presentation. *J Biol Chem,* 272**,** 13437-45.
CROSS, B. C., MCKIBBIN, C., CALLAN, A. C., ROBOTI, P., PIACENTI, M., RABU, C., WILSON, C. M., WHITEHEAD, R., FLITSCH, S. L., POOL, M. R., HIGH, S. & SWANTON, E. 2009. Eeyarestatin I inhibits Sec61-mediated protein translocation at the endoplasmic reticulum. *J Cell Sci,* 122**,** 4393-400.
CUI, S., EISENACHER, K., KIRCHHOFER, A., BRZOZKA, K., LAMMENS, A., LAMMENS, K., FUJITA, T., CONZELMANN, K. K., KRUG, A. & HOPFNER, K. P. 2008. The C-terminal regulatory domain is the RNA 5'-triphosphate sensor of RIG-I. *Mol Cell,* 29**,** 169-79.
CULP, T. D., BUDGEON, L. R., MARINKOVICH, M. P., MENEGUZZI, G. & CHRISTENSEN, N. D. 2006. Keratinocyte-secreted laminin 5 can function as a transient receptor for human papillomaviruses by binding virions and transferring them to adjacent cells. *J Virol,* 80**,** 8940-50.
DANTUR, K., ALONSO, L., CASTANO, E., MORELLI, L., CENTENO-CROWLEY, J. M., VIGHI, S. & DE PRAT-GAY, G. 2009. Cytosolic accumulation of HPV16 E7 oligomers supports different transformation routes for the prototypic viral oncoprotein: the amyloid-cancer connection. *Int J Cancer,* 125**,** 1902-11.
DAPIC, V., ABDOMEROVIC, V., MARRINGTON, R., PEBERDY, J., RODGER, A., TRENT, J. O. & BATES, P. J. 2003. Biophysical and biological properties of quadruplex oligodeoxyribonucleotides. *Nucleic Acids Res,* 31**,** 2097-107.
DAVIES, R., HICKS, R., CROOK, T., MORRIS, J. & VOUSDEN, K. 1993. Human papillomavirus type 16 E7 associates with a histone H1 kinase and with p107 through sequences necessary for transformation. *J Virol,* 67**,** 2521-8.
DAVY, C. E., JACKSON, D. J., WANG, Q., RAJ, K., MASTERSON, P. J., FENNER, N. F., SOUTHERN, S., CUTHILL, S., MILLAR, J. B. & DOORBAR, J. 2002. Identification of a G(2) arrest domain in the E1 wedge E4 protein of human papillomavirus type 16. *J Virol,* 76**,** 9806-18.
DE SANJOSE, S., QUINT, W. G., ALEMANY, L., GERAETS, D. T., KLAUSTERMEIER, J. E., LLOVERAS, B., TOUS, S., FELIX, A., BRAVO, L. E., SHIN, H. R., VALLEJOS, C. S., DE RUIZ, P. A., LIMA, M. A., GUIMERA, N., CLAVERO, O., ALEJO, M., LLOMBART-BOSCH, A., CHENG-YANG, C., TATTI, S. A., KASAMATSU, E., ILJAZOVIC, E., ODIDA, M., PRADO, R., SEOUD, M., GRCE, M., USUBUTUN, A., JAIN, A., SUAREZ, G. A., LOMBARDI, L. E., BANJO, A., MENENDEZ, C., DOMINGO, E. J., VELASCO, J., NESSA, A., CHICHAREON, S. C., QIAO, Y. L., LERMA, E., GARLAND, S. M., SASAGAWA, T., FERRERA, A., HAMMOUDA, D., MARIANI, L., PELAYO, A., STEINER, I., OLIVA, E., MEIJER, C. J., AL-JASSAR, W. F., CRUZ, E., WRIGHT, T. C., PURAS, A., LLAVE, C. L., TZARDI, M., AGORASTOS, T., GARCIA-BARRIOLA, V., CLAVEL, C., ORDI, J., ANDUJAR, M., CASTELLSAGUE, X., SANCHEZ, G. I., NOWAKOWSKI, A. M., BORNSTEIN, J., MUNOZ, N., BOSCH, F. X., RETROSPECTIVE INTERNATIONAL, S. & GROUP, H. P. V. T. T. S. 2010. Human papillomavirus genotype attribution in invasive cervical cancer: a retrospective cross-sectional worldwide study. *Lancet Oncol,* 11**,** 1048-56.

DECAPRIO, J. A. 2014. Human papillomavirus type 16 E7 perturbs DREAM to promote cellular proliferation and mitotic gene expression. *Oncogene,* 33**,** 4036-8.
DECAPRIO, J. A., LUDLOW, J. W., FIGGE, J., SHEW, J. Y., HUANG, C. M., LEE, W. H., MARSILIO, E., PAUCHA, E. & LIVINGSTON, D. M. 1988. SV40 large tumor antigen forms a specific complex with the product of the retinoblastoma susceptibility gene. *Cell,* 54**,** 275-83.
DELEAVEY, G. F., WATTS, J. K., ALAIN, T., ROBERT, F., KALOTA, A., AISHWARYA, V., PELLETIER, J., GEWIRTZ, A. M., SONENBERG, N. & DAMHA, M. J. 2010. Synergistic effects between analogs of DNA and RNA improve the potency of siRNA-mediated gene silencing. *Nucleic Acids Res,* 38**,** 4547-57.
DELURY, C. P., MARSH, E. K., JAMES, C. D., BOON, S. S., BANKS, L., KNIGHT, G. L. & ROBERTS, S. 2013. The role of protein kinase A regulation of the E6 PDZ-binding domain during the differentiation-dependent life cycle of human papillomavirus type 18. *J Virol,* 87**,** 9463-72.
DERKAY, C. S. 1995. Task force on recurrent respiratory papillomas. A preliminary report. *Arch Otolaryngol Head Neck Surg,* 121**,** 1386-91.
DESAINTES, C., GOYAT, S., GARBAY, S., YANIV, M. & THIERRY, F. 1999. Papillomavirus E2 induces p53-independent apoptosis in HeLa cells. *Oncogene,* 18**,** 4538-45.
DESHAIES, R. J. 1999. SCF and Cullin/Ring H2-based ubiquitin ligases. *Annu Rev Cell Dev Biol,* 15**,** 435-67.
DEY, A. K., GRIFFITHS, C., LEA, S. M. & JAMES, W. 2005a. Structural characterization of an anti-gp120 RNA aptamer that neutralizes R5 strains of HIV-1. *RNA,* 11**,** 873-84.
DEY, A. K., KHATI, M., TANG, M., WYATT, R., LEA, S. M. & JAMES, W. 2005b. An aptamer that neutralizes R5 strains of human immunodeficiency virus type 1 blocks gp120-CCR5 interaction. *J Virol,* 79**,** 13806-10.
DIENER, J. L., DANIEL LAGASSE, H. A., DUERSCHMIED, D., MERHI, Y., TANGUAY, J. F., HUTABARAT, R., GILBERT, J., WAGNER, D. D. & SCHAUB, R. 2009. Inhibition of von Willebrand factor-mediated platelet activation and thrombosis by the anti-von Willebrand factor A1-domain aptamer ARC1779. *J Thromb Haemost,* 7**,** 1155-62.
DILLNER, J., ARBYN, M., UNGER, E. & DILLNER, L. 2011. Monitoring of human papillomavirus vaccination. *Clin Exp Immunol,* 163**,** 17-25.
DOBLE, R., MCDERMOTT, M. F., CESUR, O., STONEHOUSE, N. J. & WITTMANN, M. 2014. IL-17A RNA aptamer: possible therapeutic potential in some cells, more than we bargained for in others? *J Invest Dermatol,* 134**,** 852-5.
DOCHEZ, C., BOGERS, J. J., VERHELST, R. & REES, H. 2014. HPV vaccines to prevent cervical cancer and genital warts: an update. *Vaccine,* 32**,** 1595-601.
DOHERTY, G. J. & MCMAHON, H. T. 2009. Mechanisms of endocytosis. *Annu Rev Biochem,* 78**,** 857-902.
DOKKA, S., COOPER, S. R., KELLY, S., HARDEE, G. E. & KARRAS, J. G. 2005. Dermal delivery of topically applied oligonucleotides via follicular transport in mouse skin. *J Invest Dermatol,* 124**,** 971-5.
DOMINSKA, M. & DYKXHOORN, D. M. 2010. Breaking down the barriers: siRNA delivery and endosome escape. *J Cell Sci,* 123**,** 1183-9.
DOORBAR, J., ELY, S., STERLING, J., MCLEAN, C. & CRAWFORD, L. 1991. Specific interaction between HPV-16 E1-E4 and cytokeratins results in collapse of the epithelial cell intermediate filament network. *Nature,* 352**,** 824-7.

DOORBAR, J., QUINT, W., BANKS, L., BRAVO, I. G., STOLER, M., BROKER, T. R. & STANLEY, M. A. 2012. The biology and life-cycle of human papillomaviruses. *Vaccine,* 30 Suppl 5**,** F55-70.
DOWHANICK, J. J., MCBRIDE, A. A. & HOWLEY, P. M. 1995. Suppression of cellular proliferation by the papillomavirus E2 protein. *J Virol,* 69**,** 7791-9.
DREIER, K., SCHEIDEN, R., LENER, B., EHEHALT, D., PIRCHER, H., MULLER-HOLZNER, E., ROSTEK, U., KAISER, A., FIEDLER, M., RESSLER, S., LECHNER, S., WIDSCHWENDTER, A., EVEN, J., CAPESIUS, C., JANSEN-DURR, P. & ZWERSCHKE, W. 2011. Subcellular localization of the human papillomavirus 16 E7 oncoprotein in CaSki cells and its detection in cervical adenocarcinoma and adenocarcinoma in situ. *Virology,* 409**,** 54-68.
DUA, P., KANG, H. S., HONG, S. M., TSAO, M. S., KIM, S. & LEE, D. K. 2013. Alkaline phosphatase ALPPL-2 is a novel pancreatic carcinoma-associated protein. *Cancer Res,* 73**,** 1934-45.
DUAN, X., PONOMAREVA, L., VEERANKI, S., PANCHANATHAN, R., DICKERSON, E. & CHOUBEY, D. 2011. Differential roles for the interferon-inducible IFI16 and AIM2 innate immune sensors for cytosolic DNA in cellular senescence of human fibroblasts. *Mol Cancer Res,* 9**,** 589-602.
DUNAIEF, J. L., STROBER, B. E., GUHA, S., KHAVARI, P. A., ALIN, K., LUBAN, J., BEGEMANN, M., CRABTREE, G. R. & GOFF, S. P. 1994. The retinoblastoma protein and BRG1 form a complex and cooperate to induce cell cycle arrest. *Cell,* 79**,** 119-30.
DUXBURY, M. S., ASHLEY, S. W. & WHANG, E. E. 2005. RNA interference: a mammalian SID-1 homologue enhances siRNA uptake and gene silencing efficacy in human cells. *Biochem Biophys Res Commun,* 331**,** 459-63.
DYSON, N. 1998. The regulation of E2F by pRB-family proteins. *Genes Dev,* 12**,** 2245-62.
DYSON, N., GUIDA, P., MUNGER, K. & HARLOW, E. 1992. Homologous sequences in adenovirus E1A and human papillomavirus E7 proteins mediate interaction with the same set of cellular proteins. *J Virol,* 66**,** 6893-902.
DYSON, N., HOWLEY, P. M., MUNGER, K. & HARLOW, E. 1989. The human papilloma virus-16 E7 oncoprotein is able to bind to the retinoblastoma gene product. *Science,* 243**,** 934-7.
EINSTEIN, M. H., BARON, M., LEVIN, M. J., CHATTERJEE, A., EDWARDS, R. P., ZEPP, F., CARLETTI, I., DESSY, F. J., TROFA, A. F., SCHUIND, A., DUBIN, G. & GROUP, H. P. V. S. 2009. Comparison of the immunogenicity and safety of Cervarix and Gardasil human papillomavirus (HPV) cervical cancer vaccines in healthy women aged 18-45 years. *Hum Vaccin,* 5**,** 705-19.
EL AWADY, M. K., KAPLAN, J. B., O'BRIEN, S. J. & BURK, R. D. 1987. Molecular analysis of integrated human papillomavirus 16 sequences in the cervical cancer cell line SiHa. *Virology,* 159**,** 389-98.
ELIYAHU, H., SERVEL, N., DOMB, A. J. & BARENHOLZ, Y. 2002. Lipoplex-induced hemagglutination: potential involvement in intravenous gene delivery. *Gene Ther,* 9**,** 850-8.
ELLINGHAM, M., BUNKA, D. H., ROWLANDS, D. J. & STONEHOUSE, N. J. 2006. Selection and characterization of RNA aptamers to the RNA-dependent RNA polymerase from foot-and-mouth disease virus. *RNA,* 12**,** 1970-9.
ENGELS, E. A., PFEIFFER, R. M., GOEDERT, J. J., VIRGO, P., MCNEEL, T. S., SCOPPA, S. M., BIGGAR, R. J. & STUDY, H. A. C. M. 2006. Trends in cancer risk among people with AIDS in the United States 1980-2002. *AIDS,* 20**,** 1645-54.

EPSTEIN, M. A., HENLE, G., ACHONG, B. G. & BARR, Y. M. 1965. Morphological and Biological Studies on a Virus in Cultured Lymphoblasts from Burkitt's Lymphoma. *J Exp Med,* 121**,** 761-70.
ERALES, J. & COFFINO, P. 2014. Ubiquitin-independent proteasomal degradation. *Biochim Biophys Acta,* 1843**,** 216-21.
EULBERG, D. & KLUSSMANN, S. 2003. Spiegelmers: biostable aptamers. *Chembiochem,* 4**,** 979-83.
EVANDER, M., FRAZER, I. H., PAYNE, E., QI, Y. M., HENGST, K. & MCMILLAN, N. A. 1997. Identification of the alpha6 integrin as a candidate receptor for papillomaviruses. *J Virol,* 71**,** 2449-56.
EWEN, M. E., SLUSS, H. K., SHERR, C. J., MATSUSHIME, H., KATO, J. & LIVINGSTON, D. M. 1993. Functional interactions of the retinoblastoma protein with mammalian D-type cyclins. *Cell,* 73**,** 487-97.
EYETECH STUDY, G. 2002. Preclinical and phase 1A clinical evaluation of an anti-VEGF pegylated aptamer (EYE001) for the treatment of exudative age-related macular degeneration. *Retina,* 22**,** 143-52.
EYETECH STUDY, G. 2003. Anti-vascular endothelial growth factor therapy for subfoveal choroidal neovascularization secondary to age-related macular degeneration: phase II study results. *Ophthalmology,* 110**,** 979-86.
FAROKHZAD, O. C., CHENG, J., TEPLY, B. A., SHERIFI, I., JON, S., KANTOFF, P. W., RICHIE, J. P. & LANGER, R. 2006. Targeted nanoparticle-aptamer bioconjugates for cancer chemotherapy in vivo. *Proc Natl Acad Sci U S A,* 103**,** 6315-20.
FAY, A., YUTZY, W. H. T., RODEN, R. B. & MOROIANU, J. 2004. The positively charged termini of L2 minor capsid protein required for bovine papillomavirus infection function separately in nuclear import and DNA binding. *J Virol,* 78**,** 13447-54.
FEHRMANN, F. & LAIMINS, L. A. 2003. Human papillomaviruses: targeting differentiating epithelial cells for malignant transformation. *Oncogene,* 22**,** 5201-7.
FEINBERG, E. H. & HUNTER, C. P. 2003. Transport of dsRNA into cells by the transmembrane protein SID-1. *Science,* 301**,** 1545-7.
FELSANI, A., MILEO, A. M. & PAGGI, M. G. 2006. Retinoblastoma family proteins as key targets of the small DNA virus oncoproteins. *Oncogene,* 25**,** 5277-85.
FENG, G. & KAPLOWITZ, N. 2002. Mechanism of staurosporine-induced apoptosis in murine hepatocytes. *Am J Physiol Gastrointest Liver Physiol,* 282**,** G825-34.
FENG, H., SHUDA, M., CHANG, Y. & MOORE, P. S. 2008. Clonal integration of a polyomavirus in human Merkel cell carcinoma. *Science,* 319**,** 1096-100.
FERNANDES, A. P., GONCALVES, M. A., DUARTE, G., CUNHA, F. Q., SIMOES, R. T. & DONADI, E. A. 2005. HPV16, HPV18, and HIV infection may influence cervical cytokine intralesional levels. *Virology,* 334**,** 294-8.
FIRZLAFF, J. M., GALLOWAY, D. A., EISENMAN, R. N. & LUSCHER, B. 1989. The E7 protein of human papillomavirus type 16 is phosphorylated by casein kinase II. *New Biol,* 1**,** 44-53.
FOGH, J., FOGH, J. M. & ORFEO, T. 1977. One hundred and twenty-seven cultured human tumor cell lines producing tumors in nude mice. *J Natl Cancer Inst,* 59**,** 221-6.
FORREST, S., LEAR, Z., HEROD, M. R., RYAN, M., ROWLANDS, D. J. & STONEHOUSE, N. J. 2014. Inhibition of the foot-and-mouth disease virus subgenomic replicon by RNA aptamers. *J Gen Virol,* 95**,** 2649-57.
FRIBORG, J., JR., KONG, W., HOTTIGER, M. O. & NABEL, G. J. 1999. p53 inhibition by the LANA protein of KSHV protects against cell death. *Nature,* 402**,** 889-94.

FUJII, T., SAITO, M., IWASAKI, E., OCHIYA, T., TAKEI, Y., HAYASHI, S., ONO, A., HIRAO, N., NAKAMURA, M., KUBUSHIRO, K., TSUKAZAKI, K. & AOKI, D. 2006. Intratumor injection of small interfering RNA-targeting human papillomavirus 18 E6 and E7 successfully inhibits the growth of cervical cancer. *Int J Oncol,* 29**,** 541-8.

FUMOTO, S., NISHI, J., ISHII, H., WANG, X., MIYAMOTO, H., YOSHIKAWA, N., NAKASHIMA, M., NAKAMURA, J. & NISHIDA, K. 2009. Rac-mediated macropinocytosis is a critical route for naked plasmid DNA transfer in mice. *Mol Pharm,* 6**,** 1170-9.

GAMMOH, N., GRM, H. S., MASSIMI, P. & BANKS, L. 2006. Regulation of human papillomavirus type 16 E7 activity through direct protein interaction with the E2 transcriptional activator. *J Virol,* 80**,** 1787-97.

GAO, Y. S., HUBBERT, C. C., LU, J., LEE, Y. S., LEE, J. Y. & YAO, T. P. 2007. Histone deacetylase 6 regulates growth factor-induced actin remodeling and endocytosis. *Mol Cell Biol,* 27**,** 8637-47.

GARCIA-ALAI, M. M., ALONSO, L. G. & DE PRAT-GAY, G. 2007. The N-terminal module of HPV16 E7 is an intrinsically disordered domain that confers conformational and recognition plasticity to the oncoprotein. *Biochemistry,* 46**,** 10405-12.

GARG, M., KANOJIA, D., SAINI, S., SURI, S., GUPTA, A., SUROLIA, A. & SURI, A. 2010. Germ cell-specific heat shock protein 70-2 is expressed in cervical carcinoma and is involved in the growth, migration, and invasion of cervical cells. *Cancer,* 116**,** 3785-96.

GARNETT, T. O. & DUERKSEN-HUGHES, P. J. 2006. Modulation of apoptosis by human papillomavirus (HPV) oncoproteins. *Arch Virol,* 151**,** 2321-35.

GILBERT, J. C., DEFEO-FRAULINI, T., HUTABARAT, R. M., HORVATH, C. J., MERLINO, P. G., MARSH, H. N., HEALY, J. M., BOUFAKHREDDINE, S., HOLOHAN, T. V. & SCHAUB, R. G. 2007. First-in-human evaluation of anti von Willebrand factor therapeutic aptamer ARC1779 in healthy volunteers. *Circulation,* 116**,** 2678-86.

GIROGLOU, T., FLORIN, L., SCHAFER, F., STREECK, R. E. & SAPP, M. 2001. Human papillomavirus infection requires cell surface heparan sulfate. *J Virol,* 75**,** 1565-70.

GIRVAN, A. C., TENG, Y., CASSON, L. K., THOMAS, S. D., JULIGER, S., BALL, M. W., KLEIN, J. B., PIERCE, W. M., JR., BARVE, S. S. & BATES, P. J. 2006. AGRO100 inhibits activation of nuclear factor-kappaB (NF-kappaB) by forming a complex with NF-kappaB essential modulator (NEMO) and nucleolin. *Mol Cancer Ther,* 5**,** 1790-9.

GITLIN, L., BARCHET, W., GILFILLAN, S., CELLA, M., BEUTLER, B., FLAVELL, R. A., DIAMOND, M. S. & COLONNA, M. 2006. Essential role of mda-5 in type I IFN responses to polyriboinosinic:polyribocytidylic acid and encephalomyocarditis picornavirus. *Proc Natl Acad Sci U S A,* 103**,** 8459-64.

GOLDBERG, A. L. 2003. Protein degradation and protection against misfolded or damaged proteins. *Nature,* 426**,** 895-9.

GOMEZ-OUTES, A., SUAREZ-GEA, M. L., LECUMBERRI, R., ROCHA, E., POZO-HERNANDEZ, C. & VARGAS-CASTRILLON, E. 2011. New parenteral anticoagulants in development. *Ther Adv Cardiovasc Dis,* 5**,** 33-59.

GONZALEZ, G., PFANNES, L., BRAZAS, R. & STRIKER, R. 2007. Selection of an optimal RNA transfection reagent and comparison to electroporation for the delivery of viral RNA. *J Virol Methods,* 145**,** 14-21.

GONZALEZ, S. L., STREMLAU, M., HE, X., BASILE, J. R. & MUNGER, K. 2001. Degradation of the retinoblastoma tumor suppressor by the human papillomavirus type 16 E7 oncoprotein is important for functional inactivation and is separable from proteasomal degradation of E7. *J Virol,* 75**,** 7583-91.

GOODWIN, E. C. & DIMAIO, D. 2000. Repression of human papillomavirus oncogenes in HeLa cervical carcinoma cells causes the orderly reactivation of dormant tumor suppressor pathways. *Proc Natl Acad Sci U S A,* 97**,** 12513-8.
GOODWIN, E. C., YANG, E., LEE, C. J., LEE, H. W., DIMAIO, D. & HWANG, E. S. 2000. Rapid induction of senescence in human cervical carcinoma cells. *Proc Natl Acad Sci U S A,* 97**,** 10978-83.
GOPINATH, S. C., MISONO, T. S., KAWASAKI, K., MIZUNO, T., IMAI, M., ODAGIRI, T. & KUMAR, P. K. 2006. An RNA aptamer that distinguishes between closely related human influenza viruses and inhibits haemagglutinin-mediated membrane fusion. *J Gen Virol,* 87**,** 479-87.
GOURRONC, F. A., ROCKEY, W. M., THIEL, W. H., GIANGRANDE, P. H. & KLINGELHUTZ, A. J. 2013. Identification of RNA aptamers that internalize into HPV-16 E6/E7 transformed tonsillar epithelial cells. *Virology,* 446**,** 325-33.
GRAHAM, J. C. & ZARBL, H. 2012. Use of cell-SELEX to generate DNA aptamers as molecular probes of HPV-associated cervical cancer cells. *PLoS One,* 7**,** e36103.
GRANT, B. D. & DONALDSON, J. G. 2009. Pathways and mechanisms of endocytic recycling. *Nat Rev Mol Cell Biol,* 10**,** 597-608.
GREEN, K. L., BROWN, C., ROEDER, G. E., SOUTHGATE, T. D. & GASTON, K. 2007. A cancer cell-specific inducer of apoptosis. *Hum Gene Ther,* 18**,** 547-61.
GREEN, L. S., JELLINEK, D., JENISON, R., OSTMAN, A., HELDIN, C. H. & JANJIC, N. 1996. Inhibitory DNA ligands to platelet-derived growth factor B-chain. *Biochemistry,* 35**,** 14413-24.
GRIFFIN, L. C., TIDMARSH, G. F., BOCK, L. C., TOOLE, J. J. & LEUNG, L. L. 1993. In vivo anticoagulant properties of a novel nucleotide-based thrombin inhibitor and demonstration of regional anticoagulation in extracorporeal circuits. *Blood,* 81**,** 3271-6.
GRUNBERG-MANAGO, M. 1967. Polynucleotide phosphorylase: structure and mechanism of action. *Biochem J,* 103**,** 62P.
GUO, N. & PENG, Z. 2013. MG132, a proteasome inhibitor, induces apoptosis in tumor cells. *Asia Pac J Clin Oncol,* 9**,** 6-11.
HALL, A. H. & ALEXANDER, K. A. 2003. RNA interference of human papillomavirus type 18 E6 and E7 induces senescence in HeLa cells. *J Virol,* 77**,** 6066-9.
HAN, R., CLADEL, N. M., REED, C. A. & CHRISTENSEN, N. D. 1998. Characterization of transformation function of cottontail rabbit papillomavirus E5 and E8 genes. *Virology,* 251**,** 253-63.
HAO, R., NANDURI, P., RAO, Y., PANICHELLI, R. S., ITO, A., YOSHIDA, M. & YAO, T. P. 2013. Proteasomes activate aggresome disassembly and clearance by producing unanchored ubiquitin chains. *Mol Cell,* 51**,** 819-28.
HARDING, H. P., ZHANG, Y. & RON, D. 1999. Protein translation and folding are coupled by an endoplasmic-reticulum-resident kinase. *Nature,* 397**,** 271-4.
HEALY, J. M., LEWIS, S. D., KURZ, M., BOOMER, R. M., THOMPSON, K. M., WILSON, C. & MCCAULEY, T. G. 2004. Pharmacokinetics and biodistribution of novel aptamer compositions. *Pharm Res,* 21**,** 2234-46.
HECK, D. V., YEE, C. L., HOWLEY, P. M. & MUNGER, K. 1992. Efficiency of binding the retinoblastoma protein correlates with the transforming capacity of the E7 oncoproteins of the human papillomaviruses. *Proc Natl Acad Sci U S A,* 89**,** 4442-6.
HELLNER, K. & MUNGER, K. 2011. Human papillomaviruses as therapeutic targets in human cancer. *J Clin Oncol,* 29**,** 1785-94.

HELT, A. M. & GALLOWAY, D. A. 2003. Mechanisms by which DNA tumor virus oncoproteins target the Rb family of pocket proteins. *Carcinogenesis,* 24**,** 159-69.
HENICS, T. & ZIMMER, C. 2006. RNA delivery by heat shock protein-70 into mammalian cells: a preliminary study. *Cell Biol Int,* 30**,** 480-4.
HERMONAT, P. L., SANTIN, A. D. & ZHAN, D. 2000. Binding of the human papillomavirus type 16 E7 oncoprotein and the adeno-associated virus Rep78 major regulatory protein in vitro and in yeast and the potential for downstream effects. *J Hum Virol,* 3**,** 113-24.
HICKE, B. J., MARION, C., CHANG, Y. F., GOULD, T., LYNOTT, C. K., PARMA, D., SCHMIDT, P. G. & WARREN, S. 2001. Tenascin-C aptamers are generated using tumor cells and purified protein. *J Biol Chem,* 276**,** 48644-54.
HICKE, B. J. & STEPHENS, A. W. 2000. Escort aptamers: a delivery service for diagnosis and therapy. *J Clin Invest,* 106**,** 923-8.
HILLEMAN, M. R. & WERNER, J. H. 1954. Recovery of new agent from patients with acute respiratory illness. *Proc Soc Exp Biol Med,* 85**,** 183-8.
HOFMANN, H. P., LIMMER, S., HORNUNG, V. & SPRINZL, M. 1997. Ni2+-binding RNA motifs with an asymmetric purine-rich internal loop and a G-A base pair. *RNA,* 3**,** 1289-300.
HOMANN, M. & GORINGER, H. U. 2001. Uptake and intracellular transport of RNA aptamers in African trypanosomes suggest therapeutic "piggy-back" approach. *Bioorg Med Chem,* 9**,** 2571-80.
HORNUNG, V., ELLEGAST, J., KIM, S., BRZOZKA, K., JUNG, A., KATO, H., POECK, H., AKIRA, S., CONZELMANN, K. K., SCHLEE, M., ENDRES, S. & HARTMANN, G. 2006. 5'-Triphosphate RNA is the ligand for RIG-I. *Science,* 314**,** 994-7.
HSUEH, P. R. 2009. Human papillomavirus, genital warts, and vaccines. *J Microbiol Immunol Infect,* 42**,** 101-6.
HUANG, D. B., VU, D., CASSIDAY, L. A., ZIMMERMAN, J. M., MAHER, L. J., 3RD & GHOSH, G. 2003. Crystal structure of NF-kappaB (p50)2 complexed to a high-affinity RNA aptamer. *Proc Natl Acad Sci U S A,* 100**,** 9268-73.
HUANG, H., SUSLOV, N. B., LI, N. S., SHELKE, S. A., EVANS, M. E., KOLDOBSKAYA, Y., RICE, P. A. & PICCIRILLI, J. A. 2014. A G-quadruplex-containing RNA activates fluorescence in a GFP-like fluorophore. *Nat Chem Biol,* 10**,** 686-91.
HUANG, Y., CHEN, X., DUAN, N., WU, S., WANG, Z., WEI, X. & WANG, Y. 2015. Selection and characterization of DNA aptamers against Staphylococcus aureus enterotoxin C1. *Food Chem,* 166**,** 623-9.
HUANG, Y., ECKSTEIN, F., PADILLA, R. & SOUSA, R. 1997. Mechanism of ribose 2'-group discrimination by an RNA polymerase. *Biochemistry,* 36**,** 8231-42.
HUBBERT, N. L., SEDMAN, S. A. & SCHILLER, J. T. 1992. Human papillomavirus type 16 E6 increases the degradation rate of p53 in human keratinocytes. *J Virol,* 66**,** 6237-41.
HUGHES, F. J. & ROMANOS, M. A. 1993. E1 protein of human papillomavirus is a DNA helicase/ATPase. *Nucleic Acids Res,* 21**,** 5817-23.
HUH, K., ZHOU, X., HAYAKAWA, H., CHO, J. Y., LIBERMANN, T. A., JIN, J., HARPER, J. W. & MUNGER, K. 2007. Human papillomavirus type 16 E7 oncoprotein associates with the cullin 2 ubiquitin ligase complex, which contributes to degradation of the retinoblastoma tumor suppressor. *J Virol,* 81**,** 9737-47.
HUH, K. W., DEMASI, J., OGAWA, H., NAKATANI, Y., HOWLEY, P. M. & MUNGER, K. 2005. Association of the human papillomavirus type 16 E7 oncoprotein with the 600-kDa retinoblastoma protein-associated factor, p600. *Proc Natl Acad Sci U S A,* 102**,** 11492-7.

HUIBREGTSE, J. M., SCHEFFNER, M. & HOWLEY, P. M. 1991. A cellular protein mediates association of p53 with the E6 oncoprotein of human papillomavirus types 16 or 18. *EMBO J,* 10**,** 4129-35.
HUIBREGTSE, J. M., SCHEFFNER, M. & HOWLEY, P. M. 1993. Cloning and expression of the cDNA for E6-AP, a protein that mediates the interaction of the human papillomavirus E6 oncoprotein with p53. *Mol Cell Biol,* 13**,** 775-84.
HUMANS, I. W. G. O. T. E. O. C. R. T. 2007. Human papillomaviruses. *IARC Monogr Eval Carcinog Risks Hum,* 90**,** 1-636.
HWANG, S. Y., SUN, H. Y., LEE, K. H., OH, B. H., CHA, Y. J., KIM, B. H. & YOO, J. Y. 2012. 5'-Triphosphate-RNA-independent activation of RIG-I via RNA aptamer with enhanced antiviral activity. *Nucleic Acids Res,* 40**,** 2724-33.
IRESON, C. R. & KELLAND, L. R. 2006. Discovery and development of anticancer aptamers. *Mol Cancer Ther,* 5**,** 2957-62.
ISHIGURO, A., AKIYAMA, T., ADACHI, H., INOUE, J. & NAKAMURA, Y. 2011. Therapeutic potential of anti-interleukin-17A aptamer: suppression of interleukin-17A signaling and attenuation of autoimmunity in two mouse models. *Arthritis Rheum,* 63**,** 455-66.
IWATA, A., RILEY, B. E., JOHNSTON, J. A. & KOPITO, R. R. 2005. HDAC6 and microtubules are required for autophagic degradation of aggregated huntingtin. *J Biol Chem,* 280**,** 40282-92.
JACKSON, G. W. & GILLIET, M. 2013. Topical DNA aptamers to the antimicrobial peptide LL37 for the potential treatment of psoriasis. *Aptamers in Medicine and Perspectives, Naples, Italy*.
JAVIER, R. T. & BUTEL, J. S. 2008. The history of tumor virology. *Cancer Res,* 68**,** 7693-706.
JENSEN, K., ANDERSON, J. A. & GLASS, E. J. 2014. Comparison of small interfering RNA (siRNA) delivery into bovine monocyte-derived macrophages by transfection and electroporation. *Vet Immunol Immunopathol,* 158**,** 224-32.
JEON, J. H., CHOI, K. H., CHO, S. Y., KIM, C. W., SHIN, D. M., KWON, J. C., SONG, K. Y., PARK, S. C. & KIM, I. G. 2003. Transglutaminase 2 inhibits Rb binding of human papillomavirus E7 by incorporating polyamine. *EMBO J,* 22**,** 5273-82.
JEON, S. H., KAYHAN, B., BEN-YEDIDIA, T. & ARNON, R. 2004. A DNA aptamer prevents influenza infection by blocking the receptor binding region of the viral hemagglutinin. *Journal of Biological Chemistry,* 279**,** 48410-48419.
JIANG, M. & MILNER, J. 2002. Selective silencing of viral gene expression in HPV-positive human cervical carcinoma cells treated with siRNA, a primer of RNA interference. *Oncogene,* 21**,** 6041-8.
JOHNSON, J. A. & GANGEMI, J. D. 2000. Quantitative immunodetection of viral oncoprotein levels in human papillomavirus-transformed human cells. *Methods Mol Med,* 24**,** 361-4.
JONES, E. E. & WELLS, S. I. 2006. Cervical cancer and human papillomaviruses: inactivation of retinoblastoma and other tumor suppressor pathways. *Curr Mol Med,* 6**,** 795-808.
KAHN, J. A., BROWN, D. R., DING, L., WIDDICE, L. E., SHEW, M. L., GLYNN, S. & BERNSTEIN, D. I. 2012. Vaccine-type human papillomavirus and evidence of herd protection after vaccine introduction. *Pediatrics,* 130**,** e249-56.
KAMEYAMA, S., HORIE, M., KIKUCHI, T., OMURA, T., TADOKORO, A., TAKEUCHI, T., NAKASE, I., SUGIURA, Y. & FUTAKI, S. 2007. Acid wash in determining cellular uptake of Fab/cell-permeating peptide conjugates. *Biopolymers,* 88**,** 98-107.
KAMPER, N., DAY, P. M., NOWAK, T., SELINKA, H. C., FLORIN, L., BOLSCHER, J., HILBIG, L., SCHILLER, J. T. & SAPP, M. 2006. A membrane-

destabilizing peptide in capsid protein L2 is required for egress of papillomavirus genomes from endosomes. *J Virol,* 80**,** 759-68.
KANG, J., LEE, M. S., COPLAND, J. A., 3RD, LUXON, B. A. & GORENSTEIN, D. G. 2008. Combinatorial selection of a single stranded DNA thioaptamer targeting TGF-beta1 protein. *Bioorg Med Chem Lett,* 18**,** 1835-9.
KANG, S. W., RANE, N. S., KIM, S. J., GARRISON, J. L., TAUNTON, J. & HEGDE, R. S. 2006. Substrate-specific translocational attenuation during ER stress defines a pre-emptive quality control pathway. *Cell,* 127**,** 999-1013.
KARANAM, B., JAGU, S., HUH, W. K. & RODEN, R. B. 2009. Developing vaccines against minor capsid antigen L2 to prevent papillomavirus infection. *Immunol Cell Biol,* 87**,** 287-99.
KARIKO, K., BHUYAN, P., CAPODICI, J. & WEISSMAN, D. 2004. Small interfering RNAs mediate sequence-independent gene suppression and induce immune activation by signaling through toll-like receptor 3. *J Immunol,* 172**,** 6545-9.
KATO, H., TAKEUCHI, O., MIKAMO-SATOH, E., HIRAI, R., KAWAI, T., MATSUSHITA, K., HIIRAGI, A., DERMODY, T. S., FUJITA, T. & AKIRA, S. 2008. Length-dependent recognition of double-stranded ribonucleic acids by retinoic acid-inducible gene-I and melanoma differentiation-associated gene 5. *J Exp Med,* 205**,** 1601-10.
KATO, H., TAKEUCHI, O., SATO, S., YONEYAMA, M., YAMAMOTO, M., MATSUI, K., UEMATSU, S., JUNG, A., KAWAI, T., ISHII, K. J., YAMAGUCHI, O., OTSU, K., TSUJIMURA, T., KOH, C. S., REIS E SOUSA, C., MATSUURA, Y., FUJITA, T. & AKIRA, S. 2006. Differential roles of MDA5 and RIG-I helicases in the recognition of RNA viruses. *Nature,* 441**,** 101-5.
KATO, Y., MINAKAWA, N., KOMATSU, Y., KAMIYA, H., OGAWA, N., HARASHIMA, H. & MATSUDA, A. 2005. New NTP analogs: the synthesis of 4'-thioUTP and 4'-thioCTP and their utility for SELEX. *Nucleic Acids Res,* 33**,** 2942-51.
KAUR, G. & ROY, I. 2008. Therapeutic applications of aptamers. *Expert Opin Investig Drugs,* 17**,** 43-60.
KAWADA, J., ZOU, P., MAZITSCHEK, R., BRADNER, J. E. & COHEN, J. I. 2009. Tubacin kills Epstein-Barr virus (EBV)-Burkitt lymphoma cells by inducing reactive oxygen species and EBV lymphoblastoid cells by inducing apoptosis. *J Biol Chem,* 284**,** 17102-9.
KAWAGUCHI, Y., KOVACS, J. J., MCLAURIN, A., VANCE, J. M., ITO, A. & YAO, T. P. 2003. The deacetylase HDAC6 regulates aggresome formation and cell viability in response to misfolded protein stress. *Cell,* 115**,** 727-38.
KAWAMURA, T., OGAWA, Y., AOKI, R. & SHIMADA, S. 2014. Innate and intrinsic antiviral immunity in skin. *J Dermatol Sci*.
KEEFE, A. D. & CLOAD, S. T. 2008. SELEX with modified nucleotides. *Curr Opin Chem Biol,* 12**,** 448-56.
KEEFE, A. D., PAI, S. & ELLINGTON, A. 2010. Aptamers as therapeutics. *Nat Rev Drug Discov,* 9**,** 537-50.
KEMP, T. J., HILDESHEIM, A., SAFAEIAN, M., DAUNER, J. G., PAN, Y., PORRAS, C., SCHILLER, J. T., LOWY, D. R., HERRERO, R. & PINTO, L. A. 2011. HPV16/18 L1 VLP vaccine induces cross-neutralizing antibodies that may mediate cross-protection. *Vaccine,* 29**,** 2011-4.
KENNY, E. F. & O'NEILL, L. A. 2008. Signalling adaptors used by Toll-like receptors: an update. *Cytokine,* 43**,** 342-9.
KHATI, M., SCHUMAN, M., IBRAHIM, J., SATTENTAU, Q., GORDON, S. & JAMES, W. 2003. Neutralization of infectivity of diverse R5 clinical isolates of human immunodeficiency virus type 1 by gp120-binding 2'F-RNA aptamers. *J Virol,* 77**,** 12692-8.

KIKIN, O., D'ANTONIO, L. & BAGGA, P. S. 2006. QGRS Mapper: a web-based server for predicting G-quadruplexes in nucleotide sequences. *Nucleic Acids Res,* 34**,** W676-82.

KIKUCHI, K., UMEHARA, T., FUKUDA, K., KUNO, A., HASEGAWA, T. & NISHIKAWA, S. 2005. A hepatitis C virus (HCV) internal ribosome entry site (IRES) domain III-IV-targeted aptamer inhibits translation by binding to an apical loop of domain IIId. *Nucleic Acids Res,* 33**,** 683-92.

KIKUCHI, K., UMEHARA, T., NISHIKAWA, F., FUKUDA, K., HASEGAWA, T. & NISHIKAWA, S. 2009. Increased inhibitory ability of conjugated RNA aptamers against the HCV IRES. *Biochem Biophys Res Commun,* 386**,** 118-23.

KIM, D., JEONG, Y. Y. & JON, S. 2010. A drug-loaded aptamer-gold nanoparticle bioconjugate for combined CT imaging and therapy of prostate cancer. *ACS Nano,* 4**,** 3689-96.

KIM, D. H., LONGO, M., HAN, Y., LUNDBERG, P., CANTIN, E. & ROSSI, J. J. 2004. Interferon induction by siRNAs and ssRNAs synthesized by phage polymerase. *Nat Biotechnol,* 22**,** 321-5.

KIM, E. Y., KIM, J. W., KIM, W. K., HAN, B. S., PARK, S. G., CHUNG, B. H., LEE, S. C. & BAE, K. H. 2014. Selection of aptamers for mature white adipocytes by cell SELEX using flow cytometry. *PLoS One,* 9**,** e97747.

KIM, S. J., KIM, M. Y., LEE, J. H., YOU, J. C. & JEONG, S. 2002. Selection and stabilization of the RNA aptamers against the human immunodeficiency virus type-1 nucleocapsid protein. *Biochem Biophys Res Commun,* 291**,** 925-31.

KISSEL, J. D., HELD, D. M., HARDY, R. W. & BURKE, D. H. 2007. Single-stranded DNA aptamer RT1t49 inhibits RT polymerase and RNase H functions of HIV type 1, HIV type 2, and SIVCPZ RTs. *AIDS Res Hum Retroviruses,* 23**,** 699-708.

KNAPP, A. A., MCMANUS, P. M., BOCKSTALL, K. & MOROIANU, J. 2009. Identification of the nuclear localization and export signals of high risk HPV16 E7 oncoprotein. *Virology,* 383**,** 60-8.

KONG, H. Y. & BYUN, J. 2013. Nucleic Acid aptamers: new methods for selection, stabilization, and application in biomedical science. *Biomol Ther (Seoul),* 21**,** 423-34.

KOTULA, J. W., PRATICO, E. D., MING, X., NAKAGAWA, O., JULIANO, R. L. & SULLENGER, B. A. 2012. Aptamer-mediated delivery of splice-switching oligonucleotides to the nuclei of cancer cells. *Nucleic Acid Ther,* 22**,** 187-95.

KRAWCZYK, E., SUPRYNOWICZ, F. A., SUDARSHAN, S. R. & SCHLEGEL, R. 2010. Membrane orientation of the human papillomavirus type 16 E5 oncoprotein. *J Virol,* 84**,** 1696-703.

KULKARNI, O., EULBERG, D., SELVE, N., ZOLLNER, S., ALLAM, R., PAWAR, R. D., PFEIFFER, S., SEGERER, S., KLUSSMANN, S. & ANDERS, H. J. 2009. Anti-Ccl2 Spiegelmer permits 75% dose reduction of cyclophosphamide to control diffuse proliferative lupus nephritis and pneumonitis in MRL-Fas(lpr) mice. *J Pharmacol Exp Ther,* 328**,** 371-7.

KULKARNI, O., PAWAR, R. D., PURSCHKE, W., EULBERG, D., SELVE, N., BUCHNER, K., NINICHUK, V., SEGERER, S., VIELHAUER, V., KLUSSMANN, S. & ANDERS, H. J. 2007. Spiegelmer inhibition of CCL2/MCP-1 ameliorates lupus nephritis in MRL-(Fas)lpr mice. *J Am Soc Nephrol,* 18**,** 2350-8.

KUNII, T., OGURA, S., MIE, M. & KOBATAKE, E. 2011. Selection of DNA aptamers recognizing small cell lung cancer using living cell-SELEX. *Analyst,* 136**,** 1310-2.

KUWAHARA, M. & SUGIMOTO, N. 2010. Molecular evolution of functional nucleic acids with chemical modifications. *Molecules,* 15**,** 5423-44.

LATHAM, J. A., JOHNSON, R. & TOOLE, J. J. 1994. The application of a modified nucleotide in aptamer selection: novel thrombin aptamers containing 5-(1-pentynyl)-2'-deoxyuridine. *Nucleic Acids Res,* 22**,** 2817-22.
LATO, S. M., OZEROVA, N. D., HE, K., SERGUEEVA, Z., SHAW, B. R. & BURKE, D. H. 2002. Boron-containing aptamers to ATP. *Nucleic Acids Res,* 30**,** 1401-7.
LAURSON, J. & RAJ, K. 2011. Localisation of human papillomavirus 16 E7 oncoprotein changes with cell confluence. *PLoS One,* 6**,** e21501.
LEA, J. S., SUNAGA, N., SATO, M., KALAHASTI, G., MILLER, D. S., MINNA, J. D. & MULLER, C. Y. 2007. Silencing of HPV 18 oncoproteins With RNA interference causes growth inhibition of cervical cancer cells. *Reprod Sci,* 14**,** 20-8.
LEIJA-MONTOYA, A. G., BENITEZ-HESS, M. L., TOSCANO-GARIBAY, J. D. & ALVAREZ-SALAS, L. M. 2014. Characterization of an RNA aptamer against HPV-16 L1 virus-like particles. *Nucleic Acid Ther,* 24**,** 344-55.
LI, L., HOU, J., LIU, X., GUO, Y., WU, Y., ZHANG, L. & YANG, Z. 2014. Nucleolin-targeting liposomes guided by aptamer AS1411 for the delivery of siRNA for the treatment of malignant melanomas. *Biomaterials,* 35**,** 3840-50.
LIANG, H. R., HU, G. Q., LI, L., GAO, Y. W., YANG, S. T. & XIA, X. Z. 2014. Aptamers targeting rabies virus-infected cells inhibit street rabies virus in vivo. *Int Immunopharmacol,* 21**,** 432-8.
LISITSYN, N., LISITSYN, N. & WIGLER, M. 1993. Cloning the differences between two complex genomes. *Science,* 259**,** 946-51.
LIU, C. Y. & KAUFMAN, R. J. 2003. The unfolded protein response. *J Cell Sci,* 116**,** 1861-2.
LIU, J., YANG, Y., HU, B., MA, Z. Y., HUANG, H. P., YU, Y., LIU, S. P., LU, M. J. & YANG, D. L. 2010. Development of HBsAg-binding aptamers that bind HepG2.2.15 cells via HBV surface antigen. *Virol Sin,* 25**,** 27-35.
LIU, X., CLEMENTS, A., ZHAO, K. & MARMORSTEIN, R. 2006. Structure of the human Papillomavirus E7 oncoprotein and its mechanism for inactivation of the retinoblastoma tumor suppressor. *J Biol Chem,* 281**,** 578-86.
LIVAK, K. J. & SCHMITTGEN, T. D. 2001. Analysis of relative gene expression data using real-time quantitative PCR and the 2(-Delta Delta C(T)) Method. *Methods,* 25**,** 402-8.
LONGWORTH, M. S. & LAIMINS, L. A. 2004. Pathogenesis of human papillomaviruses in differentiating epithelia. *Microbiol Mol Biol Rev,* 68**,** 362-72.
LORGER, M., ENGSTLER, M., HOMANN, M. & GORINGER, H. U. 2003. Targeting the variable surface of African trypanosomes with variant surface glycoprotein-specific, serum-stable RNA aptamers. *Eukaryot Cell,* 2**,** 84-94.
LOVE, K. T., MAHON, K. P., LEVINS, C. G., WHITEHEAD, K. A., QUERBES, W., DORKIN, J. R., QIN, J., CANTLEY, W., QIN, L. L., RACIE, T., FRANK-KAMENETSKY, M., YIP, K. N., ALVAREZ, R., SAH, D. W., DE FOUGEROLLES, A., FITZGERALD, K., KOTELIANSKY, V., AKINC, A., LANGER, R. & ANDERSON, D. G. 2010. Lipid-like materials for low-dose, in vivo gene silencing. *Proc Natl Acad Sci U S A,* 107**,** 1864-9.
LU, J. J., LANGER, R. & CHEN, J. 2009. A novel mechanism is involved in cationic lipid-mediated functional siRNA delivery. *Mol Pharm,* 6**,** 763-71.
LUO, Y., BATALAO, A., ZHOU, H. & ZHU, L. 1997. Mammalian two-hybrid system: a complementary approach to the yeast two-hybrid system. *Biotechniques,* 22**,** 350-2.
LUPOLD, S. E., HICKE, B. J., LIN, Y. & COFFEY, D. S. 2002. Identification and characterization of nuclease-stabilized RNA molecules that bind human prostate cancer cells via the prostate-specific membrane antigen. *Cancer Res,* 62**,** 4029-33.

MAASCH, C., BUCHNER, K., EULBERG, D., VONHOFF, S. & KLUSSMANN, S. 2008. Physicochemical stability of NOX-E36, a 40mer L-RNA (Spiegelmer) for therapeutic applications. *Nucleic Acids Symp Ser (Oxf)*, 61-2.
MAGALDI, T. G., ALMSTEAD, L. L., BELLONE, S., PREVATT, E. G., SANTIN, A. D. & DIMAIO, D. 2012. Primary human cervical carcinoma cells require human papillomavirus E6 and E7 expression for ongoing proliferation. *Virology,* 422, 114-24.
MAGEE, W. E. & GRIFFITH, M. J. 1972. The liver as a site for interferon production in response to poly I:poly C. *Life Sci II,* 11, 1081-6.
MAJOR, T., SZARKA, K., SZIKLAI, I., GERGELY, L. & CZEGLEDY, J. 2005. The characteristics of human papillomavirus DNA in head and neck cancers and papillomas. *J Clin Pathol,* 58, 51-5.
MALAGON, T., DROLET, M., BOILY, M. C., FRANCO, E. L., JIT, M., BRISSON, J. & BRISSON, M. 2012. Cross-protective efficacy of two human papillomavirus vaccines: a systematic review and meta-analysis. *Lancet Infect Dis,* 12, 781-9.
MANETTI, R., ANNUNZIATO, F., TOMASEVIC, L., GIANNO, V., PARRONCHI, P., ROMAGNANI, S. & MAGGI, E. 1995. Polyinosinic acid: polycytidylic acid promotes T helper type 1-specific immune responses by stimulating macrophage production of interferon-alpha and interleukin-12. *Eur J Immunol,* 25, 2656-60.
MANNIRONI, C., SCERCH, C., FRUSCOLONI, P. & TOCCHINI-VALENTINI, G. P. 2000. Molecular recognition of amino acids by RNA aptamers: the evolution into an L-tyrosine binder of a dopamine-binding RNA motif. *RNA,* 6, 520-7.
MARTHA LUCÍA, S., ADRIANA, U.-P., DIANA, J. G.-B. & MYRIAM CORRESPONDING AUTHOR, S.-G. 2012. New Biomarkers for Cervical Cancer – Perspectives from the IGF System.
MATHEWS, D. H., SABINA, J., ZUKER, M. & TURNER, D. H. 1999. Expanded sequence dependence of thermodynamic parameters improves prediction of RNA secondary structure. *J Mol Biol,* 288, 911-40.
MATSUOKA, M. & JEANG, K. T. 2011. Human T-cell leukemia virus type 1 (HTLV-1) and leukemic transformation: viral infectivity, Tax, HBZ and therapy. *Oncogene,* 30, 1379-89.
MCEWAN, D. L., WEISMAN, A. S. & HUNTER, C. P. 2012. Uptake of extracellular double-stranded RNA by SID-2. *Mol Cell,* 47, 746-54.
MCINTYRE, M. C., FRATTINI, M. G., GROSSMAN, S. R. & LAIMINS, L. A. 1993. Human papillomavirus type 18 E7 protein requires intact Cys-X-X-Cys motifs for zinc binding, dimerization, and transformation but not for Rb binding. *J Virol,* 67, 3142-50.
MCLAUGHLIN-DRUBIN, M. E. & MUNGER, K. 2009. The human papillomavirus E7 oncoprotein. *Virology,* 384, 335-44.
MCNAMARA, J. O., 2ND, ANDRECHEK, E. R., WANG, Y., VILES, K. D., REMPEL, R. E., GILBOA, E., SULLENGER, B. A. & GIANGRANDE, P. H. 2006. Cell type-specific delivery of siRNAs with aptamer-siRNA chimeras. *Nat Biotechnol,* 24, 1005-15.
MEADE, B. R. & DOWDY, S. F. 2009. The road to therapeutic RNA interference (RNAi): Tackling the 800 pound siRNA delivery gorilla. *Discov Med,* 8, 253-6.
MENAGER, J., EBSTEIN, F., OGER, R., HULIN, P., NEDELLEC, S., DUVERGER, E., LEHMANN, A., KLOETZEL, P. M., JOTEREAU, F. & GUILLOUX, Y. 2014. Cross-presentation of synthetic long peptides by human dendritic cells: a process dependent on ERAD component p97/VCP but Not sec61 and/or Derlin-1. *PLoS One,* 9, e89897.
MI, J., LIU, Y., RABBANI, Z. N., YANG, Z., URBAN, J. H., SULLENGER, B. A. & CLARY, B. M. 2010. In vivo selection of tumor-targeting RNA motifs. *Nat Chem Biol,* 6, 22-4.

MIDDLETON, K., PEH, W., SOUTHERN, S., GRIFFIN, H., SOTLAR, K., NAKAHARA, T., EL-SHERIF, A., MORRIS, L., SETH, R., HIBMA, M., JENKINS, D., LAMBERT, P., COLEMAN, N. & DOORBAR, J. 2003. Organization of human papillomavirus productive cycle during neoplastic progression provides a basis for selection of diagnostic markers. *J Virol,* 77**,** 10186-201.

MINCHEVA, A., GISSMANN, L. & ZUR HAUSEN, H. 1987. Chromosomal integration sites of human papillomavirus DNA in three cervical cancer cell lines mapped by in situ hybridization. *Med Microbiol Immunol,* 176**,** 245-56.

MONGELARD, F. & BOUVET, P. 2010. AS-1411, a guanosine-rich oligonucleotide aptamer targeting nucleolin for the potential treatment of cancer, including acute myeloid leukemia. *Curr Opin Mol Ther,* 12**,** 107-14.

MOORE, P. S. & CHANG, Y. 2010. Why do viruses cause cancer? Highlights of the first century of human tumour virology. *Nat Rev Cancer,* 10**,** 878-89.

MORRISSEY, D. V., LOCKRIDGE, J. A., SHAW, L., BLANCHARD, K., JENSEN, K., BREEN, W., HARTSOUGH, K., MACHEMER, L., RADKA, S., JADHAV, V., VAISH, N., ZINNEN, S., VARGEESE, C., BOWMAN, K., SHAFFER, C. S., JEFFS, L. B., JUDGE, A., MACLACHLAN, I. & POLISKY, B. 2005. Potent and persistent in vivo anti-HBV activity of chemically modified siRNAs. *Nat Biotechnol,* 23**,** 1002-7.

MUNGER, K., WERNESS, B. A., DYSON, N., PHELPS, W. C., HARLOW, E. & HOWLEY, P. M. 1989. Complex formation of human papillomavirus E7 proteins with the retinoblastoma tumor suppressor gene product. *EMBO J,* 8**,** 4099-105.

MUNGER, K., YEE, C. L., PHELPS, W. C., PIETENPOL, J. A., MOSES, H. L. & HOWLEY, P. M. 1991. Biochemical and biological differences between E7 oncoproteins of the high- and low-risk human papillomavirus types are determined by amino-terminal sequences. *J Virol,* 65**,** 3943-8.

NAUENBURG, S., ZWERSCHKE, W. & JANSEN-DURR, P. 2001. Induction of apoptosis in cervical carcinoma cells by peptide aptamers that bind to the HPV-16 E7 oncoprotein. *FASEB J,* 15**,** 592-4.

NEUMANN, E., SCHAEFER-RIDDER, M., WANG, Y. & HOFSCHNEIDER, P. H. 1982. Gene transfer into mouse lyoma cells by electroporation in high electric fields. *EMBO J,* 1**,** 841-5.

NEVINS, J. R. 2001. The Rb/E2F pathway and cancer. *Hum Mol Genet,* 10**,** 699-703.

NG, E. W. & ADAMIS, A. P. 2006. Anti-VEGF aptamer (pegaptanib) therapy for ocular vascular diseases. *Ann N Y Acad Sci,* 1082**,** 151-71.

NG, E. W., SHIMA, D. T., CALIAS, P., CUNNINGHAM, E. T., JR., GUYER, D. R. & ADAMIS, A. P. 2006. Pegaptanib, a targeted anti-VEGF aptamer for ocular vascular disease. *Nat Rev Drug Discov,* 5**,** 123-32.

NGUYEN, M. L., NGUYEN, M. M., LEE, D., GRIEP, A. E. & LAMBERT, P. F. 2003. The PDZ ligand domain of the human papillomavirus type 16 E6 protein is required for E6's induction of epithelial hyperplasia in vivo. *J Virol,* 77**,** 6957-64.

NI, X., ZHANG, Y., RIBAS, J., CHOWDHURY, W. H., CASTANARES, M., ZHANG, Z., LAIHO, M., DEWEESE, T. L. & LUPOLD, S. E. 2011. Prostate-targeted radiosensitization via aptamer-shRNA chimeras in human tumor xenografts. *J Clin Invest,* 121**,** 2383-90.

NICOL, C. January 2011. *Selection and characterisation of RNA aptamers to the human papillomavirus 16 (HPV16) E7 oncoprotein.* Ph.D., University of Leeds.

NICOL, C., BUNKA, D. H., BLAIR, G. E. & STONEHOUSE, N. J. 2011. Effects of single nucleotide changes on the binding and activity of RNA aptamers to

human papillomavirus 16 E7 oncoprotein. *Biochem Biophys Res Commun,* 405**,** 417-21.
NICOL, C., CESUR, O., FORREST, S., BELYAEVA, T. A., BUNKA, D. H., BLAIR, G. E. & STONEHOUSE, N. J. 2013. An RNA aptamer provides a novel approach for the induction of apoptosis by targeting the HPV16 E7 oncoprotein. *PLoS One,* 8**,** e64781.
NIMJEE, S. M., RUSCONI, C. P. & SULLENGER, B. A. 2005. Aptamers: an emerging class of therapeutics. *Annu Rev Med,* 56**,** 555-83.
NISHIMURA, A., NAKAHARA, T., UENO, T., SASAKI, K., YOSHIDA, S., KYO, S., HOWLEY, P. M. & SAKAI, H. 2006. Requirement of E7 oncoprotein for viability of HeLa cells. *Microbes Infect,* 8**,** 984-93.
NOMA, T., IKEBUKURO, K., SODE, K., OHKUBO, T., SAKASEGAWA, Y., HACHIYA, N. & KANEKO, K. 2005. Screening of DNA aptamers against multiple proteins in tissue. *Nucleic Acids Symp Ser (Oxf)***,** 357-8.
NUJIC, K., BANJANAC, M., MUNIC, V., POLANCEC, D. & ERAKOVIC HABER, V. 2012. Impairment of lysosomal functions by azithromycin and chloroquine contributes to anti-inflammatory phenotype. *Cell Immunol,* 279**,** 78-86.
OGANESIAN, L. & BRYAN, T. M. 2007. Physiological relevance of telomeric G-quadruplex formation: a potential drug target. *Bioessays,* 29**,** 155-65.
OH, K. J., KALININA, A., WANG, J., NAKAYAMA, K., NAKAYAMA, K. I. & BAGCHI, S. 2004. The papillomavirus E7 oncoprotein is ubiquitinated by UbcH7 and Cullin 1- and Skp2-containing E3 ligase. *J Virol,* 78**,** 5338-46.
OH, S. T., KYO, S. & LAIMINS, L. A. 2001. Telomerase activation by human papillomavirus type 16 E6 protein: induction of human telomerase reverse transcriptase expression through Myc and GC-rich Sp1 binding sites. *J Virol,* 75**,** 5559-66.
OHLENSCHLAGER, O., SEIBOTH, T., ZENGERLING, H., BRIESE, L., MARCHANKA, A., RAMACHANDRAN, R., BAUM, M., KORBAS, M., MEYER-KLAUCKE, W., DURST, M. & GORLACH, M. 2006. Solution structure of the partially folded high-risk human papilloma virus 45 oncoprotein E7. *Oncogene,* 25**,** 5953-9.
OVERMEYER, J. H., KAUL, A., JOHNSON, E. E. & MALTESE, W. A. 2008. Active ras triggers death in glioblastoma cells through hyperstimulation of macropinocytosis. *Mol Cancer Res,* 6**,** 965-77.
PADILLA, R. & SOUSA, R. 1999. Efficient synthesis of nucleic acids heavily modified with non-canonical ribose 2'-groups using a mutantT7 RNA polymerase (RNAP). *Nucleic Acids Res,* 27**,** 1561-3.
PALLAN, P. S., GREENE, E. M., JICMAN, P. A., PANDEY, R. K., MANOHARAN, M., ROZNERS, E. & EGLI, M. 2011. Unexpected origins of the enhanced pairing affinity of 2'-fluoro-modified RNA. *Nucleic Acids Res,* 39**,** 3482-95.
PARK, H. C., BAIG, I. A., LEE, S. C., MOON, J. Y. & YOON, M. Y. 2014. Development of ssDNA aptamers for the sensitive detection of Salmonella typhimurium and Salmonella enteritidis. *Appl Biochem Biotechnol,* 174**,** 793-802.
PASTOR, F., KOLONIAS, D., GIANGRANDE, P. H. & GILBOA, E. 2010. Induction of tumour immunity by targeted inhibition of nonsense-mediated mRNA decay. *Nature,* 465**,** 227-30.
PEART, M. J., SMYTH, G. K., VAN LAAR, R. K., BOWTELL, D. D., RICHON, V. M., MARKS, P. A., HOLLOWAY, A. J. & JOHNSTONE, R. W. 2005. Identification and functional significance of genes regulated by structurally different histone deacetylase inhibitors. *Proc Natl Acad Sci U S A,* 102**,** 3697-702.
PEI, X., ZHANG, J. & LIU, J. 2014. Clinical applications of nucleic acid aptamers in cancer. *Mol Clin Oncol,* 2**,** 341-348.

PICHLMAIR, A., SCHULZ, O., TAN, C. P., NASLUND, T. I., LILJESTROM, P., WEBER, F. & REIS E SOUSA, C. 2006. RIG-I-mediated antiviral responses to single-stranded RNA bearing 5'-phosphates. *Science,* 314**,** 997-1001.

POECK, H., BESCH, R., MAIHOEFER, C., RENN, M., TORMO, D., MORSKAYA, S. S., KIRSCHNEK, S., GAFFAL, E., LANDSBERG, J., HELLMUTH, J., SCHMIDT, A., ANZ, D., BSCHEIDER, M., SCHWERD, T., BERKING, C., BOURQUIN, C., KALINKE, U., KREMMER, E., KATO, H., AKIRA, S., MEYERS, R., HACKER, G., NEUENHAHN, M., BUSCH, D., RULAND, J., ROTHENFUSSER, S., PRINZ, M., HORNUNG, V., ENDRES, S., TUTING, T. & HARTMANN, G. 2008. 5'-Triphosphate-siRNA: turning gene silencing and Rig-I activation against melanoma. *Nat Med,* 14**,** 1256-63.

PURTILO, D. T., CASSEL, C. K., YANG, J. P. & HARPER, R. 1975. X-linked recessive progressive combined variable immunodeficiency (Duncan's disease). *Lancet,* 1**,** 935-40.

QUE-GEWIRTH, N. S. & SULLENGER, B. A. 2007. Gene therapy progress and prospects: RNA aptamers. *Gene Ther,* 14**,** 283-91.

RADKOV, S. A., KELLAM, P. & BOSHOFF, C. 2000. The latent nuclear antigen of Kaposi sarcoma-associated herpesvirus targets the retinoblastoma-E2F pathway and with the oncogene Hras transforms primary rat cells. *Nat Med,* 6**,** 1121-7.

RAHIMI, F., MURAKAMI, K., SUMMERS, J. L., CHEN, C. H. & BITAN, G. 2009. RNA aptamers generated against oligomeric Abeta40 recognize common amyloid aptatopes with low specificity but high sensitivity. *PLoS One,* 4**,** e7694.

RAJENDRAN, M. & ELLINGTON, A. D. 2008. Selection of fluorescent aptamer beacons that light up in the presence of zinc. *Anal Bioanal Chem,* 390**,** 1067-75.

RAMALINGAM, D., DUCLAIR, S., DATTA, S. A., ELLINGTON, A., REIN, A. & PRASAD, V. R. 2011. RNA aptamers directed to human immunodeficiency virus type 1 Gag polyprotein bind to the matrix and nucleocapsid domains and inhibit virus production. *J Virol,* 85**,** 305-14.

REIKINE, S., NGUYEN, J. B. & MODIS, Y. 2014. Pattern Recognition and Signaling Mechanisms of RIG-I and MDA5. *Front Immunol,* 5**,** 342.

REINSTEIN, E., SCHEFFNER, M., OREN, M., CIECHANOVER, A. & SCHWARTZ, A. 2000. Degradation of the E7 human papillomavirus oncoprotein by the ubiquitin-proteasome system: targeting via ubiquitination of the N-terminal residue. *Oncogene,* 19**,** 5944-50.

REYES-REYES, E. M., TENG, Y. & BATES, P. J. 2010. A new paradigm for aptamer therapeutic AS1411 action: uptake by macropinocytosis and its stimulation by a nucleolin-dependent mechanism. *Cancer Res,* 70**,** 8617-29.

RICHARDS, K. H., DOBLE, R., WASSON, C. W., HAIDER, M., BLAIR, G. E., WITTMANN, M. & MACDONALD, A. 2014. Human papillomavirus E7 oncoprotein increases production of the anti-inflammatory interleukin-18 binding protein in keratinocytes. *J Virol,* 88**,** 4173-9.

ROBINSON, M. A., WOOD, J. P., CAPALDI, S. A., BARON, A. J., GELL, C., SMITH, D. A. & STONEHOUSE, N. J. 2006. Affinity of molecular interactions in the bacteriophage phi29 DNA packaging motor. *Nucleic Acids Res,* 34**,** 2698-709.

ROCCHI, P., TONELLI, R., CAMERIN, C., PURGATO, S., FRONZA, R., BIANUCCI, F., GUERRA, F., PESSION, A. & FERRERI, A. M. 2005. p21Waf1/Cip1 is a common target induced by short-chain fatty acid HDAC inhibitors (valproic acid, tributyrin and sodium butyrate) in neuroblastoma cells. *Oncol Rep,* 13**,** 1139-44.

RODAN, S. B., IMAI, Y., THIEDE, M. A., WESOLOWSKI, G., THOMPSON, D., BAR-SHAVIT, Z., SHULL, S., MANN, K. & RODAN, G. A. 1987.

Characterization of a human osteosarcoma cell line (Saos-2) with osteoblastic properties. *Cancer Res,* 47**,** 4961-6.
ROMAN, A. & MUNGER, K. 2013. The papillomavirus E7 proteins. *Virology,* 445**,** 138-68.
ROMANOWSKI, B. 2011. Long term protection against cervical infection with the human papillomavirus: review of currently available vaccines. *Hum Vaccin,* 7**,** 161-9.
ROSENBERG, J. E., BAMBURY, R. M., VAN ALLEN, E. M., DRABKIN, H. A., LARA, P. N., JR., HARZSTARK, A. L., WAGLE, N., FIGLIN, R. A., SMITH, G. W., GARRAWAY, L. A., CHOUEIRI, T., ERLANDSSON, F. & LABER, D. A. 2014. A phase II trial of AS1411 (a novel nucleolin-targeted DNA aptamer) in metastatic renal cell carcinoma. *Invest New Drugs,* 32**,** 178-87.
ROUS, P. 1993. A transmissible avian neoplasm (sarcoma of the common fowl). 1910. *Clin Orthop Relat Res***,** 3-8.
ROUS, P. & BEARD, J. W. 1935. The Progression to Carcinoma of Virus-Induced Rabbit Papillomas (Shope). *J Exp Med,* 62**,** 523-48.
ROWE, W. P., HUEBNER, R. J., GILMORE, L. K., PARROTT, R. H. & WARD, T. G. 1953. Isolation of a cytopathogenic agent from human adenoids undergoing spontaneous degeneration in tissue culture. *Proc Soc Exp Biol Med,* 84**,** 570-3.
RUSSELL, M. R., NICKERSON, D. P. & ODORIZZI, G. 2006. Molecular mechanisms of late endosome morphology, identity and sorting. *Curr Opin Cell Biol,* 18**,** 422-8.
RYHANEN, T., HYTTINEN, J. M., KOPITZ, J., RILLA, K., KUUSISTO, E., MANNERMAA, E., VIIRI, J., HOLMBERG, C. I., IMMONEN, I., MERI, S., PARKKINEN, J., ESKELINEN, E. L., UUSITALO, H., SALMINEN, A. & KAARNIRANTA, K. 2009. Crosstalk between Hsp70 molecular chaperone, lysosomes and proteasomes in autophagy-mediated proteolysis in human retinal pigment epithelial cells. *J Cell Mol Med,* 13**,** 3616-31.
SAGE, J., MILLER, A. L., PEREZ-MANCERA, P. A., WYSOCKI, J. M. & JACKS, T. 2003. Acute mutation of retinoblastoma gene function is sufficient for cell cycle re-entry. *Nature,* 424**,** 223-8.
SALEH, M. C., VAN RIJ, R. P., HEKELE, A., GILLIS, A., FOLEY, E., O'FARRELL, P. H. & ANDINO, R. 2006. The endocytic pathway mediates cell entry of dsRNA to induce RNAi silencing. *Nat Cell Biol,* 8**,** 793-802.
SANDGREN, S., WITTRUP, A., CHENG, F., JONSSON, M., EKLUND, E., BUSCH, S. & BELTING, M. 2004. The human antimicrobial peptide LL-37 transfers extracellular DNA plasmid to the nuclear compartment of mammalian cells via lipid rafts and proteoglycan-dependent endocytosis. *J Biol Chem,* 279**,** 17951-6.
SANTOSH, B. & YADAVA, P. K. 2014. Nucleic acid aptamers: research tools in disease diagnostics and therapeutics. *Biomed Res Int,* 2014**,** 540451.
SATO, H., WATANABE, S., FURUNO, A. & YOSHIIKE, K. 1989. Human papillomavirus type 16 E7 protein expressed in Escherichia coli and monkey COS-1 cells: immunofluorescence detection of the nuclear E7 protein. *Virology,* 170**,** 311-5.
SAYYED, S. G., HAGELE, H., KULKARNI, O. P., ENDLICH, K., SEGERER, S., EULBERG, D., KLUSSMANN, S. & ANDERS, H. J. 2009. Podocytes produce homeostatic chemokine stromal cell-derived factor-1/CXCL12, which contributes to glomerulosclerosis, podocyte loss and albuminuria in a mouse model of type 2 diabetes. *Diabetologia,* 52**,** 2445-54.
SCHERER, W. F., SYVERTON, J. T. & GEY, G. O. 1953. Studies on the propagation in vitro of poliomyelitis viruses. IV. Viral multiplication in a stable strain of human malignant epithelial cells (strain HeLa) derived from an epidermoid carcinoma of the cervix. *J Exp Med,* 97**,** 695-710.

SCHLEE, M., HARTMANN, E., COCH, C., WIMMENAUER, V., JANKE, M., BARCHET, W. & HARTMANN, G. 2009a. Approaching the RNA ligand for RIG-I? *Immunol Rev,* 227**,** 66-74.

SCHLEE, M., ROTH, A., HORNUNG, V., HAGMANN, C. A., WIMMENAUER, V., BARCHET, W., COCH, C., JANKE, M., MIHAILOVIC, A., WARDLE, G., JURANEK, S., KATO, H., KAWAI, T., POECK, H., FITZGERALD, K. A., TAKEUCHI, O., AKIRA, S., TUSCHL, T., LATZ, E., LUDWIG, J. & HARTMANN, G. 2009b. Recognition of 5' triphosphate by RIG-I helicase requires short blunt double-stranded RNA as contained in panhandle of negative-strand virus. *Immunity,* 31**,** 25-34.

SCHMIDT, A., SCHWERD, T., HAMM, W., HELLMUTH, J. C., CUI, S., WENZEL, M., HOFFMANN, F. S., MICHALLET, M. C., BESCH, R., HOPFNER, K. P., ENDRES, S. & ROTHENFUSSER, S. 2009. 5'-triphosphate RNA requires base-paired structures to activate antiviral signaling via RIG-I. *Proc Natl Acad Sci U S A,* 106**,** 12067-72.

SCHMIDT, K. S., BORKOWSKI, S., KURRECK, J., STEPHENS, A. W., BALD, R., HECHT, M., FRIEBE, M., DINKELBORG, L. & ERDMANN, V. A. 2004. Application of locked nucleic acids to improve aptamer in vivo stability and targeting function. *Nucleic Acids Res,* 32**,** 5757-65.

SCHUBERT, U., OTT, D. E., CHERTOVA, E. N., WELKER, R., TESSMER, U., PRINCIOTTA, M. F., BENNINK, J. R., KRAUSSLICH, H. G. & YEWDELL, J. W. 2000. Proteasome inhibition interferes with gag polyprotein processing, release, and maturation of HIV-1 and HIV-2. *Proc Natl Acad Sci U S A,* 97**,** 13057-62.

SCHWOEBEL, F., VAN EIJK, L. T., ZBORALSKI, D., SELL, S., BUCHNER, K., MAASCH, C., PURSCHKE, W. G., HUMPHREY, M., ZOLLNER, S., EULBERG, D., MORICH, F., PICKKERS, P. & KLUSSMANN, S. 2013. The effects of the anti-hepcidin Spiegelmer NOX-H94 on inflammation-induced anemia in cynomolgus monkeys. *Blood,* 121**,** 2311-5.

SEDMAN, J. & STENLUND, A. 1998. The papillomavirus E1 protein forms a DNA-dependent hexameric complex with ATPase and DNA helicase activities. *J Virol,* 72**,** 6893-7.

SEO, Y. S., MULLER, F., LUSKY, M. & HURWITZ, J. 1993. Bovine papilloma virus (BPV)-encoded E1 protein contains multiple activities required for BPV DNA replication. *Proc Natl Acad Sci U S A,* 90**,** 702-6.

SERRANO, B., ALEMANY, L., TOUS, S., BRUNI, L., CLIFFORD, G. M., WEISS, T., BOSCH, F. X. & DE SANJOSE, S. 2012. Potential impact of a nine-valent vaccine in human papillomavirus related cervical disease. *Infect Agent Cancer,* 7**,** 38.

SHEN, Y., WANG, B., LU, Y., OUAHAB, A., LI, Q. & TU, J. 2011. A novel tumor-targeted delivery system with hydrophobized hyaluronic acid-spermine conjugates (HHSCs) for efficient receptor-mediated siRNA delivery. *Int J Pharm,* 414**,** 233-43.

SHERMAN, M. Y. & GOLDBERG, A. L. 2001. Cellular defenses against unfolded proteins: a cell biologist thinks about neurodegenerative diseases. *Neuron,* 29**,** 15-32.

SHIGDAR, S., LIN, J., YU, Y., PASTUOVIC, M., WEI, M. & DUAN, W. 2011. RNA aptamer against a cancer stem cell marker epithelial cell adhesion molecule. *Cancer Sci,* 102**,** 991-8.

SHINTANI, T. & KLIONSKY, D. J. 2004. Autophagy in health and disease: a double-edged sword. *Science,* 306**,** 990-5.

SHOPE, R. E. & HURST, E. W. 1933. Infectious Papillomatosis of Rabbits : With a Note on the Histopathology. *J Exp Med,* 58**,** 607-24.

SHRIMAL, S., SAHA, A., BHATTACHARYA, S. & BHATTACHARYA, A. 2012. Lipids induce expression of serum-responsive transmembrane kinase

EhTMKB1-9 in an early branching eukaryote Entamoeba histolytica. *Sci Rep,* 2**,** 333.
SIMA, N., WANG, W., KONG, D., DENG, D., XU, Q., ZHOU, J., XU, G., MENG, L., LU, Y., WANG, S. & MA, D. 2008. RNA interference against HPV16 E7 oncogene leads to viral E6 and E7 suppression in cervical cancer cells and apoptosis via upregulation of Rb and p53. *Apoptosis,* 13**,** 273-81.
SINAL, S. H. & WOODS, C. R. 2005. Human papillomavirus infections of the genital and respiratory tracts in young children. *Semin Pediatr Infect Dis,* 16**,** 306-16.
SIOUD, M. 2005. Induction of inflammatory cytokines and interferon responses by double-stranded and single-stranded siRNAs is sequence-dependent and requires endosomal localization. *J Mol Biol,* 348**,** 1079-90.
SMITH-MCCUNE, K., KALMAN, D., ROBBINS, C., SHIVAKUMAR, S., YUSCHENKOFF, L. & BISHOP, J. M. 1999. Intranuclear localization of human papillomavirus 16 E7 during transformation and preferential binding of E7 to the Rb family member p130. *Proc Natl Acad Sci U S A,* 96**,** 6999-7004.
SMITH, J. S., LINDSAY, L., HOOTS, B., KEYS, J., FRANCESCHI, S., WINER, R. & CLIFFORD, G. M. 2007. Human papillomavirus type distribution in invasive cervical cancer and high-grade cervical lesions: a meta-analysis update. *Int J Cancer,* 121**,** 621-32.
SMOTKIN, D. & WETTSTEIN, F. O. 1987. The major human papillomavirus protein in cervical cancers is a cytoplasmic phosphoprotein. *J Virol,* 61**,** 1686-9.
SOUNDARARAJAN, S., CHEN, W., SPICER, E. K., COURTENAY-LUCK, N. & FERNANDES, D. J. 2008. The nucleolin targeting aptamer AS1411 destabilizes Bcl-2 messenger RNA in human breast cancer cells. *Cancer Res,* 68**,** 2358-65.
SOUSA, R. & PADILLA, R. 1995. A mutant T7 RNA polymerase as a DNA polymerase. *EMBO J,* 14**,** 4609-21.
STAKAITYTE, G., WOOD, J. J., KNIGHT, L. M., ABDUL-SADA, H., ADZAHAR, N. S., NWOGU, N., MACDONALD, A. & WHITEHOUSE, A. 2014. Merkel cell polyomavirus: molecular insights into the most recently discovered human tumour virus. *Cancers (Basel),* 6**,** 1267-97.
STANLEY, M. A., BROWNE, H. M., APPLEBY, M. & MINSON, A. C. 1989. Properties of a non-tumorigenic human cervical keratinocyte cell line. *Int J Cancer,* 43**,** 672-6.
STANLEY, M. A., PETT, M. R. & COLEMAN, N. 2007. HPV: from infection to cancer. *Biochem Soc Trans,* 35**,** 1456-60.
STOPPLER, H., STOPPLER, M. C., JOHNSON, E., SIMBULAN-ROSENTHAL, C. M., SMULSON, M. E., IYER, S., ROSENTHAL, D. S. & SCHLEGEL, R. 1998. The E7 protein of human papillomavirus type 16 sensitizes primary human keratinocytes to apoptosis. *Oncogene,* 17**,** 1207-14.
SULLENGER, B. A., GALLARDO, H. F., UNGERS, G. E. & GILBOA, E. 1990. Overexpression of TAR sequences renders cells resistant to human immunodeficiency virus replication. *Cell,* 63**,** 601-8.
SUN, H., ZHU, X., LU, P. Y., ROSATO, R. R., TAN, W. & ZU, Y. 2014. Oligonucleotide aptamers: new tools for targeted cancer therapy. *Mol Ther Nucleic Acids,* 3**,** e182.
SUNDARAM, P., KURNIAWAN, H., BYRNE, M. E. & WOWER, J. 2013. Therapeutic RNA aptamers in clinical trials. *Eur J Pharm Sci,* 48**,** 259-71.
TAKAGI, T., HASHIGUCHI, M., MAHATO, R. I., TOKUDA, H., TAKAKURA, Y. & HASHIDA, M. 1998. Involvement of specific mechanism in plasmid DNA uptake by mouse peritoneal macrophages. *Biochem Biophys Res Commun,* 245**,** 729-33.

TAN, A., YEH, S. H., LIU, C. J., CHEUNG, C. & CHEN, P. J. 2008. Viral hepatocarcinogenesis: from infection to cancer. *Liver Int,* 28**,** 175-88.
TANIDA, I., UENO, T. & KOMINAMI, E. 2008. LC3 and Autophagy. *Methods Mol Biol,* 445**,** 77-88.
TEDESCO, D., LUKAS, J. & REED, S. I. 2002. The pRb-related protein p130 is regulated by phosphorylation-dependent proteolysis via the protein-ubiquitin ligase SCF(Skp2). *Genes Dev,* 16**,** 2946-57.
TENG, Y., GIRVAN, A. C., CASSON, L. K., PIERCE, W. M., JR., QIAN, M., THOMAS, S. D. & BATES, P. J. 2007. AS1411 alters the localization of a complex containing protein arginine methyltransferase 5 and nucleolin. *Cancer Res,* 67**,** 10491-500.
THOMPSON, D. A., ZACNY, V., BELINSKY, G. S., CLASSON, M., JONES, D. L., SCHLEGEL, R. & MUNGER, K. 2001. The HPV E7 oncoprotein inhibits tumor necrosis factor alpha-mediated apoptosis in normal human fibroblasts. *Oncogene,* 20**,** 3629-40.
THOMSEN, P., VAN DEURS, B., NORRILD, B. & KAYSER, L. 2000. The HPV16 E5 oncogene inhibits endocytic trafficking. *Oncogene,* 19**,** 6023-32.
THORLAND, E. C., MYERS, S. L., GOSTOUT, B. S. & SMITH, D. I. 2003. Common fragile sites are preferential targets for HPV16 integrations in cervical tumors. *Oncogene,* 22**,** 1225-37.
THYRELL, L., SANGFELT, O., ZHIVOTOVSKY, B., POKROVSKAJA, K., WANG, Y., EINHORN, S. & GRANDER, D. 2005. The HPV-16 E7 oncogene sensitizes malignant cells to IFN-alpha-induced apoptosis. *J Interferon Cytokine Res,* 25**,** 63-72.
TOSCANO-GARIBAY, J. D., BENITEZ-HESS, M. L. & ALVAREZ-SALAS, L. M. 2011. Isolation and characterization of an RNA aptamer for the HPV-16 E7 oncoprotein. *Arch Med Res,* 42**,** 88-96.
TOTA, J. E., RAMANAKUMAR, A. V., JIANG, M., DILLNER, J., WALTER, S. D., KAUFMAN, J. S., COUTLEE, F., VILLA, L. L. & FRANCO, E. L. 2013. Epidemiologic approaches to evaluating the potential for human papillomavirus type replacement postvaccination. *Am J Epidemiol,* 178**,** 625-34.
TRAVERS, K. J., PATIL, C. K., WODICKA, L., LOCKHART, D. J., WEISSMAN, J. S. & WALTER, P. 2000. Functional and genomic analyses reveal an essential coordination between the unfolded protein response and ER-associated degradation. *Cell,* 101**,** 249-58.
TRENTIN, J. J., YABE, Y. & TAYLOR, G. 1962. The quest for human cancer viruses. *Science,* 137**,** 835-41.
TRIMBLE, C. L., PENG, S., KOS, F., GRAVITT, P., VISCIDI, R., SUGAR, E., PARDOLL, D. & WU, T. C. 2009. A phase I trial of a human papillomavirus DNA vaccine for HPV16+ cervical intraepithelial neoplasia 2/3. *Clin Cancer Res,* 15**,** 361-7.
TUERK, C. & GOLD, L. 1990. Systematic evolution of ligands by exponential enrichment: RNA ligands to bacteriophage T4 DNA polymerase. *Science,* 249**,** 505-10.
TUERK, C., MACDOUGAL, S. & GOLD, L. 1992. RNA pseudoknots that inhibit human immunodeficiency virus type 1 reverse transcriptase. *Proc Natl Acad Sci U S A,* 89**,** 6988-92.
TUGIZOV, S., BERLINE, J., HERRERA, R., PENARANDA, M. E., NAKAGAWA, M. & PALEFSKY, J. 2005. Inhibition of human papillomavirus type 16 E7 phosphorylation by the S100 MRP-8/14 protein complex. *J Virol,* 79**,** 1099-112.
UVERSKY, V. N., ROMAN, A., OLDFIELD, C. J. & DUNKER, A. K. 2006. Protein intrinsic disorder and human papillomaviruses: increased amount of disorder

in E6 and E7 oncoproteins from high risk HPVs. *J Proteome Res,* 5**,** 1829-42.
UZRI, D. & GEHRKE, L. 2009. Nucleotide sequences and modifications that determine RIG-I/RNA binding and signaling activities. *J Virol,* 83**,** 4174-84.
VALDOVINOS-TORRES, H., OROZCO-MORALES, M., PEDROZA-SAAVEDRA, A., PADILLA-NORIEGA, L., ESQUIVEL-GUADARRAMA, F. & GUTIERREZ-XICOTENCATL, L. 2008. Different Isoforms of HPV-16 E7 Protein are Present in Cytoplasm and Nucleus. *Open Virol J,* 2**,** 15-23.
VARKOUHI, A. K., SCHOLTE, M., STORM, G. & HAISMA, H. J. 2011. Endosomal escape pathways for delivery of biologicals. *J Control Release,* 151**,** 220-8.
VERMES, I., HAANEN, C., STEFFENS-NAKKEN, H. & REUTELINGSPERGER, C. 1995. A novel assay for apoptosis. Flow cytometric detection of phosphatidylserine expression on early apoptotic cells using fluorescein labelled Annexin V. *J Immunol Methods,* 184**,** 39-51.
WADIA, J. S., STAN, R. V. & DOWDY, S. F. 2004. Transducible TAT-HA fusogenic peptide enhances escape of TAT-fusion proteins after lipid raft macropinocytosis. *Nat Med,* 10**,** 310-5.
WALLACE, S. T. & SCHROEDER, R. 1998. In vitro selection and characterization of streptomycin-binding RNAs: recognition discrimination between antibiotics. *RNA,* 4**,** 112-23.
WAN, Y., KIM, Y. T., LI, N., CHO, S. K., BACHOO, R., ELLINGTON, A. D. & IQBAL, S. M. 2010. Surface-immobilized aptamers for cancer cell isolation and microscopic cytology. *Cancer Res,* 70**,** 9371-80.
WANG, Q., LI, L. & YE, Y. 2008. Inhibition of p97-dependent protein degradation by Eeyarestatin I. *J Biol Chem,* 283**,** 7445-54.
WANG, Q., SHINKRE, B. A., LEE, J. G., WENIGER, M. A., LIU, Y., CHEN, W., WIESTNER, A., TRENKLE, W. C. & YE, Y. 2010. The ERAD inhibitor Eeyarestatin I is a bifunctional compound with a membrane-binding domain and a p97/VCP inhibitory group. *PLoS One,* 5**,** e15479.
WANG, R., ZHAO, J., JIANG, T., KWON, Y. M., LU, H., JIAO, P., LIAO, M. & LI, Y. 2013. Selection and characterization of DNA aptamers for use in detection of avian influenza virus H5N1. *J Virol Methods,* 189**,** 362-9.
WANG, X., QI, M., YU, X., YUAN, Y. & ZHAO, W. 2012. Type-specific interaction between human papillomavirus type 58 E2 protein and E7 protein inhibits E7-mediated oncogenicity. *J Gen Virol,* 93**,** 1563-72.
WATERS, E. K., GENGA, R. M., SCHWARTZ, M. C., NELSON, J. A., SCHAUB, R. G., OLSON, K. A., KURZ, J. C. & MCGINNESS, K. E. 2011. Aptamer ARC19499 mediates a procoagulant hemostatic effect by inhibiting tissue factor pathway inhibitor. *Blood,* 117**,** 5514-22.
WEBSTER, K., PARISH, J., PANDYA, M., STERN, P. L., CLARKE, A. R. & GASTON, K. 2000. The human papillomavirus (HPV) 16 E2 protein induces apoptosis in the absence of other HPV proteins and via a p53-dependent pathway. *J Biol Chem,* 275**,** 87-94.
WELLS, S. I., FRANCIS, D. A., KARPOVA, A. Y., DOWHANICK, J. J., BENSON, J. D. & HOWLEY, P. M. 2000. Papillomavirus E2 induces senescence in HPV-positive cells via pRB- and p21(CIP)-dependent pathways. *EMBO J,* 19**,** 5762-71.
WETHERILL, L. F., HOLMES, K. K., VEROW, M., MULLER, M., HOWELL, G., HARRIS, M., FISHWICK, C., STONEHOUSE, N., FOSTER, R., BLAIR, G. E., GRIFFIN, S. & MACDONALD, A. 2012. High-risk human papillomavirus E5 oncoprotein displays channel-forming activity sensitive to small-molecule inhibitors. *J Virol,* 86**,** 5341-51.
WHITE, P. J., GRAY, A. C., FOGARTY, R. D., SINCLAIR, R. D., THUMIGER, S. P., WERTHER, G. A. & WRAIGHT, C. J. 2002. C-5 propyne-modified

oligonucleotides penetrate the epidermis in psoriatic and not normal human skin after topical application. *J Invest Dermatol,* 118**,** 1003-7.
WHO 2014. Human papillomavirus vaccines: WHO position paper, October 2014-Recommendations. *Vaccine.*
WHYTE, P., BUCHKOVICH, K. J., HOROWITZ, J. M., FRIEND, S. H., RAYBUCK, M., WEINBERG, R. A. & HARLOW, E. 1988. Association between an oncogene and an anti-oncogene: the adenovirus E1A proteins bind to the retinoblastoma gene product. *Nature,* 334**,** 124-9.
WILLIAMS, K. P., LIU, X. H., SCHUMACHER, T. N., LIN, H. Y., AUSIELLO, D. A., KIM, P. S. & BARTEL, D. P. 1997. Bioactive and nuclease-resistant L-DNA ligand of vasopressin. *Proc Natl Acad Sci U S A,* 94**,** 11285-90.
WITTRUP, A., SANDGREN, S., LILJA, J., BRATT, C., GUSTAVSSON, N., MORGELIN, M. & BELTING, M. 2007. Identification of proteins released by mammalian cells that mediate DNA internalization through proteoglycan-dependent macropinocytosis. *J Biol Chem,* 282**,** 27897-904.
WU, E. W., CLEMENS, K. E., HECK, D. V. & MUNGER, K. 1993. The human papillomavirus E7 oncoprotein and the cellular transcription factor E2F bind to separate sites on the retinoblastoma tumor suppressor protein. *J Virol,* 67**,** 2402-7.
XIAO, B., SPENCER, J., CLEMENTS, A., ALI-KHAN, N., MITTNACHT, S., BROCENO, C., BURGHAMMER, M., PERRAKIS, A., MARMORSTEIN, R. & GAMBLIN, S. J. 2003. Crystal structure of the retinoblastoma tumor suppressor protein bound to E2F and the molecular basis of its regulation. *Proc Natl Acad Sci U S A,* 100**,** 2363-8.
YE, F., ZHENG, Y., WANG, X., TAN, X., ZHANG, T., XIN, W., WANG, J., HUANG, Y., FAN, Q. & WANG, J. 2014. Recognition of Bungarus multicinctus venom by a DNA aptamer against beta-bungarotoxin. *PLoS One,* 9**,** e105404.
YEE, C., KRISHNAN-HEWLETT, I., BAKER, C. C., SCHLEGEL, R. & HOWLEY, P. M. 1985. Presence and expression of human papillomavirus sequences in human cervical carcinoma cell lines. *Am J Pathol,* 119**,** 361-6.
YONEYAMA, M., KIKUCHI, M., NATSUKAWA, T., SHINOBU, N., IMAIZUMI, T., MIYAGISHI, M., TAIRA, K., AKIRA, S. & FUJITA, T. 2004. The RNA helicase RIG-I has an essential function in double-stranded RNA-induced innate antiviral responses. *Nat Immunol,* 5**,** 730-7.
YOO, J. W., HONG, S. W., KIM, S. & LEE, D. K. 2006. Inflammatory cytokine induction by siRNAs is cell type- and transfection reagent-specific. *Biochem Biophys Res Commun,* 347**,** 1053-8.
YOON, S. W., LEE, T. Y., KIM, S. J., LEE, I. H., SUNG, M. H., PARK, J. S. & POO, H. 2012. Oral administration of HPV-16 L2 displayed on Lactobacillus casei induces systematic and mucosal cross-neutralizing effects in Balb/c mice. *Vaccine,* 30**,** 3286-94.
YOSHIOKA, N., INOUE, H., NAKANISHI, K., OKA, K., YUTSUDO, M., YAMASHITA, A., HAKURA, A. & NOJIMA, H. 2000. Isolation of transformation suppressor genes by cDNA subtraction: lumican suppresses transformation induced by v-src and v-K-ras. *J Virol,* 74**,** 1008-13.
YU, D., WANG, D., ZHU, F. G., BHAGAT, L., DAI, M., KANDIMALLA, E. R. & AGRAWAL, S. 2009. Modifications incorporated in CpG motifs of oligodeoxynucleotides lead to antagonist activity of toll-like receptors 7 and 9. *J Med Chem,* 52**,** 5108-14.
YU, S. L., CHAN, P. K., WONG, C. K., SZETO, C. C., HO, S. C., SO, K., YU, M. M., YIM, S. F., CHEUNG, T. H., WONG, M. C., CHEUNG, J. L., YEUNG, A. C., LI, E. K. & TAM, L. S. 2012. Antagonist-mediated down-regulation of Toll-like receptors increases the prevalence of human papillomavirus infection in systemic lupus erythematosus. *Arthritis Res Ther,* 14**,** R80.

YU, T., FERBER, M. J., CHEUNG, T. H., CHUNG, T. K., WONG, Y. F. & SMITH, D. I. 2005. The role of viral integration in the development of cervical cancer. *Cancer Genet Cytogenet,* 158**,** 27-34.

YUAN, H., FU, F., ZHUO, J., WANG, W., NISHITANI, J., AN, D. S., CHEN, I. S. & LIU, X. 2005. Human papillomavirus type 16 E6 and E7 oncoproteins upregulate c-IAP2 gene expression and confer resistance to apoptosis. *Oncogene,* 24**,** 5069-78.

ZANIER, K., OULD M'HAMED OULD SIDI, A., BOULADE-LADAME, C., RYBIN, V., CHAPPELLE, A., ATKINSON, A., KIEFFER, B. & TRAVE, G. 2012. Solution structure analysis of the HPV16 E6 oncoprotein reveals a self-association mechanism required for E6-mediated degradation of p53. *Structure,* 20**,** 604-17.

ZATSEPINA, O., BRASPENNING, J., ROBBERSON, D., HAJIBAGHERI, M. A., BLIGHT, K. J., ELY, S., HIBMA, M., SPITKOVSKY, D., TRENDELENBURG, M., CRAWFORD, L. & TOMMASINO, M. 1997. The human papillomavirus type 16 E7 protein is associated with the nucleolus in mammalian and yeast cells. *Oncogene,* 14**,** 1137-45.

ZHANG, B., CHEN, W. & ROMAN, A. 2006. The E7 proteins of low- and high-risk human papillomaviruses share the ability to target the pRB family member p130 for degradation. *Proc Natl Acad Sci U S A,* 103**,** 437-42.

ZHANG, X. D., GILLESPIE, S. K. & HERSEY, P. 2004. Staurosporine induces apoptosis of melanoma by both caspase-dependent and -independent apoptotic pathways. *Mol Cancer Ther,* 3**,** 187-97.

ZHENG, Z. M. & BAKER, C. C. 2006. Papillomavirus genome structure, expression, and post-transcriptional regulation. *Front Biosci,* 11**,** 2286-302.

ZHOU, J., LI, H., LI, S., ZAIA, J. & ROSSI, J. J. 2008. Novel dual inhibitory function aptamer-siRNA delivery system for HIV-1 therapy. *Mol Ther,* 16**,** 1481-9.

ZHOU, J., PENG, C., LI, B., WANG, F., ZHOU, C., HONG, D., YE, F., CHENG, X., LU, W. & XIE, X. 2012. Transcriptional gene silencing of HPV16 E6/E7 induces growth inhibition via apoptosis in vitro and in vivo. *Gynecol Oncol,* 124**,** 296-302.

ZHOU, J., SHU, Y., GUO, P., SMITH, D. D. & ROSSI, J. J. 2011. Dual functional RNA nanoparticles containing phi29 motor pRNA and anti-gp120 aptamer for cell-type specific delivery and HIV-1 inhibition. *Methods,* 54**,** 284-94.

ZIMMERMANN, H., DEGENKOLBE, R., BERNARD, H. U. & O'CONNOR, M. J. 1999. The human papillomavirus type 16 E6 oncoprotein can down-regulate p53 activity by targeting the transcriptional coactivator CBP/p300. *J Virol,* 73**,** 6209-19.

ZUHORN, I. S., ENGBERTS, J. B. & HOEKSTRA, D. 2007. Gene delivery by cationic lipid vectors: overcoming cellular barriers. *Eur Biophys J,* 36**,** 349-62.

ZUKER, M. 2003. Mfold web server for nucleic acid folding and hybridization prediction. *Nucleic Acids Res,* 31**,** 3406-15.

ZUR HAUSEN, H. 2002. Papillomaviruses and cancer: from basic studies to clinical application. *Nat Rev Cancer,* 2**,** 342-50.

ZUR HAUSEN, H. 2009. Papillomaviruses in the causation of human cancers - a brief historical account. *Virology,* 384**,** 260-5.